

Stephan Ulmer  
Olav Jansen  
*Editors*

# fMRI

Basics and Clinical  
Applications

 Springer

---

fMRI

---

Stephan Ulmer  
Olav Jansen (Eds.)

# fMRI

Basics and Clinical Applications

 Springer

Dr. Stephan Ulmer  
Institute of Neuroradiology  
Neurocenter  
University Hospital of Schleswig-Holstein  
Schittenhelmstr. 10  
24105 Kiel  
Germany  
ulmer@email.com

Prof. Dr. Olav Jansen  
Institute of Neuroradiology  
Neurocenter  
University Hospital of Schleswig-Holstein  
Schittenhelm Str. 10  
24105 Kiel  
Germany  
o.jansen@neurorad.uni-kiel.de

ISBN: 978-3-540-68131-1

e-ISBN: 978-3-540-68132-8

DOI: 10.1007/978-3-540-68132-8

Springer Dordrecht Heidelberg London New York

Library of Congress Control Number: 2009931051

© Springer-Verlag Berlin Heidelberg 2010

This work is subject to copyright. All rights are reserved, whether the whole or part of the material is concerned, specifically the rights of translation, reprinting, reuse of illustrations, recitation, broadcasting, reproduction on microfilm or in any other way, and storage in data banks. Duplication of this publication or parts thereof is permitted only under the provisions of the German Copyright Law of September 9, 1965, in its current version, and permission for use must always be obtained from Springer. Violations are liable to prosecution under the German Copyright Law.

The use of general descriptive names, registered names, trademarks, etc. in this publication does not imply, even in the absence of a specific statement, that such names are exempt from the relevant protective laws and regulations and therefore free for general use.

Product liability: The publishers cannot guarantee the accuracy of any information about dosage and application contained in this book. In every individual case the user must check such information by consulting the relevant literature.

*Cover design:* eStudioCalamar, Figueres/Berlin

Printed on acid-free paper

Springer is part of Springer Science+Business Media ([www.springer.com](http://www.springer.com))

---

## Dedication

*“To our beloved ones  
for your continuing support, unfailing patience and humour.  
Thank you for making this project come true!”*

*And to all contributors and colleagues:  
thank you for your invaluable assistance!”*

*Stephan Ulmer and Olav Jansen*

# Contents

## Section 1 Basics

<b>1 Introduction</b> .....	3
Stephan Ulmer	
<b>2 Neuroanatomy and Cortical Landmarks</b> .....	5
Stephan Ulmer	
<b>3 Spatial Resolution of fMRI techniques</b> .....	15
Seong-Gi Kim, Tao Jin, and Mitsuhiro Fukuda	
<b>4 The Electrophysiological Background of the fMRI Signal</b> .....	23
Christoph Kayser and Nikos K. Logothetis	
<b>5 High-Field fMRI</b> .....	35
Elke R. Gizewski	
<b>6 Press Button Solutions</b> .....	43
Kerstin Schmidt and Stephan Ulmer	

## Section 2 Clinical Applications

<b>7 Preoperative Blood Oxygen Level Dependent (BOLD) Functional Magnetic Resonance Imaging (fMRI) of Motor and Somatosensory Function</b> .....	51
Christoph Stippich	
<b>8 The Functional Anatomy of Speech Processing: From Auditory Cortex to Speech Recognition and Speech Production</b> .....	69
Gregory Hickok	
<b>9 Use of fMRI Language Lateralization for Quantitative Prediction of Naming and Verbal Memory Outcome in Left Temporal Lobe Epilepsy Surgery</b> .....	77
Jeffrey R. Binder	

---

<b>10 Mapping of Recovery from Poststroke Aphasia: Comparison of PET and fMRI</b> . . . . .	95
Wolf-Dieter Heiss	
<b>11 Functional Magnetic Resonance-Guided Brain Tumor Resection</b> . . . . .	107
Peter D. Kim, Charles L. Truwit, and Walter A. Hall	
<b>12 Direct Cortical Stimulation and fMRI</b> . . . . .	121
Maximillian H. Mehdorn, Simone Goebel, and Arya Nabavi	
<b>13 Imaging Epileptic Seizures Using fMRI</b> . . . . .	127
Simon Glynn and John A. Detre	
<b>14 Special Issues in fMRI-Studies Involving Children</b> . . . . .	141
Marko Wilke	
<b>15 Multimodal Brain Mapping in Patients with Early Brain Lesions</b> . . . . .	149
Martin Staudt	
<b>16 Combining Transcranial Magnetic Stimulation with (f)MRI</b> . . . . .	155
Gesa Hartwigsen, Tanja Kassuba, and Hartwig Roman Siebner	
<b>17 Clinical Magnetoencephalography and fMRI</b> . . . . .	169
Steven M. Stufflebeam	
<b>Index</b> . . . . .	179

## Contributors

**Jeffrey R. Binder** Department of Neurology, Medical College of Wisconsin,  
8701 Watertown Plank Road, Milwaukee, WI 53226, USA  
jbinder@mcw.edu

**John A. Detre** The Mahoney Institute of Neurological Sciences, University of  
Pennsylvania, 3 W Gates Building, 3400 Spruce Street, Philadelphia,  
PA 19104, USA  
detre@mail.med.upenn.edu

**Mitsuhiro Fukuda** Department of Radiology, University of Pittsburgh,  
3025 East Carson Street, Pittsburgh, PA 15203, USA  
kimsg@pitt.edu

**Elke R. Gizewski** Department of Diagnostic and Interventional Radiology  
and Neuroradiology, University Hospital Essen, Hufelandstrasse 55,  
45127 Essen, Germany  
elke.gizewski@uni-due.de

**Simon Glynn** The Mahoney Institute of Neurological Sciences,  
University of Pennsylvania, 3 W Gates Building, 3400 Spruce Street,  
Philadelphia, PA 19104, USA  
simongly@med.umich.edu

**Simone Goebel** Department of Neurosurgery, University Hospital of Schleswig-  
Holstein (UKSH), Campus Kiel, Schittenhelmstrasse 10, 24105 Kiel, Germany

**Walter A. Hall** Department of Neurosurgery, State University of New York Upstate,  
612 Jacobsen Hall, Upstate Medical University, 750 East Adams Street, Syracuse,  
NY 13210, USA  
hallw@upstate.edu

**Gesa Hartwigsen** Department of Neurology, Neurocenter, University Hospital of  
Schleswig-Holstein, Schittenhelmstrasse 10, 24105 Kiel, Germany  
g.hartwigsen@neurologie.uni-kiel.de

**Wolf-Dieter Heiss** Max Planck Institute for Neurological Research,  
Gleueler Str. 50, 50931 Köln, Germany  
wdh@nf.mpg.de

**Gregory Hickok** Department of Cognitive Sciences, Center for Cognitive Neuroscience, University of California, SSPA4109, Irvine, CA 92697, USA  
gshickok@uci.edu

**Tao Jin** Department of Radiology, University of Pittsburgh, 3025 East Carson Street, Pittsburgh, PA 15203, USA

**Tanja Kassuba** Department of Neurology, Neurocenter, University Hospital of Schleswig-Holstein, Schittenhelmstrasse 10, 24105 Kiel, Germany

**Christoph Kayser** Max Planck Institute for Biological Cybernetics, Spemannstrasse 38, 72076 Tübingen, Germany  
christoph.kayser@tuebingen.mpg.de

**Peter D. Kim** Department of Neurosurgery, State University of New York Upstate, 612 Jacobsen Hall, Upstate Medical University, 750 East Adams Street, Syracuse, NY 13210, USA

**Seong-Gi Kim** Department of Radiology, University of Pittsburgh, 3025 East Carson Street, Pittsburgh, PA 15203, USA  
kimsg@pitt.edu, taj6@pitt.edu

**Nikos K. Logothetis** Max Planck Institute for Biological Cybernetics, Spemannstrasse 38, 72076 Tübingen, Germany

**Maximillian H. Mehdorn** Department of Neurosurgery, University Hospital of Schleswig-Holstein (UKSH), Campus Kiel, Schittenhelmstrasse 10, 24105 Kiel, Germany  
mehdorn@nch.uni-kiel

**Arya Nabavi** Department of Neurosurgery, University Hospital of Schleswig-Holstein (UKSH), Campus Kiel, Schittenhelmstrasse 10, 24105 Kiel, Germany  
nabavia@nch.uni-kiel.de

**Kerstin Schmidt** Institute of Neuroradiology, Neurocenter, University Hospital of Schleswig-Holstein, Schittenhelmstrasse 10, 24015 Kiel, Germany

**Hartwig Roman Siebner** Danish Research Center for Magnetic Resonance, Copenhagen University Hospital-Hvidovre, Kettegaards Alle 30, 2650 Hvidovre, Denmark  
hartwig.siebner@drcmr.dk

**Martin Staudt** Neuropediatric Clinic and Clinic for Neurorehabilitation/Epilepsy, Center for Children and Adolescents, Krankenhausstrasse 20, 83569 Vogtareuth, Germany  
mstaudt@schoen-kliniken.de

**Christoph Stippich** Department of Diagnostic and Interventional Neuroradiology, University Hospital of Basel, Petersgraben 4, 4031 Basel, Switzerland  
stippich@uhbs.ch

**Steven M. Stuffelbeam** Harvard Medical School/Massachusetts Institute of Technology, Athinoula A. Martinos Center for Biomedical Imaging, Massachusetts General Hospital, 149 Thirteenth Street - 2301, Charlestown, MA 02129  
sms@nmr.mgh.harvard.edu

**Charles L. Truwit** Department of Neurosurgery, State University of New York Upstate, 612 Jacobsen Hall, Upstate Medical University, 750 East Adams Street, Syracuse, NY 13210, USA

**Stephan Ulmer** Institute of Neuroradiology, Neurocenter, University Hospital of Schleswig-Holstein, Schittenhelmstrasse 10, 24015 Kiel, Germany  
ulmer@email.com

**Marko Wilke** Department Paediatric Neurology and Developmental Medicine, University Children's Hospital, Hoppe-Seyler-Straße 3, 72076 Tübingen, Germany  
Marko.Wilke@med.uni-tuebingen.de

---

**Section 1**  
**Basics**

Within the past two decades, functional magnetic resonance imaging (fMRI) has developed tremendously, from initial descriptions of changes in blood oxygenation that can be mapped with MRI (Ogawa) using T2\*-weighted images to very basic investigations performing studies of the visual and motor cortex. From there, it has further evolved into a very powerful research tool and has also become an imaging modality of daily clinical routine, especially in presurgical mapping. This book focuses on these clinical applications starting from the basics and the backgrounds leading to current concepts and their application in a clinical environment.

Understanding brain function and localizing functional areas has ever since been the goal in neuroscience, and fMRI is a very powerful tool to approach this aim. Studies on healthy volunteers usually have a different approach and often a very complex study design, while clinical applications face other problems most commonly related to the limited compliance of the patients. Therefore, the application of fMRI in a clinical setting is a different challenge reflected in the study designs as well as in the analysis of algorithms of the data.

Besides the classical definition of functional areas that might have been shifted through a lesion or could be present in a distorted anatomy prior to neurosurgical resection, further clinical applications are mapping of recovery from stroke or trauma, cortical reorganization, if these areas were affected, and changes during the development of the brain or during the course of a disease. For psychiatric disorders fMRI offers new horizons in understanding the disease.

Coming back to the issue of reduced compliance of patients, the results obtained with our tool require the knowledge of basic neuroanatomy, an understanding of the physiology that lies behind it, especially the possible pathophysiology of the disease that might affect the results to start with. The results in volunteers are mandatory to understand the results in patients, and they can only be as good as the design. There is a need to monitor the patient in the scanner to guarantee that the results obtained will reflect activation caused by the stimulation, or to understand that reduced, or even missing activation, could have hampered the results, and to analyse how they were generated. Obviously, we have to realize that while the patient is still in the scanner, a repetition of the measurement can be enabled or an unnecessary scan can be avoided if the patient is not capable of performing the task. Performing motor tasks seems pretty straight forward, because the patient can be seen in the scanner. Cognitive and language tasks are more challenging. Also, a vascular stenosis or the steal effects of a brain tumor or an arteriovenous malformation (AVM) might corrupt the results. There are some sources of disturbance of the results that might depict no activation in a patient, e.g., in language tasks that usually depict reliable results in volunteers. It is mandatory to have a person with expertise in training and testing patients on the cognitive tasks involved, such as a neuropsychologist or a cognitive neurologist.

Task performance and development of a paradigm usually follows a graduated scheme. Initially, experiments are performed in healthy volunteers. This, however, has the disadvantage that our volunteers are most likely healthy students or staff who are used to the scanner environment and can therefore, focus unrestrictedly on the task while patients could be scared or too nervous with regard to their disease and about what might happen in the near future (like a brain tumor resection).

---

S. Ulmer  
Institute of Neuroradiology, Neurocenter, University Hospital of  
Schleswig-Holstein, Schittenhelmstr. 10, 24105 Kiel, Germany  
e-mail: ulmer@email.com

The same paradigm has to be used in less affected patients first, to confirm the feasibility in this setting that might become more specific after some experience. Test-retest reliability finally enables clinical application to address specific questions. Passive or “covert” tasks might be helpful; however, at least in cognitive studies performance cannot be measured. Semantic and cognitive processes continue during passive conditions, including rest and other passive baseline conditions. Regions involved will therefore be eliminated in the analysis when such conditions are used as a baseline.

Mapping children represents a twofold challenge. Normative data is not available, and compliance is limited. In early childhood or in cognitively impaired children, or just simply during brain development, cognitive tasks need to be modified individually, and that again causes problems in analyzing the data and interpreting the results.

Analysing data is a science on its own. Fortunately, there is a variety of software solutions available free of charge for the most part. Manufacturers also offer analysing software. Task-synchronous or singular voluntary head motion during the experiment might corrupt the data tremendously, to an extent that excludes a reliable interpretation of the data. Better than any available motion correction is avoidance of head movement altogether. As already stated, absence of an expected activation represents a real challenge and raises the question of the reliability of the method per se. Suppression of activation or task-related signal intensity decrease has also not been fully understood. Missing activation in a language task could mislead the neurosurgeon to resect a low-grade lesion close to the inferior frontal lobule and still cause speech disturbance or memory loss after resection of a lesion close to the mesial temporal lobe, and therefore – depending on the close cooperation between the clinicians – healthy skepticism and combination with other modalities like

direct cortical stimulation might be advisory. Hemispheric (language) dominance is only the tip of the iceberg and we have to ask ourselves again how sensitive our method and paradigm is to depict minor deficits. The same is true for clinical bedside testing and thus questions “silent” regions in the brain.

Sequence selection is important in terms of what we want to see and how to achieve it. Prior to the introduction of echo planar imaging, temporal resolution was restricted. Spatial resolution requirements are much more important in individual cases than in a healthy control group, especially in the presurgical definition of the so called “eloquent areas.”

For clinical applications, there is a variety of questions to be answered. To address specific questions, complex study designs are necessary. Integration of complex designs into a clinical setting can be difficult. Analysing data is very time consuming; therefore, push-button solutions to analyse the data would be welcomed as time has become so short in our daily routine. Higher field strengths might enable us to depict more signals, but possibly more noise as well in the data. From a clinician’s point of view, reliability of individual results is desired. This aspect will be discussed, and a comparison to other modalities of mapping brain functions will also be covered in detail.

It is interesting to see how fMRI became a clinical application over recent years of which the neurosurgeons were very suspicious in the initial phase of first clinical experiments in presurgical mapping. Its acceptance can be recognized based on increased numbers of studies performed on demand.

With this book we try to answer some questions and give an overview on how fMRI can be applied for clinical purposes. It is a great honor for me to have this board of experts in the field involved in this project. I hope that you as a reader will enjoy this book as much as I have, and that it will help you in your own daily work.

## 2.1 Neuroanatomy and Cortical Landmarks of Functional Areas

Prior to any type of functional mapping, a profound knowledge of neuroanatomy is mandatory. Focusing on the clinical applications of fMRI, this chapter will present methods to identify characteristic anatomical landmarks, and describe the course and shape of some gyri and sulci and how they can be recognized on MR imaging. As anatomy will be presented in neuro-functional systems, some redundancy is desired in order to course over cortical landmarks. If fMRI is not performed during clinical routine imaging, usually a 3D data set is acquired to overlay the results. Nowadays, fMRI is performed using echo planar imaging (EPI) with anisotropic distortion, whereas 3D T1-weighted data sets, such as MPRage (magnetization prepared rapid acquisition gradient echo) or SPGR (spoiled gradient recalled acquisition in steady state) sequences, are usually isotropic. Normalization of the fMRI data may reduce this systemic error to some extent that is more pronounced at the very frontal aspect of the frontal lobe and the very posterior aspect of the occipital lobe. However, for individual data, normalization and overlaying fMRI results on anatomy remains crucial. No two brains, not even the two hemispheres within one subject, are identical at a macroscopic level, and anatomical templates represent only a compromise (Devlin and Poldrack 2007). Usage of templates like the Talairach space (based on the anatomy of one brain) or the MNI template (based on 305 brains) can cause

registration error as well as additional variation, and reduce accuracy; indeed, it does not warrant the shammed anatomical precision in the individual case.

### 2.1.1 Sensorimotor Cortex

#### 2.1.1.1 Transverse Sections

There are various methods to identify the precentral gyrus (preCG; [3]), the central sulcus (CS) and the postcentral gyrus (postCG; [4]). From a craniocaudal point-of-view, the sensorimotor strip follows (from the apex to the Sylvian fissure [35b]) a medial–posterior–superior to lateral–anterior–inferior course. The precentral gyrus [3] fuses with the superior frontal gyrus (SFG; [1]) at the very upper convexity (Ebeling et al. 1986; Kido et al. 1980; Naidich et al. 1995; Ono et al. 1990). This can be well depicted on transverse sections (see Figs. 2.1 and 2.2). The precentral gyrus [3] is the most posterior part of the frontal lobe that extends inferiorly to the Sylvian fissure [35b]. The precentral gyrus [3] is thicker than the postcentral gyrus [4] in anterior–posterior (ap) dimension (Naidich et al. 1995) as is the grey matter (Meyer et al. 1996). At the apex, the pre- [3] and postcentral gyri [4] form the paracentral lobule [b] as they fuse. Making a little detour to a lateral view (see Fig. 2.3), the cingulate sulcus [5] ascends at the medial interhemispheric surface dorsal to the paracentral lobule (pars marginalis) [b], and thus separates it from the precuneus [6]. This intersection can be appreciated on axial sections as the “bracket”-sign (see Fig. 2.2; Naidich and Brightbill 1996) that borders the postcentral gyrus [4]. Somatotopographically, the apex harbours the cortical representation the lower extremity (Penfield and Rasmussen 1950). Following its course along the

---

S. Ulmer  
Institute of Neuroradiology, Neurocenter, University Hospital  
of Schleswig-Holstein, Schittenhelmstr. 10, 24105 Kiel,  
Germany  
e-mail: ulmer@email.com

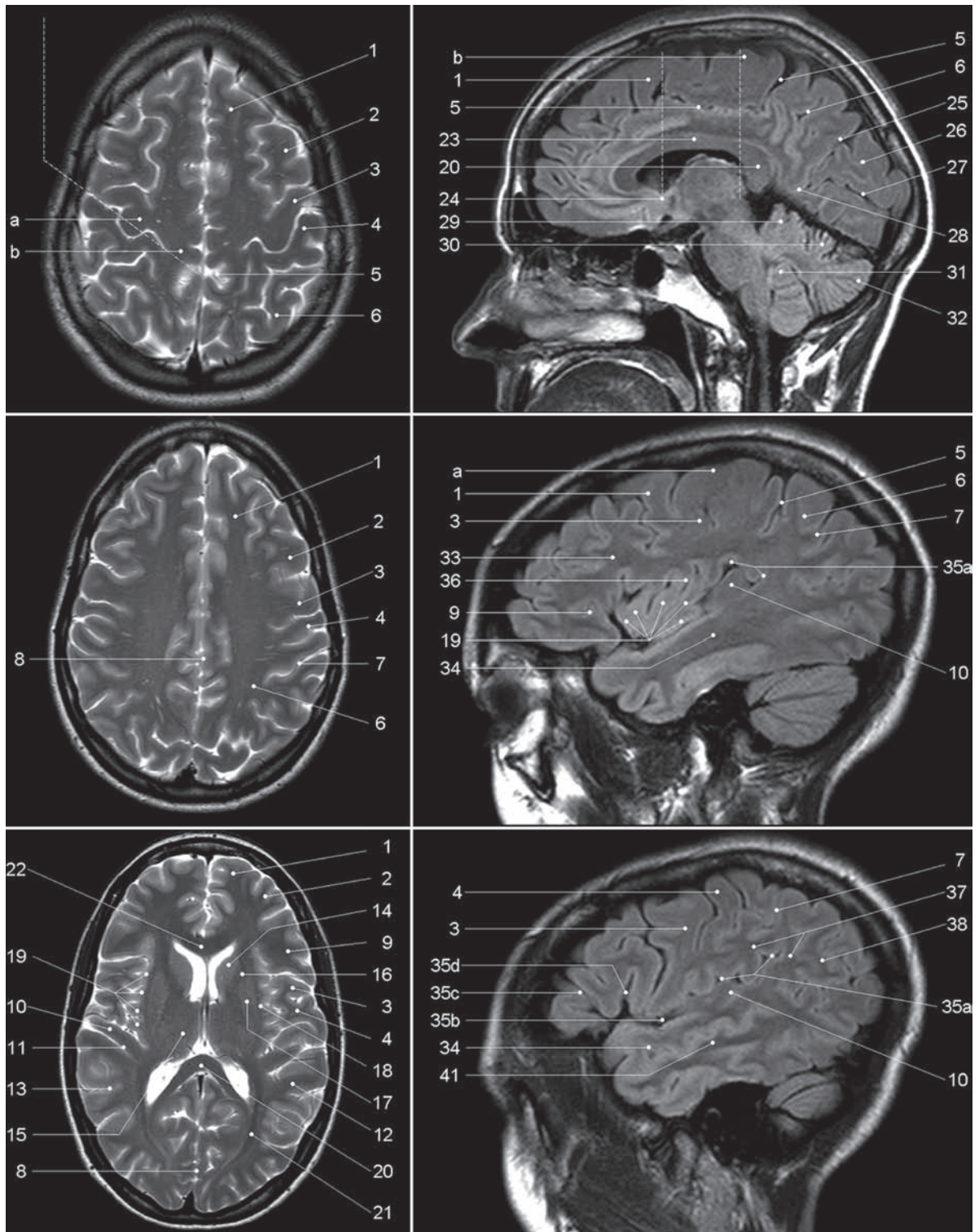
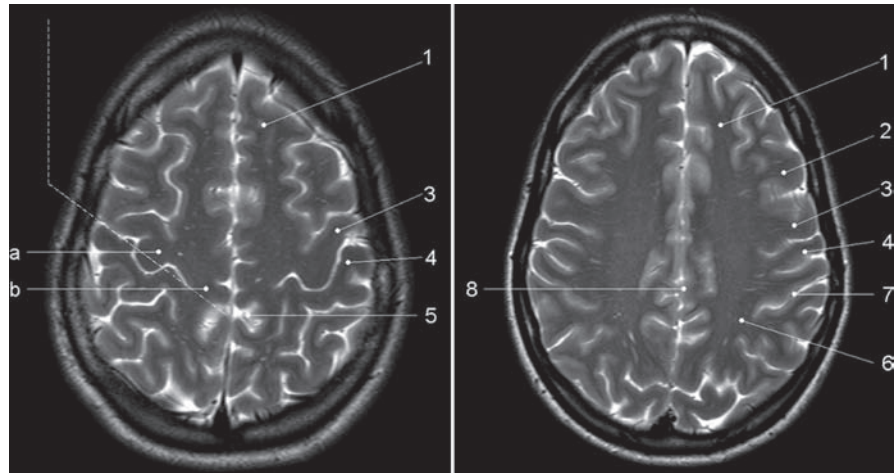


**Fig. 2.1** Overview of the used sections. The numbers are explained within the text as well as in the other figure legends in detail

**Fig. 2.2** Axial T2-weighted TSE MR images. 1 superior frontal gyrus; 2 medial frontal gyrus; 3 precentral gyrus; 4 postcentral gyrus; 5 “pars bracket,” cingulate sulcus; 6 precuneus, parietal lobe; 7 intraparietal sulcus; 8 interhemispheric fissure; *a* hand knob; *b* paracentral lobule



superficial convexity (from medial–posterior–superior to lateral–anterior–inferior), the cortical surface of the precentral gyrus increases at its posterior margin, building the omega-shaped motor hand knob ([a]; Yousry et al. 1995, 1997). Within this primary motor cortex (M1) of the hand, there is an additional somatotopic order of the individual digits (with interindividual overlap and variation). From medial to lateral, the hand is organized beginning with digit 5 (D5), to the thumb representation (D1) being the most lateral (Dechent and Frahm 2003). The motor hand knob [a] is another typical landmark of the precentral gyrus [3]; however, as the CS and the postcentral gyrus [4] follow this course, there is also an omega-shaped structure in the postcentral gyrus (harboring the somatosensory hand area). However, as described above, the ap-dimension of the postcentral gyrus [4] is smaller compared to the precentral gyrus [3], thus often enabling a differentiation. Somatotopographically, the cortical somatosensory representation follows the distribution of the precentral gyrus [3] (Penfield and Rasmussen 1950; Overduin and Servos 2004). Lateral to the SFG [1], the medial frontal gyrus [2] zigzags posteriorly and points towards the motor hand knob [a]. Beginning at this “junction” and lateral–inferior to this landmark, the ap-diameter of the PreCG [3] decreases, but it increases again along the lower convexity. This has already been recognized by Eberstaller (1890). Using modern imaging techniques, the diameter had been measured and the previous findings validated that the biggest diameter of the preCG [3] is found at the lower portion of the gyrus adjacent to the Sylvian fissure [35b] (Ono et al. 1990). This is the primary motor cortex (M1) of lip representation and tongue

movements. In the axial sections, there is neither a typical shape or landmark of the gyrus, nor does measuring from the motor hand area or the ac (anterior commissure) help us to describe the location precisely. This can be solved on sagittal sections (see below).

Previously, the anatomy of the frontal lobe has been described partially. As the course of the medial frontal gyrus [2] can be followed nicely on axial sections, the lateral inferior aspect of the frontal lobe represents the inferior frontal gyrus. Anterior to the preCG [3] the prefrontal motor areas can be found. The inferior frontal gyrus borders and overhangs the insula [19] anteriorly. This part is the frontal operculum [9] harbouring the motor speech area of Broca (see below sagittal sections).

The lateral ventricles with its anterior and posterior horn can easily be depicted on axial sections due to its typical form and typical signal caused by cortico-spinal fluid (CSF, see Figs. 2.1, 2.5 and 2.6). Their shape is formed through, the head of the caudate nucleus [10] lateral to the anterior horn, the thalamus [11] lateral at its waist (III. ventricle) and posteriorly by the fibers of the anterior–posteriorly running optic radiation [21] and left–right running fibers of the splenium [20] (see Figs. 2.5 and 2.6). Lateral to these structures, descending corticospinal fibers pass the internal capsule [16] and follow a certain somatotopic organization. The internal capsule is framed medial by the head of the caudate nucleus [10], the third ventricle and the thalamus [11] (at the posterior aspect of the third ventricle) and lateral by the globus pallidus [17]. From medial to lateral towards the insula [19] the globus pallidus, putamen and claustrum within the lentiform nucleus [17] can be differentiated. In the anterior limb and the



**Fig. 2.3** Sagittal FLAIR image at the midline. 1 superior frontal gyrus; 5 “pars bracket,” cingulate sulcus; 6 precuneus, parietal lobe; 23 body of the corpus callosum; 24 anterior commissure; 25 parieto-occipital sulcus; 27 calcarine fissure; b paracentral lobule; 28 cuneal point

genu of the internal capsule, [16] corticospinal fibers from the tongue, lip and face descend, whereas, in the posterior limb, fibers from the upper extremity, body and finally lower extremity are found.

### 2.1.1.2 Sagittal Sections

Previously sagittal sections have been described at the interhemispheric surface (see Fig. 2.3). The corpus callosum [20, 22, 23] represents the biggest connection between the two hemispheres. The frontal aspect is the genu [22], the medial part is the the body [23] and the most rostral part is the splenium [20]. The corpus callosum encases the lateral ventricles. At the base the anterior commissure (ac; [24]) can be identified as a roundish structure. Sometimes, the posterior commissure (pc) can also be defined, which represents a bundle of white fibers crossing the midline, at the dorsal aspect of the upper end of the cerebral aqueduct. Previously slice orientation of most fMRI studies had been performed according to this ac-pc line in order to have a reference system.

From the base to the apex, the corpus callosum is abutted by the callosal sulcus and the cingulate gyrus. The gyrus abutting the cingulate sulcus [5] is the medial part of the SFG [1]. In the region (at the medial cortical surface) framed by vertical lines perpendicular to the ac (Vac) or pc (Vpc; see Fig. 2.3) the supplementary motor area (SMA) is harboured in the cingulate gyrus and

superior frontal gyrus. As described above, the cingulate sulcus [5] ascends at the medial interhemispheric surface (see Fig. 2.3) dorsal to the paracentral lobule ([b]; pars marginalis) and thus separates it from the precuneus [6]. This intersection can be nicely appreciated on axial sections as the “bracket”-sign (see Fig. 2.2; Naidich and Brightbill 1996) that borders the postcentral gyrus [4]. The postcentral gyrus is already a part of the parietal lobe. The precuneus [6] is located dorsal to the postcentral sulcus. There is another important landmark that separates the parietal lobe from the occipital lobe (cuneus [26]), the parieto-occipital sulcus [25]. It can be easily recognized in sagittal views (see Fig. 2.3), as the dorsal sulcus that follows an inferior–anterior to superior–posterior course, posterior to the ascending part of the cingulate sulcus [5]. It is advisable to follow one of these structures moving laterally through the brain in sagittal sections. Once the Sylvian fissure [35b] can be identified, anatomical landmarks are again easy to define.

In mid-sagittal sections (see Fig. 2.6) the motor hand knob [a] can again be recognized as a “hook” that rises out of the parenchyma and points dorsally. Further, laterally the sensorimotor cortex overhangs the insula [19]. The Sylvian fissure [35b] that separates the frontal lobe and the temporal lobe has an inferior–anterior to superior–posterior course. At its anterior margin, it ascends into the anterior horizontal ramus [35c], and more dorsally into the anterior ascending ramus [35d] of the frontal operculum, [9] that also overhangs the anterior aspect of the insula [19]. The anterior horizontal ramus [35c] separates the pars orbitalis [40] from the pars triangularis [39], whereas the anterior ascending ramus [35d] separates the pars triangularis [39] from the pars opercularis [9] of the frontal operculum of the inferior frontal gyrus and thus form a “M” (Naidich et al. 1995). The pars opercularis [9] of the frontal operculum of the inferior frontal lobe harbours Broca’s area. At its posterior margin, the pars opercularis is delimited by the anterior subcentral sulcus. At the base of the sensorimotor strip the precentral [3] and postcentral gyrus [4] fuse (Eberstaller 1890, Ono et al. 1990). This junction is delimited dorsally by the posterior subcentral sulcus. Movement of the lips or tongue induce an increase in BOLD signal at this portion (Fesl et al. 2003, own observations). The base of the sensorimotor area has, depending on anatomical variations, a “K”- or “N”-shape that is built by the anterior subcentral sulcus and inferior precentral sulcus, the precentral gyrus, posterior subcentral

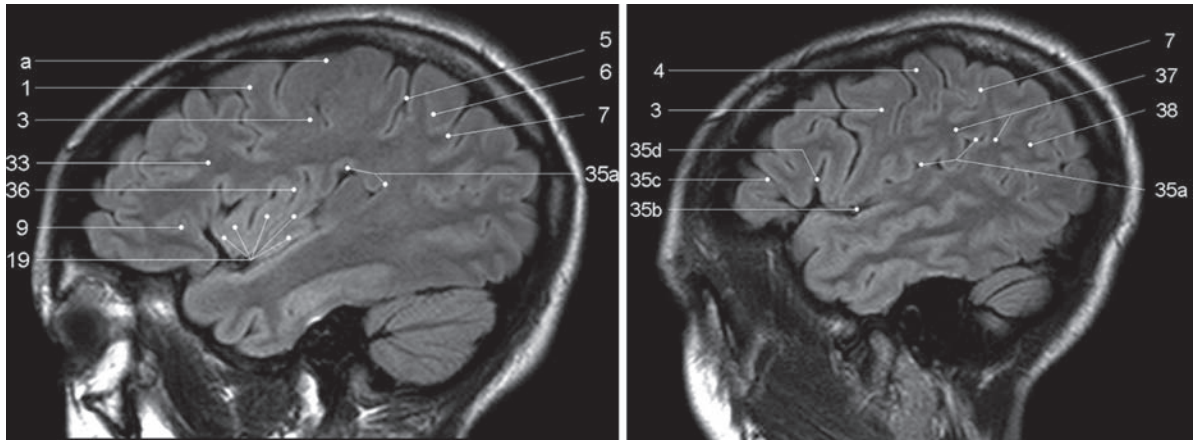


**Fig. 2.4** Sagittal FLAIR images. 1 superior frontal gyrus; 3 precentral gyrus; 4 postcentral gyrus; 5 “pars bracket,” cingulate sulcus; 6 precuneus, parietal lobe; 7 intraparietal sulcus; 9 pars opercularis, inferior frontal lobe, frontal operculum; 19 insula (anterior, posterior short insular gyri, anterior and posterior long

insular gyri); 33 medial frontal gyrus; 35a posterior ascending ramus of the sylvian fissure; 35b sylvian fissure; 35c anterior horizontal ramus of the sylvian fissure; 35d anterior ascending ramus of the sylvian fissure; 36 central sulcus of the insula; 37 supramarginal gyrus; 38 angular gyrus; a hand knob

sulcus, postcentral gyrus and postcentral sulcus that again borders the angular gyrus [38] (Eberstaller 1890, Ono et al. 1990, own observations; see Fig. 2.6). The posterior part of the Sylvian fissure separates - following its superior–posterior course - ascends into the posterior ascending ramus [35a] flanked by the anterior and posterior aspect of the supramarginal gyrus [37] that has a horseshoe appearance.

## 2.1.2 The Insula

The insula [19] is covered by the superior temporal gyrus [34], the frontal operculum [9] and the base of the sensorimotor strip. Its anatomy is best depicted in sagittal sections (see Fig. 2.6).

### 2.1.2.1 Sagittal Sections

The insula [19] is separated by the CS [36] that runs from the superior–posterior towards the inferior–anterior located apex of the insula into an anterior lobule and a posterior lobule (see Fig. 2.6). The anterior lobule consists of three gyri (anterior, medial and posterior short insular gyri), the posterior lobule consists of two gyri, the anterior long insular gyrus and the posterior long insular gyrus separated by the postcentral gyrus (Naidich et al. 2004).

From a neurofunctional point of view, the insula has various functional areas. The anterior lobule was found to cause word finding difficulties during electrical stimulation in epilepsy surgery (Ojemann and Whitaker 1978a, b), and to be responsible for speech planning (Wise et al. 1999; Price 2000). Speech apraxia is induced through lesions in the left precentral gyrus of the insula (Dronkers 1996; Nagao et al. 1999) whereas the right anterior lobule becomes activated during vocal repetition of nonlyrical tunes (Riecker et al. 2000). Stimulation of the right insula increases sympathetic tone and stimulation of the left insula increases parasympathetic tone (Oppenheimer 1993), possibly playing a role in cardiac mortality in left insular stroke. Finally visual-vestibular interactions have been found (Brandt et al. 1998) to name a few systems.

### 2.1.2.2 Transverse Sections

The insular cortex [19] is delimited medially by the globus pallidus, putamen and claustrum (lentiform nucleus [17]) and separated by a small border of white matter (extreme capsula [18]). The gyri can be differentiated by counting each knob starting ventrally at the anterior peri-insular sulcus that abuts the pars opercularis [9] of the frontal operculum of the inferior frontal gyrus (see Figs. 2.4 and 2.5). Five knobs can be defined (anterior, medial and posterior short insular gyri; anterior and posterior long insular gyrus).

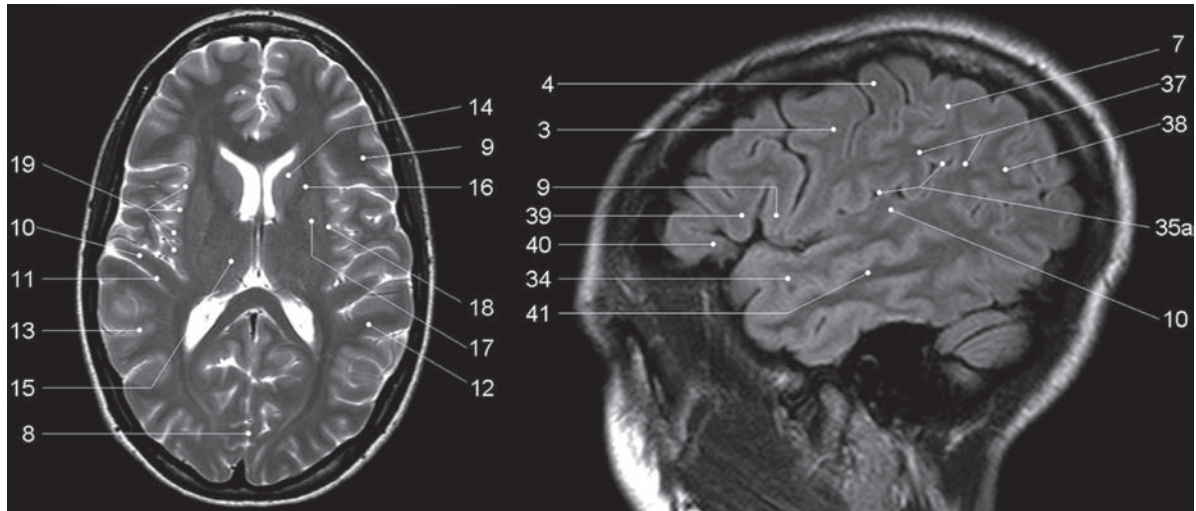


**Fig. 2.5** Axial T2-weighted TSE MR and sagittal FLAIR images. 3 precentral gyrus; 4 postcentral gyrus; 7 intraparietal sulcus; 8 interhemispheric fissure; 9 pars opercularis, inferior frontal lobe, frontal operculum; 10 Heschl's gyrus; 11 Heschl's sulcus; 12 planum temporale; 13 superior temporal sulcus; 14 head of the caudate nucleus; 15 thalamus; 16 internal capsule; 17 globus pallidus, putamen, claustrum (lentiform nucleus); 18 extreme capsule; 19

insula (anterior, posterior short insular gyri, anterior and posterior long insular gyri); 34 superior temporal gyrus; 35a posterior ascending ramus of the sylvian fissure; 37 supramarginal gyrus; 38 angular gyrus; 39 pars triangularis, frontal operculum, inferior frontal gyrus; 40 pars orbitalis, frontal operculum, inferior frontal gyrus; 41 medial temporal gyrus

## 2.1.3 Speech Associated Frontal Areas

### 2.1.3.1 Transverse Sections

In axial sections the insula [19] can be found easily (see Figs. 2.5 and 2.6). From medial (ventricles) to lateral, the globus pallidus, putamen and claustrum, within the lentiform nucleus, [17] can be differentiated followed by the extreme capsula [18] and the cortex of the insula [19]. The sylvian fissure [35b] separates the insula [19] from the temporal lobe. As stated above, the insula – taking anatomic variations into account – has four to five knobs (anterior, medial and posterior short insular gyrus divided, by the CS, from the anterior and posterior long insular gyrus). The insula [19] is covered by the superior temporal gyrus [34], the frontal operculum [9] and the base of the sensorimotor strip. After identifying the anterior short gyrus of the anterior lobule of the insular cortex, on a transverse view, the anterior border between the insula and inferior frontal lobe is the anterior peri-insular sulcus. It abuts the insula [19] on one hand and the pars opercularis [9] of the frontal operculum of the inferior frontal gyrus on the other. The pars opercularis [9] has a triangular shape in axial sections and covers the anterior part of the insula [19]. It can be followed into the anterior cranial fossa where it abuts the gyrus orbitalis that

runs parallel to the gyrus rectus. The convolution anterior to the pars opercularis [9] on the lateral surface is the pars triangularis [39], separated by the anterior ascending ramus [35d] of the sylvian fissure.

### 2.1.3.2 Sagittal Sections

Beginning at the lateral border of the brain (in sagittal views, see Figs. 2.4 and 2.5) there is the sylvian fissure [35b] that runs anterior–inferior to posterior–superior. Previously, the posterior margins have been described (see above). The Sylvian fissure separates the temporal lobe from the frontal lobe. At its anterior margin, it ascends into the anterior horizontal ramus [35c] and more dorsally into the anterior ascending ramus [35d] of the frontal operculum [9] that also overhangs the anterior aspect of the insula [19]. The anterior horizontal ramus [35c] separates the pars orbitalis [40] from the pars triangularis [39], whereas the anterior ascending ramus [35d] separates the pars triangularis [39] from the pars opercularis [9] of the frontal operculum of the inferior frontal gyrus that form an “M” (Naidich et al. 1995). The pars opercularis of the frontal operculum of the inferior frontal lobe harbours Broca's area. At its posterior margin the pars opercularis is delimited by the anterior subcentral sulcus.

## 2.1.4 Auditory Cortex and Speech Associated Temporo-Parietal Areas

### 2.1.4.1 Transverse Sections

From medial to lateral (see Figs. 2.5 and 2.6) towards the insula [19] the globus pallidus, putamen and claustrum within the lentiform nucleus [17] can be differentiated. Between the lentiform nucleus [17] and the cortex of the insula [19] the extreme capsula [18] is depicted as a small rim of white matter. The sylvian fissure [35b] separates the insula [19] from the temporal lobe. This is an easy definable landmark on axial views. The insula – taking anatomic variations into account – has four to five knobs (anterior, medial and posterior short insular gyrus divided by the CS [36] from the anterior and posterior long insular gyrus). Posterior to the convolution that represents the section of the posterior long insular gyrus, a gyrus in the superior temporal lobe can be identified with a dorso-medial to anterior–lateral course, called the transverse temporal gyrus or Heschl’s gyrus [10]. This is the primary auditory cortex (Mukamel et al. 2005, Devlin et al. 2007). Number and size may vary (Penhune et al. 1996; Rademacher et al. 2001); however, this is another good landmark that is easy to define. Heschl’s gyrus

[10] might be interrupted by the sulcus intermedius of Beck. Two gyri on the right and only one on the left hemisphere can be found frequently (Shapleske et al. 1999). Heschl’s sulcus [11], which borders Heschl’s gyrus [10] posteriorly is the anterior border of the planum temporale [12]. Although direct cortical stimulation intraoperatively may cause speech disturbances in this area (Sanai et al. 2008, Shapleske et al. 1999), the planum temporale [12] represents, more likely, the auditory association cortex. The planum temporale [12] extends on the superior surface of the temporal lobe and is delimited laterally by the superior temporal sulcus [13], posterior by the posterior ascending ramus and/or descending ramus of the sylvian fissure and medially in the depth of the sylvian fissure, which is less well defined (Shapleske et al. 1999). These borders are easier depicted in sagittal views; however, in transverse sections, remaining in the same plane in which Heschl’s gyrus [10] can be found, the superior temporal sulcus [13] is the next biggest sulcus posterior to Heschl’s sulcus [11]. Heschl’s gyrus [10] bulges into the sylvian fissure [35b]. The sylvian fissure can therefore also be followed in ascending axial images. At the parieto-temporal junction, sulci such as the sylvian fissure or the superior temporal sulcus [13] ascend whereas the sulcus intermedius primus descends. This

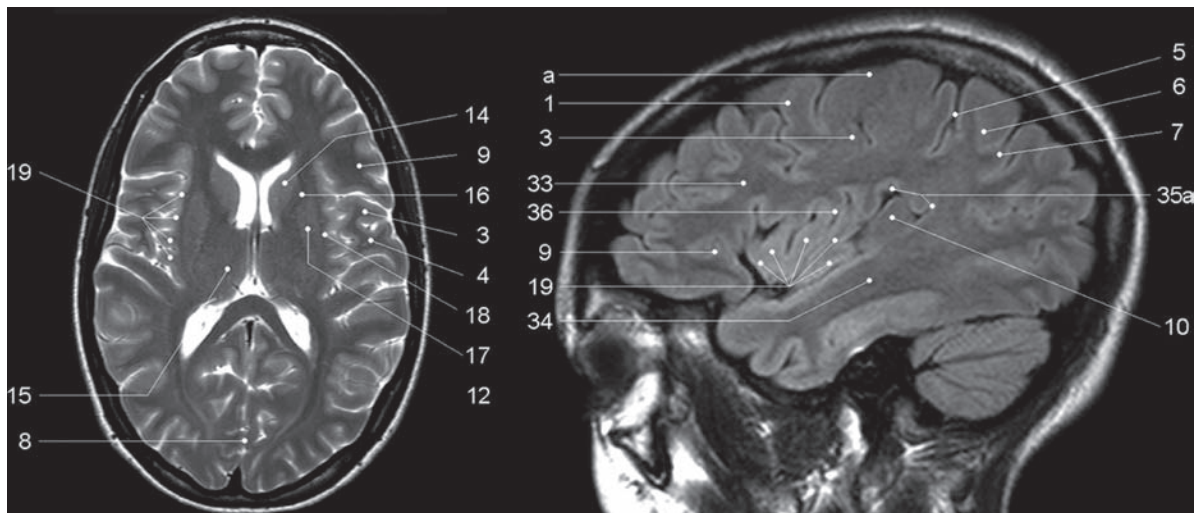


**Fig. 2.6** Axial T2-weighted TSE MR and sagittal FLAIR images. 1 superior frontal gyrus; 3 precentral gyrus; 4 postcentral gyrus; 5 “pars bracket,” cingulate sulcus; 6 precuneus, parietal lobe; 7 intraparietal sulcus; 8 interhemispheric fissure; 9 pars opercularis, inferior frontal lobe, frontal operculum; 10 Heschl’s gyrus; 12 planum temporale; 14 head of the caudate

nucleus; 15 thalamus; 16 internal capsule; 17 globus pallidum, putamen, claustrum (lentiform nucleus); 18 extreme capsula; 19 insula (anterior, posterior short insular gyri, anterior and posterior long insular gyri); 33 medial frontal gyrus; 34 superior temporal gyrus; 35a posterior ascending ramus of the sylvian fissure; 36 central sulcus of the insula

hampers anatomical description in axial sections. Ascending in axial slice order, the superior temporal sulcus [13] diminishes. As Heschl's gyrus [10] bulges into the sylvian fissure [35b], the sylvian fissure can be followed on its course as posterior ascending ramus [35a] up to the level of the cella media of the lateral ventricles (in bicommissural orientation), as a big intersection posterior to Heschl's sulcus [11]. The posterior ascending ramus [35a] of the sylvian fissure is imbedded in the supramarginal gyrus [37] which again is separated from the angular gyrus [38] by the sulcus intermedius primus. Descending in axial slice order, pre- and postcentral gyri can be identified as described above. The next sulcus dorsal to the postcentral sulcus is the intraparietal sulcus [7] which can be followed from the medial apical surface, laterally and dorsally in the parietal lobe [6]. Laterally, it ends above the sulcus intermedius primus and abuts the angular gyrus [38]. Size of the planum temporale [12] varies depending on sex, handedness and hemispherical dominance (Shapleske et al. 1999). Activation in functional imaging studies was found in verb generation tasks (Wise et al. 1991), listening to tones, words and tone sequences (Binder et al. 1996, 1997, 2000).

#### 2.1.4.2 Sagittal Sections

According to its dorso-medial to anterior-lateral course (see Fig. 2.6), the transverse temporal gyrus or Heschl's gyrus [10] abuts the base of the inferior sensorimotor strip (most likely the postcentral gyrus) at the lateral aspect and the posterior long gyrus of the insula [19] in more medially located sections. It is erected into the sylvian fissure [35b]. Heschl's sulcus [11], which borders Heschl's gyrus [10] posteriorly, is the anterior border of the planum temporale [12]. The planum temporale [12] extends on the superior surface of the temporal lobe and is delimited laterally by the superior temporal sulcus [13], posteriorly by the posterior ascending ramus and/or descending ramus of the sylvian fissure and medially in the depth of the sylvian fissure, which is less well defined (Shapleske et al. 1999). The sylvian fissure can be followed from the anterior ascending [35d] and horizontal rami [35c] in the frontal operculum [9] of the inferior frontal gyrus, dorsally to the ascending [35a] and descending rami at the temporo-parietal junction. Medially it is flanked by the insula [19], laterally by the superior temporal gyrus

[34] and inferior parts of the pre- and postcentral gyrus. Parallel to the sylvian fissure [35b], the superior temporal gyrus [34] also demonstrates an anterior-posterior course. The posterior ascending ramus [35a] of the sylvian fissure is imbedded in the supramarginal gyrus [37] which has a horseshoe appearance. Posterior to the supramarginal gyrus [37], the superior-inferior running sulcus intermedius primus separates it from the angular gyrus [38]. The superior temporal sulcus [13] ascends at its posterior end and diminishes.

#### 2.1.4.3 Coronal Sections

In coronal views, the sylvian fissure separating the temporal lobe from the insula and the frontal lobe can easily be seen. Originating from the temporal lobe, Heschl's gyrus points towards the insula (not shown).

### 2.1.5 Visual Cortex

#### 2.1.5.1 Sagittal Sections

At the medial surface of the occipital lobe, there is a sulcus that zigzags anterior-posteriorly called the calcarine sulcus [27], along which the visual cortex is located. The calcarine sulcus [27] separates the superior lip from the inferior lip of the visual cortex.

## References

- Fesl G, Moriggl B, Schmid UD, Naidich TP, Herholz K, Yousry TA (2003) Inferior central sulcus: variations of anatomy and function on the example of the motor tongue area. *Neuroimage* 20(1):601–610
- Binder JR, Frost JA, Hammeke TA, Rao SM, Cox RM (1996) Function of the left planum temporale in auditory and linguistic processing. *Brain* 119:1239–1247
- Binder JR, Frost JA, Hammeke TA, Cox RM, Rao SM, Prieto T (1997) Human brain language areas identified by functional imaging. *J Neurosci* 17:353–362
- Binder JR, Frost JA, Hammeke TA, Bellgowan PSF, Springer JA, Kaufman JN, Possing ET (2000) Human temporal lobe activation by speech and nonspeech sounds. *Cereb Cortex* 10:512–528
- Brandt T, Bartenstein P, Janek A, Dieterich M (1998) Reciprocal inhibitory visual-vestibular interactions: visual motion stimulation deactivates the parieto-insular vestibular cortex. *Brain* 121:1749–1758

- Dechent P, Frahm J (2003) Functional somatotopy of finger representations in human primary motor cortex. *Hum Brain Mapp* 18:272–283
- Devlin JT, Poldrack RA (2007) In praise of tedious anatomy. *Neuroimage* 37:1033–1041
- Dronkers NF (1996) A new brain region for coordinating speech articulation. *Nature* 384:159–161
- Ebeling U, Huber P, Reulen HJ (1986) Localization of the precentral gyrus in the computed tomogram and its clinical application. *J Neurol* 233(2):73–6
- Eberstaller O (1890) Ein Beitrag zur Anatomie der Oberfläche des Grosshirns. Urban & Schwarzenberg, Wien, Leipzig
- Kido DK, LeMay M, Levinson AW, Benson WE (1980) Computed tomographic localization of the precentral gyrus. *Radiology* 135:373–377
- Meyer JR, Roychowdhury S, Russell EJ, Callahan C, Gitelman D, Mesulam MM (1996) Location of the central sulcus via cortical thickness of the precentral and postcentral gyri on MR. *AJNR Am J Neuroradiol* 17(9):1699–706
- Mukamel R, Hagar G, Arieli A, Hasson U, Fried I, Malach R (2005) Coupling between neuronal firing, field potentials, and fMRI in human auditory cortex. *Science* 309:951–954
- Nagao M, Takeda K, Komori T, Isozaki E, Hirai S (1999) Apraxia of speech associated with an infarct in the precentral gyrus of the insula. *Neuroradiology* 41:356–357
- Naidich TP, Brightbill TC (1996) The pars marginalis: part I. A “bracket” sign for the central sulcus in axial plane CT and MRI. *Int J Neuroradiol* 2:3–19
- Naidich TP, Valavanis AG, Kubik S (1995) Anatomic relationships along the low-middle convexity: part I – normal specimens and magnetic resonance imaging. *Neurosurgery* 36:517–532
- Naidich TP, Kang E, Fatterpekar GM, Delman BN, Gultekin SH, Wolfe D, Ortiz O, Yousry I, Wieman M, Yousry TA (2004) The insula: anatomic study and MR imaging display at 1.5 T. *AJNR Am J Neuroradiol* 25:222–232
- Ojemann GA, Whitaker HA (1978a) The bilingual brain. *Arch Neurol* 35(7):409–12
- Ojemann GA, Whitaker HA (1978b) Language localization and variability. *Brain Lang* 6(2):239–60
- Ono M, Kubik S, Abernathy CD (eds) (1990) *Atlas of the cerebral sulci*. Georg Thieme, Stuttgart, New York
- Oppenheimer S (1993) The anatomy and physiology of cortical mechanisms of cardiac control. *Stroke* 24:13–15
- Overduin SA, Servos P (2004) Distributed digit somatotopy in primary somatosensory cortex. *Neuroimage* 23(2):462–72
- Penfield W, Rasmussen T (1950) *The cerebral cortex in man*. Macmillan, New York
- Penhune VB, Zatorre RJ, Macdonald JD, Evans AC (1996) Interhemispheric anatomical differences in human primary auditory cortex: probabilistic mapping and volume measurement from magnetic resonance scans. *Cereb Cortex* 6:661–672
- Price CJ (2000) The anatomy of language: contributions from functional neuroimaging. *J Anat* 197:335–359
- Rademacher J, Galaburda AM, Kennedy DN, Filipek PA, Caviness VS Jr. (1992) Human Cerebral Cortex: Localization, Parcellation, and Morphometry with Magnetic Resonance Imaging. *J Cogn Neurosci* 4(4):352–374
- Rademacher J, Morosan P, Schormann T, Schleicher A, Werner C (2001) Probabilistic mapping and volume measurement of human auditory cortex. *Neuroimage* 13:669–683
- Riecker A, Ackermann H, Wildgruber D, Dogil G, Grodd W (2000) Opposite hemispheric lateralization effects during speaking and singing at motor cortex, insula and cerebellum. *Neuroreport* 11:1997–2000
- Sanai N, Mirzadeh Z, Berger MS (2008) Functional outcome after language mapping for glioma resection. *N Engl J Med* 358(1):18–27
- Shapleske J, Rossell SL, Woodruff PWR, David AS (1999) The planum temporale: a systematic review of its structural, functional and clinical significance. *Brain Res Rev* 29:26–49
- Wise R, Chollet U, Hadar K, Friston E, Hoffner R, Frackowiak R (1991) Distribution of cortical neuronal networks involved in word comprehension and word retrieval. *Brain* 114: 1803–1817
- Wise RJ, Greene J, Buchel C, Scott SK (1999) Brain regions involved in articulation. *Lancet* 353:1057–1061
- Yousry TA, Schmid UD, Jassoy AG, Schmidt D, Eisner WE, Reulen HJ, Reiser MF, Lissner J (1995) Topography of the cortical motor hand area: prospective study with functional MR imaging and direct motor mapping at surgery. *Radiology* 195(1):23–9
- Yousry TA, Schmid UD, Alkadhi H, Schmidt D, Peraud A, Buettner A, Winkler P (1997) Localization of the motor hand area to a knob on the precentral gyrus. A new landmark. *Brain* 120(Pt 1):141–57

## 3.1 Introduction

Following its introduction over a decade ago, functional magnetic resonance imaging (fMRI) based on the blood oxygenation level dependent (BOLD) contrast (Ogawa et al. 1990) has become the tool of choice for visualizing neural activity in the human brain. The conventional BOLD approach has been extensively used for pinpointing functional foci of vision, motor, language and memory in normal and clinical patients. Intraoperative localization of functional foci will greatly improve surgical planning for epilepsy and tumor dissection, and potentially, for deep brain stimulation. Therefore, it is critical to understand the spatial resolution of fMRI relative to the actual neural active site (see review articles, (Kim and Ogawa 2002; Kim and Ugurbil 2003)).

In order to reliably determine the functional foci, high signal-to-noise ratio (SNR), which can be achieved using optimized imaging techniques, is critical. However, high SNR of fMRI techniques is not sufficient for high-resolution functional mapping if the signals that are being imaged do not have a high *specificity* to the local neural activity. Therefore, it is important to understand the signal source of BOLD fMRI and its fundamental limit of spatial resolution. Increased neural activity induces an increase in tissue metabolic demands. Thus, imaging the metabolic change (e.g., 2-fluorodeoxyglucose positron emission tomography) will yield high spatial specificity as metabolism will occur at the tissue at the site of the neuronal activity, and not in the vasculature. Changes in neural activity and metabolism

could directly or indirectly modulate the hemodynamic responses, including the cerebral blood flow (CBF), the cerebral blood volume (CBV), and the venous oxygenation levels. It has been well-established that the magnitude of CBF change is well-correlated with that of metabolic change. Thus, CBF mapping can pinpoint the most active spot of neural activity even if the exact spatial extent of the CBF response is controversial ((Malonek and Grinvald 1996) vs. (Duong et al. 2001)). The most commonly used BOLD technique is sensitive to paramagnetic deoxyhemoglobin (dHb), which is located at the capillaries and the venous draining vascular system (Ogawa et al. 1993), reducing spatial specificity of the gradient-echo BOLD signal. Often in fMRI studies, higher resolution BOLD images appear localized to large venous vessels because of larger contributions of venous signals due to the reduced partial volume of tissue.

To understand the spatial resolution of hemodynamic responses, functional changes of different vascular origins should be carefully considered. In this chapter, we will discuss the intrinsic limitations and the improvements of spatial resolution.

## 3.2 Vascular Structure and Hemodynamic Response

As all fMRI signals originate from changes in hemodynamics, it is important to examine vascular structure. Detailed human brain vasculature was studied anatomically by Duvernoy (Duvernoy et al. 1981). In short, vessels can be classified into pial and parenchymal vessels. Superficial pial arterial and venous vessels are numerous; arterial vessels with ~40–280  $\mu\text{m}$  diameter have lesser branches than venous vessels with

---

S.-G. Kim (✉)  
Department of Radiology, University of Pittsburgh,  
3025 East Carson Street, Pittsburgh, PA 15203, USA  
e-mail: kimsg@pitt.edu

a  $\sim 130\text{--}380\ \mu\text{m}$  diameter. These vessels can run a few centimeters and even longer. At the surface of the cortex, pial vessels connect to penetrating arteries and emerging veins at a right angle.

Parenchymal vessels can be divided into arteries, veins and capillary network. Capillaries with  $\sim 5\ \mu\text{m}$  average diameter and  $\sim 100\ \mu\text{m}$  length are most abundant at the middle of the cortex (Pawlik et al. 1981). Intracortical arteries and veins can be further classified into their cortical depths (Duvernoy et al. 1981); group 1 and 2 vessels (with  $10\text{--}25\ \mu\text{m}$  diameter for arterial vessels and  $20\text{--}30\ \mu\text{m}$  for venous vessels) reach the upper cortical layers (layer 2–3), group 3 (with  $15\text{--}30\ \mu\text{m}$  for arterial vessels and  $45\ \mu\text{m}$  for venous vessels) the middle of the cortex (layer 3–5), group 4 (with  $30\text{--}40\ \mu\text{m}$  for arterial vessels and  $65\ \mu\text{m}$  for venous vessels) the lower cortical region (layer 6), and group 5 (with  $30\text{--}75\ \mu\text{m}$  for arterial vessels and  $80\text{--}125\ \mu\text{m}$  for venous vessels) the white matter. The number of intracortical arteries is  $\sim 4$  times the number of intracortical veins (Duvernoy et al. 1981).

The intrinsic limit of spatial specificity of hemodynamic-based fMRI can be dependent on how finely CBF and CBV are regulated. Blood in each intracortical artery will supply a certain tissue volume, which is referred to as “the volume of arterial unit;” the volume of arterial unit is a volume with  $0.33\text{--}0.5\ \text{mm}$  diameter around a vessel for group 2–3 and for  $0.5\text{--}2\ \text{mm}$  for group 5 (Duvernoy et al. 1981). If an individual intracortical artery can be independently controlled, spatial resolution can be  $0.33\text{--}0.5\ \text{mm}$  if arterial vessels or capillary changes are detected. Our fMRI studies suggest that intrinsic CBF and CBV changes are reasonably specific to sub-millimeter functional domains (Duong et al. 2001; Zhao et al. 2005), which are in the order of  $0.5\text{--}0.7\ \text{mm}$  diameter in cats. If the regulation point exists at precapillary arterioles, then spatial resolution is even better. Recent papers indicate that precapillary arterioles indeed dilate during stimulation via astrocyte-capillary signaling (Zonta et al. 2003; Mulligan and MacVicar 2004; Metea and Newman 2006). In fact, the capillary network responds precisely in regions of neural activity in rat olfactory bulb, suggesting that spatial resolution of  $\sim 100\ \mu\text{m}$  is achievable (Chaigneau et al. 2003).

When an imaging technique is sensitive to changes in intracortical veins, its spatial resolution is determined by the volume of tissue draining to each vein, which is considered to be “the volume of venous unit.”

The volume of venous units is a volume with  $0.75\text{--}1\ \text{mm}$  diameter around a vessel for group 3–4 vessels, and  $1\text{--}4\ \text{mm}$  diameter for group 5 (Duvernoy et al. 1981). Thus, spatial resolution can not be better than  $0.75\ \text{mm}$  even if one single intracortical artery regulates precisely and downstream vessels respond. Intracortical venous vascular structures can be visualized with MRI. Figure 3.1 shows venographic images of cat brain, which were obtained using the BOLD contrast at  $9.4\ \text{T}$ . Venous vessels appear as dark lines or dots because venous blood has short  $T_2^*$  relative to tissue and arterial blood. Furthermore, blood susceptibility effect extends to tissue, enlarging apparent venous vessel size. Clearly, group 3–5 intracortical veins can be easily visualized, and group 3 are most numerous. Typical distance between intercortical veins is  $\sim 0.5\text{--}1\ \text{mm}$  (Fig. 3.1).

### 3.3 Spatial Resolution of BOLD fMRI

Since blood travels from capillaries to intracortical veins, and finally pial veins, a change in dHb concentration in blood can also occur far away from the actual gray matter region with increased neural activity, reducing effective spatial resolution. However, there is considerably more dilution of dHb change at farther downstream from the neuronally active region due to larger blood contribution from inactive regions. This dilution issue is also closely related to strength and spatial extent of neural activity; stronger and spatially larger neural activity induces more dHb change, and results in less effective dilution.

Conventional BOLD response is related to a change in dHb contents within a voxel, thus directly correlated with (baseline dHb content) time (oxygenation change). Since a pixel with draining veins has high baseline dHb content, the BOLD response is particularly sensitive to large draining veins. Thus, spatial resolution of conventional BOLD signal can be much worse than that determined by the volume of venous unit. It is a reasonable assumption that conventional BOLD-based *high-resolution* fMRI may mostly detect the functionally less-specific large-vessel contribution. To precisely localize functional foci, it is desirable to remove or minimize large vessel contributions.

In order to understand which size of venous vessels can be detected by BOLD fMRI, we review the source of BOLD fMRI signals. Detailed biophysical models

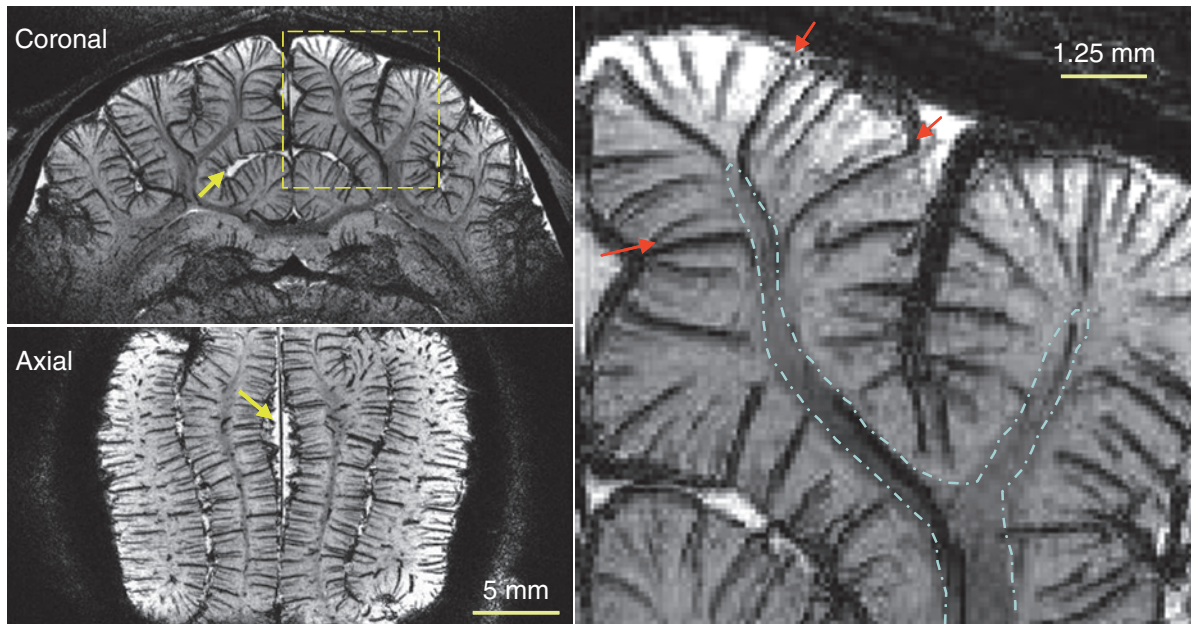


**Fig. 3.1** Visualization of venous vessels in a cat brain. A 3-D  $T_2^*$ -weighted MR image was obtained at 9.4 T with  $78 \mu\text{m}$  isotropic resolution and field of view of  $2 \times 2 \times 4 \text{ cm}^3$ . A gradient echo time of 20 ms was used to maximize the contrast between venous vessels and tissue. Data acquisition and processing methods were reported elsewhere (Park et al. 2008). 1.25-mm-thick slabs were selected, and minimum intensity projection was performed to enhance the contrast of venous

vessels. As a surface coil was used, the ventral section in the coronal slice (*top left*) had poor signal-to-noise ratio (SNR), and thus vessels could not be detected in that region. White matter areas (*contours in right*) can be distinguished from gray matter. *Dotted yellow box* in the coronal image was expanded 4 times into right. *Yellow arrows*, cerebrospinal fluid (CSF) areas; *red arrows*, venous vessels draining from white matter, which are “group 5”

and explanations can be found in others (Ogawa et al. 1993; Weisskoff et al. 1994; Kim and Ugurbil 2003). The BOLD contrast induced by dHb arises from both intravascular (IV) and extravascular (EV) components. Since exchange of water between these two compartments (typical lifetime of the water in capillaries  $>500 \text{ ms}$ ) is relatively slow when compared with the imaging time (echo time  $<100 \text{ ms}$ ), MRI signals from these can be treated as separate pools.

The IV component is considered to be uniform within vessels because water rapidly exchanges between red blood cells (RBC) with paramagnetic dHb and plasma (average water residence time in RBCs  $\approx 5 \text{ ms}$ ) and travels through space by exchange and diffusion. Thus, “dynamic” time-averaging occurs over the many different fields induced by dHb. All water molecules inside the vessel will experience similar dynamic averaging, resulting in reduction of blood water  $T_2$  in the venous pool. At high magnetic fields, venous blood  $T_2$  can be shorter than tissue  $T_2$  because  $R_2 (=1/T_2)$  of venous blood is quadratically dependent on magnetic

field (Thulborn et al. 1982). Thus, at a higher magnetic field, IV contribution can be reduced by setting echo time much longer than blood  $T_2$  (or  $T_2^*$ ) (Lee et al. 1999; Jin et al. 2006). Alternatively, the IV signal can be reduced by applying bipolar gradients (as employed in diffusion-weighted images), which, with a “ $b$ ” value of  $\sim 30 \text{ s/mm}^2$ , are expected to leave only the microvascular/extravascular contribution (Le Bihan et al. 1986).

The EV BOLD phenomenon has two biophysical sources (Ogawa et al. 1993; Weisskoff et al. 1994); one is due to intra-voxel dephasing of the magnetization in the presence of susceptibility-induced gradients, and the other is due to diffusion across the steep, susceptibility-induced gradients around small vessels (capillaries and venules). The first component induces high percentage signal changes around large venous vessels, regardless of magnetic field strength. Since field gradient decreases by  $(r/a)^2$  where  $r$  is the distance from vessel to the region of interest and  $a$  is the vessel radius, the dephasing effect around a larger vessel is more spatially widespread. However, the dephasing effect of the

static field can be refocused by the  $180^\circ$  radiofrequency (RF) pulse. Therefore, the EV contribution of large vessels can be reduced by using the spin-echo technique (which is similar to  $T_2$ -weighting in diagnostic imaging). The second component induces small signal changes in diffuse areas around capillaries and small venules. The reason is that tissue water around capillaries and small venules will be “dynamically” averaged over the many different fields during TE, similar to the IV component. This effect is larger at a higher magnetic field due to an increased susceptibility gradient within the water diffusion distance during TE. The dynamic diffusion-induced signals can be detected by either GE or SE approach. It is conceivable that the  $T_2$ -based BOLD technique is better localized to neuronal active region than  $T_2^*$ -based BOLD if the IV component of large vessels is removed (Zhao et al. 2004; Zhao et al. 2006). However, the sensitivity of spin-echo techniques is less than gradient-echo BOLD signal.

To examine the spatial resolution of GE and SE BOLD fMRI, we used cortical layers as a model because layer 4 has the highest metabolic and CBF responses during neural activity as well as the highest synapse density and cytochrome oxidase activity (Woolsey et al. 1996). If the fMRI technique is highly specific to metabolic response and/or neural activity, the middle of the cortex should have the highest signal change. **Figure 3.2** shows GE and SE BOLD fMRI maps of one isoflurane-anesthetized cat obtained during visual stimulation at 9.4 T (Zhao et al. 2006).

To view the cortical cross-section within-a plane resolution of  $156 \times 156 \mu\text{m}^2$ , a 2-mm thick imaging slice was selected perpendicular to the cortical surface. In both GE and SE BOLD maps, signal intensities increased during visual stimulation, indicating an increase in venous oxygenation. In conventional GE BOLD fMRI (**Fig. 3.2**), the highest percentage signal changes (yellow pixels) were seen in the CSF space (within the green contours), where pial veins are located. This large vessel contribution to BOLD signals is reduced using the SE technique (**Fig. 3.2**) because the dephasing around large vessels refocuses. This result is consistent with previous high-field SE BOLD observations (Lee et al. 1999; Yacoub et al. 2003; Zhao et al. 2004).

SE BOLD fMRI is an excellent alternative approach if high spatial resolution is required and high magnetic field (such as 7 T) is available. Otherwise, conventional GE BOLD fMRI should be used with postprocessing approaches to remove or minimize large vessel contributions. Location of large pial venous vessels can be determined from venographic images obtained with high-resolution  $T_2^*$ -weighted MR techniques (see **Fig. 3.1**) or from anatomical structures such as sulci and CSF. Large venous vessel areas tend to induce large BOLD percent change (see also **Fig. 3.2**) (Kim et al. 1994), delayed response (Lee et al. 1995), significant phase change (Menon 2002), and large baseline fluctuations (Kim et al. 1994). Although these criteria are subjective, they are effective in detecting and reducing large vessels contamination.

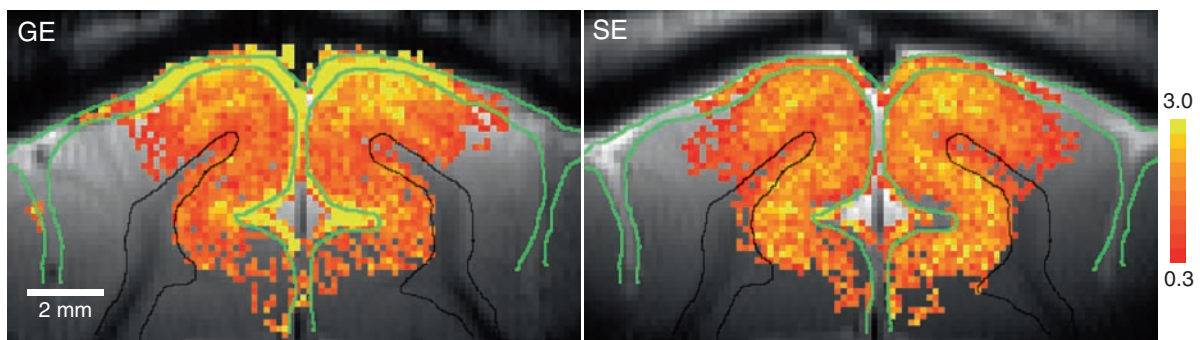


**Fig. 3.2** High resolution GE and SE BOLD fMRI maps of cat brain during visual stimulation overlaid on anatomical EPI images (Zhao et al. 2006). Coronal 2-mm thick images with  $156 \times 156 \mu\text{m}^2$  in-plane resolution were acquired using the four-shot EPI technique at 9.4 T with gradient-echo time of 20 ms and

spin-echo time of 40 ms. To determine statistically significant pixels, Student’s t-test was performed on a pixel-by-pixel basis with a t-value threshold of 2.0. Then, percentage signal changes were calculated for statistically active pixels. *Green contours*, CSF area; *black contours*, white matter

### 3.4 Perfusion-Based fMRI Approaches

Alternative to the BOLD approach, CBF-weighted techniques which are sensitive mainly to parenchyma should be considered for mapping functional foci. CBF-weighted functional images can be obtained using MR by employing arterial blood water as an endogenous flow tracer. Arterial spin labeling (ASL) can be achieved by RF pulse(s). Then, labeled spins move into capillaries in the imaging slice and exchange with tissue water spins. To obtain only perfusion-related images, two images are acquired, one with ASL and the other without labeling. The difference between the two images is directly related to CBF, and relative CBF changes due to physiological perturbations can be measured. Most of the labeled water molecules extract into tissue and the remaining labeled water lose most of their labeling by the time they reach the draining veins due to its relatively short half-life (i.e.,  $T_1$  of blood). Thus, CBF-

weighted MRI signals predominantly originate from tissue/capillary as well as arterial vessels (Ye et al. 1997; Lee et al. 2002; Kim and Kim 2005). Sensitivity of perfusion-weighted signals increases with magnetic field strength due to an increase in arterial blood  $T_1$ . ASL techniques include continuous ASL (Detre et al. 1992), flow-sensitive alternating inversion recovery (FAIR) (Kim 1995; Kwong et al. 1995), and various other techniques (Edelman et al. 1994; Wong et al. 1998).

Perfusion-based MR techniques have been used for fMRI studies. The spatial specificity of CBF-based fMRI is superior compared to GE BOLD techniques (Duong et al. 2001). Figure 3.3 shows BOLD and CBF functional maps during finger movements obtained at 4 T (Kim et al. 1997). The FAIR technique was used with inversion time of 1.4 s; the BOLD map was obtained from nonslice selective inversion recovery images, while the CBF map was from subtraction of nonslice selective from slice-selective inversion recovery images.

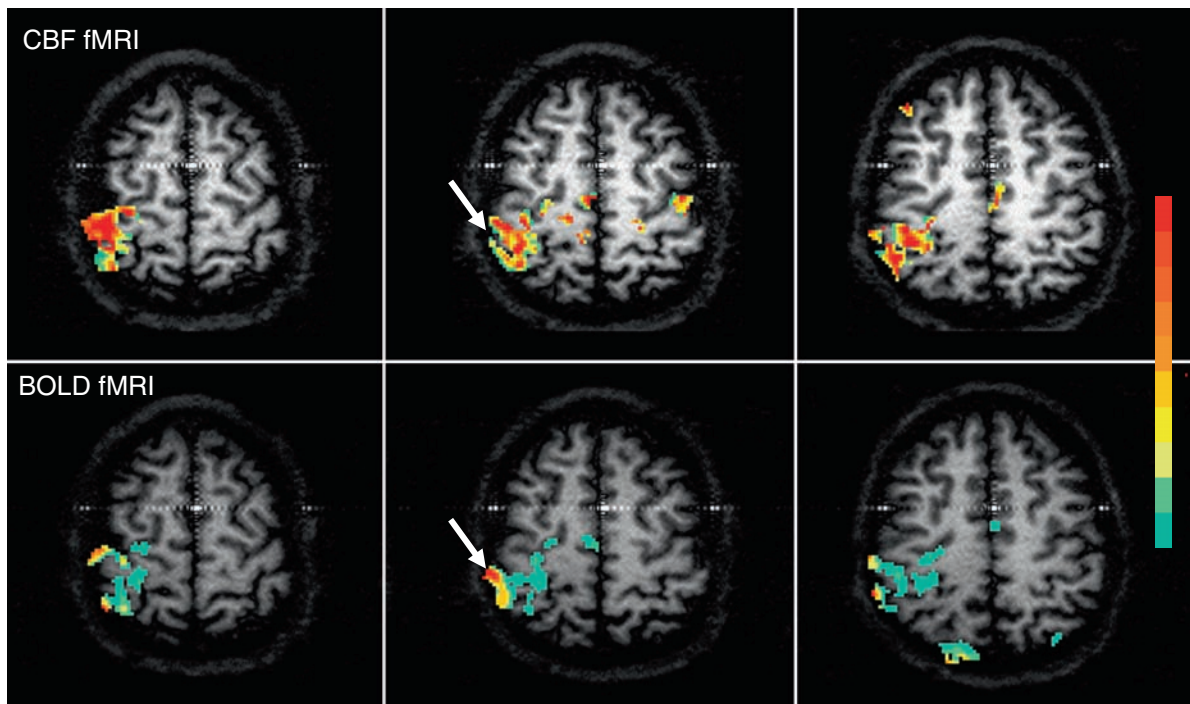


**Fig. 3.3** BOLD and CBF functional maps of left hand finger opposition, overlaid on  $T_1$ -weighted EPI (Kim et al. 1997). The flow-sensitive alternating inversion recovery (FAIR) technique was used to acquire BOLD (*top*) and CBF (*bottom*) contrast simultaneously at 4.0 T. BOLD maps were obtained from nonslice selective inversion recovery (IR) images, while CBF maps were calculated from differences between slice-selective and nonslice selective IR images. A cross-correlation value of 0.3

was used for threshold. For BOLD images, each color increment represents a 1% increment starting from the bottom 1%, while for CBF images, each color increment represents a 10% increment starting from the bottom 10%. The oblique arrow at the middle slice, indicating the right (contralateral) central sulcus, shows no activation in the CBF map, but large signal increase in the BOLD map, suggesting BOLD is sensitive to large draining veins

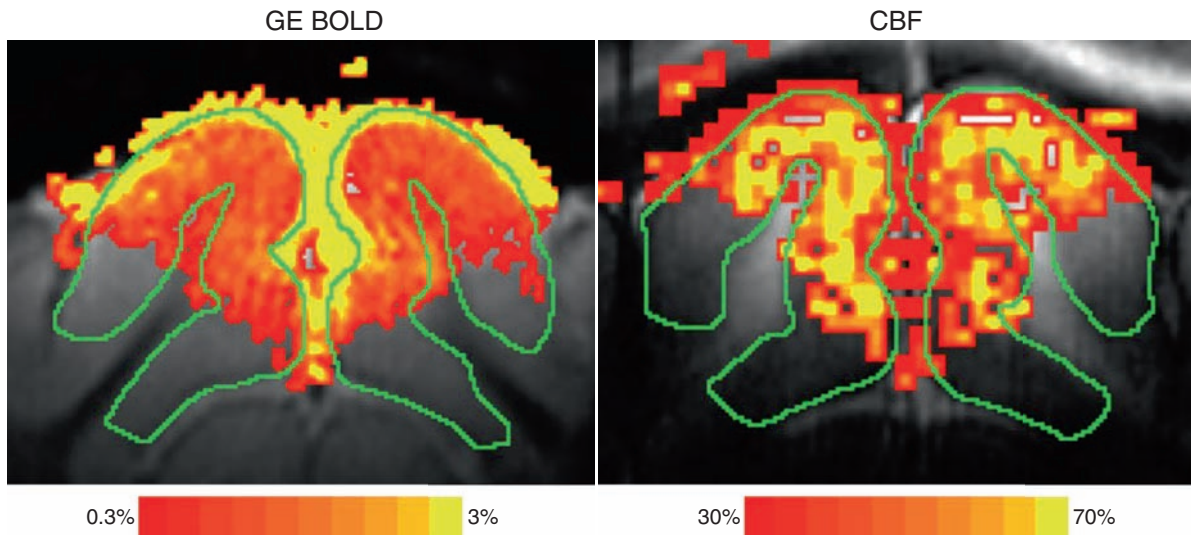


**Fig. 3.4** BOLD and CBF fMRI maps of cat brain during visual stimulation overlaid on anatomical EPI images (Jin and Kim 2008). Coronal 2 mm thick images with  $312 \times 312 \mu\text{m}^2$  in-plane resolution were acquired at 9.4 T; BOLD fMRI was obtained with TE of 20ms, while CBF was detected with the FAIR technique

with inversion time of 1.25 s. Maps were obtained by thresholding with a P-value  $<0.05$  and number of contiguous active pixels  $\geq 3$ . The gray matter areas are outlined by *green contours*. The highest BOLD signal changes are observed at the surface of the cortex, while the highest CBF changes occur at the middle of the cortex

Generally, activation areas are consistent between the maps measured by both techniques. However, pixel-wise comparison shows discrepancy between the two maps. Large signal changes in BOLD are located at draining veins indicated by arrows in the middle slice, while no signal change was observed in CBF. Tissue areas with high percent CBF changes have low BOLD signal changes. This indicates that the CBF approach is more specific to tissue than GE BOLD fMRI. To further confirm human fMRI results, BOLD and CBF fMRI were also compared in the cat's layer model. **Figure 3.4** shows GE BOLD and CBF fMRI maps obtained during visual stimulation at 9.4 T. CBF data were obtained using the FAIR technique with inversion time of 1.25s, while gradient BOLD data were obtained with TE of 20ms. The highest GE BOLD signal changes occur at the surface of the cortex, while the highest CBF changes occur at the middle of the cortex. This again demonstrates that perfusion-based fMRI technique is superior to GE BOLD for pinpointing functional foci precisely.

Proper CBF contrast is achieved only when enough time is allowed for the labeled arterial water to travel into the region of interest and exchange with tissue water. This makes it difficult to detect changes in CBF with a temporal resolution greater than  $T_1$  of arterial blood water. Acquisition of a pair of images can further reduce temporal resolution and consequently

SNR. Thus, it is difficult to obtain whole brain fMRI rapidly. However, baseline CBF value can be obtained, in addition to quantitative functional response. An additional advantage is less sensitivity to baseline signal drifts because slow non-activation-related signal changes can be removed by the pair-wise subtraction, and it is more stable to low-frequency stimulation compared to BOLD. Therefore, perfusion-based fMRI techniques are preferable for repetitive measurements over a long time period such as weeks and months, allowing investigations of functional reorganization and development. In clinical applications of fMRI where precise mapping is required around abnormal regions, the CBF-based fMRI technique is most appropriate because parenchymal signals are dominant.

**Acknowledgments** This work was supported in part by NIH (EB003324, EB003375 & NS44589). The authors thank their colleagues in the laboratory for providing the figures, and for the discussion.

## References

- Chaigneau E, Oheim M, Audinat E, Charpak S (2003) Two-photon imaging of capillary blood flow in olfactory bulb glomeruli. *Proc Nat Acad Sci* 100(22):13081–13086

- Detre JA, Leigh JS, Williams DS, Koretsky AP (1992) Perfusion imaging. *Magn Reson Med* 23:37–45
- Duong TQ, Kim D-S, Ugurbil K, Kim S-G (2001) Localized cerebral blood flow response at submillimeter columnar resolution. *Proc Natl Acad Sci USA* 98:10904–10909
- Duvernoy HM, Delon S, Vannson JL (1981) Cortical blood vessels of the human brain. *Brain Res Bull* 7(5):519–579
- Edelman RR, Siewert B, Darby DG, Thangaraj V, Nobre AC, Mesulam MM, Warach S (1994) Qualitative mapping of cerebral blood flow and functional localization with echo-planar MR imaging and signal targeting with alternating radio frequency. *Radiology* 192:513–520
- Jin T, Kim SG (2008) Cortical layer-dependent dynamic blood oxygenation, cerebral blood flow and cerebral blood volume responses during visual stimulation. *Neuroimage* 43(1):1–9
- Jin T, Wang P, Tasker M, Zhao F, Kim S-G (2006) Source of nonlinearity in echo-time-dependent BOLD fMRI. *Magn Reson Med* 55:1281–1290
- Kim S-G (1995) Quantification of relative cerebral blood flow change by flow-sensitive alternating inversion recovery (FAIR) technique: application to functional mapping. *Magn Reson Med* 34:293–301
- Kim S-G, Ogawa S (2002) Insights into new techniques for high resolution functional MRI. *Curr Opin Neurobiol* 12:607–615
- Kim S-G, Ugurbil K (2003) High-resolution functional magnetic resonance imaging of the animal brain. *Sci Direct Methods* 30:28–41
- Kim SG, Hendrich K, Hu X, Merkle H, Ugurbil K (1994) Potential pitfalls of functional MRI using conventional gradient-recalled echo techniques. *NMR Biomed* 7(1–2):69–74
- Kim S-G, Tsekos NV, Ashe J (1997) Multi-slice perfusion-based functional MRI using the FAIR technique: comparison of CBF and BOLD effects. *NMR Biomed* 10:191–196
- Kim T, Kim S-G (2005) Quantification of cerebral arterial blood volume and cerebral blood flow using MRI with modulation of tissue and vessel (MOTIVE) signals. *Magn Reson Med* 54:333–342
- Kwong KK, Chesler DA, Weisskoff RM, Donahue KM, Davis TL, Ostergaard L, Campbell TA, Rosen BR (1995) MR perfusion studies with T1-weighted echo planar imaging. *Magn Reson Med* 34:878–887
- Le Bihan D, Breton E, Lallemand D, Grenier P, Cabanis E, Laval-Jeantet M (1986) MR imaging of intravoxel incoherent motions: application to diffusion and perfusion in neurologic disorders. *Radiology* 161:401–407
- Lee AT, Glover GH, Meyer CH (1995) Discrimination of large venous vessels in time-course spiral blood-oxygen-level-dependent magnetic resonance functional neuroimaging. *Magn Reson Med* 33:745–754
- Lee S-P, Silva AC, Ugurbil K, Kim S-G (1999) Diffusion-weighted spin-echo fMRI at 9.4 T: microvascular/tissue contribution to BOLD signal change. *Magn Reson Med* 42:919–928
- Lee S-P, Silva AC, Kim S-G (2002) Comparison of diffusion-weighted high-resolution CBF and spin-echo BOLD fMRI at 9.4 T. *Magn Reson Med* 47:736–741
- Malonek D, Grinvald A (1996) Interactions between electrical activity and cortical microcirculation revealed by imaging spectroscopy: implication for functional brain mapping. *Science* 272:551–554
- Menon RS (2002) Postacquisition suppression of large-vessel BOLD signals in high-resolution fMRI. *Magn Reson Med* 47:1–9
- Metea M, Newman E (2006) Glial cells dilate and constrict blood vessels: a mechanism of neurovascular coupling. *J Neurosci* 26:2862–2870
- Mulligan S, MacVicar B (2004) Calcium transients in astrocyte endfeet cause cerebrovascular constrictions. *Nature* 431:195–199
- Ogawa S, Lee T-M, Nayak AS, Glynn P (1990) Oxygenation-sensitive contrast in magnetic resonance image of rodent brain at high magnetic fields. *Magn Reson Med* 14:68–78
- Ogawa S, Menon RS, Tank DW, Kim SG, Merkle H, Ellermann JM, Ugurbil K (1993) Functional brain mapping by blood oxygenation level-dependent contrast magnetic resonance imaging. A comparison of signal characteristics with a biophysical model. *Biophys J* 64(3):803–812
- Park SH, Masamoto K, Hendrich K, Kanno I, Kim SG (2008) Imaging brain vasculature with BOLD microscopy: MR detection limits determined by in vivo two-photon microscopy. *Magn Reson Med* 59:855–865
- Pawlik G, Rackl A, Bing RJ (1981) Quantitative capillary topography and blood flow in the cerebral cortex of cats: an in vivo microscopic study. *Brain Res* 208:35–58
- Thulborn KR, Waterton JC, Matthews PM, Radda GK (1982) Oxygenation dependence of the transverse relaxation time of water protons in whole blood at high field. *Biochem Biophys Acta* 714:265–270
- Weisskoff RM, Zuo CS, Boxerman JL, Rosen BR (1994) Microscopic susceptibility variation and transverse relaxation: theory and experiment. *Magn Reson Med* 31: 601–610
- Wong E, Buxton R, Frank L (1998) Quantitative imaging of perfusion using a single subtraction (QUIPSS and QUIPSS II). *Magn Reson Med* 39:702–708
- Woolsey TA, Rovainen CM, Cox SB, Henegar MH, Liang GE, Liu D, Moskalenko YE, Sui J, Wei L (1996) Neuronal units linked to microvascular modules in cerebral cortex: response elements for imaging the brain. *Cereb Cortex* 6:647–660
- Yacoub E, Duong TQ, Van De Moortele P, Lindquist M, Adriany G, Kim S-G, Ugurbil K, Hu X (2003) Spin-echo fMRI in humans using high spatial resolutions and high magnetic fields. *Magn Reson Med* 49:665–664
- Ye FQ, Mattay VS, Jezzard P, Frank JA, Weinberger DR, McLaughlin AC (1997) Correction for vascular artifacts in cerebral blood flow values by using arterial spin tagging techniques. *Magn Reson Med* 37:226–235
- Zhao F, Wang P, Kim S-G (2004) Cortical depth-dependent gradient-echo and spin-echo BOLD fMRI at 9.4 T. *Magn Reson Med* 51:518–524
- Zhao F, Wang P, Hendrich K, Kim S-G (2005) Spatial specificity of cerebral blood volume-weighted fMRI responses at columnar resolution. *Neuroimage* 27:416–424
- Zhao F, Wang P, Hendrich K, Ugurbil K, Kim S-G (2006) Cortical layer-dependent BOLD and CBV responses measured by spin-echo and gradient-echo fMRI: insights into hemodynamic regulation. *Neuroimage* 30:1149–1160
- Zonta M, Angulo MC, Gobbo S, Rosengarten B, Hossmann K-A, Pozzan T, Carmignoto G (2003) Neuron-to-astrocyte signaling is central to the dynamic control of brain microcirculation. *Nat Neurosci* 6:43–50

# The Electrophysiological Background of the fMRI Signal

# 4

Christoph Kayser and Nikos K. Logothetis

## 4.1 Introduction

The ability to non-invasively study the architecture and function of the human brain constitutes one of the most exciting cornerstones for modern medicine, psychology and neuroscience. Current *in vivo* imaging techniques not only provide clinically essential information and allow new forms of treatment, but also reveal insights into the mechanisms behind brain function and malfunction. This supremacy of modern imaging rests on its ability to study the structural properties of the nervous system simultaneously with the functional changes related to neuronal activity. As a result, imaging allows us to combine information about the spatial organization and connectivity of the nervous system with information about the underlying neuronal processes and provides the only means to link perception and cognition with the neural substrates in the human brain.

Functional imaging techniques build on the interconnections of cerebral blood flow (CBF), the brain's energy demand and the neuronal activity (for reviews on this topic see for example (Heeger and Ress 2002; Logothetis 2002; Logothetis and Wandell 2004; Lauritzen 2005)). Indeed, elaborate mechanisms exist to couple changes in CBF and blood-oxygenation to the maintenance and restoration of ionic gradients, and the synthesis, transport and reuptake of neurotransmitters. More than 125 years ago, Angelo Mosso had already realized that there must be a relation between energy demand and CBF, when he observed increasing brain

pulsations in a patient with a permanent skull defect performing a mental task (Mosso 1881). Similar observations on the coupling of blood flow to neuronal activity (from experiments on animals) led Roy and Sherrington to make the insightful statement that "... the chemical products of cerebral metabolism contained in the lymph that bathes the walls of the arterioles of the brain can cause variations of the caliber of the cerebral vessels: that is, in this reaction, the brain possesses an intrinsic mechanism by which its vascular supply can be varied locally in correspondence with local variations of functional activity" (Roy and Sherrington 1890).

Nowadays, there is little doubt about the usefulness of imaging to basic research and clinical diagnosis. In fact, with the wide availability of magnetic resonance imaging (MRI), functional imaging has become a self-sustaining branch of neuroscience research. Yet, and despite all this progress, it is still not clear how faithfully functional imaging replicates the patterns of neuronal activity underlying the changes in brain perfusion. Debating over the spatial and temporal precision of the imaging signal, researchers have compared it to more direct measurements of electrical neuronal activity from electrophysiological approaches. This holds especially true for the blood-oxygenation level-dependent signal (BOLD-fMRI), which is probably the most widely used functional imaging technique (Ogawa et al. 1998). As direct measurements of neuronal activity can be obtained from mesoscopic recordings of electrical potentials on the scalp (EEG) as well as from spatially localized recordings using fine microelectrodes, they offer a wide variety of signals that characterize neuronal processes. Hence, before reviewing the neurophysiological basis of the functional imaging signal, it is worth considering the properties of the signals recorded using electrophysiological methods.

---

C. Kayser (✉)  
Max Planck Institute for Biological Cybernetics,  
Spemannstrasse 38, 72076 Tübingen, Germany  
e-mail: christoph.kayser@tuebingen.mpg.de

## 4.2 The Compound Neural Signal

Electrophysiological studies at the systems level typically record extracellular signals, defined by the superposition of local currents. In contrast to the intracellular recordings that directly assess the membrane potential of individual neurons, extracellular signals can arise from a number of sources and are more difficult to interpret. Neurons are embedded in the extracellular medium, which acts as a volume conductor, allowing the passive spread of electrical signals across considerable spatial distances. For an extracellular recording point, the inflow of positively charged ions into the active sites of a neuron appears as a current sink (inward currents), while inactive membrane sites act as a source (outward currents) for the active regions. Given the resistive nature of the extracellular medium, these currents generate so-called extracellular field potentials (EFP) (Freeman 1975). The signal measured by an electrode placed at a neural site represents the mean EFP from the spatially weighted sum of sinks and sources along multiple cells at this particular site. In addition, by the superposition principle, the EFPs from multiple cells add up linearly throughout the volume conductor. Thus, for cells, or cell compartments, with diametrically opposite orientations currents of equal magnitude but opposite polarity will generate potentials that tend to cancel each other; while for well aligned and elongated processes of neural elements the currents add, resulting in a strongly oriented electric field. Despite these difficulties in interpreting the measured signals, EFP remain the most important tool for the systems neurophysiologist, as they convey a great deal of information about the underlying brain function.

If a small-tipped microelectrode is placed sufficiently close to the soma or axon of a neuron, then the measured EFP directly reports the spike (action potentials) of that neuron, and possibly also of its immediate neighbours. The firing rates of such well isolated neurons have been the critical measure for comparing neural activity with sensory processing or behaviour, ever since the early development of microelectrodes (Adrian and Zotterman 1929). Indeed, measuring firing rates has been the mainstay of systems neuroscience for decades. Although a great deal has been learned from this measure of neuronal activity, the single unit technique has the drawback of not providing information about subthreshold integrative processes or associational operations taking place at a given site. In

addition, this recording technique suffers from a bias toward certain cell types and sizes (Towe and Harding 1970; Stone 1973). For large neurons the active and passive regions are further apart, resulting in a substantially greater flow of membrane current and a larger extracellular spike than for a small cell. As a result, spikes generated by large neurons will remain above noise level over a greater distance from the cell than spikes from small neurons. It follows that typically measured spiking activity mostly represents the small population of large cells, which are the pyramidal cells in the neocortex. This bias is particularly pronounced in experiments with alert behaving animals or humans, in which even slight movements of the subjects make it extremely difficult to record from smaller neurons for a sufficiently long time (Fried et al. 1997; Kreiman et al. 2000). As a result, most of the experiments using single-unit extracellular recordings report on the activity of large principal cells, which represent the output of the cortical area under study.

If the impedance of the microelectrode is sufficiently low, or when no clear signal from individual neurons can be isolated, then the electrode can be used to monitor the totality of the action potentials in that region. Often, the multi-unit activity (MUA) is characterized as compound electrical signal in a frequency range above 300–500 Hz. This signal has been shown to be site specific (Buchwald and Grover 1970) and to vary systematically with stimulus properties, in the same way as the activity of single neurons (e.g. Kayser et al. (2007a)). There is good evidence that MUA activity reflects variations in the magnitude of extracellular spike potentials, with large-amplitude signal variations in the MUA reflecting large-amplitude extracellular potentials. Overall, the MUA seems to incorporate signals from a sphere with a radius of 150–300  $\mu\text{m}$ , depending on the detailed electrode properties (Buchwald and Grover 1970; Legatt et al. 1980; Gray et al. 1989). Typically, such a region will contain thousands of neurons, suggesting that the MUA is especially sensitive to the synchronous firings of many cells, which is further enhanced by the principle of superposition mentioned above.

While the fast, high-frequency, components of the aggregate field potentials mostly reflect the spiking activity of neighbouring neurons, the slower components of the EFP seem to reflect a different kind of activity. The so called local field potential (LFP) is defined as the low-frequency component of the EFP, and represents mostly slow events reflecting

cooperative activity in neural populations. In contrast to the MUA, the magnitude of the LFP does not correlate with cell size, but instead reflects the extent and geometry of local dendrites (Fromm and Bond 1964; Buchwald et al. 1966; Fromm and Bond 1967). A prominent geometric arrangement is formed by the pyramidal neurons with their apical dendrites running parallel to each other and perpendicular to the pial surface. They form a so called open field arrangement, in which dendrites face in one direction and somata in another, producing strong dendrite-to-soma dipoles when they are activated by synchronous synaptic input. The spatial summation of the LFP has been suggested to reflect a weighted average of synchronized dendrosomatic components of the synaptic signals of a neural population within 0.5–3 mm of the electrode tip (Mitzdorf 1985, 1987; Juergens et al. 1999). The upper limits of the spatial extent of LFP summation were indirectly calculated by computing the phase coherence as a function of inter-electrode distance in experiments with simultaneous multiple-electrode recordings (for example see Fig. 4.1). Combined intracellular and field potential recordings also suggest a synaptic/dendritic origin of the LFPs, representing locally averaged excitatory and inhibitory postsynaptic potentials, which

are considerably slower than the spiking activity (Steriade and Amzica 1994; Steriade et al. 1998). In addition, the LFP can also include other types of slow activity unrelated to synaptic events, including voltage-dependent membrane oscillations (Juergens et al. 1999) and spike after potentials (Buzsaki et al. 1988).

In summary, three different signals can commonly be extracted from extracellular microelectrode recordings, each partially covering a different frequency regime of the acquired signal. Representing fast events, the MUA reflects the averaged spiking activity of populations of neurons, with a bias for the larger, principal (projection) neurons. Covering the same frequency range the single-unit activity reports mainly on the activity of the principal neurons that form the major output of a cortical area. In contrast, and representing slower events, the LFP reflects slow waveforms such as synaptic potentials, afterpotentials, and voltage-gated membrane oscillations that mostly reflect the input of a given cortical area as well as its local intracortical processing.

### 4.3 The Passive Electric Properties of the Brain

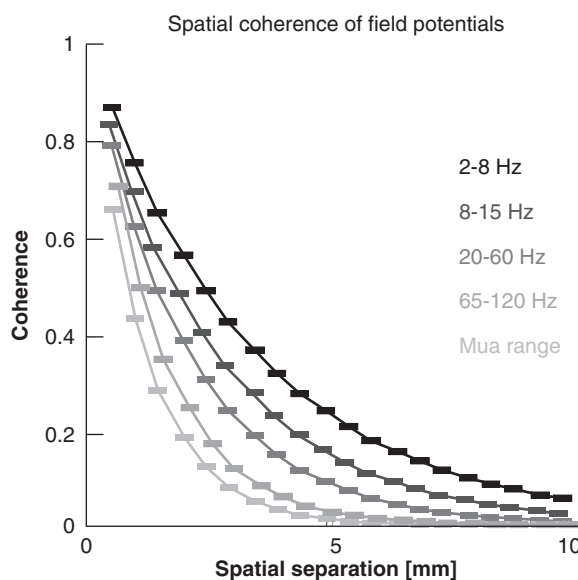


**Fig. 4.1** Spatial coherence of the local field potential in primary visual cortex. Each graph displays the average coherence of the field potentials recorded from two electrodes as a function of the electrodes' spatial separation. Each *line* indicates a different frequency band

To better understand how the signal picked up by a microelectrode emerges from the underlying neuronal processes, especially with regard to the distinction of the different frequency regimes, it is important to know the basic electrical properties of brain tissue. The extracellular microenvironment consists of narrow gaps between cellular processes, probably not more than 200 Å wide on average. These spaces form a complex three-dimensional mosaic filled with extracellular fluid. Theoretical considerations suggest that currents and ions spread within this fluid, but not through the cells (Robinson 1968). As a result, the resistance to electrical currents of this space depends on the detailed spatial layout of neuronal tissue, possibly resulting in an un-isotropic current flow that does not necessarily behave like that in a simple saline bath (Ranck 1963a, b; Mitzdorf 1985). Especially, from these considerations it is unclear whether cortical tissue behaves like an ohmic resistor, or whether signals of different frequencies experience frequency-dependent attenuation, i.e. whether the tissue behaves like a capacitive filter.

A frequency dependent behaviour was suggested by the fact that the activity of the slow wave measured by the EEG is largely independent of spiking responses, suggesting strong frequency-filtering properties of the tissue overlying the sources of the activity (Ajmone-Marsan 1965; Bedard et al. 2004, 2006). In addition, in extracellular unit recordings the shape and amplitude of recorded spikes depends on the spatial position of the electrode relative to the neuron (Gold et al. 2006), while slow potentials show much less sensitivity to position and correlate over large spatial distances. Since the lower frequencies of the field potentials typically correlate over larger spatial distances than the higher frequencies of the same signal (Fig. 4.1), this can be interpreted as strong evidence for the cortical tissue to behave as a capacitive filter (Destexhe et al. 1999). Such a frequency-dependent impedance spectrum could selectively attenuate electric signals of some frequencies more than those of others, for example, high-frequency spiking events more than low-frequency potentials.

To clarify whether the brain's tissue behaves like an ohmic or a capacitive medium we recently quantified the passive electrical spread of different signals in the brain in vivo. These measurements were conducted in the primary visual cortex, a typical model system for sensory processing, and on the scale of hundreds of

micrometers to several millimetres, i.e. the scale relevant to the typical functional imaging techniques such as fMRI-BOLD (Logothetis et al. 2007). At this scale, theoretical considerations suggest that the extracellular medium can be considered as largely homogenous and mostly isotropic (within the grey matter). Our results confirmed this, and more importantly, demonstrated that the cortical tissue does not behave like a capacitive filter, but acts like an ohmic resistor, attenuating signals of different frequencies in the same manner.

In detail, we measured the voltage drop across two neighbouring electrodes induced by an injected current of pre-defined frequency (Fig. 4.2). Our measurements employed a four point electrode system, allowing highly accurate and unperturbed measurements of resistance of cortical tissue in vivo. Over a wide range of current frequencies, and for all tested spatial arrangements of the electrodes, the brain's grey matter tissue behaved like an isotropic and ohmic resistor. The white matter in contrast, showed directional anisotropies, with lower resistance in one and higher resistance in the orthogonal direction. Yet, as for the grey matter, the white matter also behaved like an ohmic resistor. Altogether, our measurements clearly rejected the notion that the cortical tissue behaves like a frequency dependent filter, at least on the spatial scale relevant to the typical functional imaging applications.

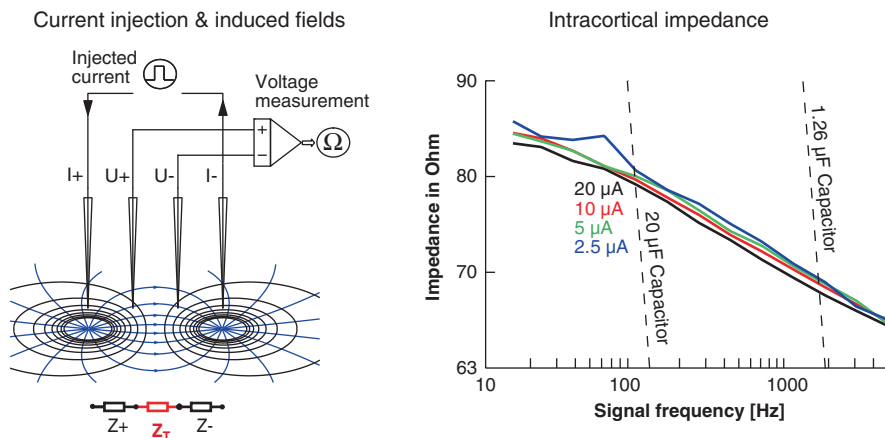


**Fig. 4.2** Impedance spectrum of cortical tissue. The *left panel* displays the schematic representation of the impedance measurement. A current of a pre-defined frequency was injected (via electrodes I+ and I-), and the voltage difference was measured across electrodes U+ and U-. From this voltage difference one can infer the cortical resistance ( $Z_T$ ) as a function of current frequency, i.e. the frequency dependent impedance spectrum. The

*right panel* displays the measured impedance values for different current strengths in cortex (*solid lines*) and for electronic capacitances. Clearly, the impedance spectrum of the cortex is nearly flat compared to that of the capacitance, suggesting that the cortex does not behave like a frequency dependent filter, but rather like an ohmic resistor. For details see (Logothetis et al. 2007)

As a consequence of this finding, one has to conclude that some of the properties of the field potentials noted above, such as the different degree of spatial correlations in different frequency bands, are not the result of passive electrical spread in the tissue. In contrast, our findings suggest that the long-range correlations of the low frequency signals, such as the theta or beta rhythms, result from properties of the generators of these signals, i.e. from the spatial patterning of the connections mediating these oscillations, and hence might be a property that is also reflected in the functional imaging signal.

#### 4.4 The Neural Correlate of the BOLD Signal

Given the distinction of the different signals that can be obtained from extracellular recordings, one can ask which signal best explains the activity patterns seen in functional imaging experiments? Or stated otherwise, which signal correlates best with the functional imaging signal? A growing body of work addresses this important question with two complementary approaches. An indirect approach asks whether both methodologies yield similar answers to a typical neuroscientific question, such as whether a certain region in the brain responds to a given stimulus. A direct approach, on the other hand, measures both signals at the same time, to directly correlate the functional imaging activation with the different signals of neuronal activity.

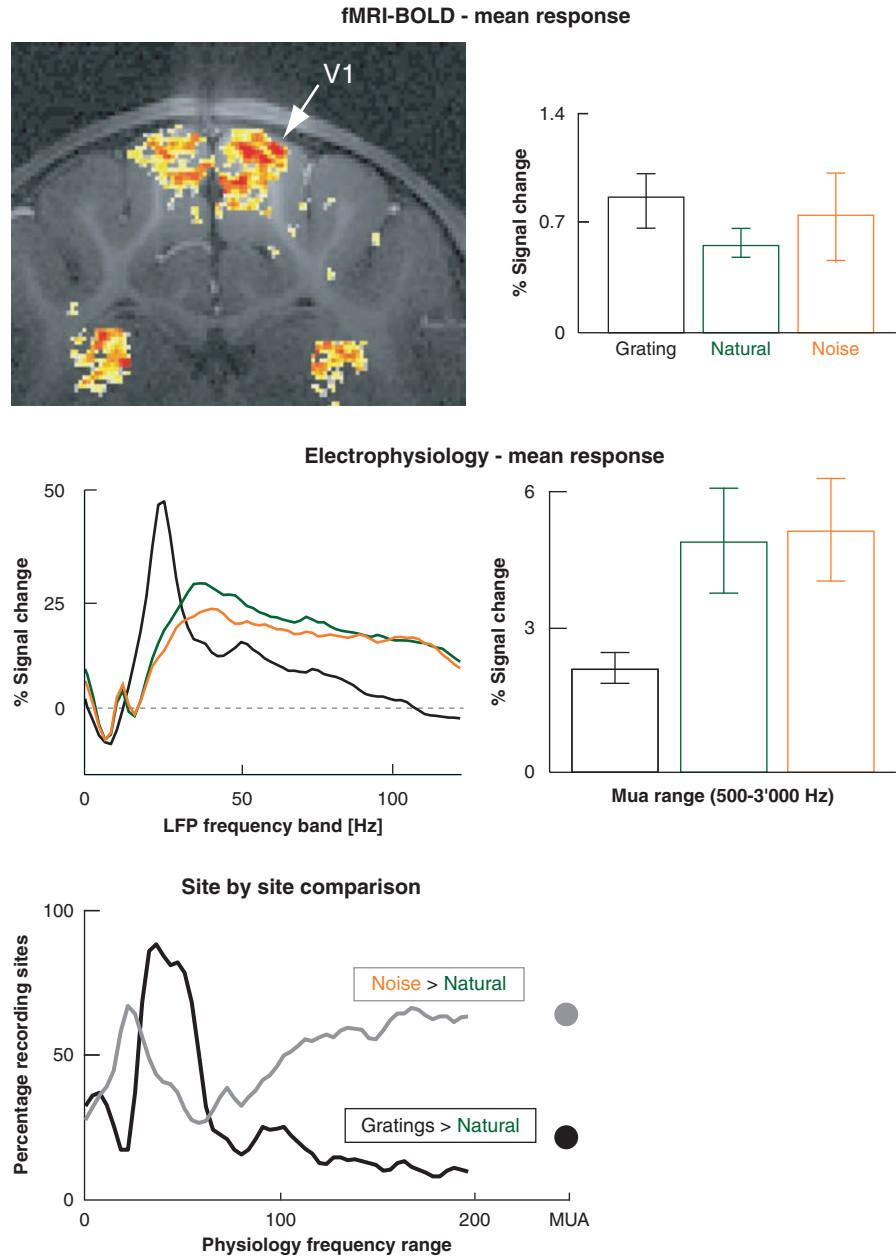
A typical example for an indirect comparison was provided by Rees et al. who compared human fMRI measurements with electrophysiological data from single-unit recordings in monkeys (Rees et al. 2000). Both datasets were obtained from the motion-specific areas of the respective species and reflected how much the respective signal changed as a function of the stimulus' motion coherence. Comparing the slope of both signals, the authors concluded that the BOLD signal was directly proportional to the average firing rate, with a constant of proportionality of approximately nine spikes per second per percentage BOLD increase. Using the same strategy, but focusing on the signal increase in primary visual cortex as a function of stimulus contrast, Heeger et al. confirmed such a linear relation of spiking activity and the BOLD signal, albeit with a smaller proportionality constant of 0.4 spikes

per percentage BOLD increase (Heeger et al. 2000). While these results suggest a good correlation of the BOLD signal and firing rates in the same cortical region, they already indicate that the details of this relation, here the constant or proportionality, depends on detailed characteristics of each area.

While the above studies focused only on firing rates, another study on primary visual cortex extended this approach to a wider range of stimuli and physiological signals (Kayser et al. 2004). Studying the cat visual system, the BOLD signal was obtained from one group of animals, while MUA and field potential responses were recorded in a second group of animals. As a metric of comparison, the authors asked which of the different electrophysiological signals would yield similar relative responses to different stimuli as found in the BOLD signal. Stated otherwise, if stimulus A elicits a stronger BOLD response than stimulus B, which of the electrophysiological signal obeys the same relation across a large fraction of recording sites sampled in the same region of interest, from which the BOLD signal is sampled (Fig. 4.3)? Overall, the MUA provided a worse match to the BOLD signal than did the LFP, although the latter showed strong frequency dependence. The best match between LFP and BOLD was obtained in the frequency range of 20–50 Hz, while slower oscillations generally showed a poor concordance with the imaging data. Noteworthy, this study also showed that the precise results of an indirect comparison can depend strongly on the specific stimuli employed: when the contrast involved grating stimuli, which elicit strong gamma band responses, a good match between the gamma band of the LFP and the BOLD was obtained. However, when the contrast involved only stimuli with less distinct activation patterns in the LFP, the correlation of LFP and BOLD also showed less frequency dependence.

While these studies only compared the average response strength of each signal, another extended the comparison to the temporal dimension and correlated the average time course obtained from fMRI with that obtained from neuronal responses (Mukamel et al. 2005). Using the human auditory cortex as a model system, these authors correlated the average fMRI responses obtained in a group of healthy subjects with intracortical recordings obtained from a group of epilepsy patients monitored for surgical treatment. While the BOLD signal again correlated well with the LFP, it showed an even stronger correlation with neuronal

**Fig. 4.3** Indirect comparison of BOLD and neurophysiological signals in cat primary visual cortex. The *upper panel* displays the average BOLD responses to the three kinds of stimuli used in this study, while the *middle panel* displays the average responses in the LFP and MUA. The *lower panel* displays the comparison between signals. This was done by counting the fraction of neurophysiological recording sites where the activity obeyed the same relations as found in the BOLD signal (noise > natural and gratings > natural). For details see (Kayser et al. 2004)



firing rates, contrasting the above result from visual cortex.

As these examples demonstrate, the results of an indirect comparison between the BOLD signal and neuronal responses may vary depending on the particular experimental paradigm and stimuli involved. In fact, an indirect comparison can only be conducted after the responses in the two measurements have each been highly averaged over trials. While such averaging will

result in a robust estimate of the stimulus related response, it will also remove the trial to trial variability of neuronal responses, the influence of the mental state and other brain state fluctuations that are not locked to the stimulus used to align the responses. As a result, one compares two “artificial” signals that do not necessarily resemble the pattern of neuronal activity seen during normal brain function. In addition, the temporal resolution of the imaging signal is often quite low, especially

in human studies, resulting in a blurred signal which cannot be adequately compared to the fast changes of neuronal activity (see also below). An indirect comparison of functional imaging and neuronal activity can hence only speak about a certain, stimulus driven aspect of the signals, but does not generalize the complex interactions of feed-forward and feed-back processing that occur during normal conditions, where each activity pattern might be unique and non-repeatable.

To overcome the limitations of these indirect comparisons, our lab examined the relationship of the BOLD signal to neural activity directly by simultaneously acquiring electrophysiological and fMRI data from the same animals. To this end we developed a 4.7 T vertical scanner environment specifically for combined neurophysiology and imaging experiments, including novel methods for interference compensation, microelectrodes and data denoising (Logothetis

et al. 2001). Our measurements showed that the fMRI-BOLD response directly reflects a local increase in neural activity as assessed by the EFP signal. For the majority of recording sites, the BOLD signal was found to be a linear but not time-invariant function of LFPs, MUA, and the firing rate of individual neurons (Fig. 4.4, upper panel). After stimulus presentation, a transient increase in power was typically observed across all LFP frequencies, followed by a lower level of activation that was maintained for the entire duration of stimulus presentation. The MUA, in contrast, often showed a more transient response, suggesting a lower correlation to the BOLD response. This hypothesis was confirmed using system identification techniques: while in general both LFPs and MUA served as good predictors for the BOLD, LFPs on average accounted for 7.6% more of the variance in the fMRI response than the MUA. This difference, albeit small, was statistically

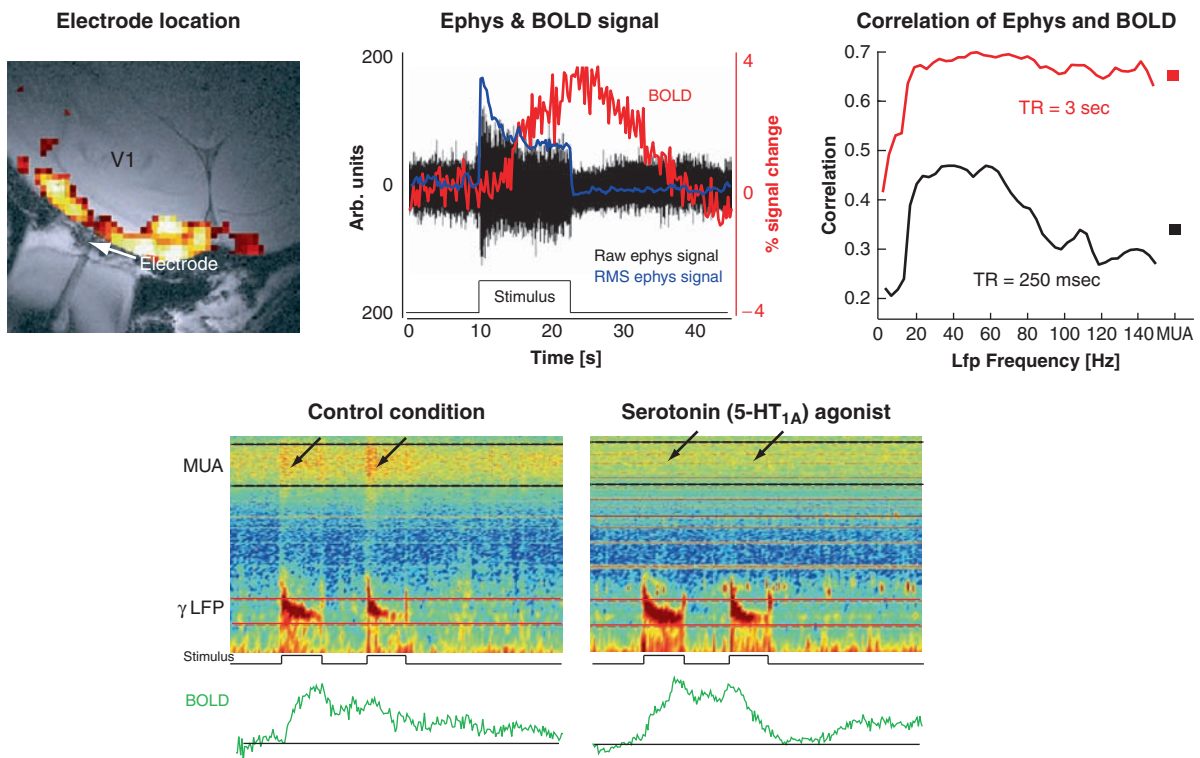


**Fig. 4.4** Simultaneous measurement of BOLD and neurophysiological signals in the monkey primary visual cortex. In the *upper row*, the *left panel* displays the electrode location in V1, together with the functional response near the electrode (*red–yellow* color code). The *middle panel* displays the simultaneously recorded BOLD and neuronal signals. The *right panel*, finally, displays the temporal correlation of both signals, once at high temporal

resolution ( $TR = 250$  ms), and once using a smoothed, low resolution signal ( $TR = 3$  s). The *lower row* displays a dissociation of BOLD, MUA and LFP induced by the application of a serotonin agonist, which suppresses the firing of pyramidal neurons. During drug application, BOLD and LFP responses persist, while the MUA response ceases. For details see (Logothetis et al. 2001; Goense and Logothetis 2008; Rauch et al. 2008)

significant across experiments. In further experiments we confirmed the same findings in alert animals, demonstrating that the correlation of BOLD and LFP holds good also during more complex, natural situations (Goense and Logothetis 2008). On the one hand, these findings confirm and extend the previous studies suggesting an analogy between spiking responses and the BOLD signal, while on the other, they reveal the strong contribution of field potentials to the BOLD signal, thereby suggesting that a direct translation of changes in the BOLD signal into changes in firing rates is misleading. Rather, we suggested on the basis of these observations, that the BOLD signal reflects the input to a local region and its local processing, as reflected by the aggregate synaptic activity, more than its output, as reflected in the spiking activity of the principal cells.

A recent study in the cat visual cortex confirmed these findings by combining optical imaging to measure hemodynamic responses with simultaneous micro-electrode recordings (Niessing et al. 2005). Along the lines of previous results, they found a frequency dependent match between the imaging signal and LFPs. Especially, frequency bands below 10Hz showed negative correlations with the imaging signal, i.e. reduced field potential during increased blood flow response. Higher frequencies, especially between 50 and 90Hz showed good correlation with the imaging signal, and importantly, stronger correlations than observed for the MUA.

It is worth noting that the exact strength of the correlation between LFP, MUA and BOLD depends on the detailed properties of the paradigm and data acquisition. Especially, the different acquisition rates for functional imaging signals and neuronal responses can have profound influences, as can easily be demonstrated (Fig. 4.4, middle panel). Starting from a BOLD signal which was acquired using a temporal resolution of 250ms, we subsequently decimated all signals to an effective temporal resolution of 3 s, the typical temporal resolution of human imaging studies. While the “fast” BOLD signal exhibits the well-established differential correlation of LFP and MUA with the BOLD, the “slow” signal shows an overall stronger correlation and less of a difference between LFP and MUA. Decreasing the temporal resolution effectively smoothes a signal and increases the coherence between LFP frequency bands; hence the increased correlation. Not surprisingly, the correlation coefficients did not increase uniformly

across frequency bands; the filtering particularly affected the high-frequency bands (>60Hz), which are typically modulated on faster timescales. As a result, the smoothing unavoidably increases the correlation of MUA to the BOLD response as well. Such simple differences of the temporal resolution of the acquired signals can explain the different degree of correlations found in ours and in indirect human studies, since the latter heavily relied on temporally smoothed signals and subject-averaged signals (Mukamel et al. 2005). To conclude, care must be taken when interpreting correlations of hemodynamic and neuronal signals, as apparent conflicts can simply arise from methodological artefacts rather than true differences.

#### 4.5 The Coupling of Synaptic Activity and CBF

A reason for the more gradual differences between LFP and MUA in their relation to the BOLD signal is that under many conditions, MUA and LFPs will vary together. In other words, in many stimulation conditions the output of any processing station in sub-cortical and early cortical structures is likely to reflect the changes of the input, and the LFP-MUA relationship will be “tight” and both will be well correlated with BOLD. Yet, this scenario might be an “exception” when generating cognitive maps during complex tasks, as in such cases, the subject’s “mental” state might be instantiated in diverse feed-forward and feed-back processes that do not necessarily increase the net-output of cortical micro-circuits. Hence, conditions might exist during which there is a dissociation of these signals, for example a condition in which an increase in local input (LFP) results in a reduction in local output activity (MUA). Clearly, such situations could reveal important insights into the different processes underlying the different signals and their mutual relations. A powerful example of such a dissociation was provided by Mathiesen et al. (Mathiesen et al. 1998; Mathiesen et al. 2000; Thomsen et al. 2004). These authors nicely exploited the synaptic organization of the cerebellar cortex, where electrical stimulation of the parallel fibres causes monosynaptic excitation of the Purkinje cells and disynaptic inhibition of the same neurons through the basket cells. This results in inhibition of the spiking activity in the Purkinje cells, while at the same time increasing the synaptic

input to these cells. Combining electrophysiological recordings with laser Doppler flowmetry to measure changes in CBF, Mathiesen et al. demonstrated a powerful dissociation of the spiking activity and the CBF. Both LFPs and CBF increased while spiking activity ceased, clearly demonstrating that increases in CBF or BOLD do not allow to make inferences about potential increases or decreases in the spiking activity of the stimulated region (Lauritzen and Gold 2003).

A similar dissociation of the imaging signal and neuronal firing rates could be seen in our studies (Logothetis et al. 2001). Often, the single or multi-unit activity showed strong response adaptation during the first few seconds, with a subsequent decay of the firing rates to baseline. In contrast to this, the BOLD signal and the LFP did persist above baseline throughout the stimulation period. As a result, during the sustained period of the stimulus only the field potential can be associated with the imaging signal, but not the spiking activity. Importantly, there was no condition or observation period during which the opposite was observed. In addition to this naturally occurring dissociation, similar situations can be induced pharmacologically. For example, the application of a serotonin receptor agonist, which causes persistent hyperpolarization of pyramidal neurons, leads to a ceasing of the MUA responses (Fig. 4.4, lower panel). However, at the very same time both the LFP and the BOLD signal still respond to visual stimulation, again demonstrating that the BOLD signal is not necessarily coupled to neuronal spiking responses (see (Rauch et al. 2008) for further results along this line).

Is the CBF signal then linearly coupled to synaptic activity? While this indeed seems to hold good under some conditions, other conditions produce a nonlinear relation between afferent input and the hemodynamic response (Mathiesen et al. 1998; Norup Nielsen and Lauritzen 2001). Especially for very low or high levels of synaptic input, the CBF response can be decoupled from the input. For example, inducing deactivation of neuronal responses by either functional deactivation or application of TTX resulted in only a small reduction in baseline CBF (Gold and Lauritzen 2002). During such instances of neuron-vascular decoupling the imaging data does not reflect all the changes in synaptic afferents, clearly highlighting the limited dynamic range of functional imaging. Such non-linear relation between synaptic activity and CBF might, for example, arise from the unequal contribution of different

receptors and channels to synaptic potentials and blood flow. For example, glutamatergic NMDA channels contribute to CBF but only little to the LFP (Hoffmeyer et al. 2007). As a result, blood flow responses might also exist in the absence of large changes in the LFP, providing strong evidence that it is not the extracellular current that causes increase in CBF, but the intracellular signalling cascades related to neurotransmitter release, uptake and recycling. Indeed, while the hemodynamic response provides supplies of glucose and oxygen, it is not the processes that require the energy that call for an increase in CBF, but rather, the processes triggered in a feed-forward manner by neurotransmitter related signalling (Lauritzen 2005).

The notion that functional imaging measures the aggregate synaptic input to a local area also resolves a number of apparently conflicting results from imaging and electrophysiological experiments. Being sensitive to the synaptic input, functional imaging “sees” modulatory lateral and feed-back projections, which might not be strong enough to induce significant changes in neuronal firing rates, but nevertheless provide a larger proportion of the total synaptic input. For example, human imaging revealed influences of spatial attention in many visual areas, including primary visual cortex. At the same time, such attentional influences have been persistently difficult to demonstrate using single-neuron recordings, or turned out to be much weaker than expected from human imaging (Luck et al. 1997; Kastner and Ungerleider 2000; Heeger and Ress 2002). Given that attentional influences are supposedly mediated by feed-back projections from higher visual and fronto-parietal regions, they might provide exactly this kind of input that is visible only using functional imaging. Along the same lines, it has been much easier to see cross-modal interactions, i.e. influences of one sensory modality on another, using functional imaging than using electrophysiology (Calvert 2001; Kayser and Logothetis 2007). For example, functional imaging demonstrated that auditory cortex can be modulated and even activated by visual or somatosensory stimuli (Kayser et al. 2007b), while the same effects are only weakly present at the level of single neuron firing rates. However, in full agreement with the above, visual modulation was well evident at the level of field potentials recorded in auditory cortex, again demonstrating a closer correspondence of the BOLD signal with field potentials than with firing rates (Kayser et al. 2008).

## 4.6 Conclusions

The hemodynamic responses characterized by functional imaging better reflect the aggregate synaptic activity and local processing that is characterized by the LFPs, rather than providing information about the typical firing rates in the same region. This partly results from the mechanisms that drive increases in blood flow, which reside upstream from the axosomatic level and near the synaptic-dendritic level. The collective findings of many studies provide good evidence for the notion that functional imaging reflects the input into a local region but not necessarily the output of the same. Under many normal conditions, the input and output of a local region will be related, and hence functional imaging will provide information about the typical neuronal firing rates in the same region. As a result of this sensitivity to synaptic input, functional imaging signals are more susceptible to modulatory feed-back input, which often might provide only a minor contribution to the response strength of large principal neurons. However, for a priori and most experimental conditions, it is unclear what relationship to expect between in- and output, and hence feed-forward and feed-back related activations cannot be distinguished. As a result, it can sometimes be misleading, if not dangerous, to make direct inferences from imaging results about the underlying neuronal processes. Especially for applications with immediate consequences, such as clinical diagnostics and surgical planning, it seems prudent to establish well defined paradigms in which the neural correlates of the imaging signal have been validated using combined electrophysiological and imaging approaches.

## References

- Adrian ED, Zotterman Y (1929) The impulses produced by sensory nerve endings, Part 2. The response of a single endorgan. *J Physiol* 61:151–171
- Ajmone-Marsan C (1965) Electrical activity of the brain: slow waves and neuronal activity. *Israel J Med Sci* 1:104–117
- Bedard C, Kroger H, Destexhe A (2004) Modeling extracellular field potentials and the frequency-filtering properties of extracellular space. *Biophys J* 86:1829–1842
- Bedard C, Kroger H, Destexhe A (2006) Model of low-pass filtering of local field potentials in brain tissue. *Phys Rev E Stat Nonlin Soft Matter Phys* 73:051911
- Buchwald JS, Grover FS (1970) Amplitudes of background fast activity characteristic of specific brain sites. *J Neurophysiol* 33:148–159
- Buchwald JS, Halas ES, Schramm S (1966) Relationships of neuronal spike populations and EEG activity in chronic cats. *Electroencephalogr Clin Neurophysiol* 21:227–238
- Buzsaki G, Bickford RG, Ponomareff G, Thal LJ, Mandel R, Gage FH (1988) Nucleus basalis and thalamic control of neocortical activity in the freely moving rat. *J Neurosci* 8:4007–4026
- Calvert GA (2001) Crossmodal processing in the human brain: insights from functional neuroimaging studies. *Cereb Cortex* 11:1110–1123
- Destexhe A, Contreras D, Steriade M (1999) Spatiotemporal analysis of local field potentials and unit discharges in cat cerebral cortex during natural wake and sleep states. *J Neurosci* 19:4595–4608
- Freeman W (1975) Mass action in the nervous system. Academic, New York
- Fried I, MacDonald KA, Wilson CL (1997) Single neuron activity in human hippocampus and amygdala during recognition of faces and objects. *Neuron* 18:753–765
- Fromm GH, Bond HW (1964) Slow changes in the electrocorticogram and the activity of cortical neurons. *Electroencephalogr Clin Neurophysiol* 17:520–523
- Fromm GH, Bond HW (1967) The relationship between neuron activity and cortical steady potentials. *Electroencephalogr Clin Neurophysiol* 22:159–166
- Goense J, Logothetis N (2008) Neurophysiology of the BOLD fMRI signal in awake monkeys. *Curr Biol* 18:631–640
- Gold C, Henze DA, Koch C, Buzsaki G (2006) On the origin of the extracellular action potential waveform: a modeling study. *J Neurophysiol* 95:3113–3128
- Gold L, Lauritzen M (2002) Neuronal deactivation explains decreased cerebellar blood flow in response to focal cerebral ischemia or suppressed neocortical function. *Proc Natl Acad Sci U S A* 99:7699–7704
- Gray CM, König P, Engel AK, Singer W (1989) Oscillatory responses in cat visual cortex exhibit inter-columnar synchronization which reflects global stimulus properties. *Nature* 338:334–337
- Heeger DJ, Ress D (2002) What does fMRI tell us about neuronal activity? *Nat Rev Neurosci* 3:142–151
- Heeger DJ, Huk AC, Geisler WS, Albrecht DG (2000) Spikes versus BOLD: what does neuroimaging tell us about neuronal activity? *Nat Neurosci* 3:631–633
- Hoffmeyer HW, Enager P, Thomsen KJ, Lauritzen MJ (2007) Nonlinear neurovascular coupling in rat sensory cortex by activation of transcallosal fibers. *J Cereb Blood Flow Metab* 27:575–587
- Juergens E, Guettler A, Eckhorn R (1999) Visual stimulation elicits locked and induced gamma oscillations in monkey intracortical- and EEG-potentials, but not in human EEG. *Exp Brain Res* 129:247–259
- Kastner S, Ungerleider LG (2000) Mechanisms of visual attention in the human cortex. *Annu Rev Neurosci* 23:315–341
- Kayser C, Logothetis NK (2007) Do early sensory cortices integrate cross-modal information? *Brain Struct Funct* 212:121–132
- Kayser C, Petkov CI, Logothetis NK (2007a) Tuning to sound frequency in auditory field potentials. *J Neurophysiol* 98:1806–1809

- Kayser C, Petkov CI, Logothetis NK (2008) Visual modulation of neurons in auditory cortex. *Cereb Cortex* 18:1560–1574. doi:10.1093/cercor/bhm187
- Kayser C, Petkov CI, Augath M, Logothetis NK (2007b) Functional imaging reveals visual modulation of specific fields in auditory cortex. *J Neurosci* 27:1824–1835
- Kayser C, Kim M, Ugurbil K, Kim DS, Konig P (2004) A comparison of hemodynamic and neural responses in cat visual cortex using complex stimuli. *Cereb Cortex* 14:881–891
- Kreiman G, Koch C, Fried I (2000) Category-specific visual responses of single neurons in the human medial temporal lobe. *Nat Neurosci* 3:946–953
- Lauritzen M (2005) Reading vascular changes in brain imaging: is dendritic calcium the key? *Nat Rev Neurosci* 6:77–85
- Lauritzen M, Gold L (2003) Brain function and neurophysiological correlates of signals used in functional neuroimaging. *J Neurosci* 23:3972–3980
- Legatt AD, Arezzo J, Vaughan HG Jr (1980) Averaged multiple unit activity as an estimate of phasic changes in local neuronal activity: effects of volume-conducted potentials. *J Neurosci Methods* 2:203–217
- Logothetis NK (2002) The neural basis of the blood-oxygen-level-dependent functional magnetic resonance imaging signal. *Philos Trans R Soc Lond B Biol Sci* 357:1003–1037
- Logothetis NK, Wandell BA (2004) Interpreting the BOLD signal. *Annu Rev Physiol* 66:735–769
- Logothetis NK, Kayser C, Oeltermann A (2007) In vivo measurement of cortical impedance spectrum in monkeys: implications for signal propagation. *Neuron* 55:809–823
- Logothetis NK, Pauls J, Augath M, Trinath T, Oeltermann A (2001) Neurophysiological investigation of the basis of the fMRI signal. *Nature* 412:150–157
- Luck SJ, Chelazzi L, Hillyard SA, Desimone R (1997) Neural mechanisms of spatial selective attention in areas V1, V2, and V4 of macaque visual cortex. *J Neurophysiol* 77:24–42
- Mathiesen C, Caesar K, Lauritzen M (2000) Temporal coupling between neuronal activity and blood flow in rat cerebellar cortex as indicated by field potential analysis. *J Physiol* 523(Pt 1):235–246
- Mathiesen C, Caesar K, Akgoren N, Lauritzen M (1998) Modification of activity-dependent increases of cerebral blood flow by excitatory synaptic activity and spikes in rat cerebellar cortex. *J Physiol* 512(Pt 2):555–566
- Mitzdorf U (1985) Current source-density method and application in cat cerebral cortex: investigation of evoked potentials and EEG phenomena. *Physiol Rev* 65:37–100
- Mitzdorf U (1987) Properties of the evoked potential generators: current source-density analysis of visually evoked potentials in the cat cortex. *Int J Neurosci* 33:33–59
- Mosso A (1881) Ueber den Kreislauf des Blutes im Menschlichen Gehirn. von Veit, Leipzig
- Mukamel R, Gelbard H, Arieli A, Hasson U, Fried I, Malach R (2005) Coupling between neuronal firing, field potentials, and fMRI in human auditory cortex. *Science* 309:951–954
- Niessing J, Ebisch B, Schmidt KE, Niessing M, Singer W, Galuske RA (2005) Hemodynamic signals correlate tightly with synchronized gamma oscillations. *Science* 309:948–951
- Norup Nielsen A, Lauritzen M (2001) Coupling and uncoupling of activity-dependent increases of neuronal activity and blood flow in rat somatosensory cortex. *J Physiol* 533:773–785
- Ogawa S, Menon RS, Kim SG, Ugurbil K (1998) On the characteristics of functional magnetic resonance imaging of the brain. *Annu Rev Biophys Biomol Struct* 27:447–474
- Ranck JB (1963a) Analysis of specific impedance or rabbit cerebral cortex. *Exp Neurol* 7:153–174
- Ranck JB (1963b) Specific impedance of rabbit cerebral cortex. *Exp Neurol* 7:144–152
- Rauch A, Rainer G, Logothetis N (2008) The effect of a serotonin induced dissociation between spiking and perisynaptic activity on BOLD fMRI. *PNAS* 108:6759–6764
- Rees G, Friston K, Koch C (2000) A direct quantitative relationship between the functional properties of human and macaque V5. *Nat Neurosci* 3:716–723
- Robinson DA (1968) The electric properties of metal microelectrodes. *Proc IEEE* 56:1065–1071
- Roy CS, Sherrington CS (1890) On the regulation of the blood supply of the brain. *J Physiol Lond* 11:85–108
- Steriade M, Amzica F (1994) Dynamic coupling among neocortical neurons during evoked and spontaneous spike-wave seizure activity. *J Neurophysiol* 72:2051–2069
- Steriade M, Amzica F, Neckelmann D, Timofeev I (1998) Spike-wave complexes and fast components of cortically generated seizures. II. Extra- and intracellular patterns. *J Neurophysiol* 80:1456–1479
- Stone J (1973) Sampling properties of microelectrodes assessed in the cat's retina. *J Neurophysiol* 36:1071–1079
- Thomsen K, Offenhauser N, Lauritzen M (2004) Principal neuron spiking: neither necessary nor sufficient for cerebral blood flow in rat cerebellum. *J Physiol* 560:181–189
- Towe AL, Harding GW (1970) Extracellular microelectrode sampling bias. *Exp Neurol* 29:366–381

## 5.1 Introduction

In recent years, functional magnetic resonance imaging (fMRI) has become a widely used approach for neuroscience. However, this method has the potential to be improved with regard to both spatial and temporal resolution. The blood-oxygenation level-dependent contrast (BOLD) represents signal changes in T2 or T2\* weighted images. These sequences are presumed to be well suited to high magnetic field strength, as fMRI sequences benefit from higher signal-to-noise ratio (SNR) and higher signal in BOLD contrast images (Vaughan et al. 2001). However, their sensitivity to susceptibility also causes problems, e.g. in-plane dephasing and signal dropouts near tissue-air boundaries.

To achieve greater insights into brain function, high-field fMRI has been applied in some studies to attain higher spatial resolutions (Duong et al. 2003; Pfeuffer et al. 2002a). These studies focused on high-resolution images which can be acquired rapidly and with good temporal resolution. Additionally, the signal increase advantage in high-field MRI has been studied (Pfeuffer et al. 2002b). Nearly all of these studies, therefore, accepted restrictions in the field-of-view and the number of slices for 7 T imaging and avoided areas near tissue-air boundaries. For broader application and for analysing cognitive functions, however, a more extended coverage of the brain is needed to reveal network activation involving multiple areas. This chapter

will give insights into the pros and cons of high- and ultra-high-field fMRI and into ongoing developments to overcome the restrictions referred to and improve the benefits.

## 5.2 Benefits and Limitations of High- and Ultra-High-Field MRI

The introduction of ultra-high-field MRI systems has brought MRI technology closer to the physical limitations, and greater development effort is required to achieve appropriate sequences and images. 3 T MRI systems are high-field systems maintaining a relatively high comfort level for the user similar to 1.5 T MRI systems (Alvarez-Linera 2008; Norris 2003). Theoretically, the SNR at high-field MRI should, according to the Boltzmann equation, show a linear increase with increasing magnetic field strength. But, the interactions of the magnetic field and other influencing factors, e.g. relaxation times, radio frequency (RF) pulses and coils performance during image acquisition, are very complex. One important factor is the change in RF pulses in higher magnetic field strengths. Changing the field strength from 1.5 to 3 T results in a fourfold increase in the required energy, resulting in an increase in specific absorption rate (SAR) (Ladd 2007). The increase in SAR leads to limitations in image acquisition, as the absorption of energy in the tissue cannot be allowed to exceed certain thresholds. Therefore, restrictions in the number of slices and achieving homogenous excitation of the nuclei increase with higher field strength.

Current 3 T scanners have been significantly improved since their introduction, especially with regard to coil developments; therefore, today the advantages, such as

---

E. R. Gizewski  
Department of Diagnostic and Interventional Radiology  
and Neuroradiology, University Hospital Essen,  
Hufelandstrasse 55, 45127 Essen, Germany  
e-mail: elke.gizewski@uni-due.de



**Fig. 5.1** 7 T MR scanner with a bore of 60cm and a length of 3.50m. The MR is surrounded by 425 tonnes of steel. The *upper figure* shows a person before positioned head first into the scanner. The *second figure* shows a person head first in the scanner with the head in the iso-centre, the feet covered with a sheet

faster acquisition time and/or higher resolution, are greater than the disadvantages, such as higher costs and in some cases, instability in running the systems (Scheef et al. 2007). For higher field strength, e.g. 7 T, the developments are still in the process of improvement.

Another important point is the magnet design. Especially at 7 T, the magnet is very long compared to a typical 1.5 T magnet. The bore is 60cm as at 1.5 T, but due to the length gives a narrow impression (Fig. 5.1). Therefore, anxiety is again a problem for imaging. A final important point is the contraindication of every metal implant at 7 T. Even non-ferromagnetic material can be influenced due to induced electrical currents. When located in the centre of imaging, such material, e.g. a surgical calotte fixation, would lead to disturbing artefacts.

### 5.3 Special Aspects of High-Field fMRI

BOLD contrast images are normally acquired using a gradient echo-planar technique (EPI). Optimal sequence design has to take into account echo times and sampling period; the variation in sensitivity between tissues with different baseline  $T2^*$ , the effects of physiological noise, and non-exponential signal decay are relevant influencing factors (Gowland and Bowtell 2007). In high-field fMRI the optimal TE is shorter than at 1.5 T. The shortening of  $T2^*$  is proportional to the magnetic field (Okada et al. 2005). The TE used in optimized 3 T fMRI imaging is between 30 and 35 ms (Preibisch et al. 2008). The optimum TE for 7 T has been reported to be around 25 ms in focused fMRI in the occipital cortex (Yacoub et al. 2001).

As mentioned above, the SNR should increase with the magnetic field strength. Some studies have revealed a BOLD signal increase up to fivefold in 7 T fMRI compared to 1.5 T BOLD signals. Studies focussing on an increase in resolution and small field-of-view (Pfeuffer et al. 2002c) could reveal a higher signal increase at 7 T than studies with whole-brain coverage (Gizewski et al. 2007). This variability can be explained taking into account the above mentioned factors influencing the SNR. Additionally, the impact of these factors increase with higher field strength, resulting in a greater variability of BOLD signal between different measurements and subjects at 7 T compared to 1.5 T. The relatively wide range of relative BOLD signal changes compared to 1.5 T and even 3 T may also be explained by the difficulty in achieving a uniform static magnetic field shim and a uniform RF excitation field at 7 T. The fMRI experiments at 7 T are therefore more dependent on field inhomogeneities, and these have to be taken into account during image analysis.

The BOLD effect at higher field strength increases less in vessels larger than the voxel size and is thus more pronounced in vessels smaller than the voxel size. By using smaller voxels at higher field strength compared to 1.5 T, the BOLD signal can become more specific and reliable (Shimada et al. 2008; Zou et al. 2005). Therefore, the signal changes should be more closely linked to the cortical activity. With the increasing signal and enhanced stability of the BOLD signal at higher field strength, the repetition of events can be reduced. At ultra-high fields even single events can give reliable BOLD signal.

A main problem at high field strength is the achievement of good response functions even in areas suffering from, for e.g., in-plane dephasing and signal dropouts near tissue-air boundaries. A further central problem is the increasing chemical shift, proportional to the magnetic field strength. All these limitations lead to errors when reading the echo. Therefore, the optimization of scanning parameters and coil construction is of much greater importance than in routine 1.5 T scanners. The following paragraphs will give some examples of developments in ultra-high-field BOLD imaging.

The shimming, especially at 7 T, should be performed manually by the user. Although the standard shimming algorithm may be used, multiple repetitions should be performed with close verification of the result before starting the EPI sequence. At higher field strengths, a per slice shimming may be necessary to account for increased  $B_0$  distortions. Additionally, the phase correction parameters can be calculated slice by slice using three non-phase-encoded navigator echoes before the EPI readout (Heid 1997).

Nevertheless, there are increased susceptibility artefacts at 3 and 7 T compared to 1.5 T. Significant improvement can be reached by using more advanced head coils than circularly polarized (CP) coils. Multi-channel coils allow application of parallel acquisition techniques (Mirrashed et al. 2004). Multiple channels provide further increases in SNR and, coupled with parallel imaging, reduce artefacts e.g. due to susceptibility differences near tissue-air boundaries as is known from experience at 1.5 T. It has been demonstrated that the use of parallel imaging at 3 T results in an increase of BOLD signal depending on the employed parallel imaging method and its implementation (Preibisch et al. 2008). At 7 T the coil equipment has to be newly developed, as the 7 T MRI systems require combined transmit and receive (t/r) coils. First t/r coils were CP designs which did not enable parallel imaging techniques, but multi-channel designs with up to 32 receiver channels are now available.

A further disadvantage at high field could be a restriction in the number of slices due to SAR restrictions and inhomogeneous resolution over the brain (Wiggins et al. 2005). Therefore, the coils and sequences have to be chosen depending on the paradigms to be applied. Again, parallel imaging can be useful for reducing the RF load on the tissue and enabling more slices. It was shown that at 3 T a reduction factor of 2

in parallel imaging can be used with only little penalty with regard to sensitivity (Preibisch et al. 2008).

Some problems in image distortion can be solved using spin-echo instead of gradient-echo EPI sequences, but they are not routinely used. The blood contribution that dominates Hahn spin-echo (HSE)-based BOLD contrast at low magnetic fields and degrades specificity is highly attenuated at high fields because the apparent  $T_2$  of venous blood in an HSE experiment decreases quadratically with increasing magnetic field. In contrast, the HSE BOLD contrast increases supralinearly with the magnetic field strength. Yacoub et al. report the results of detailed quantitative evaluations of HSE BOLD signal changes for functional imaging in the human visual cortex at 4 and 7 T (Yacoub et al. 2003). They used the increased SNR of higher field strengths and surface coils to avoid partial volume effects. Furthermore, they could show that high-resolution acquisitions lead to a CNR increase with voxel sizes  $< 1 \text{ mm}^3$ . It was concluded that the high-field HSE fMRI signals originated largely from the capillaries, and that the magnitude of the signal changes associated with brain function reached sufficiently high levels at 7 T to make it a useful approach for mapping on the millimetre to submillimetre spatial scale.

The problem that thermal and physiological noise dominates the SNR of the fMRI time-course at high spatial resolutions at high field strengths can be a prominent issue if a high-resolution matrix and a thin slice thickness are used. The problem is acquiring data at lower resolution, which is then dominated by physiological noise. A solution would be to acquire data at high resolution and smooth the data back to the desired lower resolution. In such cases the physiological noise can limit some benefits of high-field acquisition, since increases in image SNR produce only small increases in time-course SNR if the 1.5 T resolution is used (Triantafyllou et al. 2006). But, some problems even at 3 T remain; low frequency periodic fluctuations were found to have increased as well as the time-dependent increase in noise, especially in long EPI sessions (Shimada et al. 2008).

Normally, gradient-echo EPI sequences are used for fMRI, especially for clinical applications. Therefore, the optimization of EPI sequences and reduction in artefacts is of great importance. Multi-channel coils are basically an array of surface coils with higher signal in the periphery than in the centre. At higher field

strength, the signal even in the centre of multi-channel coils is higher compared to 1.5 T. Results obtained at 3 T using a combination of multi-channel coil and parallel imaging showed that BOLD sensitivity improved by 11% in all brain regions, with larger gains in areas typically affected by strong susceptibility artefacts. The use of parallel imaging markedly reduces image distortion, and hence the method should find widespread application in functional brain imaging (Poser et al. 2006).

In summary, an extended optimization of sequences and new coil developments, especially new transmit-receive coils, will be necessary to exploit all of the outstanding possibilities and advantages of ultra-high-field MRI (Scheef et al. 2007).

#### 5.4 Ultra-High Field fMRI and Possible Clinical Applications

3 T fMRI is increasingly used in clinical and experimental studies in most countries. In addition to developments in coil technology, 3 T MRI provides an excellent solution for higher resolution and/or signal changes with an acceptable increase in susceptibility artefacts (Alvarez-Linera 2008).

3 T fMRI has been used in a variety of experiments so far. The initial dip in the motor and visual areas was examined simultaneously using a visually-guided finger-tapping paradigm (Yacoub and Hu 2001). Other experiments could show that fMRI measurements quantifying the strength of activity and centres of mass in response to tasks offer sensitive measurements of change over repeated imaging sessions. Therefore, fMRI at high field strength can be used for serial investigations of individual participants using simple motor and cognitive tasks in a simple block design (Goodyear and Douglas 2008). These results are very promising in respect to advanced clinical use of high-field fMRI. At 1.5 T, one main problem is the restriction in obtaining individual activation maps due to lack of sensitivity and specificity. This can be overcome with the more stable hemodynamic response function and higher BOLD signal at 3 T and, even more at higher field strength, e.g. 7 T.

The first 7 T studies were performed to demonstrate the feasibility of BOLD fMRI using EPI and to characterize the BOLD response in humans at 7 T using visual stimulation. These results indicate that fMRI can be

reliably performed at 7 T and that at this field strength both the sensitivity and spatial specificity of the BOLD response are increased. These studies suggest that ultra-high-field MR systems are advantageous for functional mapping in humans (Yacoub, Shmuel et al. 2001).

Decreasing the voxel size at high field strength and simultaneously obtaining high temporal resolution is a major challenge and is mainly limited by gradient performance. Pfeuffer et al. used an optimized surface coil setup for zoomed functional imaging in the visual cortex (Pfeuffer et al. 2002c). With a single-shot acquisition at submillimetre resolution ( $500 \times 500 \text{ mm}^2$ ) in the human brain and a high temporal resolution of 125 ms, activation of single-trial BOLD responses were obtained. Therefore, the possibilities of event-related functional imaging in the human brain were expanded.

Further experiments have addressed retinotopic maps at 7 T. An identification of visual areas in the occipito-parietal cortex was found (Hoffmann et al. 2009). It was demonstrated that the mean coherence increased with magnetic field strength and with voxel size. At 7 T, the occipital cortex could be sampled with high sensitivity in a single short session at high resolution. Therefore, retinotopic mapping at 7 T opens the possibility of detailed understanding of the cortical visual field representations and of their plasticity in visual system pathologies.

For clinical use, the activation in eloquent areas such as the sensory-motor areas and coverage of larger brain volumes are of great importance. One study at 7 T revealed activation in all sensory-motor areas at 7 T: SI, MI, SII, SMA, thalamus, and contralateral cerebellar areas involved in sensorimotor processing (Gizewski et al. 2007). Even when using a t/r CP coil, the signal change was a factor of 2–5 higher at 7 T than at 1.5 T. At 7 T, susceptibility artefacts were present especially in the basal brain structures, but a well-fitted response curve could be detected in all sensory-motor areas at 7 T, even in areas suffering from susceptibility such as the cerebellum (Fig. 5.2). In contrast to the results at 1.5 T, thalamic activation was found in all subjects and revealed an excellent response function. Even single block analyses at 7 T revealed similar or even higher response strength than multi-block measurements at 1.5 T. These results indicate that fMRI can be robustly performed at 7 T covering the whole brain using a t/r CP head coil with higher signal and increased stability of the hemodynamic response curve. The excellent response functions and signal change elevations shown in this

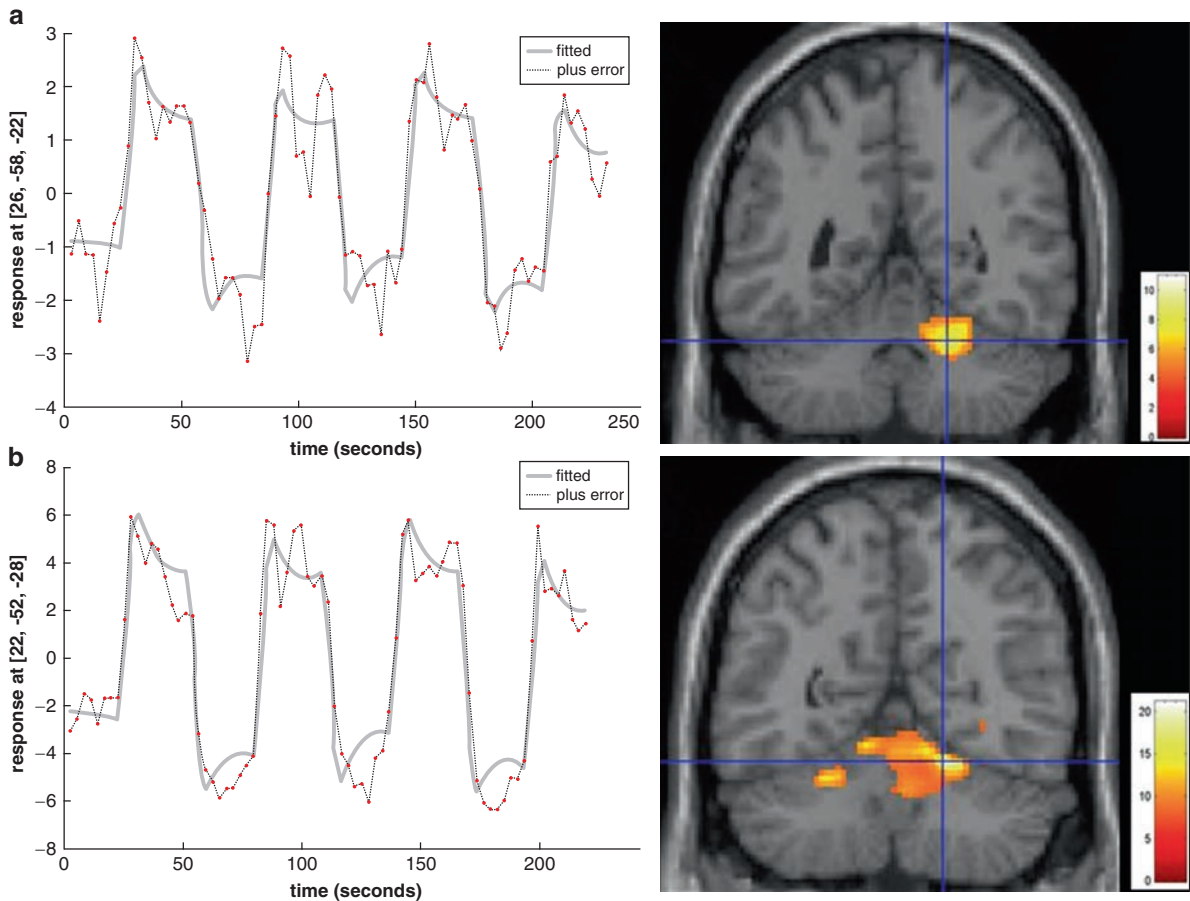


**Fig. 5.2** (a) Plot of fitted response function at the main cluster in the cerebellar sensory-motor areas at 1.5 T (representative subject). Statistical parametric maps of activation within all subjects performing the finger tapping task compared with rest period at 1.5 T. Task-related increase in MR signal is superimposed on coronal section of a 3D T1-weighted standard brain. Statistically corrected threshold is  $p < 0.05$ . Results show main activation in

cerebellum. (b) Plot of fitted response function at the main cluster in the cerebellar sensory-motor areas at 7 T (representative subject). Statistical parametric maps of activation within all subjects performing the finger tapping task compared with rest period at 7 T. Statistically corrected threshold is  $p < 0.005$ . Results show main activation in cerebellum

study using a well-established, simple sensory-motor paradigm indicate that even in susceptibility problematic brain regions ultra high-field fMRI is possible.

The signal increase in ultra-high-field fMRI depends on many factors, not only on the magnetic field strength. Some studies have revealed a signal increase of up to fivefold using imaging parameters focused on increased spatial resolution and small field-of-view (Pfeuffer et al. 2002a, b). The sensitivity is somewhat constrained by the SNR characteristics if a CP head coil is used in conjunction with standard voxel sizes from 1.5 T. It has been shown that a reduction in voxel size leads to an improvement in time series SNR through a decrease in physiological noise (Triantafyllou et al. 2005). The relatively small BOLD changes in

certain brain areas in the CP study might be explained by this effect, but the use of larger voxels allows whole-brain coverage.

It is likely that many future studies will not strive for exceptional resolution in one area of the brain but be targeted at analysing complex networks. Especially cognitive functions will require more slices and coverage of extended brain areas. Furthermore, some interesting structures such as the hippocampal region can, as in the cerebellum, suffer from signal dropouts near tissue-air boundaries.

In respect to more direct clinical application, first experiments with a speech paradigm could reveal the advantages of 7 T fMRI combined with an eight-channel head coil and a parallel acquisition technique

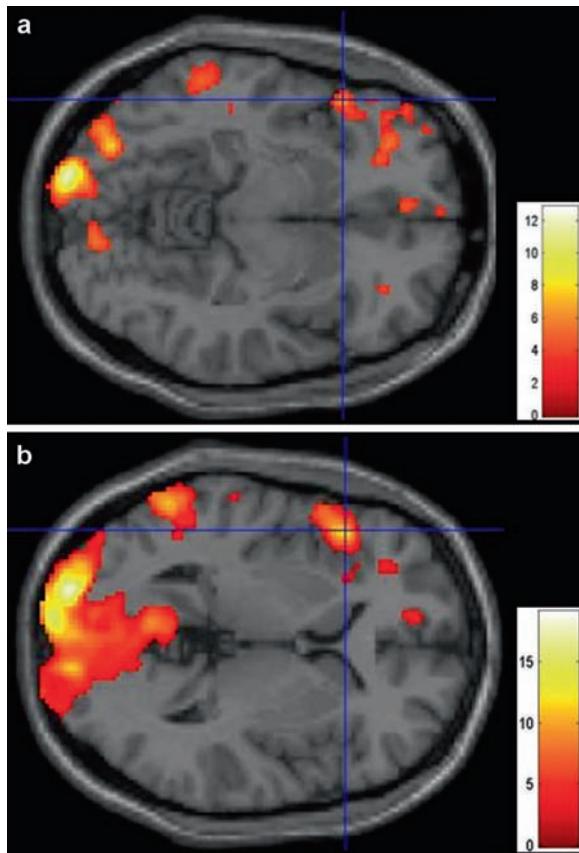


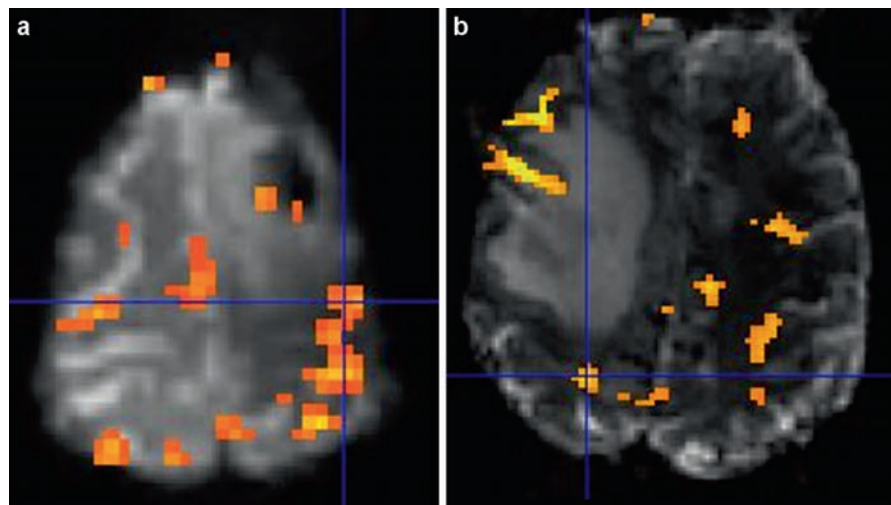
**Fig. 5.3** Statistical parametric maps of activation within all subjects performing the verb generation task compared with rest period at 1.5 T (a) and 7 T (b) superimposed on a standard brain in transverse orientation. Statistically corrected threshold is  $p < 0.005$ . Activated areas of Broca and Wernicke regions are shown at both field strengths but with more extended clusters and higher signal change at 7 T

(Fig. 5.3). Even using the parallel acquisition technique, an increase in BOLD signal could be obtained and a more extended activation and detection of lateralization could be found. Furthermore, the application of parallel imaging led to a significant reduction of artefacts (Fig. 5.4). Therefore, a reliable co-registration of high-resolution structural images with the EPI images could be performed. Figure 5.5 shows a patient with a cavernoma scanned pre-surgically at 1.5 T (a) and 7 T (b). The speech paradigm was a verb generation task in both measurements in a block design. The activation maps are superimposed on susceptibility-weighted images (SWI) at 1.5 and 7 T. In addition to the higher BOLD signal and the more extended activation at 7 T, the higher spatial resolution of the structural images confers further benefit for surgical planning.

Further studies will have to also address cognitive functions involving more challenging brain areas. One recent study evaluated BOLD responses due to visual sexual stimuli at 7 T (Walter et al. 2008). This study could demonstrate that fMRI at high fields provides an ideal tool to investigate functional anatomy of subcortical structures. Furthermore, due to an increased SNR, functional scans of short duration can be acquired at high resolution.

Besides fundamental experimental interests, e.g. for cognitive studies, clinical indications of 7 T fMRI can be imagined. Pre-surgical fMRI in patients with brain tumours could benefit from either higher resolution or faster imaging. Even patients impaired with respect to motor function are for the most part able to perform a short finger movement sufficient for a single block examination.

**Fig. 5.4** EPI images are very sensitive for susceptibility artefacts using a t/r CP head coil (a). Parallel acquisition techniques can reduce these artefacts, especially at high-field MRI (b). Both images show patients with a brain tumour performing a finger-tapping task compared to rest. Using the parallel imaging technique also allows the acquisition of a higher resolution (matrix  $128 \times 128 \text{ m}^2$  in this case) than the sequence applied with the CP head coil



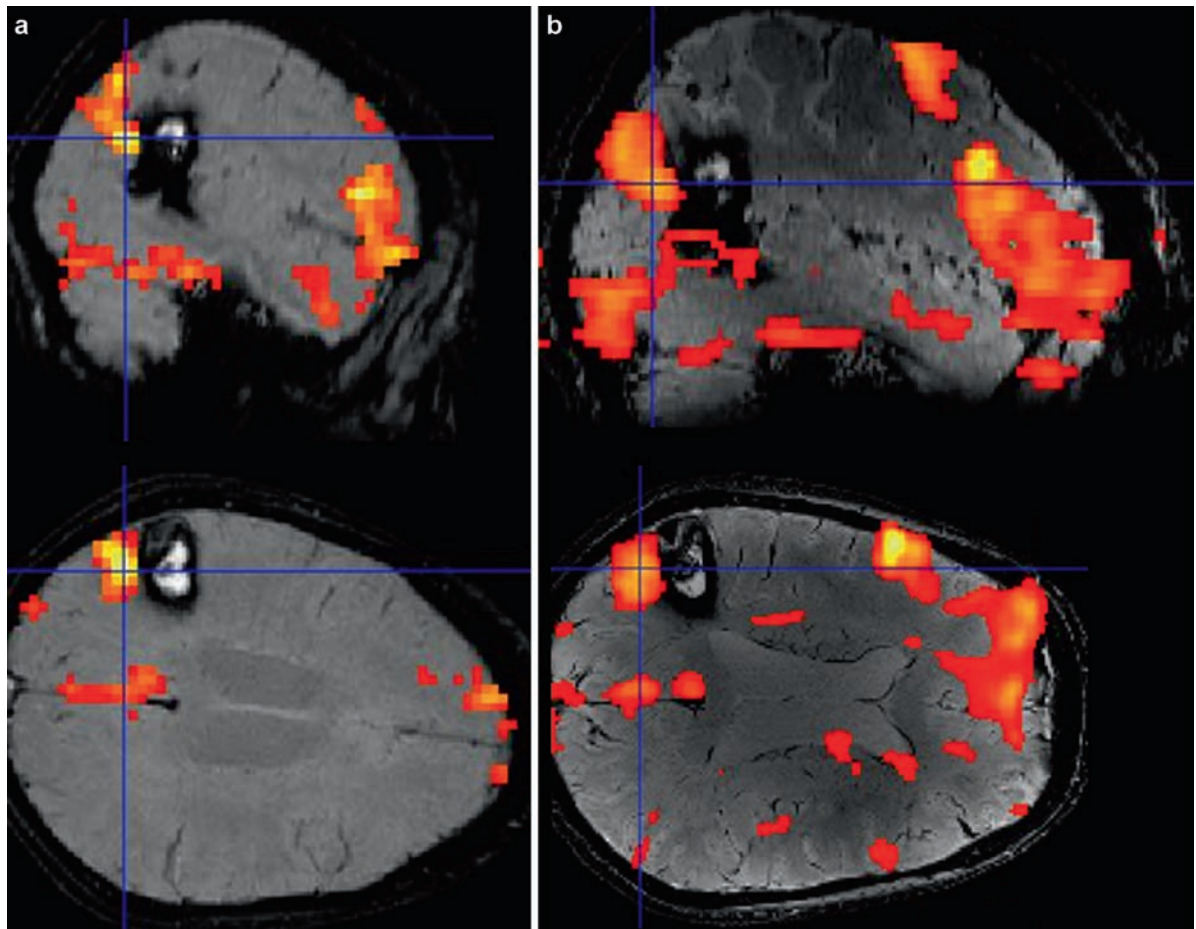


**Fig. 5.5** Statistical parametric maps of activation within one patient performing the verb generation task compared with rest period at 1.5 T (**a**) and 7 T (**b**) superimposed on SWI images. Statistically corrected threshold is  $p < 0.005$ . Activated areas of Broca and Wernicke regions are shown at both field strengths but

with more extended clusters and higher signal change at 7 T. Furthermore, the structural images have a higher in-plane resolution at 7 T with enhanced tumour-brain differentiation and superior depiction of the inner structure of the cavernoma

## References

- Alvarez-Linera J (2008) 3T MRI: advances in brain imaging. *Eur J Radiol* 67(3):415–426
- Duong TQ, Yacoub E et al (2003) Microvascular BOLD contribution at 4 and 7 T in the human brain: gradient-echo and spin-echo fMRI with suppression of blood effects. *Magn Reson Med* 49(6):1019–1027
- Gizewski ER, de Greiff A et al (2007) fMRI at 7 T: whole-brain coverage and signal advantages even infratentorially? *Neuroimage* 37(3):761–768
- Goodyear BG, Douglas EA (2008) Minimum detectable change in motor and prefrontal cortex activity over repeated sessions using 3T functional MRI and a block design. *J Magn Reson Imaging* 28(5):1055–1060
- Gowland PA, Bowtell R (2007) Theoretical optimization of multi-echo fMRI data acquisition. *Phys Med Biol* 52(7): 1801–1813
- Heid O (1997) Robust EPI phase correction. In: *Proceedings of the ISMRM, Vancouver*
- Hoffmann MB, Stadler J et al (2009) Retinotopic mapping of the human visual cortex at a magnetic field strength of 7T. *Clin Neurophysiol* 120(1):108–116
- Ladd ME (2007) High-field-strength magnetic resonance: potential and limits. *Top Magn Reson Imaging* 18(2): 139–152
- Mirashed F, Sharp JC et al (2004) High-resolution imaging at 3T and 7T with multiring local volume coils. *MAGMA* 16(4): 167–173
- Norris DG (2003) High field human imaging. *J Magn Reson Imaging* 18(5):519–529
- Okada T, Yamada H et al (2005) Magnetic field strength increase yields significantly greater contrast-to-noise ratio increase: measured using BOLD contrast in the primary visual area. *Acad Radiol* 12(2):142–147
- Pfeuffer J, Adriany G et al (2002a) Perfusion-based high-resolution functional imaging in the human brain at 7 Tesla. *Magn Reson Med* 47(5):903–911
- Pfeuffer J, Van de Moortele PF et al (2002b) Correction of physiologically induced global off-resonance effects in dynamic echo-planar and spiral functional imaging. *Magn Reson Med* 47(2):344–353

- Pfeuffer J, Van de Moortele PF et al (2002c) Zoomed functional imaging in the human brain at 7 Tesla with simultaneous high spatial and high temporal resolution. *Neuroimage* 17(1): 272–282
- Poser BA, Versluis MJ et al (2006) BOLD contrast sensitivity enhancement and artifact reduction with multiecho EPI: parallel-acquired inhomogeneity-desensitized fMRI. *Magn Reson Med* 55(6):1227–1235
- Preibisch C, Wallenhorst T et al (2008) Comparison of parallel acquisition techniques generalized autocalibrating partially parallel acquisitions (GRAPPA) and modified sensitivity encoding (mSENSE) in functional MRI (fMRI) at 3T. *J Magn Reson Imaging* 27(3):590–598
- Scheef L, Landsberg MW et al (2007) [Methodological aspects of functional neuroimaging at high field strength: a critical review.]. *Rofo* 179(9):925–931
- Shimada Y, Kochiyama T et al (2008) System stability of a 3T-MRI during continuous EPI scan. *Nippon Hoshasen Gijutsu Gakkai Zasshi* 64(12):1504–1512
- Triantafyllou C, Hoge RD et al (2005) Comparison of physiological noise at 1.5 T, 3 T and 7 T and optimization of fMRI acquisition parameters. *Neuroimage* 26(1): 243–250
- Triantafyllou C, Hoge RD et al (2006) Effect of spatial smoothing on physiological noise in high-resolution fMRI. *Neuroimage* 32(2):551–557
- Vaughan JT, Garwood M et al (2001) 7T vs. 4T: RF power, homogeneity, and signal-to-noise comparison in head images. *Magn Reson Med* 46(1):24–30
- Walter M, Stadler J et al (2008) High resolution fMRI of subcortical regions during visual erotic stimulation at 7 T. *MAGMA* 21(1–2):103–111
- Wiggins GC, Potthast A et al (2005) Eight-channel phased array coil and detunable TEM volume coil for 7 T brain imaging. *Magn Reson Med* 54(1):235–240
- Yacoub E, Duong TQ et al (2003) Spin-echo fMRI in humans using high spatial resolutions and high magnetic fields. *Magn Reson Med* 49(4):655–664
- Yacoub E, Hu X (2001) Detection of the early decrease in fMRI signal in the motor area. *Magn Reson Med* 45(2): 184–190
- Yacoub E, Shmuel A et al (2001) Imaging brain function in humans at 7 Tesla. *Magn Reson Med* 45(4):588–594
- Zou KH, Greve DN et al (2005) Reproducibility of functional MR imaging: preliminary results of prospective multi-institutional study performed by Biomedical Informatics Research Network. *Radiology* 237(3): 781–789

## 6.1 Introduction

Analyses of fMRI data is a science on its own. There is a variety of software packages available – shareware for the most part – that offers multifarious possibilities to analyze the data. AFNI, BrainVoyager, FSL or spm2” are the most commonly used packages to name a few. As they also offer options to analyze very complex study designs, they tend to be time consuming even in analyses of block-designs, which are the most commonly used paradigms in clinical routine. Integration of fMRI into clinical routine, therefore, requires either a team that focuses on the performance of the scan and analyses of the data, or fast and reliable solutions that enable doing that along with the pace of a busy schedule. Most institutions do not have dedicated work groups (besides those for research purposes); so, there is a need for “press-button” solutions. The idea is not new (Möller et al. 2005), and all manufacturers offer software packages to analyze fMRI data. Recently, it has been shown that most of the commonly used packages are similar in terms of finding areas that have been programmed into the data (Morgan et al. 2001; Cheng et al. 2006); so, the choice of software seems to be determined by the user’s preference. However, a comparison of the various software packages provided by the manufacturers has not been performed to date.

---

K. Schmidt (✉)

Institute of Neuroradiology, Neurocenter, University Hospital of Schleswig-Holstein, Schittenhelmstr. 10, 24105 Kiel, Germany

e-mail: ulmer@email.com

## 6.2 Material and Methods

### 6.2.1 Overview

Our institution is equipped with 1.5 and 3 T MR scanners from Philips (Best, The Netherlands). For preoperative mapping, we perform fMRI to locate the motor strip and speech related areas (Ogawa et al. 1990). Patients perform a fist-grasp task in a block design at an external given pace alternating for both hands, with a rest period in between. Foot motion is performed in the same setting with patients being told and trained to wiggle their toes in order to avoid too strong movements of the body and therefore, also the head. For tongue movements, patients are told to circle the tip of the tongue at the back of the front teeth keeping the mouth shut, again with rest periods in between. For language mapping, we perform silent naming with three different tasks. In the first task, the patients are instructed and trained to name words that start with a given letter. The second task is a verb generation task and the third is a group membership task that also covers word comprehension and production. Language tasks are also performed in block design. The side of the body that is supposed to move, the pace of the movement or the stimuli for the language tasks are all presented using the IFIS-SA fMRI system (Invivo, Orlando, FL, see Fig. 6.1) with a head-mounted display fixated on the eight channel head coil. All the experiments are performed at the 3 T scanner. The stimulation paradigm was programmed with E-Prime (Psychology Software Tools Inc., Pittsburgh, PA).

To compare the different software packages, we performed fMRI in ten healthy right-handed male students (mean age 24, range: 21–25 years) and selected ten consecutive patients who had recently undergone fMRI preoperatively. All ten volunteers performed all



**Fig. 6.1** Photograph of the preoperative setting. The patient/volunteer lies in a supine position with the head being placed in the eight channel coil. On *top* of the coil there is the head-

mounted display used to present the stimuli generated by the again IFIS workstation (Invivo, Orlando, FL) being outside the magnet room

six tasks in random order to avoid bias through mental or physical fatigue; the patients performed either language or motor tasks depending on the location of their lesion. Comparison of the software packages was always done one-by-one. Analysis of the data was performed using the original T2\*-weighted images as underlying anatomy to avoid overlay errors due to anisotropic voxels of the EPI-sequence compared to isotropic voxels in T1-weighted images. As spm2 is used for most research studies in our institution, we called it the Gold-standard to define the functional areas. In all the subjects, we performed the motion correction for translation and rotation, a non-rigid normalization (realignment) and used the general linear model (GLM; *t*-test). Activity was defined as a color-coded blob that was depicted by either software. We defined true positive activity as areas that were detected

by both software packages that were then being compared. If these areas differed, we analyzed the time course of the signal intensity changes over the period of the measurement in this region of interest (ROI). False positive activity was only detected with spm2 additionally proven by the time course. False negative activity was only found by the other software proven by the signal intensity changes. Activity that was found with either software but did not show the warranted signal intensity changes was defined as an artefact.

The threshold for each task was defined in the subject with the lowest activity at this task to still depict the primary motor area and ipsilateral cerebellar activity, or activation in the frontal operculum and posterior speech associated language areas for language tasks, respectively. These thresholds were used throughout the study for all the subjects. For each task and

**Table 6.1** Thresholds of the various programs used. Note the differences between the programs using identical data.

paradigm	spm2	Iview Bold	nordicIce	iPlan cranial 3.0
Hand	8.2	0.47	6.1	8.0
Foot	10.5	0.6	8.2	9.0
Tongue	8.2	0.65	9.9	4.0
LBS	8.2	0.4	7.9	5.4
Verb generation	8.2	0.4	7.9	5.4
Word groups	6.9	0.4	6.5	7.7

software, we thus defined a threshold (Table 6.1). The results of the different software packages were then compared – slice by slice – in each individual case.

Besides the obtained results, the software packages were also judged in terms of speed and user-friendliness. All the manufacturers were contacted and informed about this comparison.

Connected through a network DICOM data was transferred to the workstations. We used k-PACS (IMAGE Information Systems Ltd., London) as a server for the data.

## 6.2.2 Software Packages (in Alphabetic Order)

### 6.2.2.1 BrainLAB

BrainLAB offers iPlan3.0, which is primarily designed for neuronavigation. There is a tool in the package called “BOLD MRI Mapping” that analyzes fMRI data. The data can be loaded and is automatically recognized as a BOLD study. Loading is fast and semi-automatic. Gaussian smoothing and a motion correction are offered that correct for rotation and translation in three planes. BOLD MRI Mapping opens the data set and creates three orthogonal planes. These planes are reconstructions from the original data (also the axial orientation). A T1-weighted data set can be used instead for neuronavigation purposes. The used paradigm can be created easily with three scroll bars (block-design only) defining task and rest length. Once created, it can be used for all studies. For statistical analyses the GLM and a  $t$ -test are performed. A threshold bar allows for setting a defined statistical threshold based on the  $t$ -value. Having three orthogonal planes, activations can be seen also in coronal or saggital views

(such as in spm2) that sometimes eases anatomical allocation. To see the signal intensity changes each voxel (and rectangles of  $3 \times 3$  voxels) can be defined as ROI by simply clicking on it in a frame called “time series view”. The stimulation paradigm is overlaid to ease decision making.

iPlan is (compared to spm2) fast in loading and analyzing the data. Analysis of the signal intensity changes in defined ROIs is possible at all times and everywhere in the brain. Screen shots are available for documentation. If the data is corrupted by head motion that can not be corrected for there is an option to yield only areas defined by the investigator (after proving the correct signal intensity changes over time in these voxels) to still allow its use for neuronavigation. This, however, also offers to manipulate the data. iPlan obviously offers the advantage of having the data local on the navigation computer and can merge these data with anatomical sets for neuronavigation rather than integrating bitmaps into MPR or T1 data sets. The results can also be sent back to PACS.

### 6.2.2.2 NordicNeuroLab (NNL)/ NordicImagingLab (NIL)

NordicNeuroLab offers NordicIce that can also analyze DTI or perfusion data. As spm2, nordicICE can be run on a PC, however, no additional software (like MATLAB) is required. Loading of the data is fast and easy. The BOLD module to be selected from a pull-down menu opens a new window guiding the investigator through the steps. Being familiar with the steps in spm2 is helpful as the design is modelled on the spm2 design; however, the steps are almost self-explaining. Activity and rest conditions are specified either by seconds or time points offering also the option to vary the length of each condition within a measurement. It is however also primarily designed for block designs. Once created, these designs can be used for all studies. A variety of pre-processing steps (slice-time correction, movement correction, Gaussian smoothing and high-pass filtering) can be modified as desired. Our impression was that using the default parameter worked pretty well. Again the GLM is used for statistics that however offers to modify hemodynamic response function (HRF), temporal smoothing and data thresholding. For each of the above mentioned steps there are default options available.

Analyzing of the data is very fast and could not be beat by any other “press-button” solution. After analyzing the data a simple drag and drop enhances the activity that obviously can also be overlaid onto any other anatomical data set. Thresholding again is a mouse click away and can be done either by using a scroll bar or by typing the  $T$ -value. To analyze the signal intensity change over time various ROI shapes can be defined and the time course can be displayed from any region or voxel. Additionally the graph of the motion correction initially performed can be reviewed at any time to also depict motion related activity. Results and graphs can be saved and copied into any other image analyses program and furthermore the color-coded maps can be sent back to PACS. From there integration into a neuro-navigation system is also possible.

### 6.2.2.3 PHILIPS

The PHILIPS tool to analyze fMRI data is called IViewBOLD. It runs on the console that controls the scanner and can thus be analyzed while the patient or volunteer is still in the scanner even in an online mode. There is therefore no need to load any data or transfer it from a server as long as the data is still on the hard disc. The investigator has the option to select or deselect a motion correction; however, no graph can be seen or analyzed afterwards. Compared to the other tested software packages, IViewBOLD is the only one to use a cross correlation for statistical analysis. Handling is fast and easy. The paradigm can be created using a pull down menu and periods of activation and rest be thus defined.

Thresholding is performed through changing the cross-correlation coefficient. The activity can be overlaid onto the  $T2^*$  or any other anatomical image that is acquired in the same orientation and field of view (FOV). Results can be stored either as screenshots or as bitmaps that can be sent to PACS. From there the data can be integrated into a neuronavigation device. ROIs can be defined everywhere and analyzed in terms of the signal intensity changes over time. Each time a calculation of each timepoint is performed separately that makes analyses of various areas tiring.

### 6.2.2.4 spm2

After being on the market for more than a decade now, there is so much information about spm2 available

that could hardly be summarized in short. spm2 is free software that can be downloaded from the spm2 website (Wellcome Department, London; [www.fil.ion.ucl.ac.uk/spm2](http://www.fil.ion.ucl.ac.uk/spm2)) (Friston et al. 1994). It however requires the commercially available program MATLAB (The MathWorks, Natick, MA).

There are various websites that discuss the options that spm2 offers. Instructions can be found easily and there are dedicated training courses for spm2, so that the approach to describe what the program is capable to do would certainly go beyond the scope of this chapter. To cut a long story short, spm2 offers the biggest variety to analyze fMRI data (from this chosen selection). Its motion correction is superb. Prior to analysis the image data has to be converted into the ANALYZE format.

Offering so many options, handling of spm2 is thus complicated/awkward. As it was never meant to be a tool for clinical applications speed and user-friendliness was not the main scope of the developers. For clinical purposes however, it can only be used if a group within the department/team focuses solely on that.

One major drawback is the fact that – even though signal intensity curves can be analyzed – this is only possible in the local maxima of significance defined by the program. If one would expect activity somewhere in the brain that is not depicted by the program, changes of the signal intensity over time can not be analyzed or thresholds have to be changed accordingly.

Another drawback is that results in spm2 can not be sent back to PACS and therefore the analysis has to be done offline or a satellite solution has to be programmed. Neuronavigation based on fMRI results achieved by spm2 is thus burdensome and only achievable taking a few detours (Fig. 6.2).

## Results

As already stated under the individual subheadings, analysis of fMRI data with either software package was regarded to be more user-friendly compared to spm2. NordiICE was the fastest tool tested.

Motion correction seems to be the key issue. If subjects remained perfectly still during the scan, results were pretty much comparable independent of the software used. However, in volunteers and even

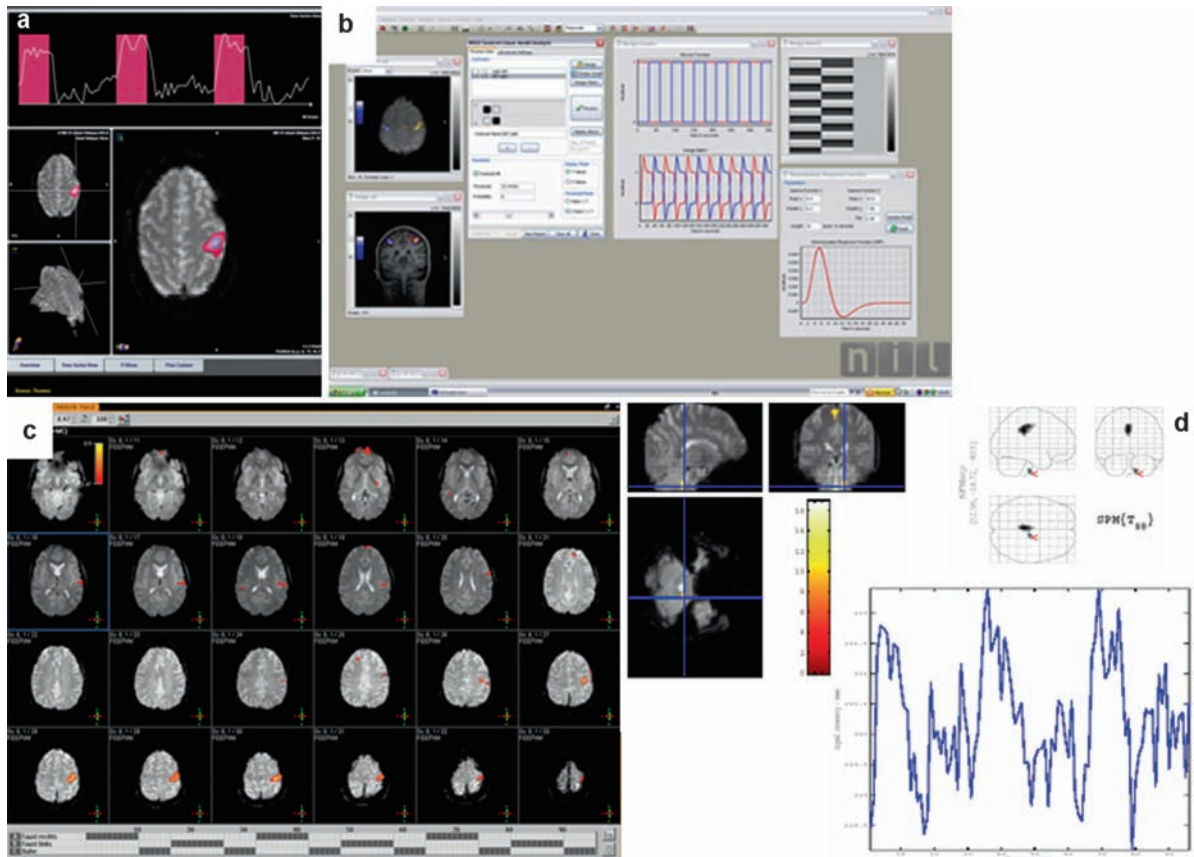


**Fig. 6.2** Screenshots of the software packages used. (a) BrainLAB: three orthogonal views can be seen. In the *upper* part of the image there is the curve of the signal intensity change over time superimposed with the blocks of activity in pink. (b) NordicNeuroLab: screenshot of analyzed data and

tool boxes including a HRF-function. Overlays can be done in various orientations. (c) Screenshot from the scanner. IViewBOLD analyzes the data while the subject is still in the scanner and presents the data overlaid in axial views. (d) spm2 – the Gold standard

worse in patients there is always head motion and the quality of the results was strongly dependent on the motion correction. In spm2 there was almost no data that demonstrated the typical rim-shaped artefact resulting in task related motion. Overall there were fewer areas activated in spm2 than with the other packages with nordicICE being neck to neck. False positive areas (only detected by one software package other than spm2 proven by the signal intensity time course) were extremely rare and only found in nordicICE. Most of the areas elucidated by any other software than spm2 turned out to be an artefact and quite frequently task related. False negative areas (only detected by spm2) occurred sometimes. Some datasets were corrupted by motion making a reliable analysis impossible.

Language tasks activated more regions besides the expected language areas than motor tasks did. This is somewhat surprising on one hand as silent naming was performed, which should thus not necessarily lead to head movements. On the other hand language stimuli will activate wide distributed networks and besides “classical defined speech areas” there are more structures involved. Language remains tricky and as long as the problem of performing active speaking has not overcome, we still map something like language or language related areas at best.

In most tasks expected activity could be found in either software however there were many additional areas in those “press-button” packages. Only the signal intensity time courses could distinguish between real activity and artefact.

### 6.3 Discussion/Future Aspects

Press button solutions represent a quick and easy tool to perform analysis for fMRI. However, they require the cooperation of the subject and little head motion – not task related if possible. This is the major drawback of these solutions, as patients are usually impaired to some extent or have less compliance. Clinicians therefore have to lower their sights. If the patient does not move much, the results are pretty much the same independent of the software used. If this is not the case, filtering of artificial false positive areas becomes the issue i.e. to guide the neurosurgeon and tell him which color-coded blob is real. As BrainLAB offers a fading of artefacts for the neuro-navigation it would be more reasonable to avoid appearance of these voxels completely. Some datasets were corrupted by motion making a reliable analysis impossible. These datasets, however, are the bottleneck of these tools. In clinical routine patients hardly follow criteria used to include healthy motivated volunteers. Any press-button solution should define real activity besides being user-friendly and fast, which was the case in all packages tested. Each package has its advantages and disadvantages. Comparing the tools IViewBOLD is obviously the fastest tool as it analyzes the data while the subject is still in the scanner. Motion correction is worse compared to other packages and analyzing signal intensity time courses becomes tiring. NordicICE was found to be the fastest tool (after transferring the data over the network) depicting the areas most reliably (compared to spm2) and also elucidating false positive areas that were proven to be valid by the signal intensity time course. All packages (except for spm2) offer the option to transfer the data into PACS to discuss the cases interdisciplinary prior to neurosurgical resection.

Whatever press-button software is used, if the data is corrupted by head motion, we strongly suggest to additionally use another software such as spm2 or similar to exclude false positive results. We would never rely on any “activity” presented by any software (not even spm2) as long as we have not proven that the depicted activity is real. The fact that it is not intended in spm2 to analyze any voxel in the brain is a major drawback especially in a clinical setting as we would sometimes like to know, why there is no activity in

expected anatomical structures i.e. caused by misunderstanding of the subject what to do.

Even almost two decades after the initial description of the BOLD effect and published methods to analyze the data it still always comes back to very simple review of the raw data. The only truth is the signal intensity change according to the paradigm in an area close to the neuronal activity. Knowledge and understanding of the signal intensity course is mandatory for all fMRI analysis and will remain the mainstay of the analysis.

New software solutions will be presented that have to maintain their ground against already available tools. The approach to ease the analysis is highly appreciated for clinical routine. We highly recommend putting maximum effort in the motion correction of these tools that will find their spot in clinical routine. As of now caution is still warranted using these programs if one will not perform a comparison of results as done here. Experience with an additional package is helpful if results are inexplicable, but analysis of the signal intensity changes remains mandatory.

**Acknowledgements** The authors would like to thank the following companies for technical support and assistance with the software packages discussed above – in alphabetic order: BrainLAB, NordicNeuroLab, and PHILIPS.

BrainLab offered hardware, software and training/instructions (as web-conference if needed) to perform this study. We are cooperation partners with NordicNeuroLab and thus received the software for test purposes for free. As we are a PHILIPS dominated institute, close collaboration with application specialists and technicians was granted at any time.

### References

- Cheng H, Zhao Q, Duensing GR, Edelstein WA, Spencer D, Browne N, Saylor C, Limkeman M. (2006) SmartPhantom—an fMRI simulator. *Magn Reson Imaging* 24(3):301–313
- Friston KJ, Jezzard P, Turner R. (1994) Analysis of functional MRI time-series. *Hum Brain Mapp* 1:153–171
- Möller M, Freund M, Greiner C, Schwindt W, Gaus C, Heindel W. (2005) Real time fMRI: a tool for the routine presurgical localisation of the motor cortex. *Eur Radiol* 15(2):292–295
- Morgan VL, Pickens DR, Hartmann SL, Price RR. (2001) Comparison of functional MRI image realignment tools using a computer-generated phantom. *Magn Reson Med* 46(3):510–514
- Ogawa S, Lee TM, Kay AR, Tank DW. (1990) Brain magnetic resonance imaging with contrast dependent on blood oxygenation. Brain magnetic resonance imaging with contrast dependent on blood oxygenation. *Magn Reson Med* 14:68–78

---

**Section 2**  
**Clinical Applications**

# Preoperative Blood Oxygen Level Dependent (BOLD) functional Magnetic Resonance Imaging (fMRI) of Motor and Somatosensory Function

Christoph Stippich

## 7.1 Rationale for fMRI in Rolandic Neurosurgery

Surgery in or around the “central region” entails a high risk for intraprocedural damage of the precentral and postcentral gyrus with consecutive motor and sensory deficits that can impact the patient’s quality of life considerably. By noninvasively providing a precise localization of the different representations of the human body in relation to the surgical target, BOLD-fMRI facilitates the selection of candidates for surgery as well as the planning and performance of more aggressive, but safe and function preserving resections (Petrella et al. 2006). This also implies that fMRI plays a role in identifying those patients who are not the ideal candidates for surgery and who may profit more from less invasive therapeutic options like radiation or chemotherapy. Such patients often present with diffusely infiltrating or recurrent malignancies of the brain, and a complete resection and a surgical cure cannot be achieved. In this situation, deficits associated with the treatment should be kept to a minimum. Prior to treatment, fMRI provides important diagnostic information to evaluate the risks and chances on an individual basis and to optimize the therapeutic strategy accordingly. In addition, functional landmarks are helpful to plan partial resections or biopsies. This also applies for awake craniotomies or epilepsy surgery. Hence, the majority of preoperative fMRI studies is performed in patients with brain tumors and epilepsies

to preserve the adjacent eloquent brain areas. In nonresective neurosurgery also fMRI can be applied, for e.g., in patients with medically intractable chronic pain. Here, it has been demonstrated that fMRI facilitates the placement of stimulation electrodes over the motor cortex (Pirotte et al. 2005). Ideally, preoperative fMRI studies are conducted for functional neuronavigation, and in combination with diffusion tensor imaging, (DTI) to also visualize important fiber bundles during surgery, e.g., the pyramidal tract (Nimsy et al. 2006).

It is important to note that the central region can be localized easily and reliably on the basis of morphological images of the brain using different anatomical structures as landmarks (for details see Chap.2) (Fig. 7.1). The most robust anatomical landmark is the “hand knob” of the precentral gyrus, representing the structural correlate of the motor hand area on transverse cross-sectional images, (Yousry et al. 1997) which also corresponds to the “precentral hook” on sagittal images. The existence of these morphological landmarks substantiates the controversy whether functional imaging is necessary at all for rolandic neurosurgery. This view, however, does not account for the important limitations of morphological brain imaging in the presence of anatomical variants or under pathological conditions (e.g., mass effects, infiltration, destruction, postoperative state in recurrent malignancies, etc.), both precluding proper identification of the different gyri and sulci. More importantly, the motor hand area is the only functional area that can be identified reliably using anatomical criteria alone. All other representations of the human body can be identified only by using functional neuroimaging (Fesl et al. 2003), both in the primary motor cortex (M1) and in the primary somatosensory cortex (S1). A substantial body of research supports the role of fMRI as a valid and valuable preoperative imaging modality (Stippich 2007).

---

C. Stippich  
Department of Diagnostic and Interventional Neuroradiology,  
University Hospital of Basel, Petersgraben 4, 4031 Basel,  
Switzerland  
e-mail: stippich@uhbs.ch

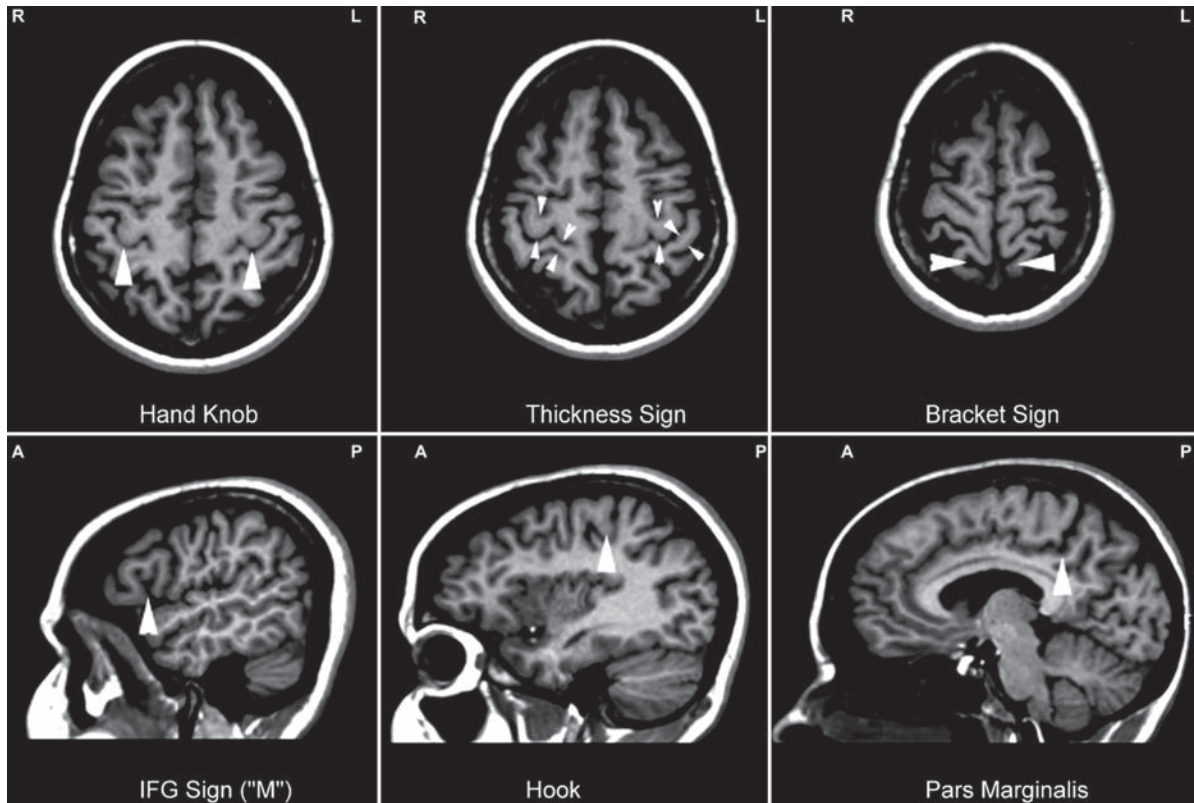


**Fig. 7.1** Anatomical landmarks on morphological MRI according to Naidich and Yousry in transverse (*upper row*) and sagittal (*lower row*) views. *White arrows* indicate the relevant anatomi-

cal structures. The “hand knob” and “hook” are synonyms for the “precentral knob.” Reprinted from Stippich (2007, p 90) with permission

Hence, the rationale for preoperative fMRI results largely from the limitations of structural brain imaging (Rolls et al. 2007). Furthermore, neuroplasticity and functional reorganization induced by the lesion or by the treatment can be assessed using fMRI (Shinoura et al. 2006), for e.g., in patients with motor and somatosensory deficits that are not explained conclusively by anatomical consideration and in patients who are candidates for repeated neurosurgery because of recurrent malignancies.

Taken together, the rationale for carrying out pre-surgical fMRI is often based on the limitations of imaging morphology, clinical and electrophysiological diagnostics and the need to include data on physiological and neuroplastic changes or pathologic (e.g., epileptic) activation of the brain in treatment planning. This diagnostic information may be generated by fMRI in a single investigation before treatment by means of a combined visualization of anatomy, pathology and function. Combination of other modern methods of MRI, for example by mapping fractional anisotropy

(FA) or DTI, may be helpful in depicting important fiber pathways such as the pyramidal tract (Schonberg et al. 2006) (Fig. 7.2).

## 7.2 Review of Literature\*

Mapping the primary motor cortex in patients with rolandic brain tumors has been the first clinical application of fMRI (Jack et al 1994). Shortly after the first reports on BOLD fMRI in healthy subjects (Belliveau et al. 1991; Bandettini et al. 1992; Kwong et al. 1992; Ogawa et al. 1993), the potential usefulness of functional imaging techniques in clinical context, and particularly in presurgical identification of motor and somatosensory cortices was postulated. The first description of presurgical fMRI as a clinically useful application dates from 1994, when

\*Acknowledgement:

We thank Dr. Maria Blatow for her substantial contribution to the review of literature.

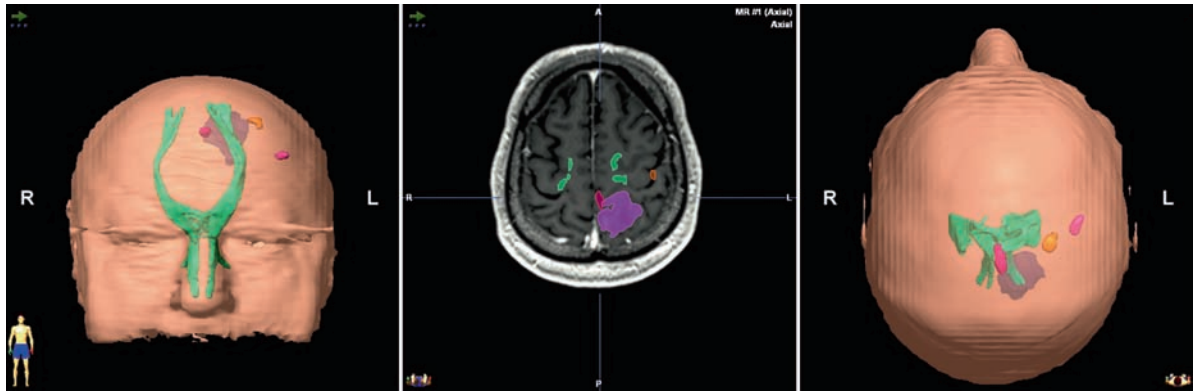


**Fig. 7.2** Integration of BOLD-fMRI and DTI-tractography for functional neuronavigation. 3D-surface projections (left: anterior – posterior, right: top – down) and 2D-navigation view (middle). The spatial relationship of the cortical toe (*red*), finger (*orange*) and tongue (*pink*) motor representations and of the

pyramidal tract (*green*) to the segmented brain tumor (*purple*) is clearly depicted. The tumor affects the superior parietal lobule, invades the postcentral gyrus extending towards the cortical motor representation of the lower extremity

Jack et al. provided proof of principle in two patients with brain tumors in the sensorimotor cortex, validating their preliminary results with established electrophysiological techniques (Jack et al. 1994). Soon after, several case studies (Baumann et al. 1995; Cosgrove et al. 1996) and reports with small numbers of patients, (Puce et al. 1995; Pujol et al. 1996; Mueller et al. 1996; Krings et al. 1998) harboring glial tumors or arteriovenous malformations (AVM), confirmed technical and practical feasibility of fMRI using motor and sensory tasks in the clinical context, and stressed the high potential value of this new upcoming technique for preoperative risk assessment, therapeutic decision making and surgical planning.

During the following years investigations with larger numbers of tumor patients (up to 50) were carried out, claiming their results to represent an important factor for surgical decision (Schlosser et al. 1997; Pujol et al. 1998). Comparisons of presurgical fMRI data with the established reference procedure intracortical stimulation (ICS) were numerous and only those specifically dealing with brain tumor patients will be mentioned here, since a detailed description of validation studies is offered in Chap. 11 and 12. Virtually all studies report highly concordant data of presurgical fMRI and ICS in patients with lesions around the central sulcus (Dymarkowski et al. 1998; Achten et al. 1999; Roux et al. 1999a, b) with agreement between fMRI and ICS data ranging from 83% in 33 patients (Majos et al. 2005) to 92% in 60 patients (Lehericy et al. 2000). Task sensitivity for identification of the sensorimotor region estimated in large groups of tumor patients was 85% in 103 patients (Krings et al. 2001)

or 97% in 125 patients (Hirsch et al. 2000). Furthermore, it should be briefly noted, that various groups focused on the correlation of fMRI results in patients with central lesions with those of other functional imaging procedures, for e.g., PET (Bittar et al. 1999).

One of the first attempts to evaluate the impact of fMRI on neurosurgical planning was published by Lee et al. The authors applied preoperative fMRI sensorimotor mapping in 32 tumor patients and reported that the results were used to determine feasibility of surgical resection in 55%, to aid in surgical planning in 22% and to select patients for invasive surgical functional mapping in 78%. Overall, the fMRI results were useful in one or more of these surgical decision making categories in 89% of all examined tumor patients (Lee et al. 1999). A similar range was documented by Ternovoi et al., who found that presurgical fMRI results had an influence on therapeutic tactics in 69% of 16 tumor patients (Ternovoi et al. 2004). Other investigators tried to establish a functional risk predictor for postoperative clinical outcome. Haberg et al. examined 25 patients with primary brain tumors near sensorimotor regions. In 80% of the patients, successful fMRI measurements were obtained, out of which 75% were used in preoperative planning. The risk of postoperative loss of function was significantly lower, when the distance between tumor periphery and BOLD activation was 10mm or more (Haberg et al. 2004). Similarly, Krishnan et al. who evaluated BOLD activation in 54 patients, found that a lesion-to-activation distance of less than 5 mm and incomplete resection were predictors of new postoperative neurological deficits and recommended

cortical stimulation within a 10-mm range (Krishnan et al. 2004). In patients with medial frontal lesions, preoperative fMRI was used to establish the area at risk for resection of specific parts of the supplementary motor area, associated with transient postoperative motor deficits and speech disorders (Krainik et al. 2001; Krainik et al. 2003; Krainik et al. 2004). In a recent study the authors used fMRI-guided resection in 16 patients with low grade gliomas. Since these tumors are generally not contrast enhancing, resection borders are particularly difficult to establish based on morphological imaging alone. Using fMRI for the determination of resection borders, no permanent neurological deficits, and no radiographic tumor progression, within a median follow-up time of 25 months, were observed (Hall et al. 2005). However, the data available to quantify a safe distance between functional activation and resection borders with respect to surgically induced neurological deficits are still very limited and do not justify any general conclusion or recommendation.

Overall, although the above mentioned studies clearly demonstrated feasibility of presurgical fMRI in clinical environment and postulated a contribution of the obtained additional clinical information to pretherapeutic decision making, an effect on the decrease in posttherapeutic morbidity was not corroborated. In order to achieve this, controlled clinical trials using optimized and standardized protocols would be required. Although most investigators agree on the necessity of a standardized routine, and several methodological studies presenting optimized protocols for clinical use were published (Hirsch et al. 2000; Ramsey et al. 2001; Rutten et al. 2002; Stippich et al. 1999; Stippich et al. 2000; Stippich et al. 2002; Stippich et al. 2004; Stippich et al. 2005), no large scale clinical trials addressing actual benefit for the patient, in terms of decrease in morbidity have been undertaken so far.

Although sensorimotor areas are identified with high success rates using fMRI in patients with central lesions by most investigators, a frequently encountered phenomenon is an altered pattern of activation as compared to the normal brain function, currently denominated as lesion-induced reorganization or plasticity. In an early study in seven patients with intracerebral gliomas of the primary sensorimotor cortex, activation was found to be displaced or reduced (Atlas et al. 1996). Roux et al. correlated the type of activation with histologic tumor characteristics in 17 patients. In infiltrating tumors, intratumoral activation was detected, which was displaced and scattered correlated with the degree of infiltration, whereas in noninfiltrating tumors activation

showed extra-tumoral shift. In tumors at a distance from the motor cortex, no intratumoral activation was measured (Roux et al. 1997). Likewise, a PET study with 51 patients describes that central lesions are more frequently associated with altered patterns of activation than lesions in noncentral locations (Bittar et al. 2000). Other studies found significant BOLD signal decrease in areas adjacent to tumor tissue in motor and sensory cortices as compared to the contralateral side. This effect was present in glial tumors, most pronounced in glioblastoma and presumably related to tumor induced changes in local cerebral hemodynamics (Holodny et al. 1999; Holodny et al. 2000; Krings et al. 2002), while in nonglial tumors (metastasis, cavernoma, abscess, AVM, meningioma) no BOLD signal decrease was found (Schreiber et al. 2000). A recent report on 33 patients with different intra- and extra-axial tumors, established the influence of tumor type and distance from eloquent cortex on activation volumes in fMRI (Liu et al. 2005). In addition to displacement or reduction of activation in the primary sensorimotor cortex harboring the tumor, other patterns of lesion-induced reorganization encompass activation of solely the contralesional cortex or an enhanced activation of nonprimary sensorimotor areas with increasing degree of paresis (Alkadhi et al. 2000; Carpentier et al. 2001; Krings et al. 2002). Also in patients with prior surgery (Kim et al. 2005) or newly acquired central paresis after resection (Reinges et al. 2005), significant decreases in BOLD activation are observed. One possible explanation for this tumor-induced BOLD signal loss was lately proposed by an fMRI study where tumor blood volume and perfusion were measured. The authors concluded that the BOLD amplitude correlates with total intratumoral blood volume and thus, reduced peritumoral perfusion due to a tumor aspirating perfusion (steal phenomenon) goes along with reduced BOLD activation (Ludemann et al. 2006). Of note is however, that resection of glioma with preoperative edema may cause transient increase of BOLD activation ipsilateral to the tumor, presumably by a decrease of pressure on the brain (Kokkonen et al. 2005). Lesion-induced functional reorganization may reflect the recruitment of plastic neuronal networks to compensate for sensory or motor impairment. On the level of a functional diagnosis in presurgical fMRI these reorganization phenomena are of major clinical significance for the planning of resections, since they can potentially cause false negative results.

During the past few years the use of combined presurgical fMRI and DTI techniques for tractography

was suggested to provide a better estimate of proximity of tumor borders to eloquent cortex than fMRI measurements alone. In particular, for space-occupying lesions affecting the central region, visualization of the origin, direction and functionality of large white matter tracts allowing imaging of functional connectivity, was put forward to improve surgical outcome and to promise a decrease in patient morbidity (Krings et al. 2001; Parmar et al. 2004; Ulmer et al. 2004; Shinoura et al. 2005; Stippich et al. 2003; Holodny et al. 2001).

Very recently, first reports on the application of real-time fMRI in clinical environment were published. This novel technique enables quick preliminary online analysis of fMRI data, which is particularly useful in surgical diagnostics, considering that fMRI data acquisition and processing are very time consuming. Möller et al. demonstrated the technical feasibility of presurgical real-time fMRI examination in ten patients with central area tumors immediately prior to surgery (Moller et al. 2005). In another study, motor and language tasks were used for real-time fMRI in 11 tumor patients. The authors reported satisfactory activation for hand motor tasks, weaker activation for foot motor tasks, and no useful activation for language tasks at the chosen threshold, concluding that the procedure needed to be optimized, but was generally feasible in clinical routine (Schwindack et al. 2005). Furthermore, Gasser et al. lately achieved the recording of intraoperative fMRI in four anesthetized patients with lesions in the vicinity of the central region. Using a passive stimulation paradigm and analyzing the data during acquisition by online statistical evaluation, they obtained intraoperative identification of eloquent brain areas taking brain shift into account (Gasser et al. 2005).

Finally, with the introduction of higher magnetic field scanners to clinical diagnostics, practicability of presurgical fMRI at 3 T was established in patients with brain tumors (Roessler et al. 2005; Van Westen et al. 2005; Feigl et al. 2008). Today the clinical implementation of preoperative fMRI is possible also in regional hospitals (Geerts et al. 2007). For a general review on the role of imaging in disease management and the development of improved image-guided therapies in neurooncology see also the latest article by Jacobs et al. (Jacobs et al. 2005).

Note: Very recently the American Medical Association ([www.ama-assn.org](http://www.ama-assn.org)) has released CPT-codes (Current Procedural Terminology) for clinical fMRI applications. General instructions for clinical fMRI can be found in the Current Protocols for Magnetic Resonance Imaging (Thulborn 2006).

### 7.3 General Considerations

Motor cortex mapping is the predominant preoperative application of fMRI because of its easy implementation in a clinical setting and the robust and valid functional localizations. Typically, a simple block-design consisting of three to five stimulation-baseline cycles is applied while the patients perform selfpaced movements with the tongue or lips, hand or fingers and foot or toes, to investigate the motor cortex somatotopy.

Essentials for the success of clinical fMRI examinations are (1) motor tasks that are feasible also in patients with paresis, (2) reduction of motion to a minimum and (3) short scanning times. Under these conditions, BOLD activations in the primary motor cortex are generally very reliable. This can be achieved, when the “most feasible” motor tasks have been selected from clinical testing, when patient positioning and head fixation is optimal during the fMRI scans, when appropriate motion correction is applied for data processing and when the fMRI scanning protocols have been evaluated in volunteers for robust functional localization, high BOLD-signal yield and low scanning time. For the diagnostic interpretation of clinical fMRI data it is indispensable, that the whole fMRI procedure is fully standardized (scanning, data processing and evaluation), that normative data are available for all applied fMRI scanning protocols (ideally including data for important influencing factors like handedness, etc.) as well as a precise assessment of each patient’s neurological deficits at the time of the preoperative fMRI measurement. For the latter, the importance of the individual training of the investigator with each patient before the actual fMRI measurement cannot be overestimated. To control for incorrect task performance, a video monitoring during the fMRI measurements is highly recommended. In uncooperative patients, it may even be necessary that the investigator is inside the scanner room to give instructions directly (e.g., by tapping the hand when the movement is started and stopped). All erroneous measurements must be excluded from evaluation and repeat measurements must be performed.

The investigation of patients with pareses can be challenging, however. Dedicated paradigms based on somatosensory stimulation (Stippich et al. 1999, 2004, 2005) or complex finger movements of the unimpaired hand (Stippich et al. 2000) may help to overcome the problem. A somatosensory stimulation can also be useful in uncooperative or sedated patients and in children. Automated devices deliver reproducible stimuli and are ideal for follow up measurements under standardized conditions

(Golaszewski et al. 2002; Kurth et al. 1998; Stippich et al. 1999). For more details see paragraphs Sect. 7.6 and 7.7. A review of literature regarding the various fMRI paradigms for motor and somatosensory function is beyond the scope of this chapter. We refer the reader to the extensive database available. It is of note that most manufacturers offer online data processing software for functional BOLD-imaging with their MR-imagers today, providing easy access to the method.

## 7.4 Diagnostic Aims

The primary diagnostic aims of preoperative fMRI are to localize the primary motor cortex and/or the primary somatosensory cortex in relation to the surgical target and the different cortical representations of the human body of the precentral gyrus and/or postcentral gyrus. The secondary aims include, the detection of neuroplastic changes and functional reorganization prior to treatment in patients with neurological deficits and in patients scheduled for repeated neurosurgery, investigating the natural course of brain activation in patients with rolandic pathologies, or the effects of a specific (surgical or alternative) treatment on brain function may represent further diagnostic aims of follow up measurements.

## 7.5 Selection of Candidates for Preoperative fMRI

Most patients referred to preoperative motor and somatosensory fMRI present with rolandic brain tumors, metastases, AVM's and epileptogenic lesions. In general, patients with meningiomas and other (non infiltrative) extraaxial masses should not be considered for fMRI, except for difficult cases on request of the surgeon. fMRI is also not necessary for patients with frontal or parietal pathologies that do not involve the central region directly.

As a basic principle, candidates for preoperative fMRI should be selected by anatomical consideration first using morphological MR images, and on the basis of clinical findings (motor and/or sensory deficit), both clearly indicating an involvement of the primary motor and/or somatosensory cortex. The appropriate examination protocol should be selected accordingly.

Depending on the site and extent of the lesion, a single fMRI reading can suffice; however, it is often necessary to examine the entire motor and, where appropriate, somatosensory somatotopy.

Preoperative fMRI studies are justified when the following anatomical criteria apply: (1) Complete destruction of the rolandic anatomy precluding identification of the precentral gyrus, central sulcus and postcentral gyrus. (2) Compression or displacement of the precentral gyrus precluding reliable localization of the hand knob – the MR-morphologic reference of the motor hand area is absent as an orientation point for the somatotopic organization of the precentral gyrus. (3) The surgical target lies below or above the hand knob and a precise localization of the cortical face or lower extremity representations is warranted. (4) The surgical target is postcentral – a somatosensory stimulation may be applied. Other (nonanatomical) criteria include (5) suspected neuroplastic changes/functional reorganization with respect to neurological signs and symptoms and (6) repeated neurosurgery.

Note: The size of the BOLD-clusters and the center of gravity varies with the statistical threshold applied for data evaluation. As a consequence, fMRI studies should not be performed to determine resection borders or a “safe” distance between lesion and functional area. In a strict sense, this is not possible to date on the basis of fMRI data as the material published on that topic is very limited (Haberg et al. 2004; Krishnan et al. 2004; Hall et al. 2005). Furthermore nonstandardized measurements in “interesting cases” are not feasible for clinical decision making and should be avoided. However, such patients may be enrolled in research trials.

## 7.6 Paradigms for Clinical Motor and Somatosensory fMRI

When designing motor paradigms in a block design, it is of principal importance to establish whether only the primary motor cortex activation needs to be measured, or secondary areas should also be considered. In the case where only the primary motor cortex is the target, paradigms can also include movements in both sides of the body (e.g., right hand vs. left hand). Since unilateral movements lead to activation of secondary areas in both hemispheres, secondary areas are active during alternating movements of the right and left

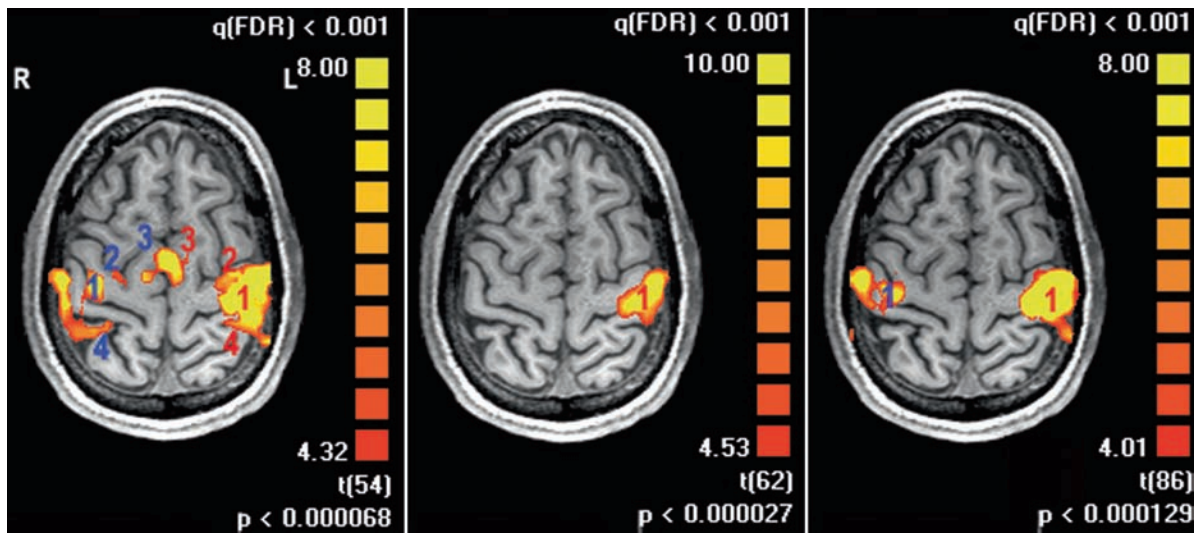


**Fig. 7.3** Variation of paradigms to localize the motor hand area results in different activation patterns. *Left*: complex finger opposition of the right hand vs. rest; strong activation of cortical motor network in both hemispheres. The large contralateral cluster (*left*) covers the primary sensorimotor cortex (1), premotor cortex (2) and parietal cortex (4). Bilateral supplementary motor activation (3, 3) is displayed in the midline, as well as ipsilateral (*right*) premotor activation (2), primary sensorimotor coactivation

(1) and parietal activation (4). *Middle*: complex finger opposition of the right vs. left hand; strong contralateral (*left*) primary sensorimotor activation (1), but no activation of secondary areas. *Right*: complex finger opposition of the right hand vs. right tongue movements; strong contralateral (*left*) primary sensorimotor activation (1) and ipsilateral primary sensorimotor coactivation (1), but no activation of secondary areas. Reprinted from Stippich (2007, p 106) with permission

body side throughout the entire measurement, but continuous activation is not shown in the statistical evaluation of fMRI data, acquired using conventional block designs, due to the lack of “contrast” between the various stimulation blocks. If information needs to be obtained regarding secondary motor activation, paradigms with strictly unilateral movements of a single body part should be applied, with “resting” as the control condition. Alternatively, three different stimulation conditions could be integrated in the paradigm, i.e., right movement – rest – left movement. However, the number of blocks per paradigm is then increased, and consequently, the examination time and susceptibility to motion artifacts also increases. In addition, it should be borne in mind that information on brain activation in the tumor-unaffected hemisphere is largely insignificant for treatment. Also, paradigms enabling the examination of several cortical body representations are problematic in brain tumor patients (e.g., foot – hand – face). Although scan time could be reduced compared to three individual measurements, the time needed is still substantially longer than for each individual measurement alone.

Particularly in the case of agitated patients or patients with paresis, the likelihood of motion artifacts increases, subsequently affecting all functional localizations. Only secondary functional areas which are exclusive to the respective movement can be localized. All jointly recruited areas escape detection on diagnostic fMRI. In conclusion, paradigms with movements of a single part of the body alternating with true rest that provide short scan times are most appropriate for preoperative fMRI (Fig. 7.3).

Clinical feasibility tests, carried out on neurosurgical patients with and without tumor-related pareses or sensory disturbances, showed that self-triggered movement tasks are better suited to preoperative fMRI than controlled paradigms, since only in this way each patient can perform within his or her ability. To keep the likelihood of motion artifacts to a minimum (Hoeller et al. 2002; Krings et al. 2001), the following movement tasks were chosen each with “rest” as control condition: repetitive tongue movements with the mouth closed, opposition of fingers D2–D5 to D1 with free choice of sequence, repetitive flexion and extension of all five toes without moving the ankle (Stippich et al. 2002)

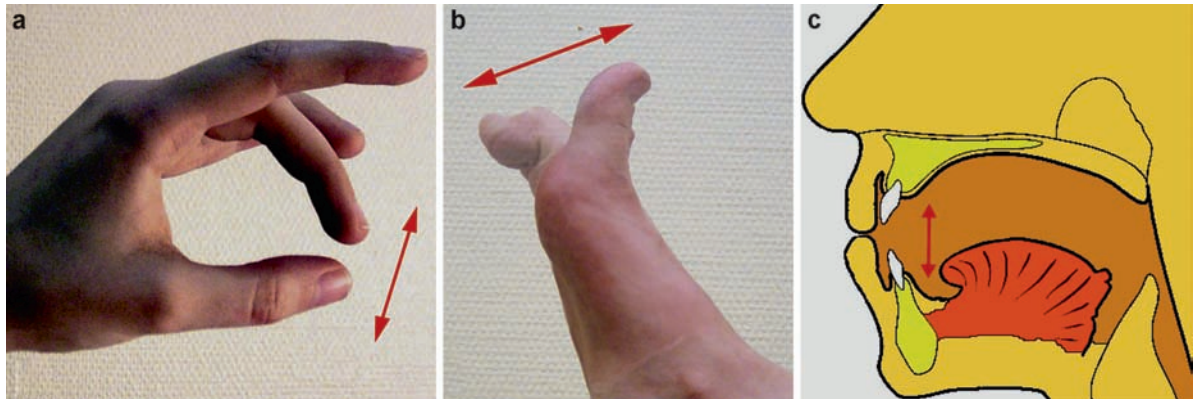


**Fig. 7.4** (a–c) Recommended self-paced movements to investigate sensorimotor somatotopy in clinical fMRI. (a) Complex finger opposition of digits 2–5 against the thumb in a random order. Movement frequency  $\sim 3$  Hz. (b) Toe up and down move-

ments, frequency  $>1$  Hz. (c) Tongue up and down movements with the mouth closed. Movement frequency  $\sim 3$  Hz. Reprinted from Stippich (2007, p 106) with permission

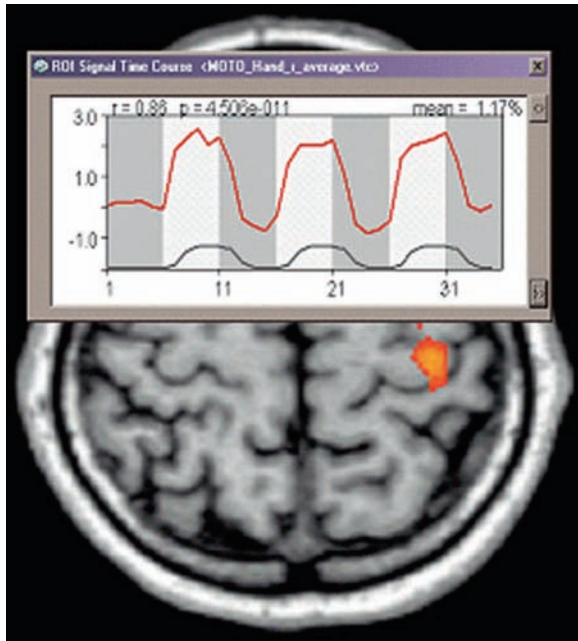


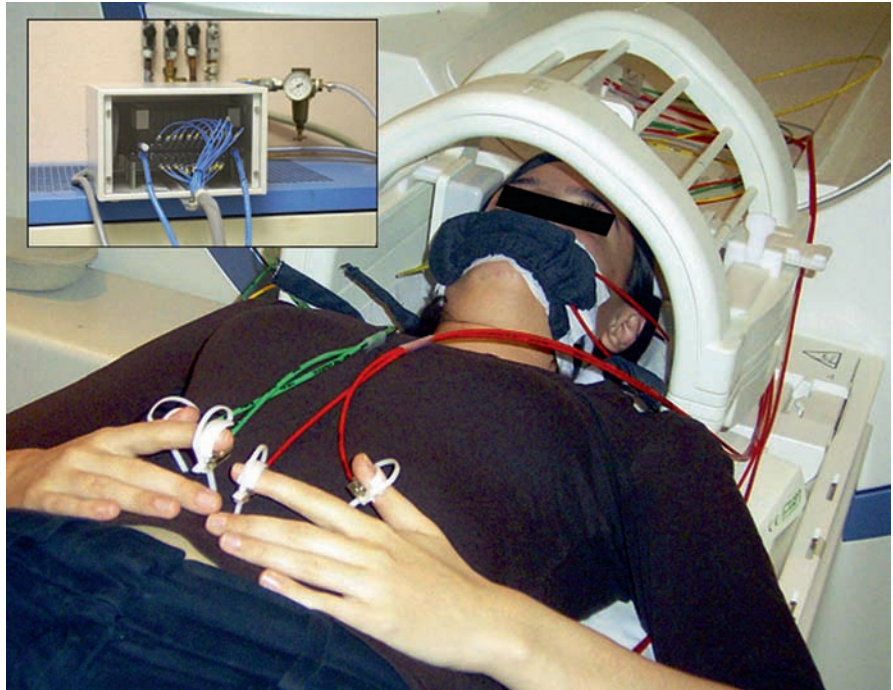
**Fig. 7.5** Clinical standard protocol for motor paradigms. The block-designed paradigm consists of four rest periods (light grey) alternating with three stimulation periods (white), each 20s in duration. The BOLD-signal time course of the motor hand area activation (red line) shows task related increases in regional hemodynamics. The black line indicates the hemodynamic reference function (hrf). Reprinted from Stippich 2007, p 107 with permission

(Fig. 7.4). Alternatively, in the case of mild paresis of the upper extremity, fist clenching/releasing can be tested. Face, arm and leg movements, or movement of the feet, can often lead to poor diagnostic evaluation of

data due to strong motion artifacts; therefore, they are not recommended for clinical fMRI. A paradigm with a block duration of 20s and three repeat cycles (four rest conditions alternating with three stimulation conditions), adding to an examination time of 140s, is a suitable compromise between robust functional localization of the primary motor cortex, high BOLD signals and short scan time (Fig. 7.5).

Determination of motor function with preoperative fMRI is limited in patients with high-grade paresis (Pujol et al. 1998; Krings et al. 2002). In the case where the fMRI protocol is based solely on self-triggered movements contralateral to the tumor, a reliable preoperative fMRI diagnosis is not guaranteed – the pareses are result of insufficient residual function of the primary motor cortex, which can lead to weak, or even absent, BOLD signals. Nevertheless, many patients with tumor-related paresis can be successfully examined by activating the primary somatosensory lip, finger and toe representations of the postcentral gyrus (Stippich et al. 1999). While most investigators apply somatosensory stimuli manually (e.g., brushing the palm), automated devices provide reproducible and standardized stimulation conditions. Electric (Kurth et al. 1998; Kampe et al. 2000; Golaszewski et al. 2004), tactile (Stippich et al. 1999; Wienbruch et al. 2006) or vibrotactile (Golaszewski et al. 2002; Golaszewski et al. 2006) stimulators are in use. The fully automatic pneumatically driven 24-channel tactile stimulation used in our institution, works artifact-free, produces reproducible stimuli and consistent examination conditions for comparative and outcome studies. The whole unit can be set up and removed

**Fig. 7.6** Fully automated pneumatically driven tactile stimulation. Flexible membranes (4D Neuroimaging, Aachen, Germany) connected to pressure resistant pneumatic tubes transmit the stimuli to the lips, fingers or toes (not shown). *Upper left:* the 24-channel high precision electromagnetic valve system was designed to investigate somatosensory somatotopy. Reprinted from Stippich 2007, p 94 with permission



within 5 min (Fig. 7.6). Scan times per measurement are 66 s for S1 (Stippich et al. 2004) or 105 s for S2 (Stippich et al. 2005). The S1-paradigm consists of five repeat cycles (six rest conditions alternating with five stimulation conditions, duration 6 s each), the S2-paradigm of three repeat cycles (four rest conditions alternating with three stimulation conditions, duration 15 s each). For the latter paradigm S1 activation is also robust.

As a further adjunct to investigate paretic patients, complex finger opposition of the nonparetic hand (ipsilateral to the pathology) can be used for the standard motor paradigm (140 s) to elicit robust premotor activation as an additional functional landmark for the precentral gyrus on the lesion side (Stippich et al. 2000) (Fig. 7.7).

## 7.7 Preoperative fMRI in Patients with Rolandic Brain Tumors

### 7.7.1 Somatotopic Mapping of the Primary Motor Cortex (Standard Protocol)

Somatotopic mapping of the motor cortex is the most frequently used preoperative fMRI protocol in

patients with rolandic lesions (Stippich et al. 2002). The protocol contains three different fMRI measurements with a scanning time of 140 s each. Typical paradigms include tongue movements, finger and toe movements contralateral to the lesion to localize the motor homunculus in relation to the surgical target (Fig. 7.8). Even in case of complete destruction of the rolandic anatomy, fMRI provides three functional landmarks for different body representations (face, upper and lower extremities). This diagnostic information is relevant to confirm the indication to operate and to plan and implement safer surgery. The same holds true for lesions that preclude proper identification of the hand knob as the anatomical reference for the motor hand area by compression or displacement (Fig. 7.9). In patients with small lesions that are – by anatomical consideration – not critical for all body representations, it seems appropriate to shorten the protocol by leaving the least relevant body representations unexamined (Fig. 7.10). However, the examination of a single body representation alone, e.g., the motor hand representation, is often not sufficient to provide the required diagnostic information. Somatotopic mapping enables also to assess plastic changes of cortical motor activation, e.g., in patients with recurrent malignancies prior to repeated surgical treatment (Fig. 7.11).

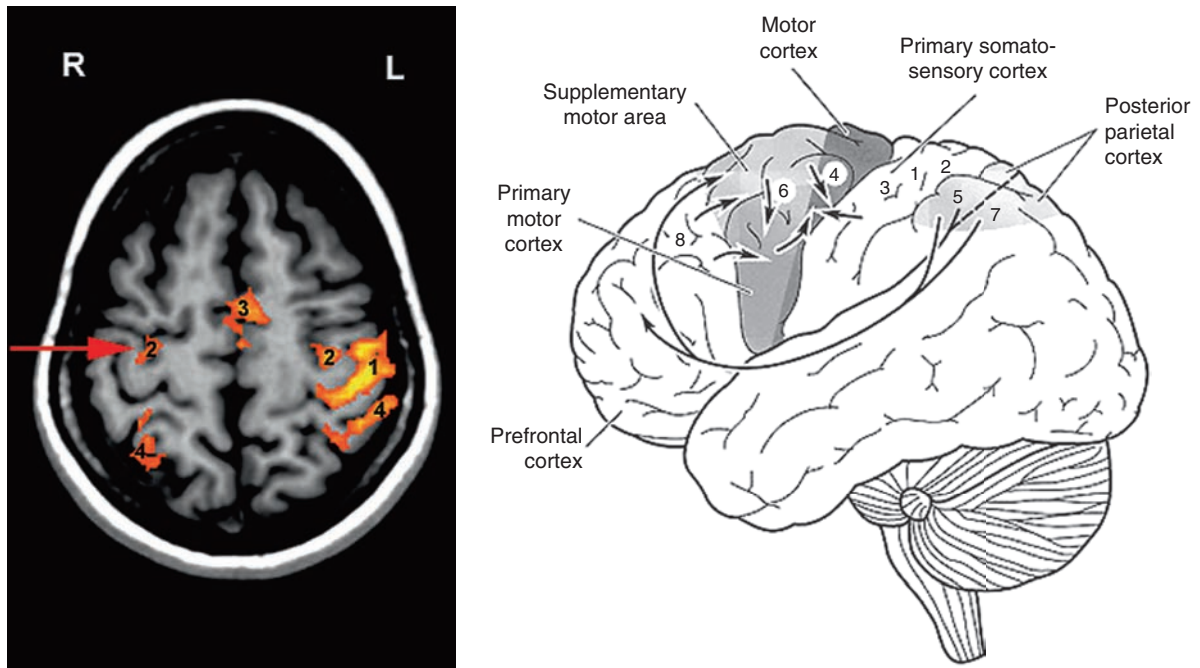


**Fig. 7.7** Typical cortical activation pattern of complex finger opposition (*right hand*). Premotor activation ipsilateral to the moving hand (*red arrow*) serves as a functional landmark for the precentral gyrus in hemiparetic patients (a clinical case is presented in [Fig. 7.13](#)). Premotor activation is typically localized at the anterior wall of the precentral gyrus directly adjacent to the

junction of the precentral sulcus with the superior frontal sulcus. It is important to note that this functional landmark does not localize the motor hand area! In the drawing of the cortical motor and somatosensory network (*right*) numbers indicate Brodmann areas. Reprinted from Stippich 2007, p 113 with permission

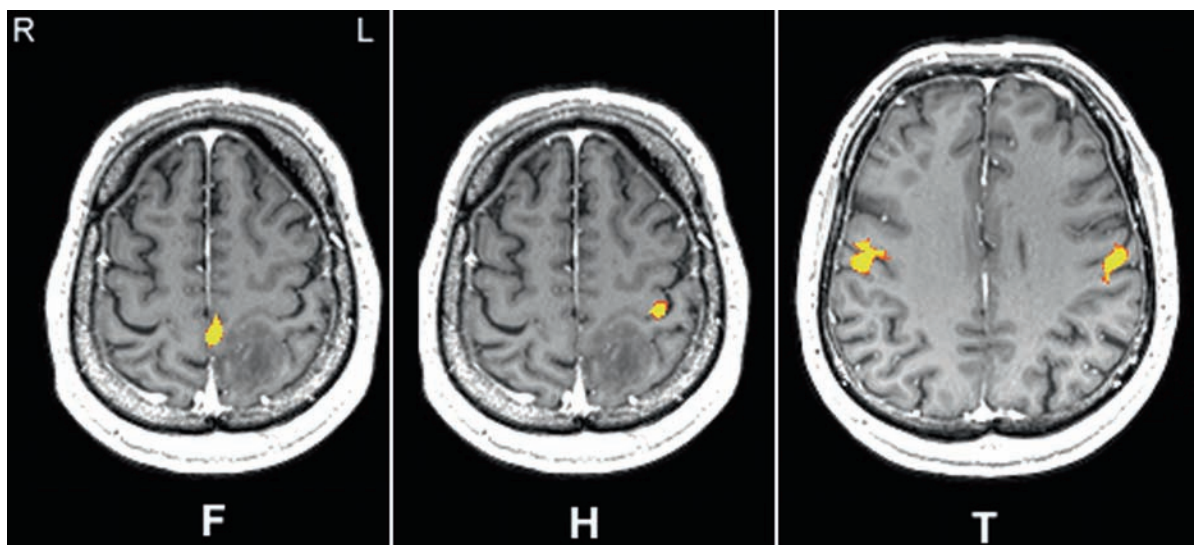


**Fig. 7.8** Standard presurgical fMRI protocol: Somatotopic mapping of the motor cortex (same patient as in [Fig. 7.2](#)). The cortical foot representation (*F*) is closely related to the left pari-

eto-postcentral anaplastic glioma. BOLD-activation of the motor hand area (*H*) is localized at the hand knob and the bilateral tongue representations (*T*) at the level of the ventricular roof

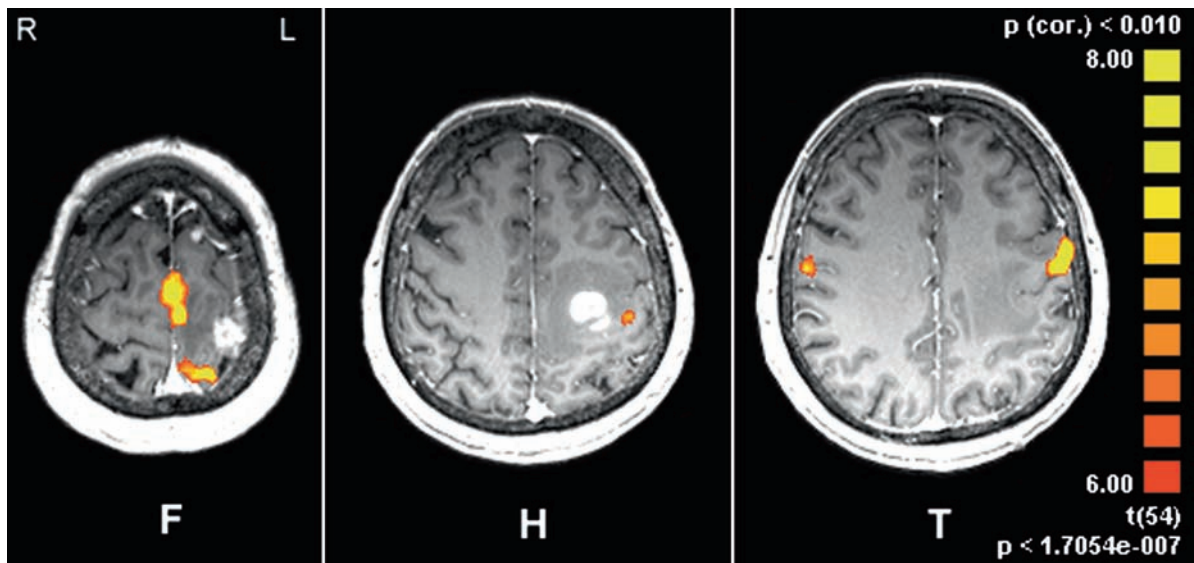


**Fig. 7.9** Somatotopic fMRI mapping of the motor cortex in a patient with a left precentral glioblastoma precluding identification of the motor hand area using morphological landmarks.

fMRI clearly indicates the position of the motor hand area during contralateral hand movements (*H*) as well as the cortical foot (*F*) and tongue representations (*T*)

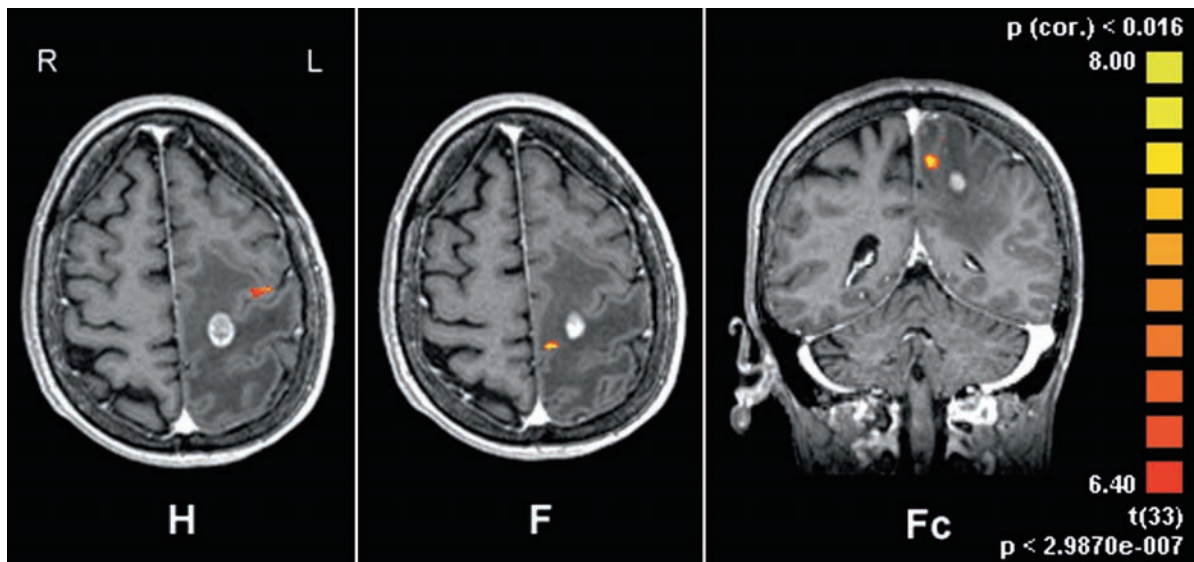


**Fig. 7.10** Somatotopic fMRI mapping of the upper motor cortex in a patient with a left central metastasis indicating the spatial relationship to the cortical hand (*H*) and foot (*F*) representation.

The latter is also displayed in coronal view (*Fc*). Additional fMRI localization of the motor tongue representations was not necessary by anatomical consideration

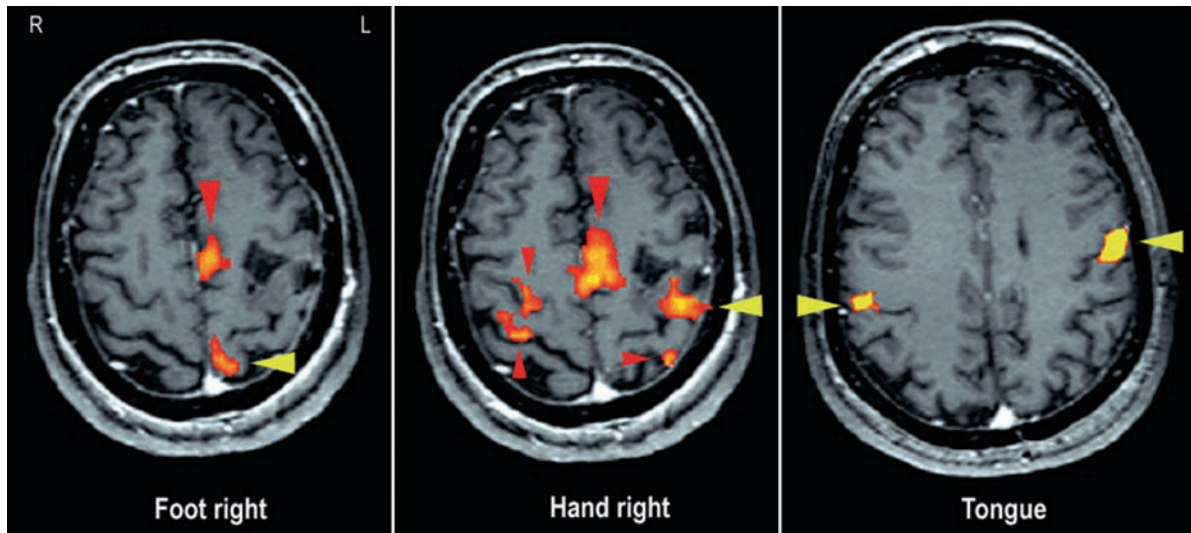


**Fig. 7.11** Presurgical fMRI somatotopic mapping of the motor cortex in a hemiparetic patient with a recurrent left rolandic astrocytoma prior to repeated surgery. Foot, hand and tongue movements revealed robust fMRI activation of the respective primary motor cortex body representations (yellow arrowheads).

Note the increased activation in secondary areas (red arrowheads): in the supplementary motor area during toe and finger movements and in the whole cortical motor network in both hemispheres during finger movements, Reprinted from Stippich 2007, p 111 with permission

### 7.7.2 Somatotopic Mapping of the Primary Somatosensory Cortex

This fMRI protocol was designed to localize the different somatosensory body representations of the postcentral gyrus (Stippich et al. 1999). The somatosensory stimuli are transmitted to the lips, fingers and toes contralateral to the brain lesion. In presurgical fMRI somatotopic somatosensory mapping is mostly used as diagnostic adjunct, when motor paradigms are difficult to apply – e.g., in uncooperative, sedated or hemiparetic patients or in children, but there is also potential for standardized follow up measurements on neuroplastic changes of the somatosensory system. This presurgical fMRI protocol enables a fully automated assessment of the spatial relationship between brain tumors and the postcentral gyrus, facilitating the estimation of possible postoperative sensory deficits (Fig. 7.12). Diagnostic information about the spatial relationship between the central sulcus or precentral gyrus and precentral or frontal brain tumors can be obtained rather indirectly as both anatomical structures are directly adjacent to the postcentral gyrus in the anterior direction.

### 7.7.3 Localization of the Precentral Gyrus in Patients with Paresis

This special protocol was designed in volunteers to help localize the precentral gyrus in patients with contralateral paresis (Stippich et al. 2000). The clinical application is still experimental and requires own validation. In these patients the primary motor cortex is commonly infiltrated by the tumor or severely compressed precluding both, reliable identification of the rolandic anatomy on morphological images and proper performance of contralateral movements for presurgical fMRI. However, as a basic principle, residual contralateral motor function and passive somatosensory stimulation should be used first for the functional localization of the pre and postcentral gyrus. As a further adjunct, complex finger opposition of the nonparetic hand ipsilateral to the brain tumor can be used to activate the whole cortical motor network in both hemispheres. The premotor activation on the tumors side, may serve as an additional functional landmark for the precentral gyrus, by localizing the anterior wall of the precentral gyrus near the junction of the precentral sulcus with the posterior part of the superior

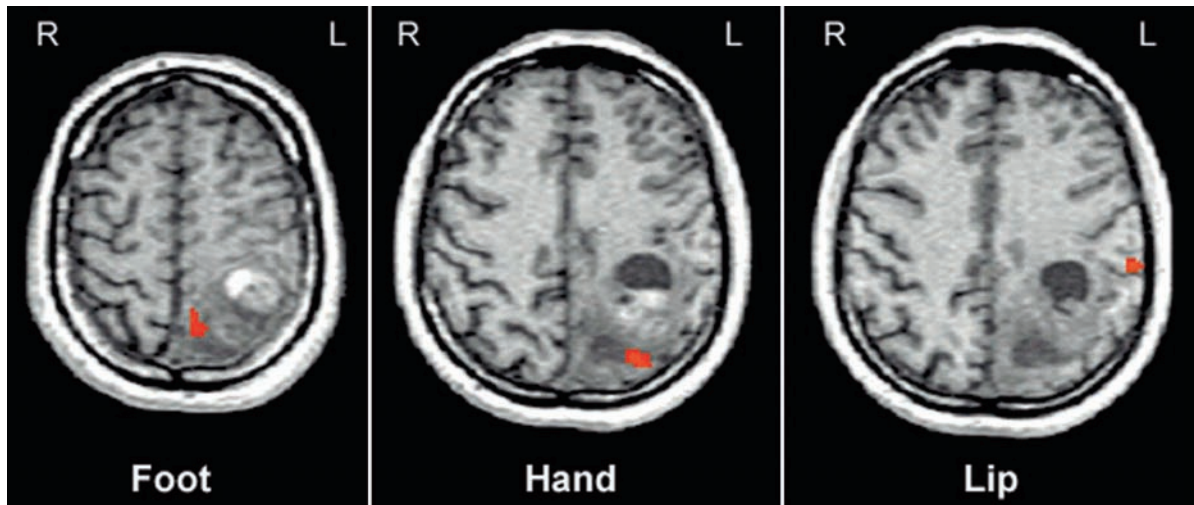


**Fig. 7.12** Presurgical fMRI somatotopic mapping of the primary somatosensory cortex (S1) in a left parietal malignant glioma indicated compression of the upper postcentral gyrus at the level

of the foot representation and tumor growth into the lower postcentral gyrus with dorsal displacement of the S1 hand representation. Reprinted from Stippich 2007, p 112 with permission

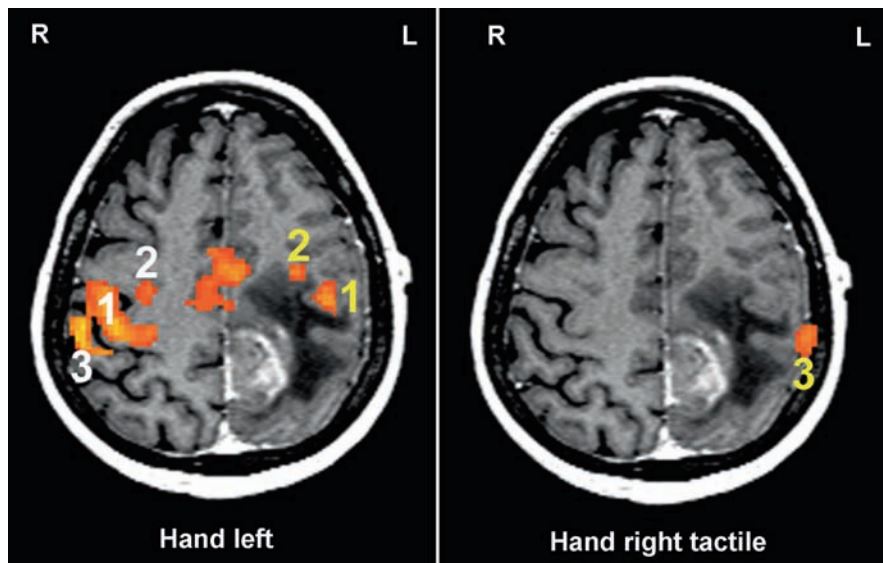


**Fig. 7.13** Presurgical fMRI protocol for patients with preexisting paresis. This protocol may serve as an adjunct to the standard protocol using movements contralateral to the brain tumor. The application is still experimental and requires own validation. In this hemiparetic patient (grade 3/5) with a left malignant glioma only weak BOLD activation was available from contralateral (*right*) hand movements precluding reliable localization of the motor hand area (not shown). By using complex finger

opposition of the unimpaired hand ipsilateral to the tumor (*left*) and fully automated tactile stimulation of the right digits BOLD activation is achievable in the motor hand area (1), premotor cortex (2) and primary somatosensory cortex (3) on the tumors side. Note the corresponding activations in the unimpaired hemisphere (*right*) associated with the left finger movements (*white numbers*). Bilateral supplementary motor activation is in the midline

frontal sulcus (Fig. 7.13). It is important to note that the risk of surgery related motor deficits cannot be estimated using premotor activation as a functional landmark! However, in healthy volunteers, primary motor

coactivation can be observed frequently localizing the motor hand area ipsilateral to the moving hand (Stippich et al. 2007). Our initial clinical experience indicates, that ipsilateral primary motor coactivation

may be supportive to localize the motor hand area on the tumor side in hemiparetic patients.

Note: For all preoperative fMRI protocols presented here, the combination with anisotropic diffusion weighted MRI or DTI (FA-mapping, DTI-tractography) is highly recommended to also delineate the effects of the rolandic pathologies on the pyramidal tract (Stippich et al. 2003).

## 7.8 Limitations and Pitfalls

Traditionally, functional areas are electrophysiologically mapped intraoperatively to reliably assess the spatial relationship between brain tumor and functional cortex (Ojemann et al. 1989; Duffau et al. 1999). Intraoperative EcoG is considered very reliable, but the sensitivity to detect motor function in the proximity of rolandic brain tumors can be low (Shinoura et al. 2005) and the method comprises several disadvantages. Surgery time can be substantially prolonged or patients need to be subjected to awake craniotomy. Furthermore, it is possible to derive activations only from the brain surface, while the by far larger portion of the cortex deep in the cerebral convolutions remains inaccessible (Cosgrove et al. 1996). Another significant disadvantage of EcoG is that the information is not available preoperatively and can not be implemented in the assessment of the indication to operate and the planning of function-preserving surgery. After all, morphological imaging provides very detailed information about intracranial pathologies (Osborn 2004), but not about brain function. fMRI is capable of overcoming these disadvantages of the “traditional diagnostic procedures” by visualizing anatomy, pathology, and function noninvasively in a single examination even prior to surgery.

When carried out in a standard way, fMRI is basically capable of providing a clinical “functional diagnosis” for individual patients (Thulborn 2006). Functional landmarks help to estimate possible therapy-related deficits and are thus particularly useful in providing patient information, verifying the indication and selecting a sparing therapeutic procedure. Once the operation has been decided upon, careful planning and appropriate selection of incision, trepanation, surgical access and resection margins are essential to function-preserving surgery. Intraoperatively, functional localizations facilitate surgical orientation, although inaccuracies

resulting from displaced brain tissue need to be taken into consideration (Stippich et al. 2002; Stippich et al. 2003). All these factors increase patient safety and reduce the risk of postoperative deficits which additionally reduce quality of life.

According to current knowledge, one can assume that presurgical fMRI is able to contribute to a reduction of invasive diagnostic procedures both before and during neurosurgical interventions in patients with brain tumors. Whether fMRI can have a positive effect on surgery-related morbidity and disease-related mortality remains to be determined in prospective studies. Prerequisites for this include a consensus on performance, analysis and medical appraisal of presurgical fMRI, as well as the delineation of recommendations and guidelines by the assigned medical societies.

Preoperative fMRI has limitations imposed by patient-specific and methodological factors. Despite intensive patient training, optimized examination protocols and appropriate head fixation, some patients cannot be examined due to poor cooperation or marked restlessness. When motor paradigms are used, undesirable continuation of movement during resting periods, mostly uncontrolled and interspersed accompanying movements in other parts of the body, can significantly compromise the quality of the examination, even if individually adjusted evaluation is used to register the error precisely. In the end, after this time-consuming process, examination results often need to be discarded. The same holds true for strong motion artifacts which cannot be corrected at later data processing stages. Stimulus-related motion artifacts can simulate activations, leading to false high BOLD signals or even to incorrect localization (Hajnal et al. 1994; Krings et al. 2001; Hoeller et al. 2002; Steger and Jackson 2004). With regard to the appearance of motion artifacts, tongue and toe movements, as well as finger opposition tasks are less critical than hand, foot and lip movements.

The problems associated with investigating motor function in patients with tumor-related hemipareses have already been addressed (see Sect. 4.4.6). In most cases, functional localization of the pre and postcentral gyrus can be achieved by using residual motor function in the affected extremities and applying special paradigms (Stippich et al. 2003). Compared to motor fMRI, BOLD signals are significantly weaker on tactile stimulation. Particularly in the lower extremities, tactile stimulation does not always achieve sufficient activation. This is accounted for by the lower number of

receptors in toe tips, the comparatively small cortical toe representation and ill defined compressed air pulses when long pneumatic tubes are used.

The BOLD signals based on fMRI originate mainly in the capillary bed of the activated brain area and downstream veins (Frahm et al. 1994; Menon et al. 1995). Thus, fMRI measures a hemodynamic secondary phenomenon and not neuronal activity directly. Possible localization errors due to BOLD signals from draining veins can be identified by superimposing functional image data onto contrast-enhanced anatomical T1-weighted image sequences (Krings et al. 1999). Careful analysis of the signal-time curves of functional raw data helps to distinguish between parenchymatous and venous activation, since these rise at different rates (Krings et al. 2001). By causing vessel compression and pathological changes in vascular autoregulation, brain tumors can affect the localization and intensity of the BOLD signals measured (Holodny et al. 1999; Holodny et al. 2000; Krings et al. 2002; Ulmer et al. 2003; Ulmer et al. 2004; Kim et al. 2005; Liu et al. 2005; Hou et al. 2006; Ludemann et al. 2006). Whether artificial activations can occur due to their neovascularization remains to be clarified. For this reason, activations within contrast-enhanced tumor portions should be assessed as artifacts until reliable study results are available. Such activations should not be used for risk assessment, surgery planning or functional neuronavigation. The same is true for BOLD signals in strongly vascularized cerebral metastases AVM (Lazar et al. 1997; Alkadhi et al. 2000; Lehericy et al. 2002; Ozdoba et al. 2002).

Investigator-dependent inaccuracies occur in manual superposition of EPI data, distorted by the method, onto anatomical 3D data sets. As a precaution, a possible localization error of approximately 0.5 cm should always be assumed (Stippich et al. 2003). Improvements are expected in the future when distortion corrections for EPI data sets are available for clinical application (Weiskopf et al. 2005; Liu and Ogawa 2006; Priest et al. 2006), enabling superposition routines to be automated. We consider defining resection margins in presurgical diagnostics on the basis of fMRI data as unreliable, since the spatial extent of activated areas depends on the evaluation parameters chosen and can therefore vary. In addition, the position of brain structures can change intraoperatively (“brain shift”), with the result that data obtained preoperatively no longer

accurately reflect the intraoperative situation (Wirtz et al. 1997; Wittek et al. 2005; Nimsy et al. 2006). Effluent cerebrospinal fluid alone can lead to shifts of several millimeters after opening of the dura. Moreover, there is often a sharp shift in the position of the brain due to tissue resection. For these reasons, preoperative fMRI cannot replace intraoperative mapping of brain function completely. Irrespective of functional imaging, additional technical inaccuracies must be taken into consideration in neuronavigation and referencing.

Text and figures have been reproduced in part from Stippich 2007 with permission.

## References

- Achten E, Jackson GD et al (1999) Presurgical evaluation of the motor hand area with functional MR imaging in patients with tumors and dysplastic lesions. *Radiology* 210(2): 529–538
- Alkadhi H, Kollias SS et al (2000) Plasticity of the human motor cortex in patients with arteriovenous malformations: a functional MR imaging study. *AJNR Am J Neuroradiol* 21(8):1423–1433
- Atlas SW, Howard RS II et al (1996) Functional magnetic resonance imaging of regional brain activity in patients with intracerebral gliomas: findings and implications for clinical management. *Neurosurgery* 38(2):329–338
- Bandettini PA, Wong EC et al (1992) Time course EPI of human brain function during task activation. *Magn Reson Med* 25(2):390–397
- Baumann SB, Noll DC et al (1995) Comparison of functional magnetic resonance imaging with positron emission tomography and magnetoencephalography to identify the motor cortex in a patient with an arteriovenous malformation. *J Image Guid Surg* 1(4):191–197
- Belliveau JW, Kennedy DN et al (1991) Functional mapping of the human visual cortex by magnetic resonance imaging. *Science* 254(5032):716–719
- Bittar RG, Olivier A et al (1999) Presurgical motor and somatosensory cortex mapping with functional magnetic resonance imaging and positron emission tomography. *J Neurosurg* 91(6):915–921
- Bittar RG, Olivier A et al (2000) Cortical motor and somatosensory representation: effect of cerebral lesions. *J Neurosurg* 92(2):242–248
- Carpentier AC, Constable RT et al (2001) Patterns of functional magnetic resonance imaging activation in association with structural lesions in the rolandic region: a classification system. *J Neurosurg* 94(6):946–954
- Cosgrove GR, Buchbinder BR, Jiang H (1996) Functional magnetic resonance imaging for intracranial navigation. *Neurosurg Clin N Am* 7(2):313–322
- Duffau H, Capelle L et al (1999) Intra-operative direct electrical stimulations of the central nervous system: the Salpêtrière experience with 60 patients. *Acta Neurochir (Wien)* 141(11):1157–1167

- Dymarkowski S, Sunaert S et al (1998) Functional MRI of the brain: localisation of eloquent cortex in focal brain lesion therapy. *Eur Radiol* 8(9):1573–1580
- Feigl GC, Safavi-Abbasi S et al (2008) Real-time 3T fMRI data of brain tumour patients for intra-operative localization of primary motor areas. *Eur J Surg Oncol* 34(6):708–715
- Fesl G, Moriggl et al (2003) Inferior central sulcus: variations of anatomy and function on the example of the motor tongue area. *Neuroimage* 20(1):601–610
- Frahm J, Merboldt KD et al (1994) Brain or vein – oxygenation or flow? On signal physiology in functional MRI of human brain activation. *NMR Biomed* 7(1–2):45–53
- Gasser T, Ganslandt O et al (2005) Intraoperative functional MRI: implementation and preliminary experience. *Neuroimage* 26(3):685–693
- Geerts J, Martens M et al (2007) Functional magnetic resonance imaging for preoperative localisation of eloquent brain areas relative to brain tumours: clinical implementation in a regional hospital. *JBR-BTR* 90(4):258–263
- Golaszewski SM, Zschiegner F et al (2002) A new pneumatic vibrator for functional magnetic resonance imaging of the human sensorimotor cortex. *Neurosci Lett* 324(2):125–128
- Golaszewski SM, Siedentopf CM et al (2004) Modulatory effects on human sensorimotor cortex by whole-hand afferent electrical stimulation. *Neurology* 62(12):2262–2269
- Golaszewski SM, Siedentopf CM et al (2006) Human brain structures related to plantar vibrotactile stimulation: a functional magnetic resonance imaging study. *Neuroimage* 29(3):923–239
- Haberg A, Kvistad KA et al (2004) Preoperative blood oxygen level-dependent functional magnetic resonance imaging in patients with primary brain tumors: clinical application and outcome. *Neurosurgery* 54(4):902–914; discussion 914–915
- Hajnal JV, Myers R et al (1994) Artifacts due to stimulus correlated motion in functional imaging of the brain. *Magn Reson Med* 31(3):283–291
- Hall WA, Liu H, Truwit CL (2005) Functional magnetic resonance imaging-guided resection of low-grade gliomas. *Surg Neurol* 64(1):20–27; discussion 27
- Hirsch J, Ruge MI et al (2000) An integrated functional magnetic resonance imaging procedure for preoperative mapping of cortical areas associated with tactile, motor, language, and visual functions. *Neurosurgery* 47(3):711–721; discussion 721–722
- Hoeller M, Krings T et al (2002) Movement artefacts and MR BOLD signal increase during different paradigms for mapping the sensorimotor cortex. *Acta Neurochir (Wien)* 144(3):279–284; discussion 284
- Holodny AI, Schulder M et al (1999) Decreased BOLD functional MR activation of the motor and sensory cortices adjacent to a glioblastoma multiforme: implications for image-guided neurosurgery. *AJNR Am J Neuroradiol* 20(4):609–612
- Holodny AI, Schulder M et al (2000) The effect of brain tumors on BOLD functional MR imaging activation in the adjacent motor cortex: implications for image-guided neurosurgery. *AJNR Am J Neuroradiol* 21(8):1415–1422
- Holodny AI, Schwartz TH et al (2001) Tumor involvement of the corticospinal tract: diffusion magnetic resonance tractography with intraoperative correlation. *J Neurosurg* 95(6):1082
- Hou BL, Bradbury M et al (2006) Effect of brain tumor neovasculation defined by rCBV on BOLD fMRI activation volume in the primary motor cortex. *Neuroimage* 32(2):489–497
- Jack CR, Thompson PM et al (1994) Sensory motor cortex: correlation of presurgical mapping with functional MR imaging and invasive cortical mapping. *Radiology* 190(1):85–92
- Jacobs AH, Kracht LW et al (2005) Imaging in neurooncology. *NeuroRx* 2(2):333–347
- Kampe KK, Jones RA, Auer DP (2000) Frequency dependence of the functional MRI response after electrical median nerve stimulation. *Hum Brain Mapp* 9(2):106–114
- Kim MJ, Holodny AI et al (2005) The effect of prior surgery on blood oxygen level-dependent functional MR imaging in the preoperative assessment of brain tumors. *AJNR Am J Neuroradiol* 26(8):1980–1985
- Kokkonen SM, Kiviniemi V et al (2005) Effect of brain surgery on auditory and motor cortex activation: a preliminary functional magnetic resonance imaging study. *Neurosurgery* 57(2):249–256; discussion 249–256
- Krainik A, Lehericy S et al (2001) Role of the supplementary motor area in motor deficit following medial frontal lobe surgery. *Neurology* 57(5):871–878
- Krainik A, Lehericy S et al (2003) Postoperative speech disorder after medial frontal surgery: role of the supplementary motor area. *Neurology* 60(4):587–594
- Krainik A, et al (2004) Role of the healthy hemisphere in recovery after resection of the supplementary motor area. *Neurology* 62(8):1323–32
- Krings T, Reul J et al (1998) Functional magnetic resonance mapping of sensory motor cortex for image-guided neurosurgical intervention. *Acta Neurochir (Wien)* 140(3):215–222
- Krings T, Erberich SG et al (1999) MR blood oxygenation level-dependent signal differences in parenchymal and large draining vessels: implications for functional MR imaging. *AJNR Am J Neuroradiol* 20(10):1907–1414
- Krings T, Reinges MH et al (2001) Functional MRI for presurgical planning: problems, artefacts, and solution strategies. *J Neurol Neurosurg Psychiatry* 70(6):749–760
- Krings T, Reinges MH et al (2002) Factors related to the magnitude of T2\* MR signal changes during functional imaging. *Neuroradiology* 44(6):459–466
- Krings T, Topper R et al (2002) Activation in primary and secondary motor areas in patients with CNS neoplasms and weakness. *Neurology* 58(3):381–390
- Krishnan R, Raabe A et al (2004) Functional magnetic resonance imaging-integrated neuronavigation: correlation between lesion-to-motor cortex distance and outcome. *Neurosurgery* 55(4):904–914; discussion 914–915
- Kurth R, Villringer K et al (1998) fMRI assessment of somatotopy in human Brodmann area 3b by electrical finger stimulation. *Neuroreport* 9(2):207–212
- Kwong KK, Belliveau JW et al (1992) Dynamic magnetic resonance imaging of human brain activity during primary sensory stimulation. *Proc Natl Acad Sci USA* 89(12):5675–5679
- Lazar RM, Marshall RS et al (1997) Anterior translocation of language in patients with left cerebral arteriovenous malformation. *Neurology* 49(3):802–808
- Lee CC, Ward HA et al (1999) Assessment of functional MR imaging in neurosurgical planning. *AJNR Am J Neuroradiol* 20(8):1511–1519

- Lehericy S, Duffau H et al (2000) Correspondence between functional magnetic resonance imaging somatotopy and individual brain anatomy of the central region: comparison with intraoperative stimulation in patients with brain tumors. *J Neurosurg* 92(4):589–598
- Lehericy S, Biondi A et al (2002) Arteriovenous brain malformations: is functional MR imaging reliable for studying language reorganization in patients? Initial observations. *Radiology* 223(3):672–682
- Liu G, Ogawa S (2006) EPI image reconstruction with correction of distortion and signal losses. *J Magn Reson Imaging* 24(3):683–689
- Liu WC, Feldman SC et al (2005) The effect of tumour type and distance on activation in the motor cortex. *Neuroradiology* 47(11):813–819
- Ludemann L, Forschler A et al (2006) BOLD signal in the motor cortex shows a correlation with the blood volume of brain tumors. *J Magn Reson Imaging* 23(4):435–443
- Majos A, Tybor K et al (2005) Cortical mapping by functional magnetic resonance imaging in patients with brain tumors. *Eur Radiol* 15(6):1148–1158
- Menon RS, Ogawa S et al (1995) BOLD based functional MRI at 4 Tesla includes a capillary bed contribution: echo-planar imaging correlates with previous optical imaging using intrinsic signals. *Magn Reson Med* 33(3):453–459
- Moller M, Freund M et al (2005) Real time fMRI: a tool for the routine presurgical localisation of the motor cortex. *Eur Radiol* 15(2):292–295
- Mueller WM, Yetkin FZ et al (1996) Functional magnetic resonance imaging mapping of the motor cortex in patients with cerebral tumors. *Neurosurgery* 39(3):515–520; discussion 520–521
- Nimsky C, Ganslandt O et al (2006) Intraoperative visualization for resection of gliomas: the role of functional neuronavigation and intraoperative 1.5 T MRI. *Neurol Res* 28(5): 482–487
- Ogawa S et al (1993) Functional brain mapping by blood oxygenation level-dependent contrast magnetic resonance imaging. A comparison of signal characteristics with a biophysical model. *Biophys J* 64(3):803–812
- Ojemann G, Ojemann J et al (1989) Cortical language localization in left, dominant hemisphere. An electrical stimulation mapping investigation in 117 patients. *J Neurosurg* 71(3):316–326
- Osborn A (2004) *Diagnostic Imaging – Brain*. Amirsys, Salt Lake City, USA
- Ozdoba C, Nirkko AC et al (2002) Whole-brain functional magnetic resonance imaging of cerebral arteriovenous malformations involving the motor pathways. *Neuroradiology* 44(1):1–10
- Parmar H, Sitoh YY, Yeo TT (2004) Combined magnetic resonance tractography and functional magnetic resonance imaging in evaluation of brain tumors involving the motor system. *J Comput Assist Tomogr* 28(4):551–556
- Petrella JR, Shah LM et al (2006) Preoperative functional MR imaging localization of language and motor areas: effect on therapeutic decision making in patients with potentially resectable brain tumors. *Radiology* 240(3):793–802
- Pirotte B, Goldman S, et al (2005) Integration of [11C]methionine-positron emission tomographic and magnetic resonance imaging for image-guided surgical resection of infiltrative low-grade brain tumors in children. *Neurosurgery*. 57 (1 Suppl):128–39
- Pirotte B, Voordecker P et al (2005) Combination of functional magnetic resonance imaging-guided neuronavigation and intraoperative cortical brain mapping improves targeting of motor cortex stimulation in neuropathic pain. *Neurosurgery* 56(2 Suppl):344–59; discussion 344–359
- Priest AN, De Vita E et al (2006) EPI distortion correction from a simultaneously acquired distortion map using TRAIL. *J Magn Reson Imaging* 23(4):597–603
- Puce A, Constable RT et al (1995) Functional magnetic resonance imaging of sensory and motor cortex: comparison with electrophysiological localization. *J Neurosurg* 83(2):262–270
- Pujol J, Conesa G et al (1996) Presurgical identification of the primary sensorimotor cortex by functional magnetic resonance imaging. *J Neurosurg* 84(1):7–13
- Pujol J, Conesa G et al (1998) Clinical application of functional magnetic resonance imaging in presurgical identification of the central sulcus. *J Neurosurg* 88(5):863–869
- Ramsey NF, Sommer IE et al (2001) Combined analysis of language tasks in fMRI improves assessment of hemispheric dominance for language functions in individual subjects. *Neuroimage* 13(4):719–733
- Reinges MH, Krings T et al (2005) Prospective demonstration of short-term motor plasticity following acquired central pareses. *Neuroimage* 24(4):1248–1255
- Roessler K, Donat M et al (2005) Evaluation of preoperative high magnetic field motor functional MRI (3 Tesla) in glioma patients by navigated electrocortical stimulation and postoperative outcome. *J Neurol Neurosurg Psychiatry* 76(8):1152–1157
- Rolls HK, Yoo SS et al (2007) Rater-dependent accuracy in predicting the spatial location of functional centers on anatomical MR images. *Clin Neurol Neurosurg* 109(3):225–235
- Roux FE, Ranjeva JP et al (1997) Motor functional MRI for presurgical evaluation of cerebral tumors. *Stereotact Funct Neurosurg* 68(1–4 Pt 1):106–111
- Roux FE, Boulanouar K et al (1999a) Cortical intraoperative stimulation in brain tumors as a tool to evaluate spatial data from motor functional MRI. *Invest Radiol* 34(3): 225–229
- Roux FE, Boulanouar K et al (1999b) Usefulness of motor functional MRI correlated to cortical mapping in Rolandic low-grade astrocytomas. *Acta Neurochir (Wien)* 141(1):71–79
- Rutten GJ, Ramsey NF et al (2002) Interhemispheric reorganization of motor hand function to the primary motor cortex predicted with functional magnetic resonance imaging and transcranial magnetic stimulation. *J Child Neurol* 17(4): 292–297
- Schlosser MJ, McCarthy G et al (1997) Cerebral vascular malformations adjacent to sensorimotor and visual cortex. Functional magnetic resonance imaging studies before and after therapeutic intervention. *Stroke* 28(6):1130–1137
- Schonberg T, Pianka P et al (2006) Characterization of displaced white matter by brain tumors using combined DTI and fMRI. *Neuroimage* 30(4):1100–1111
- Schreiber A, Hubbe U et al (2000) The influence of gliomas and nonglial space-occupying lesions on blood-oxygen-level-dependent contrast enhancement. *AJNR Am J Neuroradiol* 21(6):1055–1063
- Schwindack C, Siminotto E et al (2005) Real-time functional magnetic resonance imaging (rt-fMRI) in patients with brain tumours: preliminary findings using motor and language paradigms. *Br J Neurosurg* 19(1):25–32

- Shinoura N, Yamada R et al (2005) Preoperative fMRI, tractography and continuous task during awake surgery for maintenance of motor function following surgical resection of metastatic tumor spread to the primary motor area. *Minim Invasive Neurosurg* 48(2):85–90
- Shinoura N, Suzuki Y et al (2006) Restored activation of primary motor area from motor reorganization and improved motor function after brain tumor resection. *AJNR Am J Neuroradiol* 27(6):1275–1282
- Steger TR, Jackson EF (2004) Real-time motion detection of functional MRI data. *J Appl Clin Med Phys* 5(2):64–70
- Stippich C (2005) Clinical functional magnetic resonance imaging: basic principles and clinical applications. *Radiologie up2date* 5:317–336
- Stippich C (ed) (2007) *Clinical functional MRI: presurgical functional neuroimaging*. Springer, New York; ISBN 978-3-540-24469-1
- Stippich C, Hofmann R et al (1999) Somatotopic mapping of the human primary somatosensory cortex by fully automated tactile stimulation using functional magnetic resonance imaging. *Neurosci Lett* 277(1):25–28
- Stippich C, Kapfer D et al (2000) Robust localization of the contralateral precentral gyrus in hemiparetic patients using the unimpaired ipsilateral hand: a clinical functional magnetic resonance imaging protocol. *Neurosci Lett* 285(2): 155–159
- Stippich C, Heiland S et al (2002) Functional magnetic resonance imaging: physiological background, technical aspects and prerequisites for clinical use. *Rofo* 174(1):43–49
- Stippich C, Ochmann H, Sartor K (2002) Somatotopic mapping of the human primary sensorimotor cortex during motor imagery and motor execution by functional magnetic resonance imaging. *Neurosci Lett* 331(1):50–54
- Stippich C, Kress B et al (2003) Preoperative functional magnetic resonance tomography (fMRI) in patients with rolandic brain tumors: indication, investigation strategy, possibilities and limitations of clinical application. *Rofo* 175(8):1042–1050
- Stippich C, Romanowski A et al (2004) Fully automated localization of the human primary somatosensory cortex in one minute by functional magnetic resonance imaging. *Neurosci Lett* 364(2):90–93
- Stippich C, Blatow M et al (2007) Global activation of primary motor cortex during voluntary movements in man. *Neuroimage* 34:1227–1237
- Ternovoi SK, Sinitsyn VE et al (2004) Localization of the motor and speech zones of the cerebral cortex by functional magnetic resonance tomography. *Neurosci Behav Physiol* 34(5):431–437
- Thulborn K (2006) *Clinical functional magnetic resonance imaging, current protocols in magnetic resonance imaging*. Wiley, EM Haacke
- Ulmer JL, Krouwer HG et al (2003) Pseudo-reorganization of language cortical function at fMR imaging: a consequence of tumor-induced neurovascular uncoupling. *AJNR Am J Neuroradiol* 24(2):213–217
- Ulmer JL, Salvati CV et al (2004) The role of diffusion tensor imaging in establishing the proximity of tumor borders to functional brain systems: implications for preoperative risk assessments and postoperative outcomes. *Technol Cancer Res Treat* 3(6):567–576
- Van Westen D, Skagerberg G et al (2005) Functional magnetic resonance imaging at 3T as a clinical tool in patients with intracranial tumors. *Acta Radiol* 46(6):599–609
- Wienbruch C, et al (2006) A portable and low-cost fMRI compatible pneumatic system for the investigation of the somatosensory system in clinical and research environments. *Neurosci Lett* 398(3):183–8
- Weiskopf N, Klose U et al (2005) Single-shot compensation of image distortions and BOLD contrast optimization using multi-echo EPI for real-time fMRI. *Neuroimage* 24(4): 1068–1079
- Wirtz CR, Tronnier VM et al (1997) Image-guided neurosurgery with intraoperative MRI: update of frameless stereotaxy and radicality control. *Stereotact Funct Neurosurg* 68(1–4 Pt 1):39–43
- Wittek A, Kikinis R et al (2005) Brain shift computation using a fully nonlinear biomechanical model. *Med Image Comput Comput Assist Interv Int Conf Med Image Comput Comput Assist Interv* 8(Pt 2):583–590
- Yousry TA, Schmid UD et al (1997) Localization of the motor hand area to a knob on the precentral gyrus. A new landmark. *Brain* 120:(Pt 1):141–157

# The Functional Anatomy of Speech Processing: From Auditory Cortex to Speech Recognition and Speech Production

8

Gregory Hickok

## 8.1 Introduction

Lesion-based research has been successful in providing a broad outline of the neuroanatomy of speech/language processes (Dronkers et al. 2000; Hillis 2007), and continues to play a crucial role in the development of functional anatomic models of cognitive processes (Fellows et al. 2005). However, lesion studies lack the spatial resolution to assess more detailed functional anatomical hypotheses. Functional imaging methods such as fMRI, when appropriately, guided and constrained by lesion and other methods, can provide much needed information.

In this chapter, we will review evidence regarding the functional anatomy of the human auditory cortex as it relates to speech recognition and speech production. Fig. 8.1 displays an organizational framework for this discussion.

## 8.2 Hierarchical Organization of Auditory Cortex

The monkey auditory cortex is organized hierarchically with a core region at the center, a belt region surrounding the core, and a parabelt region surrounding the belt area, each containing subdivisions. The core corresponds to the primary auditory cortex, showing a distinct primary-type cytoarchitecture and robust single unit responses to pure tones, with sharp tuning curves relative to belt regions. Both the core and the

belt areas receive inputs from the medial geniculate nucleus (MGN), although from different subregions, MGv and MGd, respectively. The parabelt also receives direct ascending auditory input from MGd, but is distinguished from the belt area in that it does not receive direct input from the core. Instead, information reaching the parabelt from the core, appears to be mediated by the belt region which projects heavily to the parabelt (Kaas and Hackett 2000; Kaas et al. 1999).

The human auditory cortex appears to be similar in its hierarchical organization. Simple acoustic stimulation, such as noise bursts or tones, activates the auditory cortex in and around heschl's gyrus. In addition, more complex stimuli, such as speech, activate a broader region, including the superior temporal sulcus (STS) (Binder et al. 2000).

In both human and nonhuman primates, there is evidence for two broad projection streams, sometimes referred to as the ventral and dorsal pathways (Hickok and Poeppel 2000, 2007; Rauschecker 1998; Romanski et al. 1999; Scott 2005). There is a general agreement that the ventral stream supports recognition of the content of auditory information (a "what" pathway), but there is disagreement regarding the nature of the dorsal stream, with some authors promoting a location-based function ("where" pathway) (Rauschecker 1998), and others an auditory-motor integration function (Hickok et al. 2003; Hickok and Poeppel 2000, 2007; Warren et al. 2005). These hypotheses are not necessarily incompatible.

## 8.3 STS Supports Phonological Aspects of Speech Recognition

A number of studies have found that portions of the STS are important for representing and/or processing phonological information (Fig. 8.1, yellow)

---

G. Hickok  
Department of Cognitive Sciences, Center for Cognitive Neuroscience, University of California, SSPA4109, Irvine, CA 92697, USA  
e-mail: gshickok@uci.edu

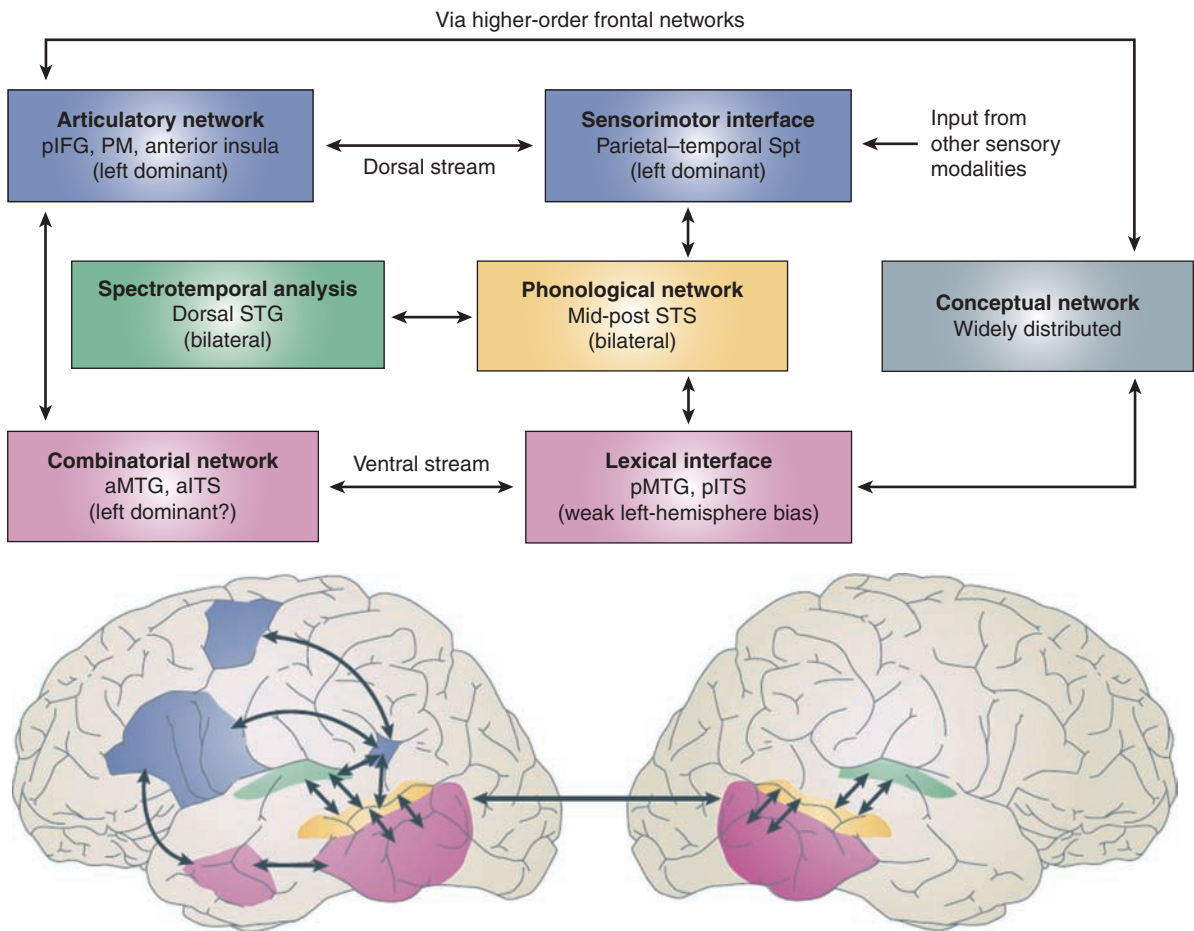


**Fig. 8.1** The dual-stream model of the functional anatomy of language. (a) Schematic diagram of the dual-stream model. The earliest stage of cortical speech processing involves some form of spectrotemporal analysis, which is carried out in auditory cortices bilaterally in the supratemporal plane. These spectrotemporal computations appear to differ between the two hemispheres. Phonological-level processing and representation involves the middle to posterior portions of the superior temporal sulcus (STS) bilaterally, although there may be a weak left-hemisphere bias at this level of processing. Subsequently, the system diverges into two broad streams, a dorsal pathway (*blue*) that maps sensory or phonological representations onto articulatory motor representations, and a ventral pathway (*pink*) that maps sensory or phonological representations onto lexical conceptual representations. (b) Approximate anatomical locations of the dual-stream model components, specified as precisely as available evidence allows. Regions shaded *green* depict areas on the dorsal surface of the superior temporal gyrus (STG) that are proposed to be involved in spectrotempo-

ral analysis. Regions shaded *yellow* in the posterior half of the STS are implicated in phonological-level processes. Regions shaded *pink* represent the ventral stream, which is bilaterally organized with a weak left-hemisphere bias. The more posterior regions of the ventral stream, posterior middle and inferior portions of the temporal lobes correspond to the lexical interface, which links phonological and semantic information, whereas the more anterior locations correspond to the proposed combinatorial network. Regions shaded *blue* represent the dorsal stream, which is strongly left dominant. The posterior region of the dorsal stream corresponds to an area in the Sylvian fissure at the parietotemporal boundary (area Spt), which is proposed to be a sensorimotor interface, whereas the more anterior locations in the frontal lobe, probably involving Broca's region and a more dorsal premotor site, correspond to portions of the articulatory network. *aITS* anterior inferior temporal sulcus; *aMTG* anterior middle temporal gyrus; *pIFG* posterior inferior frontal gyrus; *PM* premotor cortex. Reprinted with permission from Hickok and Poeppel (2007)

(Binder et al. 2000; Hickok and Poeppel 2004, 2007; Indefrey and Levelt, 2004; Liebenthal et al. 2005; Price et al., 1996). The STS is activated by several tasks that tap phonological information such as, speech perception, speech production (Indefrey and Levelt 2004),

and the active short-term maintenance of phonemic information (Buchsbaum et al. 2001; Hickok et al. 2003). Functional activation studies that have used subtraction methodologies to isolate phonological processes have found activation along the STS (Liebenthal

et al. 2005; Narain et al. 2003; Obleser et al. 2006; Scott et al. 2000; Spitsyna et al. 2006; Vouloumanos et al. 2001), as have studies that manipulate psycholinguistic variables that tap phonological networks (Okada and Hickok 2006). Although a common view is that the phonological system is strongly left dominant, both lesion and imaging evidence (Hickok and Poeppel 2007) suggests a bilateral organization.

One currently unresolved question is the relative contribution of anterior vs. posterior STS regions in phonological processing. A majority of functional imaging studies targeting phonological processing in perception have highlighted regions in the posterior half of the STS (Hickok and Poeppel 2007). Other studies, however, have reported *anterior* STS activation in perceptual speech tasks (Mazoyer et al. 1993; Narain et al. 2003; Scott et al. 2000; Spitsyna et al. 2006). These studies involved sentence-level stimuli raising the possibility that anterior STS regions may be responding to some other aspect of the stimuli such as its syntactic or prosodic organization (Friederici et al. 2000; Humphries et al. 2001, 2005, 2006; Vandenberghe et al. 2002). Lesion evidence indicates that damage to posterior temporal lobe areas is most predictive of auditory comprehension deficits (Bates et al. 2003). The weight of the available evidence, therefore, suggests that the critical portion of the STS, that is involved in phonological-level processes, is bounded anteriorly by the anterolateral-most aspect of Heschl's gyrus and posteriorly by the posterior-most extent of the Sylvian fissure (Hickok and Poeppel 2007).

#### 8.4 Access to Conceptual-Semantic Information May Involve Middle Temporal Regions

Comprehension of speech involves more than just processing and recognizing phonological information in speech. It crucially involves using speech sound information to access conceptual-semantic representations. Although the organization of semantic knowledge in the brain is far from understood, a common view is that conceptual-semantic information is widely distributed throughout the cortex (Damasio and Damasio 1994; Gage and Hickok 2005; Hickok and Poeppel 2000, 2004, 2007; Martin 1998; Martin and Chao 2001; Mesulam 1998; Squire 1986). Access to this system via auditory-linguistic channels, however, may

be more focal. The posterior, middle and ventral temporal lobe (~BA 37) appears to be an important node in the interface between auditory/speech systems and conceptual-semantic knowledge (Fig. 8.1, posterior pink-shaded area). This conclusion is supported by lesion evidence showing that damage to this region results in semantic-level deficits in both comprehension and production (Chertkow et al. 1997; Hart and Gordon 1990; Hickok and Poeppel 2004, 2007).

Functional imaging studies have implicated these same regions in lexical-semantic processing. For example, Binder and colleagues asked subjects to make semantic decisions about auditorily presented words (Binder et al. 1997). In comparison to a tone-decision control task, semantic decisions strongly activated portions of the STS and middle temporal and inferior temporal gyri (in addition to frontal and parietal regions), but did not activate the superior temporal gyrus (STG). In the context of studies on phonological level processes discussed above, a reasonable interpretation is that, the STS activation reflects phonological aspects of word processing, whereas the more ventral activations, which do not show up reliably in studies of phonological processing, reflect postphonemic mechanisms involved in processing or accessing lexical-semantic information.

Similar conclusions are derived from studies of lexical semantic processing that use different approaches. Some studies have found greater activation in inferior posterior temporal regions for words compared to nonwords (Binder et al. 2005; Rissman et al. 2003). This contrast should emphasize lexical-semantic processes as nonwords have minimal lexical-semantic associations. Posterior middle temporal regions have also been implicated in processing semantically ambiguous words. Rodd et al. found that listening to sentences that contained high levels of lexical ambiguity produced more activation in the left posterior MTG (Rodd et al. 2005).

Imaging studies of semantic priming, which also should highlight regions involved in lexical-semantic processing, have, however, led to a different conclusion. These studies (Copland et al. 2003; Rissman et al. 2003) have found a more anterior middle temporal site that shows a reduction in activation for semantically related, compared to semantically unrelated word pairs (priming is typically reflected as a reduction of brain activity (Henson, 2003)). The implication of anterior temporal regions is not consistent with stroke-based lesion studies, as noted above. However,

it is consistent with recent claims derived from studies of semantic dementia, that the anterior temporal lobes play a critical role in the representation of conceptual knowledge (Hodges and Patterson 2007; Patterson et al. 2007).

Much work remains to be done in understanding the functional anatomy of semantic-related processes, particularly the relation between the posterior and anterior regions which have been implicated. It is possible to make the generalization that while phonemic-level processes involve auditory-responsive regions in the STS, higher-level lexical- and conceptual-semantic processes involve regions surrounding the STS both ventrally and posteriorly.

## 8.5 Sensory Systems Participate in Speech Production

There is unequivocal evidence that posterior sensory-related cortex in the left, but not right, hemisphere participates in speech production. For example, damage to the left posterior temporal lobe often results not only in comprehension deficits, but also in speech *production* deficits (Damasio 1991, 1992; Geschwind 1971; Goodglass 1993; Goodglass et al. 2001). Disruption to phonological systems appears to account for some of these production deficits. Damage to the left dorsal STG and/or the supramarginal gyrus/temporal-parietal junction is associated with conduction aphasia, a syndrome that is characterized by good comprehension, but with frequent phonemic errors in speech production, naming difficulties that often involve tip-of-the-tongue states (implicating a breakdown in phonological encoding), and difficulty with verbatim repetition (Damasio and Damasio 1980; Goodglass 1992)<sup>1</sup>. Conduction aphasia has classically been considered to be a disconnection syndrome involving damage to the arcuate fasciculus (Geschwind 1965). However, there is now good evidence that this syndrome results from cortical

<sup>1</sup>Although conduction aphasia is often characterized as a disorder of repetition, it is clear that the deficit extends well beyond this one task (Hickok et al. 2000). In fact, Wernicke first identified conduction aphasia as a disorder of speech production in the face of preserved comprehension (Wernicke 1874/1969). It was only later that Lichtheim introduced repetition as a convenient diagnostic tool for assessing the integrity of the link between sensory and motor speech systems (Lichtheim 1885).

dysfunction (Anderson et al. 1999; Hickok et al. 2000). Thus, conduction aphasia provides evidence for the involvement of left posterior auditory-related brain regions in phonological aspects of speech production (Hickok 2000; Hickok et al. 2000).

Functional imaging evidence also implicates left superior posterior temporal regions in speech production generally (Hickok et al. 2000; Price et al. 1996), and phonological stages of the process in particular (Indefrey and Levelt 2004; Indefrey and Levelt 2000). With respect to the latter, the posterior portion of the left planum temporale region, which is within the distribution of lesions associated with conduction aphasia, activates during picture naming and exhibits length effects (Okada et al. 2003), frequency effects (Graves et al. 2007), and has a time-course of activation, measured electromagnetically, that is consistent with the phonological encoding stage of naming (Levelt et al. 1998).

Taken together, the lesion and physiological evidence reviewed in this section make a compelling argument for the involvement of left posterior superior temporal regions in phonological aspects of speech production.

## 8.6 The Posterior Planum Temporale Supports Sensory-Motor Integration

If left posterior superior temporal regions are involved in phonological aspects of speech *production*, there must be a mechanism for interfacing posterior and anterior brain regions. The need for such a mechanism has long been acknowledged, and in classical models was instantiated as a simple white matter pathway, the arcuate fasciculus (Geschwind 1971). More recent proposals have argued, instead, for a *cortical* system that serves to integrate sensory and motor aspects of speech (Hickok et al. 2000, 2003; Hickok and Poeppel 2000, 2004, 2007; Warren et al. 2005), which is consistent with much research on sensory-motor integration systems studied in the context of the monkey visual system (Andersen 1997; Colby and Goldberg 1999; Milner and Goodale 1995).

A series of studies over the last several years has identified a cortical network for speech and related abilities (e.g., music), which has many of the properties exhibited by sensory-motor networks studied in

other domains. These properties include, sensory-motor responses, connectivity with frontal motor systems, motor-effector specificity, and multisensory responses (Andersen 1997; Colby and Goldberg 1999). The speech-related network with these response properties includes an area (termed Spt) in the left posterior planum temporale (Okada & Hickok, 2009) region (Fig. 8.1, posterior blue-shaded region), that has been argued to support sensory-motor integration for speech (Hickok et al. 2003). We will review the evidence for this claim below.

*Spt exhibits sensory-motor response properties.* A number of studies have demonstrated the existence of an area in the left posterior planum temporale that responds both during the perception and production of speech, even when speech is produced covertly (subvocally) so that there is no overt auditory feedback (Buchsbaum et al. 2001, 2005a, b; Hickok et al. 2003). Spt is not speech-specific, however. It responds equally well to the perception and (covert) production via humming of melodic stimuli (Hickok et al. 2003; Pa and Hickok 2008).

*Spt is functionally connected to motor speech areas.* Spt activity is tightly correlated with activity in frontal speech-production related areas, such as the pars opercularis (BA 44) (Buchsbaum et al. 2001) suggesting that the two regions are functionally connected. Furthermore, cortex in the posterior portion of the planum temporale (area Tpt) has a cytoarchitectonic structure that is similar to BA44. Galaburda writes, “area Tpt “...exhibits a degree of specialization like that of Area 44 in Broca’s region. It contains prominent pyramids in layer IIIc and a broad lamina IV.... the intimate relationship and similar evolutionary status of Areas 44 and Tpt allows for a certain functional overlap” (Galaburda 1982).

*Spt activity is modulated by motor effector manipulations.* In monkey, parietal cortex sensory-motor integration areas are organized around motor effector systems (e.g., ocular vs. manual actions in LIP and AIP; (Andersen 1997; Colby and Goldberg 1999)). Recent evidence suggests that Spt may be organized around the vocal tract effector system: Spt was less active when skilled pianists listened to and then imagined playing a novel melody than when they listened to and covertly hummed the same melody (Pa and Hickok 2008).

*Spt is sensitive to speech-related visual stimuli.* Many neurons in sensory-motor integration areas of the monkey parietal cortex are sensitive to inputs from more

than one sensory modality (Andersen 1997). The planum temporale, while often thought to be an auditory area, also activates in response to sensory input from other modalities. For example, silent lip-reading has been shown to activate auditory cortex in the vicinity of the planum temporale (Calvert et al. 1997; Calvert and Campbell 2003). Although these studies typically report the location as “auditory cortex” including primary regions, group-based localizations in this region can be unreliable. Indeed, a recent fMRI study using individual subject analyses has found that activation to visual speech and activation using the standard Spt-defining auditory-motor task (listen then covertly produce) are found in the same regions of the left posterior planum temporale. Thus, Spt appears to be sensitive also to visual input that is relevant to vocal tract actions.

In summary, Spt exhibits all the features of sensory-motor integration areas as identified in the parietal cortex of the monkey. This suggests that Spt is a sensory-motor integration area for vocal tract actions (Pa and Hickok 2008), placing it in the context of a network of sensory-motor integration areas in the posterior parietal and temporal/parietal cortex, which receive multisensory input and are organized around motor-effector systems (Andersen 1997). Although area Spt is not language-specific, it counts sensory-motor integration for phonological information as a prominent function.

## 8.7 Summary

Data from functional imaging studies has augmented a long history of language-brain research based on traditional neuropsychological methods. This work converges on several broad conclusions that are particularly relevant to an understanding of the neural organization of speech processing. Human auditory cortex is hierarchically organized with early areas primarily involved in the spectrotemporal analysis of acoustic signals. Higher-order representations/processes, such as those involved in the analysis of phonological information involve auditory-related regions in the STS, which are probably several steps downstream from primary auditory cortex. Beyond these high-level auditory-related systems in the STS, portions of the middle and inferior temporal gyri are important for mapping auditory-related representations onto conceptual-semantic systems. These systems,

involved in mapping acoustic input onto conceptual-semantic representations, comprise the ventral stream, and is bilaterally organized in its early stages, becoming somewhat left dominant at the level of conceptual-semantic access. A dorsal stream connects portions of the auditory system to articulatory-motor systems, thus enabling speech production and related functions. This circuit involves the posterior planum temporale (area Spt), which may function as a sensory-motor interface system for the vocal tract.

## References

- Andersen R (1997) Multimodal integration for the representation of space in the posterior parietal cortex. *Philos Trans R Soc Lond B Biol Sci* 352:1421–1428
- Anderson JM, Gilmore R, Roper S, Crosson B, Bauer RM, Nadeau S, Beversdorf DQ, Cibula J, Rogish M III, Kortencamp S, Hughes JD, Gonzalez Rothi LJ, Heilman KM (1999) Conduction aphasia and the arcuate fasciculus: a reexamination of the Wernicke-Geschwind model. *Brain Lang* 70:1–12
- Bates E, Wilson SM, Saygin AP, Dick F, Sereno MI, Knight RT, Dronkers NF (2003) Voxel-based lesion-symptom mapping. *Nat Neurosci* 6(5):448–450
- Binder JR, Frost JA, Hammeke TA, Cox RW, Rao SM, Prieto T (1997) Human brain language areas identified by functional magnetic resonance imaging. *J Neurosci* 17:353–362
- Binder JR, Frost JA, Hammeke TA, Bellgowan PS, Springer JA, Kaufman JN, Possing ET (2000) Human temporal lobe activation by speech and nonspeech sounds. *Cerebral Cortex* 10:512–528
- Binder JR, Westbury CF, McKiernan KA, Possing ET, Medler DA (2005) Distinct brain systems for processing concrete and abstract concepts. *J Cogn Neurosci* 17(6):905–917
- Buchsbaum B, Hickok G, Humphries C (2001) Role of left posterior superior temporal gyrus in phonological processing for speech perception and production. *Cogn Sci* 25:663–678
- Buchsbaum BR, Olsen RK, Koch P, Berman KF (2005a) Human dorsal and ventral auditory streams subserve rehearsal-based and echoic processes during verbal working memory. *Neuron* 48(4):687–697
- Buchsbaum BR, Olsen RK, Koch PF, Kohn P, Kippenhan JS, Berman KF (2005b) Reading, hearing, and the planum temporale. *Neuroimage* 24(2):444–454
- Calvert GA, Campbell R (2003) Reading speech from still and moving faces: the neural substrates of visible speech. *J Cogn Neurosci* 15:57–70
- Calvert GA, Bullmore ET, Brammer MJ, Campbell R, Williams SCR, McGuire PK, Woodruff PWR, Iversen SD, David AS (1997) Activation of auditory cortex during silent lipreading. *Science* 276:593–596
- Chertkow H, Bub D, Deaudo C, Whitehead V (1997) On the status of object concepts in aphasia. *Brain Lang* 58(2):203–232
- Colby CL, Goldberg ME (1999) Space and attention in parietal cortex. *Ann Rev Neurosci* 22:319–349
- Copland DA, de Zubicaray GI, McMahon K, Wilson SJ, Eastburn M, Chenery HJ (2003) Brain activity during automatic semantic priming revealed by event-related functional magnetic resonance imaging. *Neuroimage* 20(1):302–310
- Damasio AR (1992) Aphasia. *New Engl J Med* 326:531–539
- Damasio AR, Damasio H (1994) Cortical systems for retrieval of concrete knowledge: the convergence zone framework. In: Koch C, Davis JL (eds) *Large-scale neuronal theories of the brain*. MIT Press, Cambridge, MA, pp 61–74
- Damasio H (1991) Neuroanatomical correlates of the aphasias. In: Sarno M (ed) *Acquired aphasia*, 2nd edn. Academic, San Diego, pp 45–71
- Damasio H, Damasio AR (1980) The anatomical basis of conduction aphasia. *Brain* 103:337–350
- Dronkers NF, Redfern BB, Knight RT (2000) The neural architecture of language disorders. In: Gazzaniga MS (ed) *The new cognitive neurosciences*. MIT Press, Cambridge, MA, pp 949–958
- Fellows LK, Heberlein AS, Morales DA, Shivde G, Waller S, Wu DH (2005) Method matters: an empirical study of impact in cognitive neuroscience. *J Cogn Neurosci* 17(6):850–858
- Friederici AD, Meyer M, von Cramon DY (2000) Auditory language comprehension: an event-related fMRI study on the processing of syntactic and lexical information. *Brain Lang* 74:289–300
- Gage N, Hickok G (2005) Multiregional cell assemblies, temporal binding, and the representation of conceptual knowledge in cortex: a modern theory by a “classical” neurologist, Carl Wernicke. *Cortex* 41:823–832
- Galaburda, A. M. (1982). Histology, architectonics, and asymmetry of language areas. In M. A. Arbib & D. Caplan & J. C. Marshall (Eds.), *Neural models of language processes* (pp. 435–445). San Diego: Academic Press
- Geschwind N (1965) Disconnexion syndromes in animals and man. *Brain* 88:237–294, 585–644
- Geschwind N (1971) Aphasia. *New Engl J Med* 284:654–656
- Goodglass H (1992) Diagnosis of conduction aphasia. In: Kohn SE (ed) *Conduction aphasia*. Lawrence Erlbaum, Hillsdale, NJ, pp 39–49
- Goodglass H (1993) *Understanding aphasia*. Academic, San Diego
- Goodglass H, Kaplan E, Barresi B (2001) *The assessment of aphasia and related disorders*, 3rd edn. Lippincott Williams and Wilkins, Philadelphia
- Graves WW, Grabowski TJ, Mahta S, Gordon JK (2007) A neural signature of phonological access: distinguishing the effects of word frequency from familiarity and length in overt picture naming. *J Cogn Neurosci* 19:617–631
- Hart JJ, Gordon B (1990) Delineation of single-word semantic comprehension deficits in aphasia, with anatomical correlation. *Ann Neurol* 27:226–231
- Henson RNA (2003) Neuroimaging studies of priming. *Prog Neurobiol* 70:53–81
- Hickok G (2000) Speech perception, conduction aphasia, and the functional neuroanatomy of language. In: Grodzinsky Y, Shapiro L, Swinney D (eds) *Language and the brain*. Academic, San Diego, pp 87–104
- Hickok G, Poeppel D (2000) Towards a functional neuroanatomy of speech perception. *Trends Cogn Sci* 4:131–138
- Hickok G, Poeppel D (2004) Dorsal and ventral streams: a framework for understanding aspects of the functional anatomy of language. *Cognition* 92:67–99

- Hickok G, Poeppel D (2007) The cortical organization of speech processing. *Nat Rev Neurosci* 8(5):393–402
- Hickok G, Erhard P, Kassubek J, Helms-Tillery AK, Naeve-Velguth S, Strupp JP, Strick PL, Ugarbil K (2000) A functional magnetic resonance imaging study of the role of left posterior superior temporal gyrus in speech production: implications for the explanation of conduction aphasia. *Neurosci Lett* 287: 156–160
- Hickok G, Buchsbaum B, Humphries C, Muftuler T (2003) Auditory-motor interaction revealed by fMRI: speech, music, and working memory in area Spt. *J Cogn Neurosci* 15:673–682
- Hillis AE (2007) Aphasia: progress in the last quarter of a century. *Neurology* 69(2):200–213
- Hodges JR, Patterson K (2007) Semantic dementia: a unique clinicopathological syndrome. *Lancet Neurol* 6(11): 1004–1014
- Humphries C, Willard K, Buchsbaum B, Hickok G (2001) Role of anterior temporal cortex in auditory sentence comprehension: an fMRI study. *Neuroreport* 12:1749–1752
- Humphries C, Love T, Swinney D, Hickok G (2005) Response of anterior temporal cortex to syntactic and prosodic manipulations during sentence processing. *Hum Brain Mapp* 26:128–138
- Humphries C, Binder JR, Medler DA, Liebenthal E (2006) Syntactic and semantic modulation of neural activity during auditory sentence comprehension. *J Cogn Neurosci* 18(4): 665–679
- Indefrey P, Levelt WJ (2004) The spatial and temporal signatures of word production components. *Cognition* 92(1–2): 101–144
- Indefrey P, Levelt WJM (2000) The neural correlates of language production. In: Gazzaniga MS (ed) *The new cognitive neurosciences* MIT Press, Cambridge, MA, pp 845–865
- Kaas JH, Hackett TA (2000) Subdivisions of auditory cortex and processing streams in primates. *Proc Natl Acad Sci U S A* 97(22):11793–11799
- Kaas JH, Hackett TA, Tramo MJ (1999) Auditory processing in primate cerebral cortex. *Curr Opin Neurobiol* 9(2): 164–170
- Levelt WJM, Praamstra P, Meyer AS, Helenius P, Salmelin R (1998) An MEG study of picture naming. *J Cogn Neurosci* 10:553–567
- Lichtheim L (1885) On aphasia. *Brain* 7:433–484
- Liebenthal E, Binder JR, Spitzer SM, Possing ET, Medler DA (2005) Neural substrates of phonemic perception. *Cereb Cortex* 15(10):1621–1631
- Martin A (1998) The organization of semantic knowledge and the origin of words in the brain. In: Jablonski NG, Aiello LC (eds) *The origins and diversification of language*. California Academy of Sciences, San Francisco, pp 69–88
- Martin A, Chao LL (2001) Semantic memory and the brain: structure and processes. *Curr Opin Neurobiol* 11(2):194–201
- Mazoyer BM, Tzourio N, Frak V, Syrota A, Murayama N, Levrier O, Salamon G, Dehaene S, Cohen L, Mehler J (1993) The cortical representation of speech. *J Cogn Neurosci* 5:467–479
- Mesulam M-M (1998) From sensation to cognition. *Brain* 121:1013–1052
- Milner AD, Goodale MA (1995) *The visual brain in action*. Oxford University Press, Oxford
- Narain C, Scott SK, Wise RJ, Rosen S, Leff A, Iversen SD, Matthews PM (2003) Defining a left-lateralized response specific to intelligible speech using fMRI. *Cereb Cortex* 13(12):1362–1368
- Obleser J, Zimmermann J, Van Meter J, Rauschecker JP (2006) Multiple stages of auditory speech perception reflected in event-related fMRI. *Cereb Cortex* 17:2251–2257
- Okada K, Hickok G (2006) Identification of lexical-phonological networks in the superior temporal sulcus using fMRI. *Neuroreport* 17:1293–1296
- Okada, K., & Hickok, G. (2009). Two cortical mechanisms support the integration of visual and auditory speech: A hypothesis and preliminary data. *Neurosci Lett*, 452(3), 219–223
- Okada K, Smith KR, Humphries C, Hickok G (2003) Word length modulates neural activity in auditory cortex during covert object naming. *Neuroreport* 14:2323–2326
- Pa J, Hickok G (2008) A parietal-temporal sensory-motor integration area for the human vocal tract: evidence from an fMRI study of skilled musicians. *Neuropsychologia* 46: 362–368
- Patterson K, Nestor PJ, Rogers TT (2007) Where do you know what you know? The representation of semantic knowledge in the human brain. *Nat Rev Neurosci* 8(12): 976–987
- Price CJ, Wise RJS, Warburton EA, Moore CJ, Howard D, Patterson K, Frackowiak RSJ, Friston KJ (1996) Hearing and saying: the functional neuro-anatomy of auditory word processing. *Brain* 119:919–931
- Rauschecker JP (1998) Cortical processing of complex sounds. *Curr Opin Neurobiol* 8(4):516–521
- Rissman J, Eliassen JC, Blumstein SE (2003) An event-related fMRI investigation of implicit semantic priming. *J Cogn Neurosci* 15(8):1160–1175
- Rodd JM, Davis MH, Johnsrude IS (2005) The neural mechanisms of speech comprehension: fMRI studies of semantic ambiguity. *Cerebral Cortex* 15:1261–1269
- Romanski LM, Tian B, Fritz J, Mishkin M, Goldman-Rakic PS, Rauschecker JP (1999) Dual streams of auditory afferents target multiple domains in the primate prefrontal cortex. *Nat Neurosci* 2:1131–1136
- Scott SK (2005) Auditory processing – speech, space and auditory objects. *Curr Opin Neurobiol* 15(2):197–201
- Scott SK, Blank CC, Rosen S, Wise RJS (2000) Identification of a pathway for intelligible speech in the left temporal lobe. *Brain* 123:2400–2406
- Spitsyna G, Warren JE, Scott SK, Turkheimer FE, Wise RJ (2006) Converging language streams in the human temporal lobe. *J Neurosci* 26(28):7328–7336
- Squire LR (1986) Mechanisms of memory. *Science* 232: 1612–1619
- Vandenberghe R, Nobre AC, Price CJ (2002) The response of left temporal cortex to sentences. *J Cogn Neurosci* 14(4): 550–560
- Vouloumanos A, Kiehl KA, Werker JF, Liddle PF (2001) Detection of sounds in the auditory stream: event-related fMRI evidence for differential activation to speech and non-speech. *J Cogn Neurosci* 13(7):994–1005
- Warren JE, Wise RJ, Warren JD (2005) Sounds do-able: auditory-motor transformations and the posterior temporal plane. *Trends Neurosci* 28(12):636–643
- Wernicke C (1874/1969) The symptom complex of aphasia: A psychological study on an anatomical basis. In: Cohen RS, Wartofsky MW (eds) *Boston studies in the philosophy of science*. D. Reidel, Dordrecht, pp 34–97

## Use of fMRI Language Lateralization for Quantitative Prediction of Naming and Verbal Memory Outcome in Left Temporal Lobe Epilepsy Surgery

Jeffrey R. Binder

Partial removal of the anterior temporal lobe (ATL) is the most commonly performed surgical procedure for intractable epilepsy. ATL resection is highly effective for seizure control, resulting in long-term cure rates of 60–80% (McIntosh et al. 2001; Jeong et al. 2005; Tellez-Zenteno et al. 2005). The undeniable benefit of ATL surgery is partially offset by the occurrence of neuropsychological morbidity in some patients receiving this treatment. Evidence suggests a 30–60% incidence of anomic aphasia (Hermann et al. 1994 Hermann et al. 1999a; Hermann et al. 1999b; Langfitt and Rausch 1996; Bell et al. 2000b; Sabsevitz et al. 2003) and a similar risk for decline in verbal memory ability (Chelune et al. 1993; Helmstaedter and Elger 1996; Martin et al. 1998; Sabsevitz et al. 2001; Stroup et al. 2003; Gleissner et al. 2004; Baxendale et al. 2006; Lineweaver et al. 2006; Binder et al. 2008b) after left ATL surgery. Patients are generally aware of these deficits, which adversely affect quality of life and employability (Perrine et al. 1995; Helmstaedter et al. 2003; Stroup et al. 2003; Lineweaver et al. 2004; Langfitt et al. 2007). Cognitive deficits from right ATL resection have been much less consistently observed (Loring et al. 1990a; Loring et al. 1995b; Pigot and Milner 1993); Pillon et al. 1999; Lee et al. 2002; Binder et al. 2008). Though the first priority in treating intractable epilepsy is seizure control, the importance of cognitive side effects for some patients undergoing left ATL surgery should not be underestimated or denied. Indeed, considerable resources have been devoted to developing methods for predicting and preventing cognitive mor-

bidity, and many such methods are used routinely in the evaluation of surgical candidates despite ongoing controversy regarding their effectiveness.

This chapter focuses on the recent advances in the prediction of postoperative language and verbal memory deficits using preoperative fMRI. The clinical value of such risk assessment is that it provides the patient and the physician additional information that can be useful in deciding whether to proceed with treatment in elective situations. The use of fMRI activation maps intraoperatively for defining surgical resection boundaries is a separate issue that will not be addressed in detail here.

### 9.1 Use of fMRI for Predicting Naming Outcome

#### 9.1.1 Measuring Language Lateralization

The intracarotid amobarbital (Wada) test was developed to assess the risk of language decline in patients undergoing resective brain surgery (Wada and Rasmussen 1960), based on the assumption that operating on the language-dominant hemisphere entailed increased risk. Though the Wada test has been in use for over 50 years, until recently the relationship between Wada language asymmetry and postoperative language outcome had never been quantified. The historical reasons for this relate to the fact that language lateralization was traditionally viewed as dichotomous (left or right) or trichotomous (left, right, or “bilateral”). Under this schema, it was obvious that operating on a nondominant hemisphere would be safer than operating on a language-dominant hemisphere. Several aspects of this formulation

---

J. R. Binder  
Department of Neurology, Medical College of Wisconsin,  
8701 Watertown Plank Road, Milwaukee, WI 53226, USA  
e-mail: jrbinder@mcw.edu

have changed in recent decades. First, language lateralization has come to be seen as a continuously graded rather than an all-or-none phenomenon, with relative *degrees* of dominance rather than distinct categories (Loring et al. 1990b; Binder et al. 1996; Springer et al. 1999; Knecht et al. 2000b, 2002; Chlebus et al. 2007; Seghier 2008). Thus, while the vast majority (~80%) of patients who undergo left hemisphere surgery for epilepsy are left-dominant for language, there is variation within this group in terms of the degree of left dominance. This variability raises the question of whether graded degrees of language dominance are reflected in graded levels of risk. Second, neuropsychological methods for identifying postoperative language deficits have steadily improved and become more widespread, resulting in a shift of the clinical focus, particularly in left ATL cases, from prediction of severe aphasia (which is very rare after standard left ATL resection) to prediction of more moderate degrees of language decline.

The initiative to develop fMRI methods for predicting language outcome in ATL epilepsy surgery is therefore motivated by two critical assumptions. First, it is assumed that patients show varying degrees of language (mainly naming) deficit after surgery, and that it is desirable to know before surgery what degree of decline can be expected. Second, it is assumed that the degree of decline will be related to the degree of language lateralization toward the surgical hemisphere. The goal of fMRI in this context is, thus, to provide a reliable and valid measure of language lateralization. A wide variety of fMRI language activation paradigms have been described, differing in the type of language stimuli, the stimulus modality, the language task, the control stimuli, and the control task used, raising the question of which of these paradigms, if any, is optimal. Though different paradigms have seldom been compared quantitatively, it is well known that they can produce very different, in some cases, entirely nonoverlapping, activation patterns. This variation is related primarily to the cognitive, sensory, and motor processes engaged by the tasks, and the degree to which the language and control conditions differ in engaging these specific processes (Binder 2006).

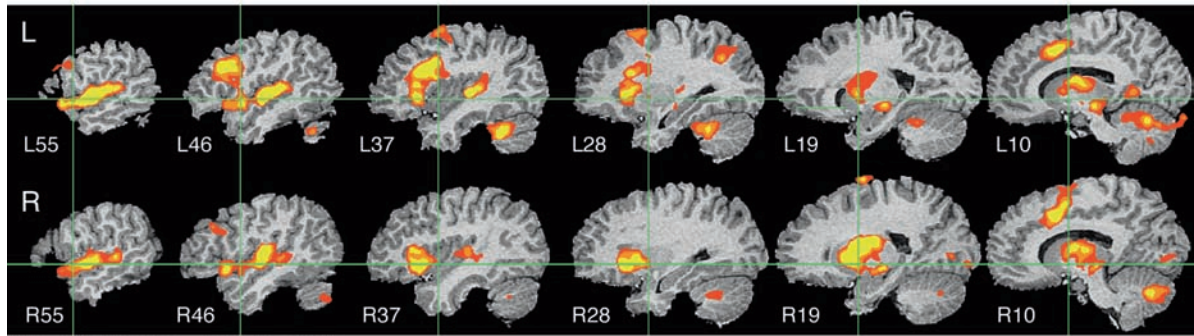
Several simple criteria can be applied in assessing the usefulness of different language paradigms. First, the pattern of activation obtained in healthy, right-handed adults should be lateralized strongly to the left hemisphere, as it is known that almost all such individuals are left-hemisphere dominant for language

(Loring et al. 1990b; Springer et al. 1999; Knecht et al. 2000a). Second, the activation should be robust, i.e., it should be reliably obtained across individuals and in the same general brain regions. Third, there should be concordance between language lateralization measured with the fMRI paradigm, and with other techniques, such as the Wada test, in the same individuals. Finally, in some cases it may be desirable that the paradigm produce activation in particular target brain regions. In the case of ATL surgery, for example, activation asymmetry in the temporal lobe might be more predictive of outcome than activation in the frontal lobe, thus a paradigm that activates the temporal lobe would have advantages over one that does not.

Figure 9.1 illustrates some of these issues. The figure shows average activation maps obtained while 26 right-handed subjects listened to spoken words and performed a semantic decision task (Binder et al. 1997, 2008a). In the top panel, BOLD signal during this task is compared to a “resting” baseline. The activated regions are largely bilateral, including bilateral auditory, working memory, general executive, and attention networks. In the lower panel of the figure, the semantic decision task is compared to a nonlinguistic auditory control task. In this case the activated regions are strongly left-lateralized, including several left temporal, parietal, and prefrontal regions (indicated by blue arrows) that were not observed when the resting baseline was used. These data illustrate in dramatic fashion how activation patterns depend on the choice of control condition. In the lower panel, the use of an active nonlinguistic control task “subtracts out” bilateral activation in early auditory, general executive, and attention networks, leaving activation in left-lateralized language networks. These results also demonstrate that certain high-level language processing regions are active during the “resting” state and can only be observed when an active nonlinguistic control condition is employed (Binder et al. 1999, 2008a).

Many fMRI language paradigms have been compared to Wada language testing (Desmond et al. 1995; Binder et al. 1996; Bahn et al. 1997; Hertz-Pannier et al. 1997; Worthington et al. 1997; Yetkin et al. 1998; Benson et al. 1999; Lehericy et al. 2000; Carpentier et al. 2001; Rutten et al. 2002; Spreer et al. 2002; Adcock et al. 2003; Sabbah et al. 2003; Woermann et al. 2003; Deblaere et al. 2004; Gaillard et al. 2004; Benke et al. 2006; Chlebus et al. 2007). These studies generally report high concordance rates, typically in

## Semantic Decision – Rest



## Semantic Decision – Tone Decision

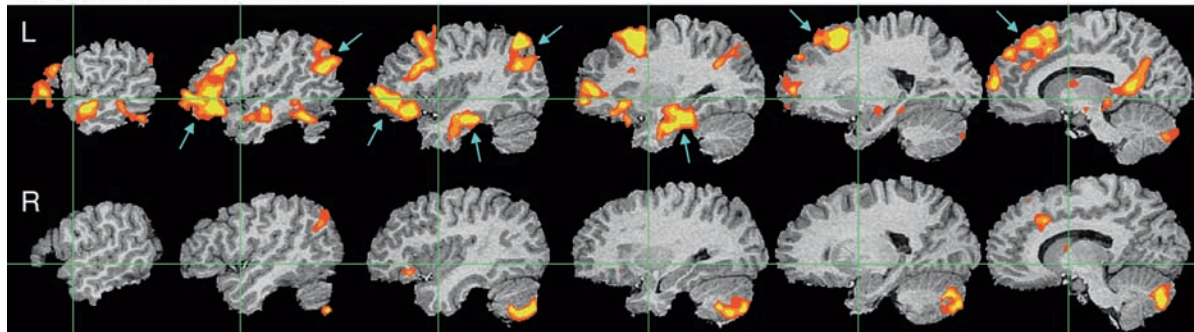


**Fig. 9.1** Group fMRI activation maps from two auditory word comprehension experiments. *Top*: Semantic Decision relative to resting. *Bottom*: Semantic Decision relative to Tone Decision. Data are displayed as serial sagittal sections through the brain at 9 mm intervals. X-axis locations for each slice are given in the *top panel*. Both maps are thresholded at a whole-brain corrected  $P < 0.05$

using voxel-wise  $P < 0.0001$  and cluster extent  $> 200 \text{ mm}^3$ . The three steps in each color continuum represent voxel-wise  $P$  thresholds of  $10^{-4}$ ,  $10^{-5}$ , and  $10^{-6}$ . Blue arrows in the lower image indicate left hemisphere language areas that are active during the resting state and thus visible only when an active nonlinguistic task is used as the baseline (adapted from Binder et al. 2008a)

the range of 90–100% (for reviews, see (Binder and Raghavan 2006; Swanson et al. 2007)). In assessing the rate of concordance, patients are usually assigned to categories such as “left dominant,” “right dominant,” or “mixed” on each test. The proportion of concordant cases depends on how these arbitrary categories are defined. Another method of comparing fMRI and Wada results is to calculate the correlation between continuous measures of lateralization on both tests. In the case of fMRI, a standard approach is to calculate a laterality index (LI) expressing the asymmetry of activation in numerical form. The first such LI was based on a simple count of the voxels that survived thresholding in each hemisphere (Binder et al. 1996). The formula  $(L - R)/(L + R)$ , where L and R refer to the voxel counts in each hemisphere, yields a number that varies from +1, when all activated voxels are on the left side, to -1, when all activated voxels are on the right. LI values obtained with this method vary as a function of the threshold used for defining activated voxels, thus

several authors have explored alternative asymmetry measures that do not require thresholding (Nagata et al. 2001; Adcock et al. 2003; Wilke and Schmithorst 2006; Chlebus et al. 2007; Seghier 2008). No consensus regarding the optimal method for calculating activation asymmetry has yet emerged from these studies.

### 9.1.2 Predicting Naming Outcome

With so many studies focusing on fMRI/Wada correlations, it is easy to forget that the actual aim of measuring language lateralization prior to brain surgery is prediction of language outcome. In the case of left ATL resection, an fMRI procedure that reliably identifies patients at risk for postoperative naming deficits would be a valuable clinical tool, especially if the fMRI results added information over and above other available tests. Previous behavioral studies have identified demographic and

behavioral variables that may predict outcome. For example, left ATL patients who develop seizures at an earlier age generally have a lower risk for postoperative language decline (Stafniak et al. 1990; Saykin et al. 1995; Hermann et al. 1999b), presumably because earlier age at onset is associated with a higher probability of language shift to the right hemisphere (Springer et al. 1999). Better preoperative naming performance is associated with a higher risk for decline (Hermann et al. 1994). As noted above, Wada language testing has always been assumed to be predictive of language outcome. Apart from a few case reports of patients with right language dominance who did not decline (Wada and Rasmussen 1960; Langfitt and Rausch 1996), however, no prior studies have formally tested this assumption.

To date, only one study has examined the value of fMRI language lateralization as a predictor of language outcome. Sabsevitz et al. (2003) studied 24 consecutively encountered patients undergoing left ATL resection. The fMRI paradigm used a contrast between an auditory semantic decision task and a nonlinguistic tone decision task (Fig. 9.1, lower panel). A previous study had shown that asymmetry of activation with this task paradigm is correlated with language lateralization on the Wada test (Binder et al. 1996). For the Sabsevitz et al. study, separate LIs were computed for the whole hemisphere, frontal lobe, temporal lobe, and angular gyrus. All patients also underwent Wada testing and preoperative assessment of confrontation naming using the 60-item Boston Naming Test (BNT). The BNT was administered again at 6 months after surgery, and a change score was calculated as the difference between postop and preop BNT scores. Surgeries were performed blind to the fMRI data.

Compared to a control group of 32 right ATL patients, the left ATL group declined postoperatively on the BNT ( $P < 0.001$ ), with an average change score of  $-9$ . Within the left ATL group, however, there was considerable variability, with 13 patients (54%) showing variable degrees of decline relative to the control group. The temporal lobe fMRI LI was the strongest predictor of outcome ( $r = -0.64$ ,  $P < 0.001$ ), indicating that language lateralization towards the left (surgical) temporal lobe was related to poorer naming outcome, whereas lateralization towards the right temporal lobe was associated with little or no decline. This fMRI measure showed 100% sensitivity, 73% specificity, and a positive predictive value of 81% in predicting significant decline. By comparison, the Wada language LI showed

a somewhat weaker correlation with outcome ( $r = -0.50$ ,  $P < 0.05$ ), 92% sensitivity, 43% specificity, and a positive predictive value of 67%. Notably, the frontal lobe fMRI LI was also less predictive ( $r = -0.47$ ,  $P < 0.05$ ), suggesting that an optimal LI is one that indexes lateralization near the surgical resection area.

Sabsevitz et al. also created multivariate models to determine the contribution of fMRI relative to other noninvasive predictors. Both age at epilepsy onset ( $r = -0.35$ ,  $P = 0.09$ ) and preoperative performance ( $r = -0.39$ ,  $P = 0.06$ ) showed strong trends towards a correlation with outcome, and together these variables predicted about 27% of the variance in outcome. Adding the temporal lobe fMRI LI to this model accounted for an additional 23% of the variance ( $P < 0.01$ ), indicating a significant increase in predictive power. Addition of the Wada language asymmetry score did not improve the model ( $R^2$  change = 0.01).

Though based on a relatively small sample, these results show how preoperative fMRI can be used to stratify patients in terms of risk for language decline in the setting of left ATL resection, allowing patients and physicians to more accurately weigh the risks and benefits of the surgery. It is crucial to note, however, that these results hold good only for the particular methods used in the study and may not generalize to other fMRI protocols, analysis methods, patient populations, or surgical procedures. Future studies should not only confirm these results using larger patient samples, but also test whether other fMRI protocols in current widespread use have similar predictive capability.

### 9.1.3 “Tailoring” Resections

It remains to be seen how useful fMRI language activation maps will be for planning surgical resection boundaries. At least three significant problems complicate progress: (a) variation in language maps produced by different activation protocols, (b) the failure, to date, to find an activation protocol that reliably activates the ATL where the majority of epilepsy surgeries are performed, and (c) an inadequate understanding of the specificity of fMRI activations.

As indicated earlier, different fMRI language activation protocols in current clinical use produce markedly different patterns of activation (Binder 2006; Binder et al. 2008a). These findings suggest that

activation maps are strongly dependent on the specific composition of cognitive processes engaged during the scan, and how these differ between the language and control tasks used (see discussion above). Of note is the fact that none of the language activation protocols currently in common use is associated with robust ATL activation. Because the dominant ATL is known to contribute to language processing (Mazoyer et al. 1993; Damasio et al. 1996; Hamberger et al. 2001; Humphries et al. 2005; Rogers et al. 2006), and left ATL resection not infrequently results in language decline (Hermann et al. 1994; Langfitt and Rausch 1996; Davies et al. 1998b; Bell et al. 2000b; Sabsevitz et al. 2003), it follows that these protocols are not detecting crucial language areas. Clearly, further language activation task development is necessary. It may also be necessary, as some have suggested (Rutten et al. 2002; Gaillard et al. 2004), to incorporate multiple activation protocols before a complete picture of the language zones in an individual can be discerned.

In addition to these issues concerning sensitivity of the activation protocol, it is conceivable that some regions activated during language tasks may play a minor or nonspecific role rather than a critical role in language. Resection of these “active” foci may not necessarily produce clinically relevant or persisting deficits. Thus, those who would use fMRI activation maps to decide which brain regions can be resected in an individual patient run two risks: (a) resection of critical language zones that are “not activated” due to insensitivity of the particular language activation protocol employed, resulting in postoperative language decline; and (b) sparing of “activated” regions that are actually not critical for language, resulting in suboptimal seizure control. Only through very carefully designed studies – in which resections are performed blind to the fMRI data, standardized procedures are used for assessing outcome, and quantitative measures are made of the anatomical and functional lesion – will the usefulness of fMRI language maps for “tailoring” surgical resections be determined.

## 9.2 Prediction of Verbal Memory Outcome

ATL resection typically involves removal of much of the anterior medial temporal lobe (MTL), including portions of the hippocampus and parahippocampus, which are

known to be critical for encoding and retrieval of long-term episodic memories (Squire 1992). Verbal memory decline after left ATL resection is a consistent finding in group studies and is observed in 30–60% of such patients (Chelune et al. 1991, 1993; Hermann et al. 1995; Kneebone et al. 1995; Loring et al. 1995b; Helmstaedter and Elger 1996; Martin et al. 1998; Chiaravalloti and Glosser 2001; Sabsevitz et al. 2001; Lee et al. 2002; Stroup et al. 2003; Gleissner et al. 2004; Baxendale et al. 2006; Lineweaver et al. 2006; Binder et al. 2008b). In contrast, nonverbal memory decline after right ATL resection is less consistently observed in groups and individuals (Lee et al. 2002; Stroup et al. 2003; Lineweaver et al. 2006; Binder et al. 2008b). A main focus of the preoperative evaluation in ATL surgery candidates is, therefore, to estimate the risk of verbal memory decline in patients undergoing left ATL resection.

The Wada memory test was originally developed for the purpose of predicting global amnesia after ATL resection (Milner et al. 1962). Studies of its ability to predict relative verbal memory decline have been inconsistent, with several studies suggesting good predictive value (Kneebone et al. 1995; Loring et al. 1995b; Bell et al. 2000a; Chiaravalloti and Glosser 2001; Sabsevitz et al. 2001) and others showing little or none, particularly when used in combination with noninvasive tests (Chelune and Najm 2000; Stroup et al. 2003; Lacruz et al. 2004; Kirsch et al. 2005; Lineweaver et al. 2006; Binder et al. 2008b). Some authors have questioned the general validity and reliability of Wada memory results (Novelly and Williamson 1989; Loring et al. 1990a; Lee et al. 1995; Kubu et al. 2000; Simkins-Bullock 2000; Martin and Grote 2002; Loddenkemper et al. 2007). Others have emphasized the sensitivity of the test to certain details of the stimulus presentation, procedures used for recall, and other methodological factors (Loring et al. 1994, 1995a; Carpenter et al. 1996; Alpherts et al. 2000). Other presurgical tests of MTL functional or anatomical asymmetry are also modestly predictive of memory outcome, including structural MRI of the hippocampus (Trenerry et al. 1993; Wendel et al. 2001; Stroup et al. 2003; Cohen-Gadol et al. 2004; Lineweaver et al. 2006) and interictal positron emission tomography (Griffith et al. 2000). Preoperative neuropsychological testing also has predictive value, in that patients with good memory abilities prior to surgery are more likely to decline than patients with poor preoperative memory (Chelune et al. 1991; Hermann et al. 1995; Helmstaedter and Elger

1996; Jokeit et al. 1997; Davies et al. 1998a; Stroup et al. 2003; Gleissner et al. 2004; Baxendale et al. 2006, 2007; Lineweaver et al. 2006; Binder et al. 2008b).

### 9.2.1 *fMRI of the Medial Temporal Lobe*

MTL activation during memory encoding and retrieval tasks has been a subject of intense research with fMRI (for reviews, see (Schacter and Wagner 1999; Gabrieli 2001; Paller and Wagner 2002; Rugg et al. 2002; Hwang and Golby 2006; Schacter and Addis 2007; Vilberg and Rugg 2008)). Hippocampal activation has been demonstrated using a variety of task paradigms (e.g., (Binder et al. 1997, 2005; Henke et al. 1997; Fernandez et al. 1998; Martin 1999; Constable et al. 2000; Eldridge et al. 2000; Otten et al. 2001; Small et al. 2001; Sperling et al. 2001; Stark and Squire 2001; Davachi and Wagner 2002; Killgore et al. 2002; Kensinger et al. 2003; Zeinah et al. 2003; Weis et al. 2004; Greene et al. 2006; Parsons et al. 2006; Vincent et al. 2006; Hassabis et al. 2007; Prince et al. 2007)), although fMRI of this region is not without technical challenges. The hippocampal formation is small relative to typical voxel sizes used in fMRI. Within-voxel averaging of signals from active and inactive structures may thus impair detection of hippocampal activity. Loss of MRI signal in the medial ATL due to macroscopic field inhomogeneity can affect the amygdala and occasionally the anterior hippocampus (Constable et al. 2000; Fransson et al. 2001; Morawetz et al. 2008). Finally, the “baseline” state employed in subtraction analyses is probably of critical importance. Hippocampal encoding processes probably continue beyond the duration of the stimulus or event (Alvarez and Squire 1994), and human imaging evidence suggests that the hippocampus is relatively activated in the “resting” state (Andreasen et al. 1995; Binder et al. 1999; Martin 1999; Stark and Squire 2001). Stark and Squire (2001), for example, showed that the hippocampus and parahippocampus both show higher BOLD signals during “rest” than during active perceptual discrimination tasks. Activation of these MTL regions during encoding of pictures was detected using the perceptual discrimination tasks as baseline, but not when “rest” was used as a baseline.

Hippocampal fMRI paradigms generally employ one of three approaches. The first of these involves a contrast

between encoding novel and repeated stimuli, based on earlier electrophysiological studies showing that the hippocampus responds more strongly to novel than to repeated stimuli (Riches et al. 1991; Li et al. 1993; Knight 1996; Grunwald et al. 1998). The encoding task might involve explicit memorization for later retrieval testing or a decision task designed to produce implicit encoding. Such novelty contrasts mainly activate the posterior parahippocampus and adjacent fusiform gyrus, with involvement of the posterior hippocampus in some but not all studies (Stern et al. 1996; Tulving et al. 1996; Gabrieli et al. 1997; Kirchhoff et al. 2000; Fransson et al. 2001; Hunkin et al. 2002; Binder et al. 2005). The second approach involves manipulating the degree of associative/semantic processing that occurs during encoding. Hippocampal encoding is thought to involve the creation of “relational” representations that tie together sensory, semantic, affective, and other codes activated by an event (Cohen and Eichenbaum 1993; McClelland et al. 1995; O’Reilly and Rudy 2001). External events that are meaningful and activate semantic and emotional associations engage the hippocampus more robustly and are, therefore, more effectively recorded (Craik and Lockhart 1972). Thus, many fMRI studies have demonstrated hippocampal activation using contrasts between a stimulus (e.g., a word or picture) or task that engages associative/semantic processing and a stimulus (e.g., a nonword or unrecognizable visual form) or task that engages only sensory processing (Binder et al. 1997; Henke et al. 1997, 1999; Wagner et al. 1998; Martin 1999; Otten et al. 2001; Small et al. 2001; Sperling et al. 2001; Davachi and Wagner 2002; Killgore et al. 2002; Bartha et al. 2003; Kensinger et al. 2003; Zeinah et al. 2003; Binder et al. 2005). Finally, a third approach uses subsequent recognition performance as a direct index of MTL activity during encoding. Items encoded during the fMRI scan are sorted according to whether they were later remembered, and a contrast is made between successfully and unsuccessfully encoded items. These studies consistently show greater MTL activation during subsequently remembered compared to subsequently forgotten stimuli, though the precise MTL regions showing this effect have varied considerably (Brewer et al. 1998; Fernandez et al. 1998; Wagner et al. 1998; Constable et al. 2000; Kirchhoff et al. 2000; Buckner et al. 2001; Otten et al. 2001; Davachi and Wagner 2002; Weis et al. 2004; Prince et al. 2005, 2007; Uncapher and Rugg 2005).

Finally, the location of MTL activation detected by fMRI depends on the type of stimulus material encoded. MTL activation is left-lateralized for verbal stimuli and generally symmetric for pictorial stimuli (Binder et al. 1997, 2005; Kelley et al. 1998; Martin 1999; Golby et al. 2001; Otten et al. 2001; Reber et al. 2002; Powell et al. 2005).

### 9.2.2 Medial Temporal Lobe fMRI as a Predictor of Memory Outcome

Several fMRI studies have examined the relationship between preoperative MTL activation and memory outcome after ATL surgery (Table 9.1). Rabin et al. (2004) studied 23 patients undergoing ATL resection (10 left, 13 right) using a scene encoding task that activates the posterior MTL bilaterally (Detre et al. 1998). Patients were tested for delayed recognition of the same pictures immediately after scanning. Delayed picture recognition was then tested again after surgery, and the change on this recognition task was used as the primary memory outcome variable. About half of the patients in both

surgery groups declined on this measure. Preoperative fMRI activation lateralization towards the side of surgery was correlated with decline, as was the extent of activation on the side of surgery. These results were the first to demonstrate a relationship between preoperative fMRI activation asymmetry and outcome; yet, they are of limited relevance to the problem of predicting verbal memory outcome. In the left ATL patients studied by Rabin et al., neither Wada memory nor fMRI activation asymmetry predicted verbal memory decline as measured by standard psychometric tests.

Richardson and colleagues studied correlations between hippocampal activation and verbal memory outcome in three small studies (Richardson et al. 2004, 2006; Powell et al. 2008). Patients performed a semantic decision task with words during the fMRI scan and then took a recognition test after scanning. Words that were subsequently recognized were contrasted with words that were judged to be familiar but not recognized. In the first of these studies (Richardson et al. 2004), the authors observed a focus in the anterior hippocampus, where *asymmetry* of activation (i.e., left – right) predicted verbal memory outcome on a standardized word list learning test after left ATL resection. Greater activation in this region on the left

**Table 9.1** fMRI studies of verbal memory outcome prediction in ATL surgery

References	N	fMRI contrast	Memory measure	Summary
Rabin et al. (2004)	10 L, 13 R	Indoor/outdoor decision on visual scenes vs. passive viewing of scrambled scenes	Recognition of scenes encoded during fMRI	MTL LI predicts outcome on scene recognition task in both surgery groups
Richardson et al. (2004)	10 L	Subsequently recognized vs. familiar but not recognized words encoded during a semantic decision task	Word list learning and story recall (Adult Memory and Information Processing Battery)	Activation asymmetry in a hippocampus ROI predicts verbal memory outcome
Richardson et al. (2006)	12 L	Same as Richardson et al. (2004)	Same as Richardson et al. (2004)	Unilateral activation in either left or right hippocampus ROI predicts verbal memory outcome
Binder et al. (2008b)	60 L	Semantic decision on auditory words vs. sensory decision on tones	Word list learning and delayed recall (Selective Reminding Test)	LI predicts verbal memory outcome, adds value beyond other predictors
Frings et al. (2008)	9 L, 10 R	Memorizing and recognizing object locations vs. comparing size of two objects	Word list learning (Verbaler Lern- and Merkfähigkeitstest)	Hippocampal LI predicts verbal memory outcome, mainly in left group
Köylü et al. (2008)	14 L, 12 R	Semantic decision on auditory words vs. sensory decision on tones	Word list learning and delayed recall (Münchener Gedächtnistest)	MTL activation correlates with pre- and postoperative memory
Powell et al. (2008)	7 L, 8 R	Subsequently recognized vs. forgotten words and faces encoded during a semantic decision task	Word list learning and visual design learning	Unilateral activation in dominant-side hippocampus ROI predicts verbal memory outcome in dominant resection

side relative to the right side predicted greater decline. The second study by the same authors, however, showed correlations between outcome and hippocampal activation on either side (Richardson et al. 2006). That is, greater activation unilaterally on the left or the right was associated with poorer outcome. The correlation between verbal memory decline after *left* ATL resection and activation in the *right* hippocampus is difficult to explain, as patients with greater activation in the right hippocampus preoperatively would be expected to have a better outcome, not a worse outcome (Chelune 1995). This finding was not replicated in the third study (Powell et al. 2008), which reported a correlation between left hippocampus activation and poor outcome but no correlation between right hippocampus activation and outcome. A methodological weakness in all of these studies is that they are based on fMRI activation values extracted from a small region of interest, defined by searching the volume for voxels that show a correlation with outcome, across a group of patients. As the coordinates of these correlated voxels have varied across the studies, it is not clear how this method of extracting activation values would be applied to a newly encountered patient.

Frings et al. studied the relationship between preoperative hippocampal activation asymmetry and verbal memory outcome in a small sample of patients undergoing left or right ATL resection (Frings et al. 2008). The fMRI protocol used a task in which patients viewed a virtual-reality environment containing colored geometric shapes and either memorized the location of these objects or performed a recognition decision following memorization. These “memory tasks” were contrasted with a control task in which patients saw two versions of a geometric object and indicated which one was larger. This fMRI contrast had been shown previously to activate posterior MTL regions (mainly posterior parahippocampus) bilaterally. An LI was computed over the entire hippocampus, defined using a stereotaxic atlas. Verbal memory change was marginally correlated (1-tailed  $P = 0.077$ ) with preoperative LI in the left ATL surgery group, but not in the right surgery group. A significant correlation (1-tailed  $P < 0.05$ ) was obtained when the groups were combined, indicating greater verbal memory decline when preoperative hippocampal activation was lateralized more towards the side of surgery.

Finally, Köylü et al. examined correlations between preoperative MTL activation and verbal memory

performance before and after ATL surgery (Koylu et al. 2008). Average fMRI activation produced by a semantic decision – tone decision contrast was measured in left and right MTL regions of interest including the hippocampus and parahippocampus. The authors observed correlations between MTL activation and both preoperative and postoperative verbal memory. In the left ATL surgery group, postoperative memory was positively correlated with preoperative activation in the right MTL. Unfortunately, the analyses examined only pre- and postoperative scores in isolation and not pre- to postoperative change, which is the primary issue of clinical interest.

Although preliminary, these studies are encouraging in that they suggest that preoperative fMRI activation asymmetry may provide information about the risk of memory decline in patients undergoing ATL resection. Among the studies that assessed verbal memory change, two (Rabin et al. 2004; Frings et al. 2008) used complex scene encoding tasks that activate the MTL bilaterally on fMRI. This bilateral pattern suggests activation of both verbal and nonverbal memory encoding systems. Prediction of verbal memory outcome using these paradigms seems to be weak at best. In contrast, the verbal memory fMRI paradigms used by Richardson et al. appear to provide better predictive information regarding verbal memory outcome, at least when the analysis is confined to a specific region of the hippocampus. The persistent difficulty in applying the latter approach, however, is identifying *a priori* the small set of voxels that will be predictive in a given individual patient.

### 9.2.3 Language Lateralization as a Predictor of Verbal Memory Outcome

Binder et al. studied the relationship between preoperative language lateralization and verbal memory outcome (Binder et al. 2008b). The premise underlying this approach is that the verbal episodic memory encoding system is likely to be colateralized with language. More generally, the authors proposed that the type of material preferentially encoded by the left or right episodic memory system depends on the type of information it receives from the ipsilateral neocortex. If this model is correct, then the MTL in the language-dominant hemisphere is likely to be more critical for

supporting verbal episodic memory, and language lateralization should be a reliable indicator of verbal memory lateralization.

The study included 60 patients who underwent left ATL resection and a control group of 63 patients who underwent right ATL resection. The fMRI paradigm used a contrast between an auditory semantic decision task and a nonlinguistic tone decision task (Fig. 9.1, lower panel). Verbal memory was measured preoperatively and 6 months after surgery using the Selective Reminding Test, a word-list learning and retention test (Buschke and Fuld 1974). Other neuropsychological testing included the story recall and visual reproduction subtests from Wechsler Memory Scale (Wechsler 1997). Language LIs were computed from the fMRI data using a large region of interest covering the lateral two-thirds of each hemisphere (Springer et al. 1999). All patients also underwent preoperative Wada language and object memory testing.

The left ATL surgery group showed substantial changes in verbal memory, with an average raw score decline of 43% on word list learning and 45% on delayed recall of the word list. Of the individual patients in this group, 33% declined significantly on the learning measure and 55% on the delayed recall measure. In contrast, the right ATL surgery group improved slightly on both measures. Neither group showed significant changes on any nonverbal memory tests. Preoperative measures that predicted verbal memory decline in the left surgery group included the preoperative score, the fMRI language LI, the Wada language asymmetry score, the age at onset of epilepsy, and the Wada memory asymmetry score (Table 9.2, Fig. 9.2).

In applying these results to real clinical situations, the main questions to resolve are: which tests make a significant independent contribution to predicting outcome, and how should results from these tests be optimally combined? Binder et al. addressed these questions in a series of stepwise multiple regression

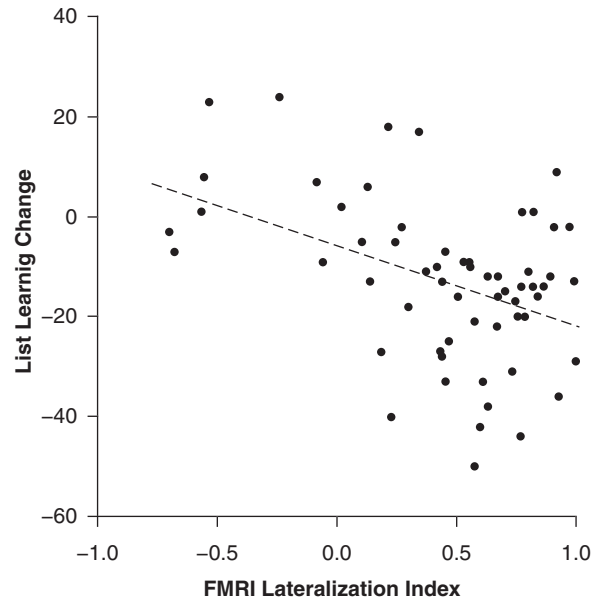


**Fig. 9.2** Relationship between fMRI lateralization indexes and individual change scores on a word-list learning verbal memory test (Continuous Long-Term Recall from the Selective Reminding Test) in 60 left ATL surgery patients ( $r = -0.432$ ,  $P < 0.001$ ) (adapted from Binder et al. 2008b)

analyses. The first variables entered in all analyses were preoperative test performance and age at onset of epilepsy. The rationale for including these variables first is that they can be obtained with relatively little expense and at no risk to the patient. Next, the fMRI language LI was added, followed by simultaneous addition of both the Wada memory and Wada language asymmetry scores. The rationale for adding fMRI in the second step is that fMRI is noninvasive and carries less risk than the Wada test. The two Wada scores were added together in the final step because these measures are typically obtained together.

Preoperative score and age at onset of epilepsy together accounted for 49% of the variance in List

**Table 9.2** Preoperative predictors of verbal memory outcome in 60 left ATL surgery patients

Predictor variable	List learning	<i>P</i>	Delayed recall	<i>P</i>
Preoperative score	-0.662	<0.0001	-0.654	<0.0001
fMRI language LI	-0.432	<0.001	-0.316	<0.05
Wada language asymmetry	-0.398	<0.01	-0.363	<0.01
Age at epilepsy onset	-0.341	<0.01	-0.390	<0.01
Wada memory asymmetry	-0.331	<0.05	-0.135	n.s.

List learning and delayed recall refer to the consistent long-term recall and delayed recall subtests of the selective reminding test. Simple correlation values and *P* values for each correlation are shown

Learning outcome and 54% of the variance in Delayed Recall outcome. The fMRI LI accounted for an additional 10% of the variance in List Learning outcome ( $P = 0.001$ ) and 7% of the variance in Delayed Recall outcome ( $P = 0.003$ ). Addition of the Wada language and memory data did not significantly improve the predictive power of either model ( $R^2$  change for List Learning = 0.025,  $R^2$  change for Delayed Recall = 0.017, both  $P > 0.1$ ). When patients were categorized as showing decline or no decline, based on a negative change score 1.5 standard deviations or more from the mean change score in the right ATL surgery group, the List Learning outcome model showed sensitivity of 90% and specificity of 80% for predicting decline on List Learning. The Delayed Recall outcome model showed sensitivity of 81% and specificity of 100% for predicting decline on Delayed Recall.

These results are interesting for several reasons. Most intriguing is the finding that *language* lateralization, whether measured by fMRI or the Wada test, was a better predictor of verbal *memory* outcome than Wada memory testing. The explanation for this paradox rests on two hypotheses. One, mentioned above, is that verbal memory encoding processes tend to

collateralize with language processes. The second hypothesis is that many tests of memory lateralization do not specifically assess verbal memory encoding. That is, visual stimuli such as objects and pictures can be dually encoded using both verbal and visual codes. Wada memory procedures that use such stimuli (including the Wada test used by Binder et al.) therefore do not provide a measure of verbal memory lateralization, but rather a measure of overall memory lateralization that includes both verbal and nonverbal encoding processes. Together, these two hypotheses suggest that language asymmetry may be more closely correlated with verbal memory lateralization than Wada memory asymmetry (Fig. 9.3). In particular, some patients with left temporal seizures show right-lateralized memory on the Wada test due to a strong nonverbal memory component in the right hemisphere, but are nevertheless at high risk for verbal memory decline because their *verbal* memory remains strongly lateralized to the left (Fig. 9.3b).

These data also have direct implications for clinical practice. First, they confirm the utility of fMRI for predicting verbal memory outcome in patients undergoing left ATL resection. The fMRI language LI is a

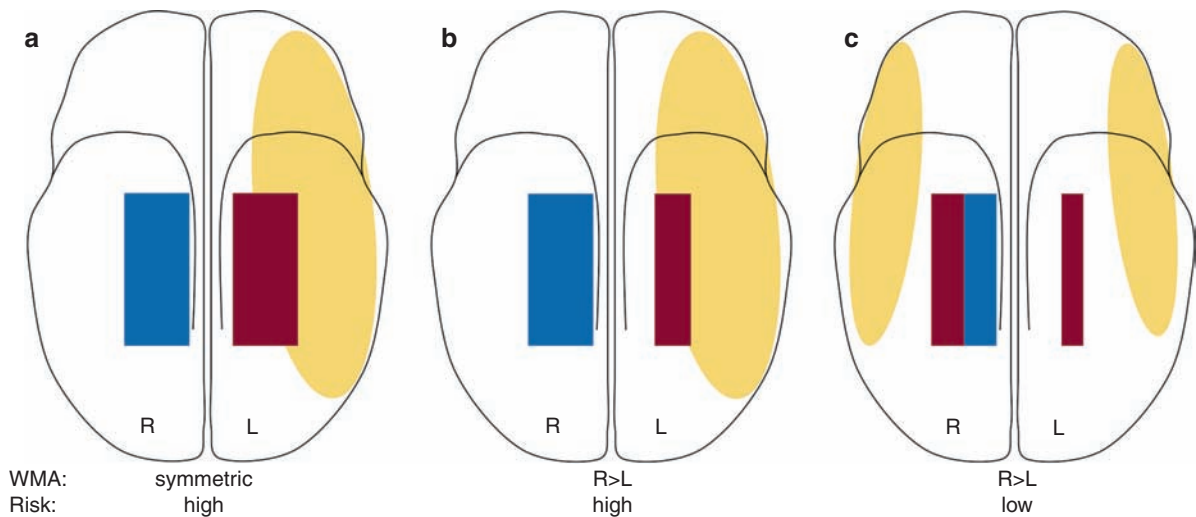


**Fig. 9.3** Schematic diagram of a hypothetical model of memory and language representation in temporal lobe epilepsy (TLE). The yellow ovals represent language systems, red rectangles represent verbal episodic memory encoding systems in the MTL, and green rectangles represent nonverbal episodic memory encoding systems in the MTL. (a) Typical state in healthy subjects and patients with late-onset epilepsy. Language and verbal memory processes are strongly left-lateralized, placing the patient at high risk for verbal memory decline.

(b) Chronic left TLE without shift. The left MTL is dysfunctional, causing Wada memory lateralization to the right, but verbal memory has not shifted, leaving the patient at high risk for verbal memory decline. (c) Chronic left TLE with shift. Both language and verbal memory functions have shifted partially to the right, lowering the risk for verbal memory decline. Note the partial lack of correspondence, across patient types, between Wada memory asymmetry and level of risk (adapted from Binder et al. 2008b)

safe, noninvasive measure that improves prediction accuracy relative to other noninvasive measures. The finding that Wada memory lateralization is not a strong predictor of verbal memory outcome and adds no predictive value beyond these noninvasive measures, confirms several previous studies that also examined multivariate prediction models (Chelune and Najm 2000; Stroup et al. 2003; Lacruz et al. 2004; Kirsch et al. 2005; Lineweaver et al. 2006). Although Binder et al. found that Wada language asymmetry is a stronger predictor of verbal memory outcome than Wada memory lateralization, even the addition of both Wada tests together did not contribute additional predictive power after inclusion of available noninvasive data (including fMRI). These results call into question the routine use of the Wada test for predicting material-specific verbal memory outcome, particularly if a validated fMRI measure of language lateralization is available. Some practitioners continue to value the Wada test as a means of predicting more severe “global” amnesia, such as is known to occur after bilateral MTL damage (Scoville and Milner 1957; Milner et al. 1962; Guerreiro et al. 2001; Di Gennaro et al. 2006). According to this theory, anesthetization of the to-be-resected MTL is necessary to discover whether the contralateral hemisphere is healthy enough to support memory on its own. Empirical observations, however, provide little support for such an approach. Cases of global amnesia following unilateral temporal lobe resection – especially modern, well-documented cases – appear to be rare in the extreme (Novelly and Williamson 1989; Loring et al. 1990a; Baxendale 1998; Kubu et al. 2000; Simkins-Bullock 2000; Kapur and Prevett 2003). Furthermore, there is ample evidence that contralateral hemisphere “memory failure” on the Wada test suffers from poor test-retest reliability and does not reliably predict amnesia (Novelly and Williamson 1989; Loring et al. 1990a; Lee et al. 1995; Kubu et al. 2000; Simkins-Bullock 2000; Martin and Grote 2002; Loddenkemper et al. 2007). Given the availability of fMRI for predicting material-specific verbal memory outcome, perhaps the use of the Wada test should be reserved only for patients at greatest risk for global amnesia, i.e., patients undergoing unilateral ATL resection and who have structural or functional evidence of damage to the contralateral MTL. Because it is noninvasive and requires fewer personnel, fMRI is also likely to be considerably less costly than Wada testing.

### 9.3 Conclusions

Recent studies demonstrate that preoperative fMRI can be used to predict postoperative naming and verbal memory changes in patients undergoing left ATL resection. Most importantly, two studies showed that fMRI significantly improves prediction accuracy when combined with other noninvasive measures (Sabsevitz et al. 2003; Binder et al. 2008b). Thus, fMRI provides patients and practitioners with a tool for making better-informed decisions based on a quantitative assessment of cognitive risk. The quantitative nature of these predictions represents something of a paradigm shift, in that traditional predictive models using the Wada test tended to be implemented as a dichotomous “pass or fail” judgment. The alternative approach followed in many recent studies involves the development of multivariable formulas that compute predicted change scores (Fig. 9.4). These quantitative predictions provide a much more realistic picture of the actual outcomes, which are not dichotomous but vary smoothly along a continuum. Ultimately, of course, the decision whether to undergo surgery is a categorical one, but the categorical nature of the decision does not obviate the need for precision regarding the factors that enter into the decision. An unemployed patient with frequent seizures may be willing to tolerate a substantial decline in naming or verbal memory, whereas a patient who depends on such cognitive abilities for her livelihood may be willing to risk a small decline but not a large one.

In practice, implementation of fMRI methods for predicting outcome in epilepsy surgery will depend on the availability of a validated fMRI protocol and involvement of clinicians with the necessary clinical expertise. Fast T2\*-weighted imaging capabilities necessary for fMRI are a standard feature on currently marketed clinical MRI systems, and fMRI is now available in some form at most medical centers. Implementation of cognitive fMRI protocols requires only installation of relatively low-cost audiovisual stimulation and response monitoring systems, together with expertise in cognitive training and testing provided by a neuropsychologist or cognitive neurologist.

**Acknowledgments** My thanks to Linda Allen, Thomas Hammeke, Wade Mueller, Romila Mushtaq, Conrad Nievera, Manoj Raghavan, David Sabsevitz, Sara Swanson, and other personnel at the Froedtert-MCW Comprehensive Epilepsy Center for assistance with this research, which was also

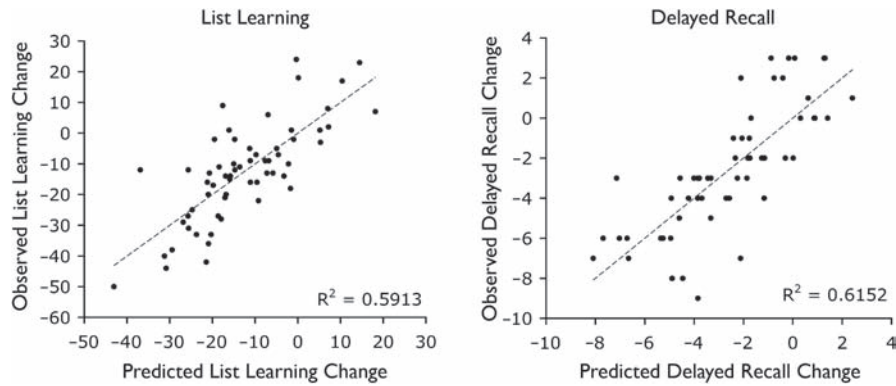


**Fig. 9.4** Predicted vs. observed individual memory change scores in 60 left ATL surgery patients on tests of word list learning and delayed recall. Predicted list learning change scores were computed from the formula:  $17.67 - 0.704(\text{preoperative score})$

$- 0.280(\text{age at onset}) - 12.19(\text{fMRI LI})$ . Predicted delayed recall change scores were computed from the formula:  $3.76 - 0.688(\text{preoperative score}) - 0.093(\text{age at onset}) - 2.14(\text{fMRI LI})$  (adapted from Binder et al. 2008b)

supported by National Institute of Neurological Diseases and Stroke grant R01 NS35929, National Institutes of Health General Clinical Research Center grant M01 RR00058, and the Charles A. Dana Foundation.

## References

- Adcock JE, Wise RG, Oxbury JM, Oxbury SM, Matthews PM (2003) Quantitative fMRI assessment of the differences in lateralization of language-related brain activation in patients with temporal lobe epilepsy. *Neuroimage* 18:423–438
- Alpherts WC, Vermeulen J, van Veelen CW (2000) The Wada test: prediction of focus lateralization by asymmetric and symmetric recall. *Epilepsy Res* 39:239–249
- Alvarez P, Squire LR (1994) Memory consolidation and the medial temporal lobe: a simple network model. *Proc Natl Acad Sci U S A* 91:7041–7045
- Andreasen NC, O’Leary DS, Cizadlo T, Arndt S, Rezai K, Watkins GL, Boles Ponto LL, Hichwa RD (1995) Remembering the past: two facets of episodic memory explored with positron emission tomography. *Am J Psychiatry* 152:1576–1585
- Bahn MM, Lin W, Silbergeld DL, Miller JW, Kuppusamy K, Cook RJ, Hammer G, Wetzel R, Cross D (1997) Localization of language cortices by functional MR imaging compared with intracarotid amobarbital hemispheric sedation. *Am J Radiol* 169:575–579
- Bartha L, Brenneis C, Schocke M, Trinka E, Koylu B, Trieb T, Kremser C, Jaschke W, Bauer G, Poewe W, Benke T (2003) Medial temporal lobe activation during semantic language processing: fMRI findings in healthy left- and right-handers. *Cogn Brain Res* 17:339–346
- Baxendale S (1998) Amnesia in temporal lobectomy patients: historical perspective and review. *Seizure* 7:15–24
- Baxendale S, Thompson P, Harkness W, Duncan J (2006) Predicting memory decline following epilepsy surgery: a multivariate approach. *Epilepsia* 47:1887–1894
- Baxendale S, Thompson P, Harkness W, Duncan J (2007) The role of the intracarotid amobarbital procedure in predicting verbal memory decline after temporal lobe resection. *Epilepsia* 48:546–552
- Bell BD, Davies KG, Haltiner AM, Walters GL (2000a) Intracarotid amobarbital procedure and prediction of postoperative memory in patients with left temporal lobe epilepsy and hippocampal sclerosis. *Epilepsia* 41:992–997
- Bell BD, Davies KG, Hermann BP, Walters G (2000b) Confrontation naming after anterior temporal lobectomy is related to age of acquisition of the object names. *Neuropsychologia* 38:83–92
- Benke T, Koylu B, Visani P, Karner E, Brenneis C, Bartha L, Trinka E, Trieb T, Felber S, Bauer G, Chemelli A, Willmes K (2006) Language lateralization in temporal lobe epilepsy: a comparison between fMRI and the Wada Test. *Epilepsia* 47:1308–1319
- Benson RR, FitzGerald DB, LeSeuer LL, Kennedy DN, Kwong KK, Buchbinder BR, Davis TL, Weisskoff RM, Talavage TM, Logan WJ, Cosgrove GR, Belliveau JW, Rosen BR (1999) Language dominance determined by whole brain functional MRI in patients with brain lesions. *Neurology* 52:798–809
- Binder JR (2006) FMRI of language systems: methods and applications. In: Faro SH, Mohammed FB (eds) *Functional MRI: basic principles and clinical applications*. Springer, New York, pp 245–277
- Binder JR, Bellgowan PSF, Hammeke TA, Possing ET, Frost JA (2005) A comparison of two fMRI protocols for eliciting hippocampal activation. *Epilepsia* 46:1061–1070
- Binder JR, Frost JA, Hammeke TA, Bellgowan PSF, Rao SM, Cox RW (1999) Conceptual processing during the conscious resting state: a functional MRI study. *J Cogn Neurosci* 11: 80–93
- Binder JR, Frost JA, Hammeke TA, Cox RW, Rao SM, Prieto T (1997) Human brain language areas identified by functional MRI. *J Neurosci* 17:353–362
- Binder JR, Raghavan M (2006) *Functional MRI in epilepsy*. In: D’Esposito ME (ed) *Functional MRI: applications in neurology and psychiatry*. Informa Healthcare, London, pp 81–114

- Binder JR, Swanson SJ, Hammeke TA, Sabsevitz DS (2008a) A comparison of five fMRI protocols for mapping speech comprehension systems. *Epilepsia* 49:1980–1997
- Binder JR, Sabsevitz DS, Swanson SJ, Hammeke TA, Raghavan M, Mueller WM (2008b) Use of preoperative functional MRI to predict verbal memory decline after temporal lobe epilepsy surgery. *Epilepsia* 49:1377–1394
- Binder JR, Swanson SJ, Hammeke TA, Morris GL, Mueller WM, Fischer M, Benbadis S, Frost JA, Rao SM, Haughton VM (1996) Determination of language dominance using functional MRI: a comparison with the Wada test. *Neurology* 46:978–984
- Brewer JB, Zhao Z, Desmond JE, Glover GH, Gabrieli JDE (1998) Making memories: brain activity that predicts how well visual experience will be remembered. *Science* 281:1185–1188
- Buckner RL, Wheeler ME, Sheridan MA (2001) Encoding processes during retrieval tasks. *J Cogn Neurosci* 13:406–415
- Buschke H, Fuld PA (1974) Evaluating storage, retention, and retrieval in disordered memory and learning. *Neurology* 24:1019–1025
- Carpenter K, Oxbury JM, Oxbury S, Wright GD (1996) Memory for objects presented after intracarotid sodium amytal: a sensitive clinical neuropsychological indicator of temporal lobe pathology. *Seizure* 5:103–108
- Carpentier A, Pugh KR, Westerveld M, Studholme C, Skrinjar O, Thompson JL, Spencer DD, Constable RT (2001) Functional MRI of language processing: dependence on input modality and temporal lobe epilepsy. *Epilepsia* 42:1241–1254
- Chelune GC (1995) Hippocampal adequacy versus functional reserve: predicting memory functions following temporal lobectomy. *Arch Clin Neuropsychol* 10:413–432
- Chelune GJ, Najm IM (2000) Risk factors associated with post-surgical decrements in memory. In: Luders HO, Comair Y (eds) *Epilepsy surgery*, 2nd edn. Lippincott, Philadelphia, pp 497–504
- Chelune GJ, Naugle RI, Lüders H, Awad IA (1991) Prediction of cognitive change as a function of preoperative ability level among temporal lobectomy patients at six months follow-up. *Neurology* 41:399–404
- Chelune GJ, Naugle RI, Lüders H, Sedlak J, Awad IA (1993) Individual change after epilepsy surgery: practice effects and base-rate information. *Neuropsychology* 7:41–52
- Chiaravalloti ND, Glosser G (2001) Material-specific memory changes after anterior temporal lobectomy as predicted by the intracarotid amobarbital test. *Epilepsia* 42:902–911
- Chlebus P, Mikl M, Brazdil M, Pazourkova M, Krupa P, Rektor I (2007) fMRI evaluation of hemispheric language dominance using various methods of laterality index calculation. *Exp Brain Res* 179:365–374
- Cohen NJ, Eichenbaum H (1993) *Memory, amnesia, and the hippocampal system*. MIT Press, Cambridge, MA
- Cohen-Gadol AA, Westerveld M, Alvarez-Carilles J, Spencer DD (2004) Intracarotid amytal memory test and hippocampal magnetic resonance imaging volumetry: validity of the Wada test as an indicator of hippocampal integrity among candidates for epilepsy surgery. *J Neurosurg* 101:926–931
- Constable RT, Carpentier A, Pugh K, Westerveld M, Oszunar Y, Spencer DD (2000) Investigation of the hippocampal formation using a randomized event-related paradigm and z-shimmed functional MRI. *Neuroimage* 12:55–62
- Craik FIM, Lockhart RS (1972) Levels of processing: a framework for memory research. *J Verbal Learn Verbal Behav* 11:671–684
- Damasio H, Grabowski TJ, Tranel D, Hichwa RD, Damasio AR (1996) A neural basis for lexical retrieval. *Nature* 380:499–505
- Davachi L, Wagner AD (2002) Hippocampal contributions to episodic memory: Insights from relational and item-based learning. *J Neurophysiol* 88:982–990
- Davies KG, Bell BD, Bush AJ, Wyler AR (1998a) Prediction of verbal memory loss in individuals after anterior temporal lobectomy. *Epilepsia* 39:820–828
- Davies KG, Bell BD, Bush AJ, Hermann BP, Dohan FC, Jaap AS (1998b) Naming decline after left anterior temporal lobectomy correlates with pathological status of resected hippocampus. *Epilepsia* 39:407–419
- Deblaere K, Boon PA, Vandemaele P, Tieleman A, Vonck K, Vingerhoets G, Backes W, Defreyne L, Achten E (2004) MRI language dominance assessment in epilepsy patients at 1.0 T: region of interest analysis and comparison with intracarotid amytal testing. *Neuroradiology* 46:413–420
- Desmond JE, Sum JM, Wagner AD, Demb JB, Shear PK, Glover GH, Gabrieli JDE, Morrell MJ (1995) Functional MRI measurement of language lateralization in Wada-tested patients. *Brain* 118:1411–1419
- Detre JA, Maccotta L, King D, Alsop DC, D’Esposito M, Zarahn E, Aguirre GK, Glosser G, French JA (1998) Functional MRI lateralization of memory in temporal lobe epilepsy. *Neurology* 50:926–932
- Di Gennaro G, Grammaldo LG, Quarato PP, Esposito V, Mascia A, Sparano A, Meldolesi GN, Picardi A (2006) Severe amnesia following bilateral medial temporal lobe damage occurring on two distinct occasions. *Neurol Sci* 27:129–133
- Eldridge LL, Knowlton BJ, Furmanski CS, Bookheimer SY, Engel SA (2000) Remembering episodes: a selective role for the hippocampus during retrieval. *Nat Neurosci* 3:1149–1152
- Fernandez G, Weyerts H, Schrader-Bölsche M, Tendolcar I, Smid HG, Tempelmann C, Hinrichs H, Scheich H, Elger CE, Mangun GR, Heinze H-J (1998) Successful verbal encoding into episodic memory engages the posterior hippocampus: a parametrically analyzed functional magnetic resonance imaging study. *J Neurosci* 18:1841–1847
- Fransson P, Merboldt KD, Ingvar M, Petersson KM, Frahm J (2001) Functional MRI with reduced susceptibility artifact: high-resolution mapping of episodic memory encoding. *Neuroreport* 12:1415–1420
- Frings L, Wagner K, Halsband U, Schwarzwald R, Zentner J, Schulze-Bonhage A (2008) Lateralization of hippocampal activation differs between left and right temporal lobe epilepsy patients and correlates with postsurgical verbal learning decrement. *Epilepsy Res* 78:161–170
- Gabrieli JDE (2001) Functional imaging of episodic memory. In: Cabeza R, Kingstone A (eds) *Handbook of functional neuroimaging of cognition*. MIT Press, Cambridge, MA, pp 253–291
- Gabrieli JDE, Brewer JB, Desmond JE, Glover GH (1997) Separate neural bases of two fundamental memory processes in human medial temporal lobe. *Science* 276:264–266
- Gaillard WD, Balsamo L, Xu B, McKinney C, Papero PH, Weinstein S, Conry J, Pearl P, Sachs B, Sato S, Vezina LG,

- Frattali C, Theodore WH (2004) fMRI language task panel improves determination of language dominance. *Neurology* 63:1403–1408
- Gleissner U, Helmstaedter C, Schramm J, Elger CE (2004) Memory outcome after selective amygdalohippocampectomy in patients with temporal lobe epilepsy: one-year follow-up. *Epilepsia* 45:960–962
- Golby AJ, Poldrack RA, Brewer JB, Spencer D, Desmond JE, Aron AP, Gabrieli JD (2001) Material-specific lateralization in the medial temporal lobe and prefrontal cortex during memory encoding. *Brain* 124:1841–1854
- Greene AJ, Gross WL, Elsingher CL, Rao SM (2006) An fMRI analysis of the human hippocampus: inference, context, and task awareness. *J Cogn Neurosci* 18:1156–1173
- Griffith HR, Perlman SB, Woodard AR, Rutecki PA, Jones JC, Ramirez LF, DeLaPena R, Seidenberg M, Hermann BP (2000) Preoperative FDG-PET temporal lobe hypometabolism and verbal memory after temporal lobectomy. *Neurology* 54:1161–1165
- Grunwald T, Lehnertz K, Heinze HJ, Helmstaedter C, Elger CE (1998) Verbal novelty detection within the human hippocampus proper. *Proc Natl Acad Sci U S A* 95:3193–3197
- Guerreiro CAM, Jones-Gotman M, Andermann F, Cendes F (2001) Severe amnesia in epilepsy: Causes, anatomopsychological considerations, and treatment. *Epilepsy Behav* 2:224–246
- Hamberger MJ, Goodman RR, Perrine K, Tamny TR (2001) Anatomic dissociation of auditory and visual naming in the lateral temporal cortex. *Neurology* 56:56–61
- Hassabis D, Kumaran D, Maguire EA (2007) Using imagination to understand the neural basis of episodic memory. *J Neurosci* 27:14365–14374
- Helmstaedter C, Elger CE (1996) Cognitive consequences of two-thirds anterior temporal lobectomy on verbal memory in 144 patients: a three-month follow-up study. *Epilepsia* 37:171–180
- Helmstaedter C, Kurthen M, Lux S, Reuber M, Elger CE (2003) Chronic epilepsy and cognition: a longitudinal study in temporal lobe epilepsy. *Ann Neurol* 54:425–432
- Henke K, Buck A, Weber B, Wieser HG (1997) Human hippocampus establishes associations in memory. *Hippocampus* 7:249–256
- Henke K, Weber B, Kneifel S, Wieser HG, Buck A (1999) Human hippocampus associates information in memory. *Proc Natl Acad Sci U S A* 96:5884–5889
- Hermann B, Davies K, Foley K, Bell B (1999a) Visual confrontation naming outcome after standard left anterior temporal lobectomy with sparing versus resection of the superior temporal gyrus: a randomized prospective clinical trial. *Epilepsia* 40:1070–1076
- Hermann BP, Wyler AR, Somes G, Clement L (1994) Dysnomia after left anterior temporal lobectomy without functional mapping: frequency and correlates. *Neurosurgery* 35:52–57
- Hermann BP, Seidenberg M, Haltiner A, Wyler AR (1995) Relationship of age at onset, chronologic age, and adequacy of preoperative performance to verbal memory change after anterior temporal lobectomy. *Epilepsia* 36:137–145
- Hermann BP, Perrine K, Chelune GJ, Barr W, Loring DW, Strauss E, Trenerry MR, Westerveld M (1999b) Visual confrontation naming following left anterior temporal lobectomy: a comparison of surgical approaches. *Neuropsychology* 13:3–9
- Hertz-Pannier L, Gaillard WD, Mott S, Cuenod CA, Bookheimer S, Weinstein S, Conry J, Papero PH, Schiff SJ, LeBihan D, Theodore WH (1997) Noninvasive assessment of language dominance in children and adolescents with functional MRI: a preliminary study. *Neurology* 48:1003–1012
- Humphries C, Swinney D, Love T, Hickok G (2005) Response of anterior temporal cortex to syntactic and prosodic manipulations during sentence processing. *Hum Brain Mapp* 26:128–138
- Hunkin NM, Mayes AR, Gregory LJ, Nicholas AK, Nunn JA, Brammer MJ, Bullmore ET, Williams SC (2002) Novelty-related activation within the medial temporal lobes. *Neuropsychologia* 40:1456–1464
- Hwang DY, Golby AJ (2006) The brain basis for episodic memory: insights from functional MRI, intracranial EEG, and patients with epilepsy. *Epilepsy Behav* 8:115–126
- Jeong S-W, Lee SK, Hong K-S, Kinn K-K, Chung C-K, Kim H (2005) Prognostic factors for the surgery for mesial temporal lobe epilepsy: longitudinal analysis. *Epilepsia* 46:1273–1279
- Jokeit H, Ebner A, Holthausen H, Markowitsch HJ, Moch A, Pannek H, Schulz R, Tuxhorn I (1997) Individual prediction of change in delayed recall of prose passages after left-sided anterior temporal lobectomy. *Neurology* 49:481–487
- Kapur N, Preveit M (2003) Unexpected amnesia: are there lessons to be learned from cases of amnesia following unilateral temporal lobe surgery? *Brain* 126:2573–2585
- Kelley WM, Miezin FM, McDermott KB, Buckner RL, Raichle ME, Cohen NJ, Ollinger JM, Akbudak E, Conturo TE, Snyder AZ, Petersen SE (1998) Hemispheric specialization in human dorsal frontal cortex and medial temporal lobe for verbal and nonverbal memory encoding. *Neuron* 20:927–936
- Kensinger EA, Clarke RJ, Corkin S (2003) What neural correlates underlie successful encoding and retrieval? A functional magnetic resonance imaging study using a divided attention paradigm. *J Neurosci* 23:2407–2415
- Killgore WD, Casasanto DJ, Yurgelun-Todd DA, Maldjian JA, Detre JA (2002) Functional activation of the left amygdala and hippocampus during associative encoding. *Neuroreport* 11:2259–2263
- Kirchhoff BA, Wagner AD, Maril A, Stern CE (2000) Prefrontal-temporal circuitry for episodic encoding and subsequent memory. *J Neurosci* 20:6173–6180
- Kirsch HE, Walker JA, Winstanley FS, Hendrickson R, Wong ST, Barbaro NM, Laxer KD, Garcia PA (2005) Limitations of Wada memory asymmetry as a predictor of outcomes after temporal lobectomy. *Neurology* 65:676–680
- Knecht S, Deppe M, Dräger B, Bobe L, Lohmann H, Ringelstein EB, Henningsen H (2000a) Language lateralization in healthy right-handers. *Brain* 123:74–81
- Knecht S, Dräger B, Deppe M, Bobe L, Lohmann H, Flöel A, Ringelstein E-B, Henningsen H (2000b) Handedness and hemispheric language dominance in healthy humans. *Brain* 123:2512–2518
- Knecht S, Flöel A, Dräger B, Breitenstein C, Sommer J, Henningsen H, Ringelstein E-B, Pascual-Leone A (2002) Degree of language lateralization determines susceptibility to unilateral brain lesions. *Nat Neurosci* 5:695–699
- Kneebone AC, Chelune GJ, Dinner DS, Naugle RI, Awad IA (1995) Intracarotid amobarbital procedure as a predictor of

- material-specific memory change after anterior temporal lobectomy. *Epilepsia* 36:857–865
- Knight RT (1996) Contribution of the human hippocampal region to novelty detection. *Nature* 383:256–259
- Koylu B, Walser G, Ischebeck A, Ortler M, Benke T (2008) Functional imaging of semantic memory predicts postoperative episodic memory functions in chronic temporal lobe epilepsy. *Brain Res* 1223:73–81
- Kubu CS, Girvin JP, McLachlan RS, Pavol M, Harnadek MC (2000) Does the intracarotid amobarbital procedure predict global amnesia after temporal lobectomy? *Epilepsia* 41:1321–1329
- Lacruz ME, Alarcon G, Akanuma N, Lum FC, Kissani N, Koutroumanidis M, Adachi N, Binnie CD, Polkey CE, Morris RG (2004) Neuropsychological effects associated with temporal lobectomy and amygdalohippocampectomy depending on Wada test failure. *J Neurol Neurosurg Psychiatry* 75:600–607
- Langfitt JT, Rausch R (1996) Word-finding deficits persist after left anterotemporal lobectomy. *Arch Neurol* 53:72–76
- Langfitt JT, Westerveld M, Hamberger MJ, Walczak TS, Cicchetti DV, Berg AT, Vickrey BG, Barr WB, Sperling MR, Masur D, Spencer SS (2007) Worsening of quality of life after epilepsy surgery: effect of seizures and memory decline. *Neurology* 68:1988–1994
- Lee GP, Loring DW, Smith JR, Flanigin HF (1995) Intraoperative hippocampal cooling and Wada memory testing in the evaluation of amnesia risk following anterior temporal lobectomy. *Arch Neurol* 52:857–861
- Lee TMC, Yip JTH, Jones-Gotman M (2002) Memory deficits after resection of left or right anterior temporal lobe in humans: a meta-analytic review. *Epilepsia* 43:283–291
- Lehéricy S, Cohen L, Bazin B, Samson S, Giacomini E, Rougetet R, Hertz-Pannier L, LeBihan D, Marsault C, Baulac M (2000) Functional MR evaluation of temporal and frontal language dominance compared with the Wada test. *Neurology* 54:1625–1633
- Li L, Miller EK, Desimone R (1993) The representation of stimulus familiarity in anterior inferior temporal cortex. *J Neurophysiol* 69:1918–1929
- Lineweaver TT, Naugle RI, Cafaro AM, Bingaman W, Luders HO (2004) Patients' perceptions of memory functioning before and after surgical intervention to treat medically refractory epilepsy. *Epilepsia* 45:1604–1612
- Lineweaver TT, Morris HH, Naugle RI, Najm IM, Diehl B, Bingaman W (2006) Evaluating the contributions of state-of-the-art assessment techniques to predicting memory outcome after unilateral anterior temporal lobectomy. *Epilepsia* 47:1895–1903
- Loddenkemper T, Morris HH, Lineweaver TT, Kellinghaus C (2007) Repeated intracarotid amobarbital tests. *Epilepsia* 48:553–558
- Loring DW, Lee GP, Meador KJ, Flanigin HF, Figueroa RE, Martin RC (1990a) The intracarotid amobarbital procedure as a predictor of memory failure following unilateral temporal lobectomy. *Neurology* 40:605–610
- Loring DW, Meador KJ, Lee GP, King DW, Gallagher BB, Murro AM, Smith JR (1994) Stimulus timing effects on Wada memory testing. *Arch Neurol* 51:806–810
- Loring DW, Hermann BP, Perrine K, Plenger PM, Lee GP, Nichols ME, Meador KJ (1995a) Memory for real objects is superior to line drawing recognition in discrimination of lateralized temporal lobe impairment during the Wada test. *J Int Neuropsychol Soc* 1:134
- Loring DW, Meador KJ, Lee GP, Murro AM, Smith JR, Flanigin HF, Gallagher BB, King DW (1990b) Cerebral language lateralization: Evidence from intracarotid amobarbital testing. *Neuropsychologia* 28:831–838
- Loring DW, Meador KJ, Lee GP, King DW, Nichols ME, Park YD, Murro AM, Gallagher BB, Smith JR (1995b) Wada memory asymmetries predict verbal memory decline after anterior temporal lobectomy. *Neurology* 45:1329–1333
- Martin A (1999) Automatic activation of the medial temporal lobe during encoding: Lateralized influences of meaning and novelty. *Hippocampus* 9:62–70
- Martin RC, Grote CL (2002) Does the Wada test predict memory decline following epilepsy surgery. *Epilepsy Behav* 3:4–15
- Martin RC, Sawrie SM, Roth DL, Giliam FG, Faught E, Morawetz RB, Kuzniecky R (1998) Individual memory change after anterior temporal lobectomy: a base rate analysis using regression-based outcome methodology. *Epilepsia* 39:1075–1082
- Mazoyer BM, Tzourio N, Frak V, Syrota A, Murayama N, Levrier O, Salamon G, Dehaene S, Cohen L, Mehler J (1993) The cortical representation of speech. *J Cogn Neurosci* 5:467–479
- McClelland JL, McNaughton BL, O'Reilly RC (1995) Why are there complementary learning systems in the hippocampus and neocortex: insights from the success and failures of connectionist models of learning and memory. *Psychol Rev* 102:409–457
- McIntosh AM, Wilson SJ, Berkovic SF (2001) Seizure outcome after temporal lobectomy: current research practice and findings. *Epilepsia* 42:1288–1307
- Milner B, Branch C, Rasmussen T (1962) Study of short-term memory after intracarotid injection of sodium amytal. *Trans Am Neurol Assoc* 87:224–226
- Morawetz C, Holz P, Lange C, Baudewig J, Weniger G, Irle E, Dechent P (2008) Improved functional mapping of the human amygdala using a standard functional magnetic resonance imaging sequence with simple modifications. *Magn Reson Imaging* 26:45–53
- Nagata S, Uchimura K, Hirakawa W, Kuratsu J (2001) Method for quantitatively evaluating the lateralization of linguistic function using functional MR imaging. *Am J Neuroradiol* 22:985–991
- Novelly RA, Williamson PD (1989) Incidence of false-positive memory impairment in the intracarotid Amytal procedure. *Epilepsia* 30:711
- O'Reilly RC, Rudy JW (2001) Conjunctive representations in learning and memory: principles of cortical and hippocampal function. *Psychol Rev* 108:311–345
- Otten LJ, Henson RNA, Rugg MD (2001) Depth of processing effects on neural correlates of memory encoding. Relationship between findings from across- and within-task comparisons. *Brain* 124:399–412
- Paller KA, Wagner AD (2002) Observing the transformation of experience into memory. *Trends Cogn Sci* 6:93–102
- Parsons MW, Haut MW, Lemieux SK, Moran MT, Leach SG (2006) Anterior medial temporal lobe activation during encoding of words: fMRI methods to optimize sensitivity. *Brain Cogn* 60:253–261
- Perrine K, Hermann BP, Meador KJ, Vickrey BG, Cramer JA, Hays RD, Devinsky O (1995) The relationship of

- neuropsychological functioning to quality of life in epilepsy. *Arch Neurol* 52:997–1003
- Pigot S, Milner B (1993) Memory for different aspects of complex visual scenes after unilateral-temporal or frontal-lobe resection. *Neuropsychologia* 13:1–15
- Pillon B, Bazin B, Deweer B, Ehrle N, Baulac M, Dubois B (1999) Specificity of memory deficits after right or left temporal lobectomy. *Cortex* 35:561–571
- Powell HW, Koepp MJ, Symms MR, Boulby PA, Salek-Haddadi A, Thompson PJ, Duncan JS, Richardson MP (2005) Material-specific lateralization of memory encoding in the medial temporal lobe: Blocked versus event-related design. *Neuroimage* 48:1512–1525
- Powell HWR, Richardson MP, Symms MR, Boulby PA, Thompson PJ, Duncan JS, Koepp MJ (2008) Preoperative fMRI predicts memory decline following anterior temporal lobe resection. *J Neurol Neurosurg Psychiatry* 79: 686–693
- Prince SE, Daselaar SM, Cabeza R (2005) Neural correlates of relational memory: Successful encoding and retrieval of semantic and perceptual associations. *J Neurosci* 25: 1203–1210
- Prince SE, Tsukiura T, Cabeza R (2007) Distinguishing the neural correlates of episodic memory encoding and semantic memory retrieval. *Psychol Sci* 18:144–151
- Rabin ML, Narayan VM, Kimberg DY, Casasanto DJ, Glosser G, Tracy JI, French JA, Sperling MR, Detre JA (2004) Functional MRI predicts post-surgical memory following temporal lobectomy. *Brain* 127:2286–2298
- Reber PJ, Wong EC, Buxton RB (2002) Encoding activity in the medial temporal lobe examined with anatomically constrained fMRI analysis. *Hippocampus* 12:363–376
- Richardson MP, Strange BA, Duncan JS, Dolan RJ (2006) Memory fMRI in left hippocampal sclerosis. Optimizing the approach to predicting postsurgical memory. *Neurology* 66:699–705
- Richardson MP, Strange BA, Thompson PJ, Baxendale SA, Duncan JS, Dolan RJ (2004) Pre-operative verbal memory fMRI predicts post-operative memory decline after left anterior temporal lobe resection. *Brain* 127:2419–2426
- Riches IP, Wilson FAW, Brown MW (1991) The effects of visual stimulation and memory on neurones of the hippocampal formation and neighboring parahippocampal gyrus and inferior temporal cortex of the primate. *J Neurosci* 11: 1763–1779
- Rogers TT, Hocking J, Noppeney U, Mechelli A, Gorno-Tempini ML, Patterson K, Price CJ (2006) Anterior temporal cortex and semantic memory: reconciling findings from neuropsychology and functional imaging. *Cogn Affect Behav Neurosci* 6:201–213
- Rugg MD, Otten LJ, Henson RNA (2002) The neural basis of episodic memory: evidence from functional neuroimaging. *Philos Trans R Soc Lond B* 357:1097–1110
- Rutten G-J, Ramsey N, van Rijen P, Alpherts W, van Veelen C (2002) fMRI-determined language lateralization in patients with unilateral or mixed language dominance according to the Wada test. *Neuroimage* 17:447–460
- Sabbah P, Chassoux F, Leveque C, Landre E, Baudoin-Chial S, Devaux B, Mann M, Godon-Hardy S, Nioche C, Ait-Ameur A, Sarrazin JL, Chodkiewicz JP (2003) Functional MR imaging in assessment of language dominance in epileptic patients. *Neuroimage* 18:460–467
- Sabsevitz DS, Swanson SJ, Morris GL, Mueller WM, Seidenberg M (2001) Memory outcome after left anterior temporal lobectomy in patients with expected and reversed Wada memory asymmetry scores. *Epilepsia* 42:1408–1415
- Sabsevitz DS, Swanson SJ, Hammeke TA, Spanaki MV, Possing ET, Morris GL, Mueller WM, Binder JR (2003) Use of preoperative functional neuroimaging to predict language deficits from epilepsy surgery. *Neurology* 60:1788–1792
- Saykin AJ, Stafiniak P, Robinson LJ, Flannery K, Gur R, O'Connor MJ, Sperling MR (1995) Language before and after temporal lobectomy: specificity of acute changes and relation to early risk factors. *Epilepsia* 36:1071–1077
- Schacter DL, Wagner AD (1999) Medial temporal lobe activations in fMRI and PET studies of episodic encoding and retrieval. *Hippocampus* 9:7–24
- Schacter DL, Addis DR (2007) The cognitive neuroscience of constructive memory: remembering the past and imagining the future. *Philos Trans R Soc Lond B* 362:773–786
- Scoville WB, Milner B (1957) Loss of recent memory after bilateral hippocampal lesions. *J Neurol Neurosurg Psychiatry* 20:11–21
- Seghier ML (2008) Laterality index in functional MRI: methodological issues. *Magn Reson Imaging* 26:594–601
- Simkins-Bullock J (2000) Beyond speech lateralization: a review of the variability, reliability, and validity of the intracarotid amobarbital procedure and its nonlanguage uses in epilepsy surgery candidates. *Neuropsychology Rev* 10:41–74
- Small SA, Nava AS, Perera GM, DeLaPaz R, Mayeux R, Stern Y (2001) Circuit mechanisms underlying memory encoding and retrieval in the long axis of the hippocampal formation. *Nat Neurosci* 4:442–449
- Sperling RA, Bates JF, Cocchiarella AJ, Schacter DL, Rosen BR, Albert MS (2001) Encoding novel face-name associations: a functional MRI study. *Hum Brain Mapp* 14: 129–139
- Spreer J, Arnold S, Quiske A, Ziyeh S, Altenmüller DM, Herpers M, Kassubek J, Klisch J, Steinhoff BJ, Honegger J, Schulze-Bonhage A, Schumacher M (2002) Determination of hemisphere dominance for language: comparison of frontal and temporal fMRI activation with intracarotid amytal testing. *Neuroradiology* 44:467–474
- Springer JA, Binder JR, Hammeke TA, Swanson SJ, Frost JA, Bellgowan PSF, Brewer CC, Perry HM, Morris GL, Mueller WM (1999) Language dominance in neurologically normal and epilepsy subjects: a functional MRI study. *Brain* 122:2033–2045
- Squire LR (1992) Memory and the hippocampus: a synthesis from findings with rats, monkeys, and humans. *Psychol Rev* 99:195–231
- Stafiniak P, Saykin AJ, Sperling MR, Kester DB, Robinson LJ, O'Connor MJ, Gur RC (1990) Acute naming deficits following dominant temporal lobectomy: prediction by age at first risk for seizures. *Neurology* 40:1509–1512
- Stark CE, Squire LR (2001) When zero is not zero: The problem of ambiguous baseline conditions in fMRI. *Proc Natl Acad Sci U S A* 98:12760–12766
- Stern CE, Corkin S, González RG, Guimaraes AR, Baker JA, Jennings PJ, Carr CA, Sugiura RM, Vedantham V, Rosen BR (1996) The hippocampal formation participates in novel picture encoding: Evidence from functional magnetic resonance imaging. *Proc Natl Acad Sci U S A* 93: 8660–8665

- Stroup E, Langfitt JT, Berg M, McDermott M, Pilcher W, Como P (2003) Predicting verbal memory decline following anterior temporal lobectomy (ATL). *Neurology* 60:1266–1273
- Swanson SJ, Sabsevitz DS, Hammeke TA, Binder JR (2007) Functional magnetic resonance imaging of language in epilepsy. *Neuropsychol Rev* 17:491–504
- Tellez-Zenteno JF, Dhar R, Wiebe S (2005) Long-term seizure outcomes following epilepsy surgery: a systematic review and meta-analysis. *Brain* 128:1188–1198
- Trenerry MR, Jack CRJ, Ivnik RJ, Sharbrough FW, Cascino GD, Hirschorn KA, Marsh WR, Kelly PJ, Meyer FB (1993) MRI hippocampal volumes and memory function before and after temporal lobectomy. *Neurology* 43:1800–1805
- Tulving E, Markowitsch HJ, Crail FIM, Habib R, Houle S (1996) Novelty and familiarity activations in PET studies of memory encoding and retrieval. *Cereb Cortex* 6:71–79
- Uncapher MR, Rugg MD (2005) Encoding and durability of episodic memory: A functional magnetic resonance imaging study. *J Neurosci* 25:7260–7267
- Vilberg KL, Rugg MD (2008) Memory retrieval and the parietal cortex: a review of evidence from a dual-process perspective. *Neuropsychologia* 46:1787–1799
- Vincent JL, Snyder AZ, Fox MD, Shannon BJ, Andrews JR, Raichle ME, Buckner RL (2006) Coherent spontaneous activity identifies a hippocampal-parietal memory network. *J Neurophysiol* 96:3517–3531
- Wada J, Rasmussen T (1960) Intracarotid injection of sodium amytal for the lateralization of cerebral speech dominance. *J Neurosurg* 17:266–282
- Wagner AD, Schacter DL, Rotte M, Koutstaal W, Maril A, Dale AM, Rosen BR, Buckner RL (1998) Building memories: remembering and forgetting of verbal experiences as predicted by brain activity. *Science* 281:1188–1191
- Wechsler D (1997) WMS-III: Wechsler memory scale administration and scoring manual, 3rd edn. Psychological Corporation, San Antonio, TX
- Weis S, Klaver P, Reul J, Elger CE, Fernández G (2004) Temporal and cerebellar brain regions that support both declarative memory formation and retrieval. *Cereb Cortex* 14:256–267
- Wendel JD, Trenerry MR, Xu YC, Sencakova D, Cascino GD, Britton JW, Lagerlund TD, Shin C, So EL, Sharbrough FW, Jack CR (2001) The relationship between quantitative T2 relaxometry and memory in nonlesional temporal lobe epilepsy. *Epilepsia* 42:863–869
- Wilke M, Schmithorst VJ (2006) A combined bootstrap/histogram analysis approach for computing a lateralization index from neuroimaging data. *Neuroimage* 33:522–530
- Woermann FG, Jokeit H, Luerding R, Freitag H, Schulz R, Guertler S, Okujava M, Wolf PA, Tuxhorn I, Ebner A (2003) Language lateralization by Wada test and fMRI in 100 patients with epilepsy. *Neurology* 61:699–701
- Worthington C, Vincent DJ, Bryant AE, Roberts DR, Vera CL, Ross DA, George MS (1997) Comparison of functional magnetic resonance imaging for language localization and intracarotid speech amytal testing in presurgical evaluation for intractable epilepsy. *Stereotact Funct Neurosurg* 69:197–201
- Yetkin FZ, Swanson S, Fischer M, Akansel G, Morris G, Mueller W, Haughton V (1998) Functional MR of frontal lobe activation: comparison with Wada language results. *Am J Neuroradiol* 19:1095–1098
- Zeinab MM, Engel SA, Thompson PM, Bookheimer SY (2003) Dynamics of the hippocampus during encoding and retrieval of face-name pairs. *Science* 299:577–580

## 10.1 The Principle of Activation Studies

The energy demand of the brain is very high and relies almost entirely on the oxidative metabolism of glucose. Glucose metabolized in neuronal cell bodies mainly supports cellular, vegetative and house-keeping functions, e.g., axonal transport, biosynthesis of nucleic acids, proteins, lipids, as well as other energy-consuming processes not related directly to action potentials. Therefore, the energy demand of neuronal cell bodies is relatively low and essentially unaffected by neuronal functional activation (Sokoloff 1999). A larger portion of energy consumption is required for signalling, mainly action potential propagation and postsynaptic ion fluxes; this might account for up to 87% of the total energy consumed with only 13% expended in maintaining membrane resting potential (Laughlin and Attwell 2001). As a consequence, the rate of glucose consumption of neuronal cell bodies is essentially unaffected by functional activation, whereas increases in metabolism (and in the coupled regional blood flow) evoked by functional activation are confined to synapse-rich regions, i.e., the neuropil that contains axonal terminals, dendritic processes, and the astrocytic processes that envelop the synapses (Magistretti 2004). The magnitudes of these increases are linearly related to the frequency of action potentials in the afferent pathways, and increases of metabolism and blood flow in the projection zones occur regardless of whether the pathway is excitatory or inhibitory. Only at the next downstream projection zones, glucose utilization (and, as a

consequence, blood supply) is depressed in inhibited neurons and increased in excited neurons.

Mapping of neuronal activity in the brain can be primarily achieved by quantitation of the regional cerebral metabolic rate for glucose (rCMRGlc), as introduced for autoradiographic experimental studies by Sokoloff (Sokoloff 1999) and adapted for positron emission tomography (PET) in humans (Reivich et al. 1979). Functional mapping, as it is widely used now, relies primarily on the hemodynamic response assuming a close association between energy metabolism and blood flow. While it is well documented that increases in blood flow and glucose consumption are closely coupled during neuronal activation, the increase in oxygen consumption is considerably delayed leading to a decreased oxygen extraction fraction (OEF) during activation (Mintun et al. 2001). PET detects and, if required, can quantify changes in CBF and CMRGlc accompanying different activation states of the brain tissue. The regional values of CBF or CMRGlc represent the brain activity due to a specific state, task or stimulus, in comparison to the resting condition, and color coded maps can be analyzed or coregistered to morphologic images. Due to the radioactivity of the necessary tracers, activation studies with PET are limited to a maximum of 12 doses of  $^{15}\text{O}$ -labeled tracers, e.g., 12 flow scans, or two doses of  $^{18}\text{F}$ -labelled tracers, e.g., two metabolic scans. Especially for studies of glucose consumption, the time to metabolic equilibrium (20–40 min) as well as the time interval between measurements required for isotope decay (HT for  $^{18}\text{F}$  108 min, for  $^{15}\text{O}$  2 min) must be taken into consideration.

Functional magnetic resonance imaging (fMRI) measures signals that depend on the differential magnetic properties of oxygenated and deoxygenated hemoglobin, termed the blood–oxygen-level-dependent (BOLD) signal, which gives an estimate of changes in oxygen

---

W.-D. Heiss  
Max Planck Institute for Neurological Research,  
Gleueler Str. 50, 50931 Köln, Germany  
email: wdh@nf.mpg.de

availability (Ogawa et al. 1990). This means that mainly the amount of deoxyhemoglobin in small blood vessels is recorded, which depends on the flow of well-oxygenated arterial blood (CBF), on the outflow of  $O_2$  to the tissue ( $CMRO_2$ ) and on the cerebral blood volume (CBV) (Turner et al. 1997). The magnitude of these changes in signal intensity relative to the resting conditions are color coded to produce fMRI images that map changes in brain function, which can be super-imposed on the anatomical image. This results in a spatial resolution of fMRI of 1–3 mm with a temporal resolution of approximately 10 s. As fMRI does not involve ionizing radiation, and thus, is also used without limitations in healthy subjects, allows more rapid signal acquisition and more flexible experimental setups, it has become the dominant technique for functional imaging. There are some advantages of PET, however – physiologically specific measures, better quantitation, better signal-to-noise ratio, fewer artifacts, actual activated and reference values – which support its continued use especially in complex clinical situation and in combination with special stimulating technique, as transcranial magnetic stimulation (TMS).

## 10.2 Language Activation in Healthy Subjects

The capacity to understand and to speak language is strictly lateralized in most subjects to the dominant hemisphere. With a few exceptions, this is the left hemisphere in right-handers, whereas in left-handers language may be represented in either hemisphere or even bilaterally (Knecht et al. 2002; Thiel et al. 1998). In addition to language dominance, details of the anatomical localization of sensory and motor language areas (Wernicke's and Broca's region) may vary considerably even in normal individuals. A considerable variety of language activation paradigms have been applied for localization of language functions by PET and fMRI (Hickok and Poeppel 2007; Petersen et al. 1988; Price 2000; Wise 2003), producing a vast amount of partly contradictory data (Demonet et al. 1996). For the analysis of aphasia after stroke or due to brain tumors, the application of a simplified scheme may be justified (Fig. 10.1) (Price 2000).

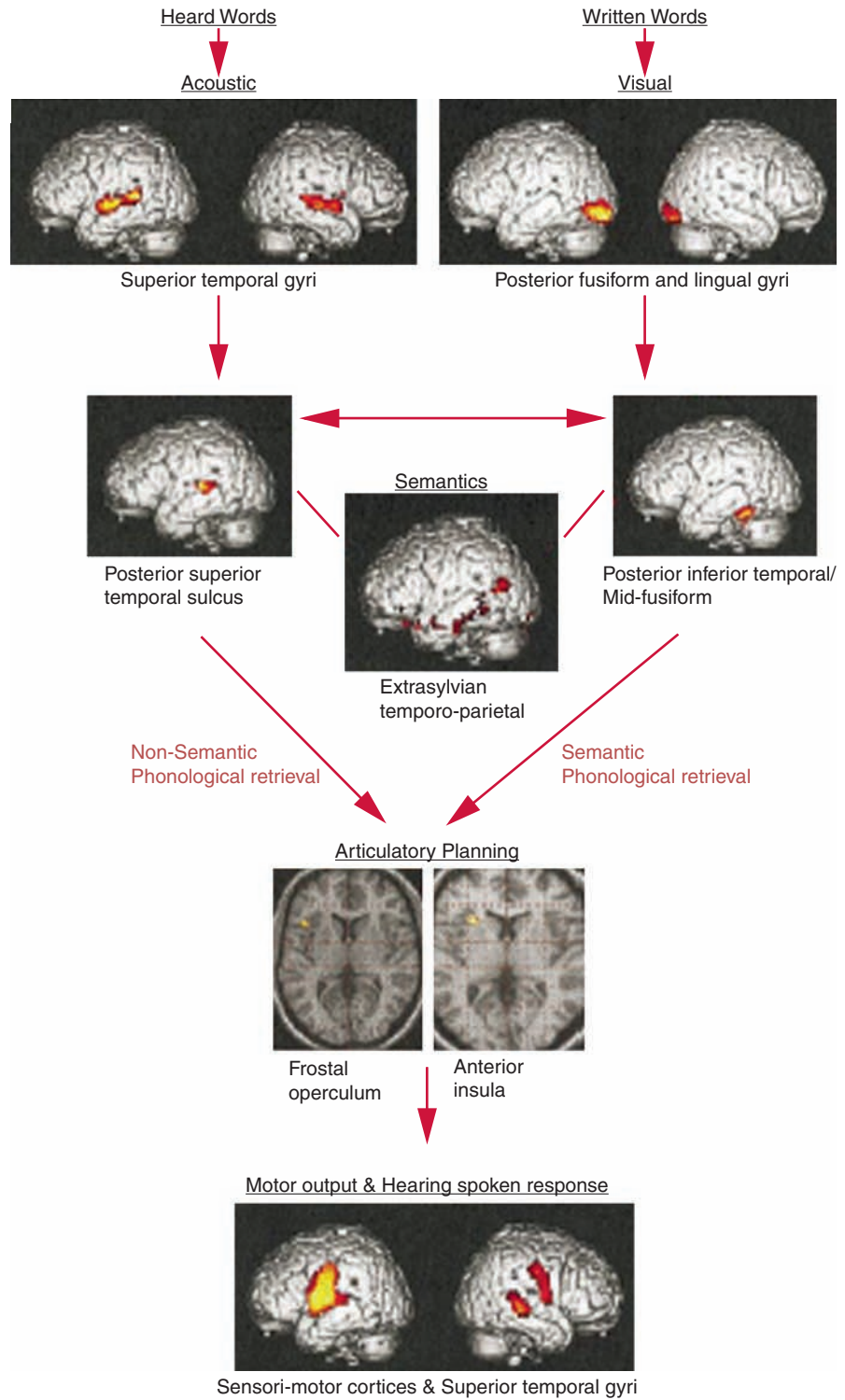
The processing of hearing words activates bilaterally the upper temporal gyrus and the semantic attribution to

a meaningful content is achieved in left posterior temporal, temporo-parietal and anterior lower cortical areas. For the production of speech, the activity in the posterior upper temporal sulcus and in the left posterior lower temporal cortex is increased. The activity in the posterior upper temporal sulci is further increased, if words or sequences are repeated or read. In contrast, the left posterior lower temporal cortex in the neighborhood of the middle fusiform semantic area is activated by word fluency. This area is participating in lexical speech production. Independently, planning of articulation activates the left anterior insula and the bordering frontal operculum. Phonologic word retrieval requires the integration of the anterior insula/operculum and the posterior upper temporal sulcus or left posterior lower temporal gyrus. Finally, the bilateral sensorimotor cortex is activated for the motoric control of speech production and the hearing of the spoken response augments the activation in the upper temporal gyrus.

In the processing of written words the same areas are involved. Reading selectively activates the posterior fusiform and lingual gyrus, which are also involved in picture naming. For reading, the visual cortex and the posterior upper temporal sulci are activated, which contribute to the functional integration of the language network. According to this model the function of the Wernicke region is represented in the upper part of the sulcus temporalis, the sulcus temporalis posterior superior; the anterior insula and not the Broca area is responsible for planning articulation; the gyrus angularis is involved in semantic connection and not specific for visualization of words; the meaning of words is located in the left lower and middle temporal gyrus; reading and retrieval of names activate the posterior lower temporal lobe. For these functions – and also for the severity of functional damage – the hierarchy of individual areas within the network and the dominance of left cortical regions is of utmost importance (Heiss and Thiel 2006), which is induced and manifested by collateral and transcallosal inhibition (Karbe et al. 1998; Nudo et al. 1996).

It has to be kept in mind that all usual language functions, which are complex, and require integration of several partial functions, activate larger parts of the bilateral network. For instance, the retrieval of substantives and verbs activates large areas in the left dorso-medial prefrontal cortex and the anterior cingulum as well as the supplementary motor area. The processing of meaningful connections activates the left

**Fig. 10.1** Proposed neurological and cognitive model of language with brain areas activated by different tasks. From Price (2000)



middle temporal gyrus, the left and right temporal pole as well as a left prefrontal area. Hearing and processing of nouns and generating verbs in relation to nouns involves a network consisting of pars opercularis and triangularis of the left lower frontal gyrus, the posterior part of the temporal sulcus up to the planum temporale and the anterior part of the left lower temporal gyrus. In this network, even some parts of the cerebellum and of the basal ganglia are integrated (Booth et al. 2007). These complex activation patterns involving widely distributed areas impair the prediction of severity and recovery of speech disturbances caused by infarcts or other localized brain damage.

### 10.3 Poststroke Aphasia

Aphasia is a severely incapacitating symptom of stroke and is a main cause of functional disturbance. Estimates suggest that more than 20% of patients suffering a stroke develop aphasia, 10–18% of survivors are left with a persistent speech deficit (Wade et al. 1986). Most patients with aphasia due to acute nonprogressive brain damage, such as in the case of stroke or head injury, show some degree of recovery of language function during the days, months, or even years following the initial insult. The recuperation is variable, ranging from the hardly noticeable improvement of auditory comprehension of the global aphasia to the apparently complete recovery of the patient with mild fluent aphasia due to small subcortical stroke. It is also well known that improvement can be observed not only in patients submitted to language rehabilitation but also in cases that have not undergone any specific treatment.

### 10.4 Disturbance of Regional Metabolism and Flow vs. Severity and Persistence of Language Deficit

Studies of glucose metabolism after stroke (Cappa et al. 1997) have shown metabolic disturbances in the ipsilateral hemisphere caused by the lesion, and contralateral hemisphere caused by functional deactivation (diaschisis) (Feeney and Baron 1986). Most studies have been performed in right-handed individuals with

language dominance in the left hemisphere. The left temporo-parietal region, in particular the angular gyrus, supramarginal gyrus, and lateral and transverse superior temporal gyrus are most frequently and consistently impaired, and the degree of impairment is related to the severity of aphasia (Karbe et al. 1989; Metter et al. 1990). In contrast, metabolic impairment in subcortical structures is related mainly to language fluency and other behavioral aspects, but not to aphasia severity (Metter et al. 1988). In patients with aphasia attributable to purely subcortical strokes, deactivation of temporo-parietal cortex is regularly found, which is probably responsible for the aphasic symptoms (Kumar et al. 1996).

Recovery of metabolism in both hemispheres was correlated with recovery of aphasia. One specific region crucial for recovery of language perception has been found in the left temporo-parietal cortex (Karbe et al. 1989; Metter et al. 1987) and metabolic disturbance in these areas is related to outcome (Heiss et al. 1993a). Investigations in the subacute state after stroke showed a highly significant correlation with language performance assessed at follow-up after 2 years (Karbe et al. 1995). The receptive language disorder is correlated with rCMRGlC in the left temporal cortex and word fluency is correlated with rCMRGlC in the left prefrontal cortex. These results indicate that the functional disturbance as measured by rCMRGlC in speech-relevant brain regions early after stroke is predictive of the eventual outcome of aphasia. However, not only functional deactivation (diaschisis) but also neuronal loss may contribute to metabolic and perfusional changes in the neighborhood of the infarct, and the condition of the surrounding tissue may affect the recovery of individual patients. In this context, it is important to note that early reperfusion to specific areas is able to restore disturbed function, as demonstrated for recovery of naming by reperfusion to the key areas BA37, BA 44/45 (Broca) and BA 22 (Wernicke) (Hillis et al. 2006).

### 10.5 Changes in Activation Patterns vs. Recovery of Language Function

On this basis, it is not surprising that in patients with a poor outcome of poststroke aphasia, metabolism in the hemisphere outside the infarct was significantly less

than in those with good language recovery, indicating significant cell loss caused by the ischemic episode outside the ischemic core (Heiss et al. 1993b). In addition, the functionality of the network was reduced in patients with an eventual poor outcome; during task performance, patients with an eventual good recovery predominantly activated structures in the ipsilateral hemisphere. It must be kept in mind that aphasia symptoms – and consequently also activation patterns – improve with restoration of regional blood flow (Jordan and Hillis 2006).

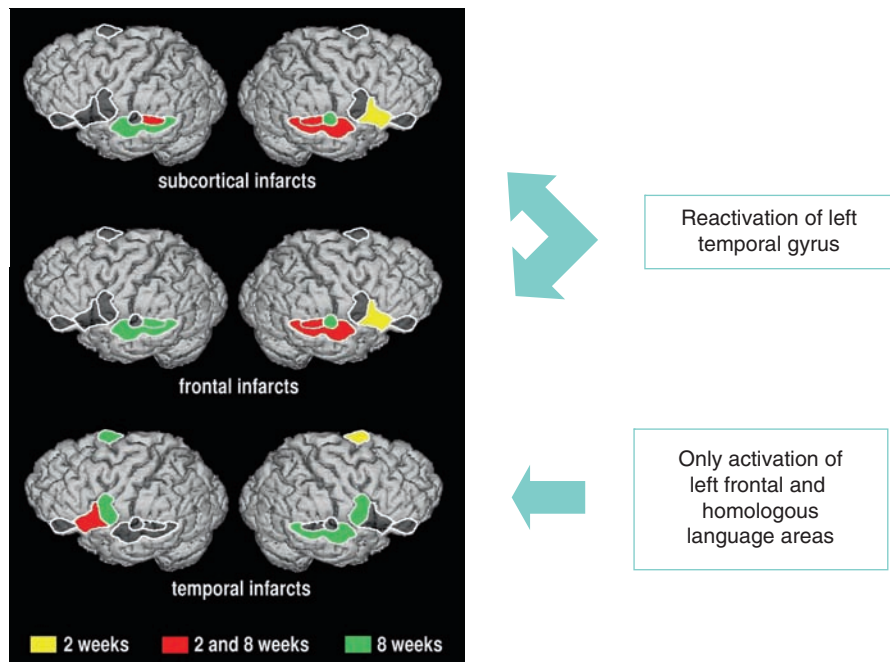
One of the central issues of aphasia research is the question why recovery from aphasia is taking place and what the responsible mechanisms for this recovery are. Converging evidence from clinical studies and neural imaging studies of aphasic patients suggest that primary candidates for recovery in right-handed, left-hemisphere language dominant patients include undamaged portions of the language network in the left hemisphere and – to a lesser extent – homologous right-hemisphere areas (Rosen et al. 2000). Since the language network is not confined to the dominant hemisphere, the role of the right hemisphere after infarcts in the left hemisphere has been addressed in several studies. Generally, more right hemispheric activations were seen in the subacute phase of an infarct with language activation than in normals with the same tasks (Ohyama et al. 1996; Price and Crinion 2005; Saur et al. 2006; Weiller et al. 1995). Despite such responses in the right superior temporal gyrus especially in fluent Wernicke's patients (Musso et al. 1999; Weiller et al. 1995) and in the inferior frontal gyrus (Ohyama et al. 1996), efficient restoration of language is usually achieved only if left temporal areas are preserved and can be reintegrated into the functional network (Gainotti 1993). Only the basic function of mere word repetition appears to be sufficiently supported by sole right hemisphere activation (Berthier et al. 1991). Based on their study in chronic nonfluent aphasia patients, Belin et al. (1996) suggested that the increased activation within the right hemisphere may be a marker of failed or faulty recovery attempts in the sense of maladaptive plasticity or the breakdown of normal interhemispheric control within the distributed neural network. Language recovery in the months immediately after aphasia onset was associated with regression of functional depression (diaschisis) in structurally unaffected regions, in particular in the right hemisphere (Cappa et al. 1997; Saur et al.

2006). Right hemispheric activations after left frontal or temporal parietal damage are not related to the level of recovery (Fernandez et al. 2004), but may reflect transcallosal inhibition as a maladaptive neuronal reorganization rather than functional compensation (Price and Crinion 2005). Despite the brain recruits right hemispheric regions for speech processing when the left-hemispheric centers are impaired (Raboyeau et al. 2008), outcome studies reveal that this strategy is significantly less effective than repair of the speech-relevant network in adults (Karbe et al. 1998). The effectiveness of right hemispheric compensation appears to be higher in childhood than later (Muller et al. 1998). In studies of reorganization of the functional network in the course of aphasia, it is important to take into consideration the specificity of the tasks, the influence of site and extent of lesion, and the effect of treatment focused on a particular language domain on recruitment of different aspects of the language network, especially if compensatory treatment to access limited functional responses would stimulate only required pathways and would do little to stimulate reorganization of the language system (Thompson 2000).

Changes in the activation pattern induced by repeating words in the course after ischemic stroke were related to recovery from poststroke aphasia (Heiss et al. 1999). Repeating words activated blood flow in 10 normal controls by more than 10% relative to resting condition in both upper temporal gyri, by 5–10% in planum temporale and Heschl gyrus of both sides and in the lower part of the central gyrus of the left side, and by less than 5% in the left Broca area. This test procedure was applied to 23 patients with aphasia of different types. Morphological defects were defined on MRI/CT, and the patients were grouped according to the site of the lesion. Activation PET studies were performed in the subacute stage approximately 2 weeks after the stroke and repeated 6 weeks later. On matched MRIs, regions of interest were defined in 14 identified structures of the bilateral language-related network.

The three groups of aphasic patients showed different patterns of activation in the acute and chronic phase, and their improvement was different: Although subcortical and frontal infarcts improved considerably in several tests, temporal infarcts showed only little improvement. These differences in improvement of speech deficits were reflected in different patterns of

**Fig. 10.2** Activation patterns in patients with left hemispheric stroke 2 and 8 weeks after stroke. In the case of subcortical and frontal infarction, the left temporal areas are reactivated correlating to better recovery of language function. From Heiss et al. (1999)



activation in the course after stroke (Fig. 10.2). The subcortical and frontal groups improved substantially and activated the right inferior frontal gyrus and the right superior temporal gyrus (STG) at baseline and regained regional left STG activation at follow-up. The temporal group improved only in word comprehension; it activated the left Broca area and supplementary motor areas at baseline and the precentral gyrus bilaterally as well as the right STG at follow-up, but could not reactivate the left STG. These differential activation patterns were also obvious when subcortical and frontal infarcts were grouped together according to the extent of improvement: Those with a decrease in Token test errors by more than 50% could activate the left STG, those with a more unfavorable and unsatisfactory outcome were not able to do this. Similar reactivation patterns were observed in smaller groups of patients (Cao et al. 1999; Warburton et al. 1999). A recent study with repeated fMRI and parallel language testing from the acute to the chronic stage after stroke, demonstrated a similar pattern (Saur et al. 2006). All 14 patients recovered clinically as shown by a set of aphasia tests. In the acute phase (mean: 1.8 days post stroke), group analysis showed little early activation of noninfarcted left-hemispheric language structures, while in the subacute phase (12.1 days post stroke) a large increase of activation in the bilateral language network, with a peak in the right Broca-

homologue was observed. In the chronic phase (1321 days post stroke) a normalization of activation with reshift to left-hemispheric areas was observed. This reorganization with recruitment of homologue language zones correlated with improvement, the normalization possibly reflected recovery and consolidation of the language system.

## 10.6 Effect of Treatment in Poststroke Aphasia

Although the effect of physiotherapy on improvement of sensorimotor deficits is unchallenged, the efficiency of speech therapy is still controversial, with several randomized controlled trials yielding no difference in outcome between treated and untreated groups (Ferro et al. 1999; Greener et al. 2001a). Many trials were undertaken to enhance the recovery from aphasia with adjuvant pharmacotherapy, but again, only a few studies demonstrated efficacy: In a double-blind placebo-controlled study Walker-Batson et al. (2001) observed a significantly increased gain in score in patients treated with dextroamphetamine before speech therapy sessions compared to the placebo group, but the difference was not significant at 6 months follow-up. Similarly, donepezil improved the effect of speech therapy only

temporarily (Berthier et al. 2006). A large Cochrane Review (Greener et al. 2001b) identified piracetam as the only drug with a significant effect on recovery of language, which was also observed in a large multicenter trial (Orgogozo 1998). In order to investigate the question if the effect of piracetam is reflected in altered activation patterns, we performed a study in 24 patients with aphasia after stroke (Kessler et al. 2000). All these patients had speech therapy and were randomly assigned to placebo or  $2 \times 2.4$  g piracetam. With respect to performance in the aphasia tests, the piracetam group did significantly better especially in subtests reflecting the ability for spontaneous speech, whereas the placebo experienced – as the verum group – improvements in Token test, reading and writing and comprehension. It was impressive to see that these differences in improvement were also reflected in differences in the achieved activation patterns: In the piracetam group increase in activation was significantly higher in the left transverse temporal gyrus, the left triangular part of the inferior frontal gyrus, and the left posterior temporal gyrus after the treatment period compared with the initial measures. In the right inferior frontal gyrus a trend toward a decrease in activation was observed. The placebo group showed an increase in the activation effect only in the left vocalization area, which is the inferior part of the precentral gyrus where the primary motor area of mouth, tongue, and larynx is localized. It might be concluded from the controlled clinical trials and our study of activation patterns that piracetam as an adjuvant to speech therapy improves recovery of various language functions and that this effect is accompanied by task-related flow activation in eloquent areas of the left hemisphere. This again points to the important role of (re)activated areas in the left hemisphere for recovery of language function. Other imaging studies with individualized aphasia treatment in small numbers of patients did not show conclusive changes in fMRI activation patterns (review in Crinion and Leff 2007).

### 10.7 Combination of Repetitive Transcranial Magnetic Stimulation (rTMS) with Activated Imaging

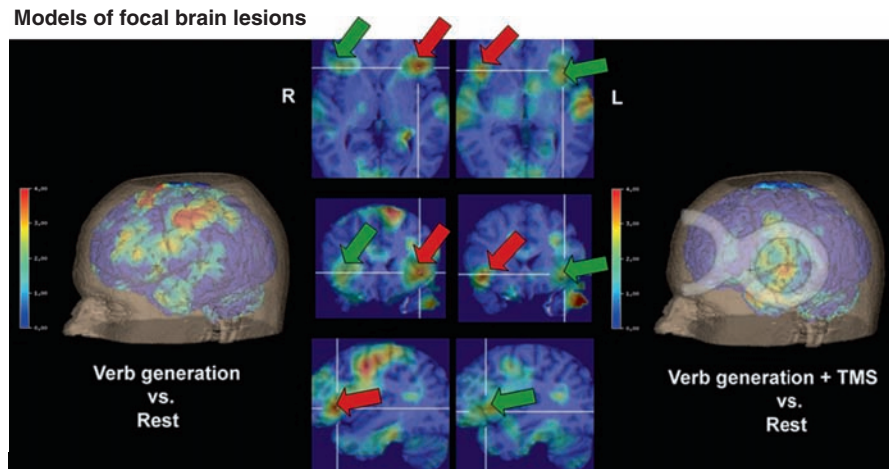
rTMS is a noninvasive procedure to create electric currents in discrete brain areas (Pascual-Leone et al. 2002) which depending on frequency, intensity, and duration can lead to transient increases and decreases in

excitability of the affected cortex. Low frequencies of rTMS (below 5 Hz) can suppress excitability of the cortex, while higher frequency stimulation (5–20 Hz) leads to an increase in cortical excitability (Kobayashi and Pascual-Leone 2003). As in the motor system (Chen et al. 1997), it can also be applied to identify the various areas involved in language processing and production by a selective disturbance of partial function with low frequency rTMS. Most frequently rTMS is used in the so-called “lesion mode” to interfere with normal brain function. In our studies cited below rTMS was applied with 4 Hz at resting motor threshold for 10–30 s. These parameter settings were chosen because Wassermann et al. (2002) has shown that 4 Hz is the lowest frequency which consistently interferes with language function and simultaneously minimizes the risk of inducing seizures.

Increases in relative cerebral blood volume (CBV) in contralateral homologous language regions during overt propositional speech fMRI in chronic, nonfluent aphasia patients indicated over-activation of right language homologues (Naeser et al. 2004). This right hemisphere over-activation may represent a maladaptive strategy, as suggested previously by Belin et al. (1996) and Rosen et al. (2000) in their studies with chronic, nonfluent aphasia patients. This over-activation in the right hemisphere homologous language areas during overt propositional speech can be interpreted as a result of decreased transcallosal inhibition due to damage of the specialized and lateralized speech areas (Karbe et al. 1998). TMS studies by Martin et al. (2004) and Naeser et al. (2005) have reported improved picture naming ability in chronic nonfluent aphasia patients following a series of ten 20 min 1 Hz rTMS sessions to suppress a portion of the right pars triangularis area in the right Broca’s area. Picture naming ability was significantly improved at 2 months following ten 20 min rTMS sessions (90% of motor threshold). The authors hypothesized that suppression of the right pars triangularis modulated the bi-hemispheric neural network for naming, resulting in improved picture naming after the rTMS treatment series.

Both types of inhibition – collateral ipsilateral and transcallosal contralateral – can be demonstrated by simultaneous rTMS and PET activation studies (Thiel et al. 2006b). In six normal male volunteers, the Broca area, as defined by maximal activation during verb generation in the left inferior frontal gyrus, was stimulated by rTMS (4 Hz at resting motor threshold for 30 s) to interfere with normal language function. Interference with language function (positive TMS-effect) is usually

**Fig. 10.3** Effect of repetitive transcranial magnetic stimulation on activation pattern by verb generation. Activation pattern (a) and coil position (d) shown in 3D rendering. Images in 3D (b) show activation of left inferior frontal gyrus during verb generation (*red arrows*), images (c) clearly show the decreased activation on the left (*green arrow*) and increased activity on the right side (*red arrows*) during rTMS interference. Modified from Thiel et al. (2006b)



classified into three types on the behavioral level: (1) No response to the stimulus (e.g., no verb generated to a presented noun). (2) Wrong response to the stimulus (e.g., a verb is generated which is not semantically related to the presented noun). (3) The reaction time latency to the stimulus is changed (e.g., faster response means facilitation, slower response means inhibition). At rest, rTMS decreased blood flow ipsilateral and contralateral. During verb generation, rCBF was decreased during rTMS ipsilateral under the coil, but increased ipsilateral outside the coil and in the contralateral homologous area (Fig. 10.3). The effect of rTMS was accompanied by a prolongation of reaction time latencies to verbal stimuli.

The role of activation in the right hemisphere for residual language performance can be investigated by combining rTMS with functional imaging, e.g., PET (Siebner et al. 2001). Such an approach was used in 11 patients with predominantly nonfluent aphasia 2 weeks after left sided middle cerebral artery infarction (Winhuisen et al. 2005). rTMS stimulation sites were selected according to maximum flow activation within left and right inferior frontal gyrus (IFG). Of these patients three activated the left, eight the bilateral IFG. rTMS (4 Hz, as described above) resulted in increased reaction time latency or error rate in the word generation task in five patients with right IFG activation, indicating essential language function. In a verbal fluency task, these patients had a lower performance than patients with effects of rTMS only over the left IFG, suggesting a less effective compensatory potential of right sided network areas. These results were supported by studies in tumor patients.

## 10.8 Language Function in Brain Tumors

The speed of the development of a brain lesion may have an effect on the functional impairment and on the mechanisms of compensation and reorganization of the involved networks. In a study on 61 patients with tumors in the dominant left hemisphere (Thiel et al. 2001), a verb generation paradigm not only increased flow in the left IFG (Brodmann 44 and 55), both superior temporal gyri and the cerebellum (the pattern observed in the control group), but additionally in the left frontal medial gyrus (BA 46) and orbital part of the IFG (BA 47), the anterior insula and the left cerebellum. Contrary to the healthy volunteers, two thirds of the right handed patients showed also an activation of the right IFG, i.e., the area homologous to the Broca area. In 18% of the patients, a reversed dominance was indicated by a negative laterality index. It was interesting to note that successful resection of a left fronto-temporal tumor improved aphasia and restored left-hemispheric dominance, suggesting the reversibility of the effect of disinhibition by removal of the cause of primary functional damage. In a further study (Thiel et al. 2005), the role of involvement of right IFG in speech performance was tested by disturbing IFG function with rTMS. In all patients, rTMS over left IFG prolonged word-generation latencies, indicating that the left IFG is still essential for performance of this task, as it is in normals. However, in patients but not in controls, significantly longer latencies were also observed during rTMS over the right IFG corresponding to higher right IFG activation. The right IFG therefore can be regarded as essential for

language performance because patients and controls activate the IFG only during word-generation, e.g., retrieval of verbs and nouns contrasted with a number of control states (Warburton et al. 1996) and TMS over the right interfered with this task in patients as over the left in controls. The lateralization indices, as determined by PET, were significantly lower in patients with right-sided TMS effect than in those without. As described in the article by Thiel et al. (2006a), there was a significant correlation between the laterality index and the performance in a verbal fluency test (FAS, (Lezak et al. 2004)) in the patients without right-positive TMS effect (4 Hz for 20 s, as described above), whereas in patients with a predominant right-positive TMS effect the performance in the verbal fluency test was comparable with that in controls. This result may indicate that in a few patients with left hemispheric brain tumors, the slow progression of damage leads to a shift in language function to the right hemisphere, which can compensate for the defect on the left side.

## 10.9 Hierarchical Organization for Recovery?

The different dynamics of recovery of language function observed in patients after stroke and with tumors in the left hemisphere suggest various mechanisms for compensation of the lesion within the functional network. Despite the limited number of longitudinal studies, the heterogeneity with respect to the type of

aphasia in the patients included and the differences among the activation and stimulation paradigms (Zahn et al. 2006), a hierarchy for effective recovery, might be deduced from these data (Fig. 10.4) (Heiss and Thiel 2006):

- Best, even complete recovery of function can usually be achieved only by the restoration of the original activation pattern within the network of the dominant hemisphere; this is only feasible after small brain damage, probably only affecting an area of minor importance, permitting functional restitution of the main interconnected components.
- If primary functional centres are damaged, reduction of collateral inhibition leads to activation of areas around the lesion; this intrahemispheric compensation involving secondary centres of the ipsilateral network is the basis for incomplete, but often satisfactory improvement of language function.
- If ipsilateral network components are severely damaged, reduction of transcallosal inhibition causes activation of contralateral homotopic areas; this interhemispheric compensation involving homotopic contralesional areas contributes to some improvement in function, which is dependent on the extent of the functional shift between the hemispheres, but usually is not as efficient as intrahemispheric compensation. However, in some patients with slowly developing brain damage – and perhaps also an a priori not highly lateralized functional network – the language function can be completely shifted to the right hemisphere, and in these cases

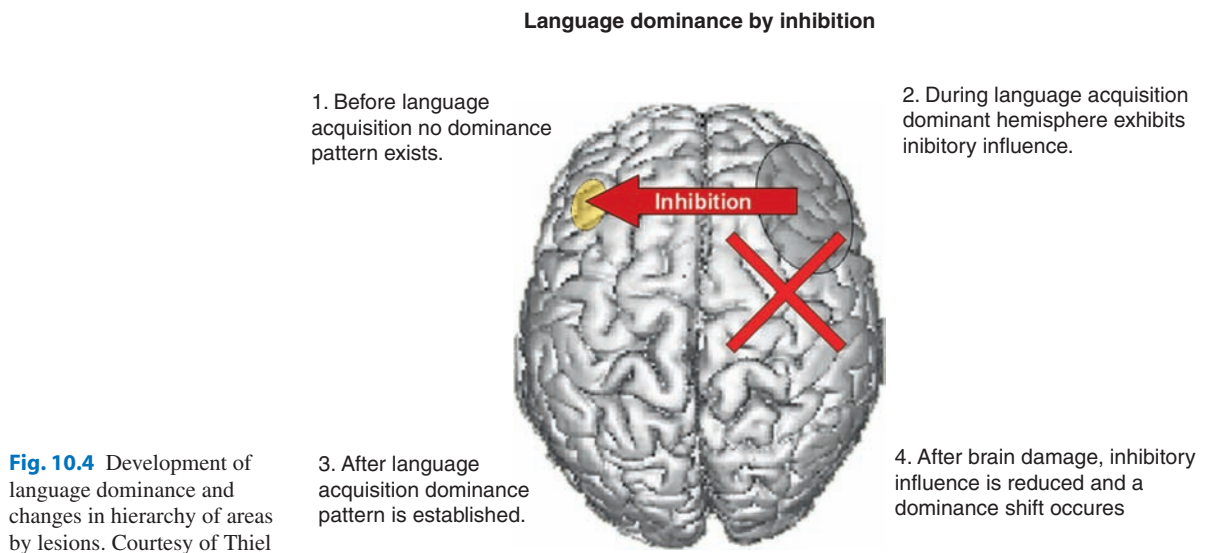


**Fig. 10.4** Development of language dominance and changes in hierarchy of areas by lesions. Courtesy of Thiel

speech performance can be preserved or completely recovered despite the damage in the left (previously dominant) hemisphere.

The concept of the difference between the effectiveness of intrahemispheric compensation and interhemispheric compensation may be taken one step further. The blockade of the contralateral intact area by rTMS can be utilized to modulate the inhibitory interactions. In a preliminary study in patients with nonfluent aphasia 5–11 years after left hemisphere stroke, Naeser et al. (2005) observed significant and persistent improvement in naming pictures on testing performed 2 months after a series of ten 20 min 1 Hz rTMS treatment to suppress a portion of the right Broca's homologue (right pars triangularis, posterior portion). The authors postulated that rTMS decreased excitation in right BA 45 which in turn modulated activity in the distributed, bihemispheric language network. This result suggests that in chronic, nonfluent aphasia patients, contralateral over-activation (likely due to transcallosal disinhibition secondary to dominant, left hemisphere lesion) may be tempered or suppressed, following a series of slow, 1 Hz rTMS treatments to a posterior portion of the right pars triangularis. The clinical and long-term efficacy of this novel complementary treatment for aphasia, however, needs to be proven in larger clinical trials.

## 10.10 Conclusion

Specific brain functions, such as language, can be localized by comparing CBF or CMRGlc during performance of a selected task with a “resting” condition. This was originally made possible by PET using FDG. With <sup>15</sup>O-water or other ultra-short-lived CBF tracers, multiple replications of conditions in the same subject could be performed. This technique was widely used, especially for the study of higher brain function (cognitive neuroscience) and for evaluating disturbed activation patterns in disease, as in post-stroke aphasia. In recent years, fMRI has become the dominating imaging technique in this field because it does not involve ionizing radiation and therefore, is easily used in normal controls, allows more rapid signal acquisition and more complex experimental designs. However, PET provides a more physiologically specific signal, a better signal-to-noise ratio and fewer artefacts in individual acquisitions. PET also provides actual activated

and reference regional values, which may show a better correlation with task performance than the difference signal provided by fMRI. Additionally, magnetic stimulations can be performed during PET examinations. These advantages support its continued use in pathophysiologically complex clinical situations such as stroke and brain tumors, where CBF responses to activation may be altered and may involve unexpected components of a functional network.

## References

- Basso A, Gardelli M, Grassi MP, Mariotti M (1989) The role of the right hemisphere in recovery from aphasia. Two case studies. *Cortex* 25:555–566
- Belin P, van Eeckhout P, Zilbovicius M, Remy P, Francois C, Guillaume S, Chain F, Rancurel G, Samson Y (1996) Recovery from nonfluent aphasia after melodic intonation therapy: a PET study. *Neurology* 47:1504–1511
- Berthier ML, Starkstein SE, Leiguarda R, Ruiz A, Mayberg HS, Wagner H, Price TR, Robinson RG (1991) Transcortical aphasia. Importance of the nonspeech dominant hemisphere in language repetition. *Brain* 114(Pt 3):1409–1427
- Berthier ML, Green C, Higuera C, Fernandez I, Hinojosa J, Martin MC (2006) A randomized, placebo-controlled study of donepezil in poststroke aphasia. *Neurology* 67:1687–1689
- Booth JR, Wood L, Lu D, Houk JC, Bitan T (2007) The role of the basal ganglia and cerebellum in language processing. *Brain Res* 1133:136–144
- Cao Y, Vikingstad EM, George KP, Johnson AF, Welch KMA (1999) Cortical language activation in stroke patients recovering from aphasia with functional MRI. *Stroke* 30:2331–2340
- Cappa SF, Perani D, Grassi F, Bressi S, Alberoni M, Franceschi M, Bettinardi V, Todde S, Fazio F (1997) A PET follow-up study of recovery after stroke in acute aphasics. *Brain Lang* 56:55–67
- Chen R, Classen J, Gerloff C, Celnik P, Wassermann EM, Hallett M, Cohen LG (1997) Depression of motor cortex excitability by low-frequency transcranial magnetic stimulation. *Neurology* 48:1398–403
- Crinion JT, Leff AP (2007) Recovery and treatment of aphasia after stroke: functional imaging studies. *Curr Opin Neurol* 20:667–673
- Demonet JF, Fiez JA, Paulesu E, Petersen SE, Zatorre RJ (1996) PET studies of phonological processing: a critical reply to Poeppel. *Brain Lang* 55:352–379
- Feeney DM, Baron JC (1986) Diaschisis. *Stroke* 17:817–830
- Fernandez B, Cardebat D, Demonet JF, Joseph PA, Mazaux JM, Barat M, Allard M (2004) Functional MRI follow-up study of language processes in healthy subjects and during recovery in a case of aphasia. *Stroke* 35:2171–2176
- Ferro JM, Mariano G, Madureira S (1999) Recovery from aphasia and neglect. *CerebrovascDis* 9(Suppl 5):6–22
- Gainotti G (1993) The riddle of the right hemisphere's contribution to the recovery of language. *Eur J Disord Commun* 28:227–246

- Greener J, Enderby P, Whurr R (2001a) Speech and language therapy for aphasia following stroke (Cochrane Review). The Cochrane Library 3 Oxford: Update Software
- Greener J, Enderby P, Whurr R (2001b) Pharmacological treatment for aphasia following stroke (Protocol for a Cochrane Review). The Cochrane Library 3 Oxford: Update Software
- Heiss WD, Emunds HG, Herholz K (1993a) Cerebral glucose metabolism as a predictor of rehabilitation after ischemic stroke. *Stroke* 24:1784–1788
- Heiss WD, Kessler J, Karbe H, Fink GR, Pawlik G (1993b) Cerebral glucose metabolism as a predictor of recovery from aphasia in ischemic stroke. *Arch Neurol* 50:958–964
- Heiss WD, Kessler J, Thiel A, Ghaemi M, Karbe H (1999) Differential capacity of left and right hemispheric areas for compensation of poststroke aphasia. *Ann Neurol* 45:430–438
- Heiss WD, Thiel A (2006) A proposed regional hierarchy in recovery of post-stroke aphasia. *Brain Lang* 98:118–123
- Hickok G, Poeppel D (2007) The cortical organization of speech processing. *Nature Rev* 8:393–402
- Hillis AE, Kleinman JT, Newhart M, Heidler-Gary J, Gottesman R, Barker PB, Aldrich E, Llinas R, Wityk R, Chaudhry P (2006) Restoring cerebral blood flow reveals neural regions critical for naming. *J Neurosci* 26:8069–8073
- Jordan LC, Hillis AE (2006) Disorders of speech and language: aphasia, apraxia and dysarthria. *Curr Opin Neurol* 19:580–585
- Karbe H, Herholz K, Szelies B, Pawlik G, Wienhard K, Heiss WD (1989) Regional metabolic correlates of Token test results in cortical and subcortical left hemispheric infarction. *Neurology* 39:1083–1088
- Karbe H, Kessler J, Herholz K, Fink GR, Heiss WD (1995) Long-term prognosis of poststroke aphasia studied with positron emission tomography. *Arch Neurol* 52:186–190
- Karbe H, Thiel A, Weber-Luxenburger G, Herholz K, Kessler J, Heiss WD (1998) Brain plasticity in poststroke aphasia: what is the contribution of the right hemisphere? *Brain Lang* 64:215–230
- Kessler J, Thiel A, Karbe H, Heiss WD (2000) Piracetam improves activated blood flow and facilitates rehabilitation of poststroke aphasic patients. *Stroke* 31:2112–2116
- Knecht S, Floel A, Dräger B, Breitenstein C, Sommer J, Henningsen H, Ringelstein EB, Pascual-Leone A (2002) Degree of language lateralization determines susceptibility to unilateral brain lesions. *Nat Neurosci* 5:695–699
- Kobayashi M, Pascual-Leone A (2003) Transcranial magnetic stimulation in neurology. *Lancet Neurol* 2:145–156
- Kumar R, Masih AK, Pardo J (1996) Global aphasia due to thalamic hemorrhage: a case report and review of the literature. *Arch Phys Med Rehabil* 77:1312–1315
- Laughlin SB, Attwell D (2001) The metabolic cost of neural information: from fly eye to mammalian cortex. *HFSP Workshop 11 – Neuroenergetics*:54–64
- Lezak M, Howieson D, Loring D (2004) *Neuropsychological assessment*. Oxford University Press, Oxford
- Magistretti PJ (2004) Brain energy metabolism. In: *From molecules to networks*. Elsevier, Amsterdam
- Martin PI, Naeser MA, Theoret H, Tormos JM, Nicholas M, Kurland J, Fregni F, Seekins H, Doron K, Pascual-Leone A (2004) Transcranial magnetic stimulation as a complementary treatment for aphasia. *Semin Speech Lang* 25:181–191
- Metter EJ, Kempler D, Jackson CA, Hanson WR, Riege WH, Camras LR, Mazziotta JC, Phelps ME (1987) Cerebellar glucose metabolism in chronic aphasia. *Neurology* 37:1599–1606
- Metter EJ, Riege WH, Hanson WR, Jackson CA, Kempler D, Van Lancker D (1988) Subcortical structures in aphasia. An analysis based on (18 F)-fluorodeoxyglucose, positron emission tomography, and computed tomography. *Arch Neurol* 45:1229–1234
- Metter EJ, Hanson WR, Jackson CA, Kempler D, Van Lancker D, Mazziotta JC, Phelps ME (1990) Temporoparietal cortex in aphasia. Evidence from positron emission tomography. *Arch Neurol* 47:1235–1238
- Mintun MA, Lundstrom BN, Snyder AZ, Vlassenko AG, Shulman GL, Raichle ME (2001) Blood flow and oxygen delivery to human brain during functional activity: theoretical modeling and experimental data. *Proc Natl Acad Sci U S A* 98:6859–6864
- Muller RA, Rothermel RD, Behen ME, Muzik O, Mangner TJ, Chakraborty PK, Chugani HT (1998) Brain organization of language after early unilateral lesion: a PET study. *Brain Lang* 62:422–451
- Musso M, Weiller C, Kiebel S, Müller SP, Bülow P, Rijntjes M (1999) Training-induced brain plasticity in aphasia. *Brain* 122(Pt 9):1781–1790
- Naeser MA, Martin PI, Baker EH, Hodge SM, Sczerzenie SE, Nicholas M, Palumbo CL, Goodglass H, Wingfield A, Samaraweera R, Harris G, Baird A, Renshaw P, Yurgelun-Todd D (2004) Overt propositional speech in chronic nonfluent aphasia studied with the dynamic susceptibility contrast fMRI method. *Neuroimage* 22:29–41
- Naeser MA, Martin PI, Nicholas M, Baker EH, Seekins H, Kobayashi M, Theoret H, Fregni F, Maria-Tormos J, Kurland J, Doron KW, Pascual-Leone A (2005) Improved picture naming in chronic aphasia after TMS to part of right Broca's area: an open-protocol study. *Brain Lang* 93:95–105
- Nudo RJ, Wise BM, SiFuentes F, Milliken GW (1996) Neural substrates for the effects of rehabilitative training on motor recovery after ischemic infarct. *Science* 272:1791–1794
- Ogawa S, Lee TM, Kay AR, Tank DW (1990) Brain magnetic resonance imaging with contrast dependent on blood oxygenation. *Proc Natl Acad Sci U S A* 87:9868–9872
- Ohyama M, Senda M, Kitamura S, Ishii K, Mishina M, Terashi A (1996) Role of the nondominant hemisphere and undamaged area during word repetition in poststroke aphasia – a PET activation study. *Stroke* 27:897–903
- Orgogozo JM (1998) Piracetam in the treatment of acute stroke. *CNS Drugs* 9:41–49
- Pascual-Leone A, Davey N, Wassermann EM, Rothwell J, Puri B. (2002). *Handbook of transcranial magnetic stimulation*. Arnold Press, London
- Petersen SE, Fox PT, Posner MI, Mintun M, Raichle ME (1988) Positron emission tomographic studies of the cortical anatomy of single-word processing. *Nature* 331:585–589
- Price CJ (2000) The anatomy of language: contributions from functional neuroimaging. *J Anat* 197(Pt 3):335–359
- Price CJ, Crinion J (2005) The latest on functional imaging studies of aphasic stroke. *Curr Opin Neurol* 18:429–434
- Raboyeau G, De Boissezon X, Marie N, Balduyck S, Puel M, Bezy C, Demonet JF, Cardebat D (2008) Right hemisphere activation in recovery from aphasia: lesion effect or function recruitment? *Neurology* 70:290–298
- Reivich M, Kuhl D, Wolf A, Greenberg J, Phelps M, Ido T, Casella V, Fowler J, Hoffman E, Alavi A, Som P, Sokoloff L

- (1979) The (18 F)fluorodeoxyglucose method for the measurement of local cerebral glucose utilization in man. *Circ Res* 44:127–137
- Rosen HJ, Petersen SE, Linenweber MR, Snyder AZ, White DA, Chapman L, Dromerick AW, Fiez JA, Corbetta MD (2000) Neural correlates of recovery from aphasia after damage to left inferior frontal cortex. *Neurology* 55:1883–1894
- Saur D, Lange R, Baumgaertner A, Schraknepper V, Willmes K, Rijntjes M, Weiller C (2006) Dynamics of language reorganization after stroke. *Brain* 129:1371–1384
- Siebner HR, Takano B, Peinemann A, Schwaiger M, Conrad B, Drzezga A (2001) Continuous transcranial magnetic stimulation during positron emission tomography: a suitable tool for imaging regional excitability of the human cortex. *Neuroimage* 14:883–890
- Sokoloff L (1999) Energetics of functional activation in neural tissues. *Neurochem Res* 24:321–329
- Thiel A, Herholz K, von Stockhausen HM, Leyen-Pilgram K, Pietrzyk U, Kessler J, Wienhard K, Klug N, Heiss WD (1998) Localization of language-related cortex with 15O-labeled water PET in patients with gliomas. *Neuroimage* 7:284–295
- Thiel A, Herholz K, Koyuncu A, Ghaemi M, Kracht L, Habedank B, Heiss WD (2001) Plasticity of language networks in patients with brain tumors: a PET activation study. *Ann Neurol* 50:620–629
- Thiel A, Habedank B, Winhuisen L, Herholz K, Kessler J, Haupt WF, Heiss WD (2005) Essential language function of the right hemisphere in brain tumor patients. *Ann Neurol* 57:128–131
- Thiel A, Habedank B, Herholz K, Kessler J, Winhuisen L, Haupt WF, Heiss WD (2006a) From the left to the right: how the brain compensates progressive loss of language function. *Brain Lang* 98:57–65
- Thiel A, Schumacher B, Wienhard K, Gairing S, Kracht LW, Wagner R, Haupt WF, Heiss WD (2006b) Direct demonstration of transcallosal disinhibition in language networks. *J Cereb Blood Flow Metab* 26:1122–1127
- Thompson CK (2000) The neurobiology of language recovery in aphasia. *Brain Lang* 71:245–248
- Turner R, Howseman A, Rees G, Josephs O (1997) Functional imaging with magnetic resonance. In: Frackowiak RSJ, Friston KJ, Frith CD, Dolan RJ, Mazziotta JC (eds) *Human brain function*. Academic, San Diego, pp 467–486
- Wade DT, Hewer RL, David RM, Enderby PM (1986) Aphasia after stroke: natural history and associated deficits. *J Neurol Neurosurg Psychiatry* 49:11–16
- Walker-Batson D, Curtis S, Natarajan R, Ford J, Dronkers N, Salmeron E, Lai J, Unwin DH (2001) A double-blind, placebo-controlled study of the use of amphetamine in the treatment of aphasia. *Stroke* 32:2093–2098
- Warburton E, Wise RJS, Price CJ, Weiller C, Hadar U, Ramsay S, Frackowiak RSJ (1996) Noun and verb retrieval by normal subjects studies with PET. *Brain* 119:159–179
- Warburton E, Price CJ, Swinburn K, Wise RJS (1999) Mechanisms of recovery from aphasia: evidence from positron emission tomography studies. *J Neurol Neurosurg Psychiatry* 66:155–161
- Wassermann EM, Pascual-Leone A, Davey NJ, Rothwell J, Wassermann EM, Puri BK (2002) Safety and side-effects of transcranial magnetic stimulation and repetitive transcranial magnetic stimulation. In: *Handbook of transcranial magnetic stimulation*. Arnold Press, London, pp 39–49
- Weiller C, Isensee C, Rijntjes M, Huber W, Müller S, Bier D, Dutschka K, Woods RP, Noth J, Diener HC (1995) Recovery from Wernicke's aphasia: a positron emission tomographic study. *Ann Neurol* 37:723–732
- Winhuisen L, Thiel A, Schumacher B, Kessler J, Rudolf J, Haupt WF, Heiss WD (2005) Role of the contralateral inferior frontal gyrus in recovery of language function in poststroke aphasia: a combined repetitive transcranial magnetic stimulation and positron emission tomography study. *Stroke* 36:1759–1763
- Wise RJ (2003) Language systems in normal and aphasic human subjects: functional imaging studies and inferences from animal studies. *Br Med Bull* 65:95–119
- Zahn R, Schwarz M, Huber W (2006) Functional activation studies of word processing in the recovery from aphasia. *J Physiol Paris* 99:370–385

## 11.1 Introduction

The ultimate goal of brain tumor surgery is maximum tumor removal without the development of a new neurologic deficit. This is especially true in the treatment of intraparenchymal tumors such as gliomas and metastatic lesions. In the treatment of glioblastoma multiforme (GBM), for example, gross total resection (GTR) has been demonstrated in a number of studies to be one of the few attainable factors that is associated with prolonged survival (Buckner 2003; Jeremic et al. 1994; Lacroix et al. 2001; Vidiri et al. 2006; Ushio et al. 2005). GTR of low grade gliomas is also supported in the literature and has been demonstrated in several retrospective studies to be associated with a lower risk of tumor recurrence and prolonged patient survival (Claus et al. 2005; Laws et al. 1984; Nicolato et al. 1995; Philippon et al. 1993; Piepmeier et al. 1996). In one reported series where complete radiologic resection was attained in the treatment of low grade glial tumors, tumor recurrence was not reported (Berger et al. 1994). Additionally, GTR has been demonstrated to result in improved postoperative control of seizures (Chang et al. 2008), a major source of disability in these patients. It should be noted, however, that the appropriate treatment of low grade gliomas is not without controversy (Keles et al. 2001), and there are reported series that have failed to demonstrate a significant correlation between GTR and survival (Medbery et al. 1988; Piepmeier 1987). Reported series of high grade gliomas (HGG) that have failed to

demonstrate a correlation between the extent of resection and prognosis have also been published (Kowalczyk et al. 1997; Lai et al. 1993).

Despite these discordant findings and the fact that most data are retrospective and nonrandomized, there is a theoretical benefit of maximal tumor resection. In the case of low grade glial tumors, GTR may reduce the number of remaining cells that have the potential for malignant degeneration. Maximal resection of high grade tumors offers the advantage of minimizing the number of residual cells capable of generating recurrent tumor at the operative site or migrating along white matter tracts into other areas of the brain. This reduction in malignant cells should also allow for maximal benefit of adjuvant therapy, and subsequently, lengthen the time to tumor recurrence. In patients with GBM, there are genetic changes that occur prior to tumor recurrence (Kim and Hall unpublished data; Joki et al. 2001; Speigl-Kreinecker et al. 2002) that may also negatively influence treatment response and thus, survival; this finding provides further rationale for aggressive surgical resection. Given the increasing body of evidence in the form of retrospective trials and the theoretical advantages of GTR as outlined above, we favor a strategy of aggressive resection for the treatment of most gliomas. Recently, a large series of patients with HGG were found to have increased survival with GTR even when stratified for patient age and tumor location near eloquent cortex (Stummer et al. 2008).

There is even less evidence-based guidance regarding the effect of the extent of resection on survival in patients with metastatic brain tumors. This is probably because of the fact that other treatment modalities are often used for these tumors instead of surgery, leading to controversy over the role of open surgery in the management of these tumors. A number of studies support the role of surgery in specific settings. Surgical resection has been demonstrated to confer increased

---

W. A. Hall (✉)

Department of Neurosurgery, State University of New York  
Upstate, 612 Jacobsen Hall, Upstate Medical University,  
750 East Adams Street, Syracuse, NY 13210, USA  
e-mail: hallw@upstate.edu

survival in patients with single metastatic lesions in the brain (Patchell et al. 1990; Vecht et al. 1993), particularly in cases where the primary source of the tumor is unknown (Nguyen et al. 1998; Weber et al. 1996).

The goal of aggressive tumor removal with the preservation of brain function has led to innovations in imaging that are part of today's surgical armamentarium. Central to the planning and execution of brain tumor surgery is appropriate neuroimaging. The advent of computed tomography (CT) and magnetic resonance imaging (MRI) has revolutionized brain tumor surgery. These modalities were used initially to demonstrate brain anatomy; however, the development of stereotactic techniques added to the accuracy of brain surgery, which in turn predated the development of neuronavigation and eventually, ioMRI.

Frameless neuronavigation systems provide surgeons with an unprecedented accuracy in surgical planning. Despite this, a major limitation of this technology is the occurrence of brain shift, that results after the resection of any significant amount of tumor (Reinges et al. 2004; Truwit and Hall 2006), the egress of cerebrospinal fluid (CSF) (Preul et al. 2004), and the combination of these factors that are further influenced by the effect of gravity on an open surgical field (Nabavi et al. 2001). Computational techniques (Clatz et al. 2005) and methods of validation based on shifting vascular anatomy (Reinertsen et al. 2007) have been used in an attempt to compensate for this effect. Intraoperative imaging circumvents the issue of brain shift, and was initially accomplished with CT (Engle and Lunsford 1987). However, ioMRI has been validated as a safe and effective surgical technique that provides near-real time feedback with respect to the extent of tumor resection, the presence of secondary pathology such as an iatrogenic intracerebral hematoma or hydrocephalus, and the location of eloquent structures after brain shift has occurred (Alexander et al. 1997; Berger et al. 1994; Bernays and Laws 1997; Bernstein et al. 2000; Hall et al. 2003, 1998; Kremer et al. 2006; Lam et al. 2001; Nimsky et al. 2004; Schwartz et al. 1999; Trantakis et al. 2003). Many different magnet strengths have been utilized for ioMRI with each magnet and format offering distinct unique advantages. The first operational system used a 0.5 T magnet with a double coil design (SIGNA SP, General Electric Medical Systems, Milwaukee, WI) in which the surgeon operated between the coils. System field strength has varied from 0.12 to 3 T, and while low field (up to 0.5 T) systems allow for

less rigorous adherence to MRI compatibility, 1.5 T field strength or greater is necessary for advanced MRI techniques that include fMRI. Although the cost of establishing an operating suite with MRI capabilities is considerable, the use of ioMRI appears to be cost effective because of the shorter length of stay in the hospital, the improved neurologic outcomes, the decreased frequency of tumor recurrence and the longer time to tumor recurrence (Kucharczyk et al. 2001).

Neuronavigation and ioMRI allow the neurosurgeon to identify functional brain tissue with respect to the surgical lesion. However, the determination of eloquent vs. noneloquent areas of brain are dependent upon the surgeon's knowledge of normal anatomy and the ability to interpret accurately the information provided by the MRI. When lesions or planned surgical corridors are in close proximity to presumed eloquent cortex or the associated white matter fiber tracts, one must consider the displacement of these vital areas that result from brain shift. An unacceptably high operative risk for neurological injury may exist in the absence of further definition of the location of eloquent areas. Awake craniotomy with direct cortical stimulation has been well described as a way to maintain neurologic function during high-risk neurosurgical procedures (Jääskeläinen and Randell 2003; Meyer et al. 2001; Picht et al. 2006). This direct surgical technique provides the surgeon with information concerning brain function during the operative procedure but does not allow for the generation of a visual image of the location of functional areas.

The need to identify and locate areas of functional importance and confirm their exact spatial relationships to brain tumors planned for resection has led to the use of fMRI for intraoperative guidance. The two most commonly used methods of employing fMRI in surgical planning are with neuronavigation and ioMRI. Additionally, fMRI has been combined with awake craniotomy and electrostimulation techniques (Amiez et al. 2008; Picht et al. 2006).

## 11.2 Functional MRI Neuronavigation

Functional imaging may be combined with frameless neuronavigation in tumor surgery to allow for the intraoperative localization of both the lesion and areas of brain activation. Blood oxygenation level dependant

(BOLD) fMRI (Ogawa et al. 1990) is performed preoperatively. Images are acquired while the patient performs tasks that involve the area of brain that is likely to be at risk during the planned surgery. These data are then coregistered with traditional high resolution structural MRI and appear on the neuronavigation images. Demonstrations of this technique were reported in a small series of patients starting in the late 1990s (Braun et al. 2000, 2001; Kamada et al. 2003; Schulder et al. 1999, 1997; Signorelli et al. 2003; Fandino et al. 1999; Wilkinson et al. 2003), while validation has been achieved by comparison of fMRI data with the results of direct cortical stimulation at the time of surgery (Braun et al. 2000; O'Shea et al. 2006; Roessler et al. 2005; Schulder et al. 1999; Signorelli et al. 2003). Algorithms for the coregistration of functional areas with structural MRI data have been demonstrated to yield accuracy within a sub-millimeter median error (Kober et al. 2002).

Neuronavigation combined with fMRI data was used in a series of 15 patients with tumors located in eloquent areas where no patient suffered a postoperative neurologic deficit (Gumprecht et al. 2002); however, in eight of these patients the tumor was only resected partially. Using a combination of fMRI neuronavigation and direct intraoperative cortical stimulation, Roessler et al. (2005) achieved GTR in nine of 22 patients, with partial resections in 11 and biopsy in 2. Another series examined the use of fMRI neuronavigation in 54 patients with tumors located near the motor strip. GTR was achieved in 45 patients (83%), however neurologic deterioration was observed in nine (Krishnan et al. 2004). In addition to the traditional mapping of sensorimotor and language functions, neuronavigation with coregistered fMRI data has been used for resection of tumors located near areas involved in short term memory (Braun et al. 2006). In this series of 14 patients, good surgical results were reported, especially with regards to verbal memory. Two patients with lesions near visual cortex have been surgically treated using fMRI coregistered neuronavigation (Schulder et al. 1999). Functional MRI has been coregistered with positron emission tomography (PET) data (Braun et al. 2001).

Preservation of functional cortex does not protect against postoperative neurologic deficits when the corresponding deep white matter tracts are surgically damaged. To address this, fMRI data have been coregistered with diffusion tensor imaging in order to

visualize both functional areas of cortex and their underlying white matter tracts (Kamada et al. 2007).

### 11.3 Intraoperative Functional MRI

Intraoperative MRI was developed in order to provide the neurosurgeon with near-real time feedback regarding the extent of tumor resection and the presence of intraoperative hemorrhage. Intraoperative imaging accounts for the effects of brain shift because the imaging data used for guidance are acquired during the surgical procedure and therefore the effects of CSF loss, tissue resection, and gravity are visualized. The main issues in developing ioMRI are magnetic compatibility, timing of intraoperative scans, maintenance of sterility, and ergonomic design of the operating MRI suite. The latter must allow for the efficient transfer of the patient to and from the scanner and ease of performing the operative procedure. The first ioMRI scanner was low field (0.5 T) (Black et al. 1999) and therefore carried a relatively low risk of magnetic mishaps. As neurosurgeons turned to high field ioMRI, issues with ferromagnetism of operative tools became more significant. Adaptation of neurosurgical procedures to allow for the presence of the magnet within the operating suite involved definition of the five gauss line, beyond which only MRI-compatible materials may be used. Large surgical series have been reported without significant rates of magnet-related mishaps or increased rates of infection (Hall et al. 2003; Nimsy et al. 2004; Nimsy et al. 2009b; Trantakis et al. 2003). Although the first ioMRI system consisted of a double coil design that allowed the surgeon to operate with the patient's head already at the ideal location for image acquisition, we have found that transfer of the patient into and out of the scanner during surgery is easily accomplished. When ioMRI is desired, the patient is moved by means of a floating top table into the scanner after a sterile towel is placed over the surgical site. Surgery is resumed within a few minutes after the acquisition of the imaging data. The timing of intraoperative scanning is variable. Although surgeons may employ slightly different algorithms, the basic technical strategy involves obtaining a scan when there is doubt regarding the completeness of the tumor resection, and then repeating this process until GTR is attained.

## 11.4 High Field Functional MRI

Intraoperative images at low field (0.12 T) and mid-field (0.5 T) have predictably demonstrated lower resolution compared to imaging obtained at high field (1.5 T); (Nimsky et al. 2004; Nimsky et al. 2009b). Despite the concerns for safety and the proven success of intraoperative high field MRI at 1.5 T, surgery at 3 T has been performed in order to explore the benefits of improved resolution (Trantakis et al. 2003). The improved resolution and signal to noise ratio afforded by high field MRI has led to its use for functional neuronavigation. Feigl et al. (2008) have used real time 3 T BOLD t-maps coregistered with MRI for neuronavigation of patients with tumors near the motor cortex, and achieved success comparable to that seen in a cohort of patients that had previously undergone awake craniotomy.

Our paradigm for fMRI guided neurosurgery utilizes preoperative high field (1.5 T or 3 T) fMRI combined with ioMRI at 1.5 T. Intraoperative MRI allows for near real-time feedback regarding the extent of tumor resection, but the shifted position of functional areas must be mentally extrapolated onto the newly acquired images by the surgeon. A novel approach reported by Archip et al. (2007), combines nonrigid registration of preoperative 3 T fMRI images with 0.5 T ioMRI to provide a quantitative estimation of brain shift in order to update fMRI localization. Using this technique, the alignment of the nonrigid system was found to be accurate (1.82 mm).

Intraoperative fMRI has been used for the resection of tumors located near eloquent cortex. In the remainder of this chapter, we will review our experience with intraoperative fMRI at 1.5 T and 3 T.

## 11.5 Materials and Methods

### 11.5.1 The Intraoperative MRI Suite

Surgery was performed at the University of Minnesota Fairview-University Medical Center. The MRI was a short-bore 1.5 T scanner (Gyrosan ACS-NT, Philips Medical Systems, Best, The Netherlands) with strong imaging gradients (23 mT/m, 105 mTm/ms) allowing for generation of echo planar imaging that is commonly used in fMRI. The total length of the MRI is

180 cm with an inner bore diameter of 60 cm and a gantry that can extend to 100 cm beyond the flared openings. The operating suite consisted of the scanner and a monitor similar to that used by the technologists to perform scanning. The operating microscope, patient monitors and anesthesia equipment were all MRI compatible. The magnet was actively shielded with a resulting 5 Gauss (G) line enclosing an area of 7.8 by 5.0 m. Surgery was performed on an angiography table with a floating table top mechanism oriented in-line with the MRI scanner, allowing for patient transfer easily into the MRI. A carbon-fiber Malcolm-Rand head frame was used that allowed for the exact reproduction of scan planes between imaging sessions. The ability to obtain high quality scans while maintaining operative access was afforded by a head coil composed of two circular loops arranged as a phased array. Surgery was performed either at the near end of the room outside the 5 G line, or alternatively on the opposite side of the scanner within the 5 G line, where only MRI-compatible materials were used. The MRI suite was cleaned the day before the surgical procedure and treated as a sterile surgical environment. Pocketless color coded scrubs were worn within the suite in order to avoid the inadvertent transport of non-MRI compatible instruments too near to the scanner.

## 11.6 Functional MRI-Guided Tumor Resection

### 11.6.1 1.5 T Functional MRI-Guided Resection

Patients underwent fMRI imaging preoperatively. For language, silent speech was used because actual physical vocalization would result in head movement and the subsequent misregistration of the areas of brain activation on the high resolution MRI obtained for surgical planning. Motor tasks included finger and toe tapping, while list retention was used for short-term memory mapping. Patients were asked to repeat each task multiple times with similar periods of rest between task performance. The fMRI protocol for the 1.5 T scanner was a single-shot EPI scan (TR/TE = 3,000/40 ms; field of view = 210 mm) with a 64 × 64 image matrix and 7 mm-thick slices with 1 mm intersection gap. Acquisition

was repeated 72 times over 4 min in sequential fashion. Test accuracy was measured by a wave pattern that was overlaid on a linear graph that indicated when the patient was performing a particular task properly. Areas of BOLD activation were calculated and these fMRI data were superimposed on high quality structural MRI scans that were displayed on the operating suite viewing monitor.

Intraoperative images were obtained in order to assist in determining the extent of residual disease and whether there was the need for more resection. The choice of imaging sequence was determined by the neurosurgeon in conjunction with the neuroradiologist. T2 weighted images, turbo FLAIR (fluid attenuated inversion recovery) and HASTE (half-Fourier-acquisition single-shot turbo-spin echo) images were used most often for intraoperative imaging of low grade glial tumors. Once the decision to obtain intraoperative imaging was made, all non-MRI compatible materials were removed from the table and the surgical site was covered with a sterile towel. All operations were performed with the patient under general anesthesia, and therefore functional scans were not obtained intraoperatively.

Follow up imaging was obtained 3 months after surgery and subsequently 1–2 times per year. All follow up films were reviewed by the neuroradiologist to exclude the presence of recurrent tumor.

### 11.6.2 3 T Functional MRI-Guided Resection

Preoperative mapping of functional areas of the brain was accomplished at 3 T. For preoperative 3 T fMRI studies, one of two scanners was used. One MR system was a short bore 3 T scanner (Intera, Philips Medical Systems, Best, The Netherlands). The fMRI protocol for this system was a single shot EPI scan (TR/TE = 3,000/35 ms; field of view = 230 mm) with an 80 × 128 image matrix and 4 mm thick slices with 1 mm intersection gap. The acquisition was repeated 100 times in a sequential fashion over an imaging interval of 7 min. The other system was the 3 T Siemens scanner (Siemens Medical Solutions, Erlangen, Germany). The fMRI protocol for this system was a single shot EPI scan (TR/TE = 2,660/30 ms; field of view = 192 mm) with a 64 × 64 image matrix and 3 mm slices with 0.8 mm intersection gap. Acquisition was repeated 60 times in

sequential fashion over an interval of 3 min. These data were acquired during repeated performances of toe tapping, finger tapping or silent speech. Tasks were repeated with periods of rest of similar length intervening. Brain activation (BOLD) imaging data were calculated using Philips software. Intraoperative guidance was still performed with the 1.5 T system as described above. Rigid fixation of the head during intraoperative scans allowed for similar acquisition planes and straightforward identification of the previously identified areas of activation on the intraoperative scans.

## 11.7 Results

### 11.7.1 Functional MRI at 1.5 T for the Treatment of Low Grade Glial Tumors

From 1997 to 2003, 16 patients whose tumors were histologically proven to be low grade gliomas were operated on using 1.5 T ioMRI-guidance after preoperative 1.5 T fMRI was obtained. Fifteen of these patients had operative resection while the last patient underwent ioMRI-guided biopsy because the tumor was determined to be located within the motor cortex. Tumors in this series included oligodendrogliomas ( $n = 10$ ), low grade astrocytomas ( $n = 4$ ), pleomorphic xanthroastrocytoma ( $n = 1$ ), and dysembryoplastic neuroepithelial tumor ( $n = 1$ ). Mean age at the time of surgery was 31 years, with a range of 10–43 years. Fifteen of the patients in this series presented with seizures, the remaining patient was asymptomatic. No patient had a neurological deficit prior to surgery. Of the 16 patients, 12 were undergoing their first surgical procedure, whereas three patients had previous resection or debulking and one patient had previously undergone biopsy. Locations were right frontal ( $n = 5$ ), left frontal ( $n = 6$ ), left temporal ( $n = 3$ ), and left parietal ( $n = 1$ ). Motor function, speech function and memory function were localized using fMRI as deemed appropriate by the location of the lesion and planned surgical corridor.

The number and frequency of intraoperative images varied depending on the operative findings; however, all the patients had imaging to determine whether the tumor was completely resected, and one final scan to exclude the presence of hemorrhage before leaving the

operative suite. For the majority of patients, the first scan obtained after resection revealed some residual tumor that was found to be resected on subsequent imaging after more surgery. In a few cases where the tumor was particularly close to areas of functional imaging, one or more additional intermediate scans were obtained as the resection progressed. In cases where there was doubt about the presence of blood on this scan, one final scan was obtained 15–20 min later.

In this series of patients, a GTR was achieved in 10 patients (63%). Of the five patients in whom resection was considered subtotal, residual tumor was left intentionally because it was felt that the lesions were entwined with functional motor cortex in four patients and both language and motor areas in the other patient.

None of the patients in whom complete radiographic resection was achieved had experienced recurrence at last follow up (mean, 31 months; range, 14–87 months). Of the patients who underwent partial resection, none had evidence of tumor progression at last follow-up (12–20 months). The patient who was treated with radiotherapy as the primary treatment modality had stable disease at last follow-up of 41 months.

Postoperative morbidity in this series was low. There were no permanent neurological deficits in any patient. One patient experienced a transient hemiparesis that was felt to be related to postoperative edema extending into the motor strip, while another patient exhibited a transient motor apraxia, which was not surprising, given the location of the tumor within the supplementary motor area. There were no mishaps involving MRI-incompatible instruments or any other objects within the magnetic field.

### 11.8 Functional MRI at 3 T

Using fMRI data acquired at 3 T, tumor surgery was performed on 13 patients with primary intracranial tumors located adjacent to eloquent cortex. These tumors included six oligodendrogliomas, three meningiomas, two astrocytomas and two GBMs. Mean age was 43 years with a median age of 48 years (range, 22–70 years). Tumors were located in the right frontal ( $n = 5$ ), left frontal ( $n = 6$ ), and left temporal ( $n = 2$ ) lobes. Ten of the 13 patients were being operated on for the first time. Twelve of the patients underwent resection with ioMRI-guidance after review of fMRI results, while one patient's tumor was within the motor cortex,

and therefore, a brain biopsy was performed. In the twelve patients whose tumors were resected, a GTR was achieved in ten (Figs. 11.1–11.3). The remaining two patients, one with an astrocytoma and the other with a GBM, had partial resections because the fMRI revealed that the tumors were infiltrating into eloquent cortex. GTR was defined either as the removal of all areas of enhancement for high grade tumors and meningiomas, or the removal of the predefined tumor imprint for nonenhancing tumors. There was no postoperative hemorrhage noted in any patient.

The number of intraoperative scans that were obtained during surgery varied widely within this series. A minimum of three scans were generally obtained with one before surgery, one to determine if there was residual tumor (Figs. 11.4–11.6), and a final scan before leaving the operative suite to determine if any hemorrhage occurred during closure. The head position was maintained constant throughout the procedure by use of the head frame, resulting in identical image planes during scanning.

There were no permanent postoperative neurologic deficits seen in this series of patients. Five patients

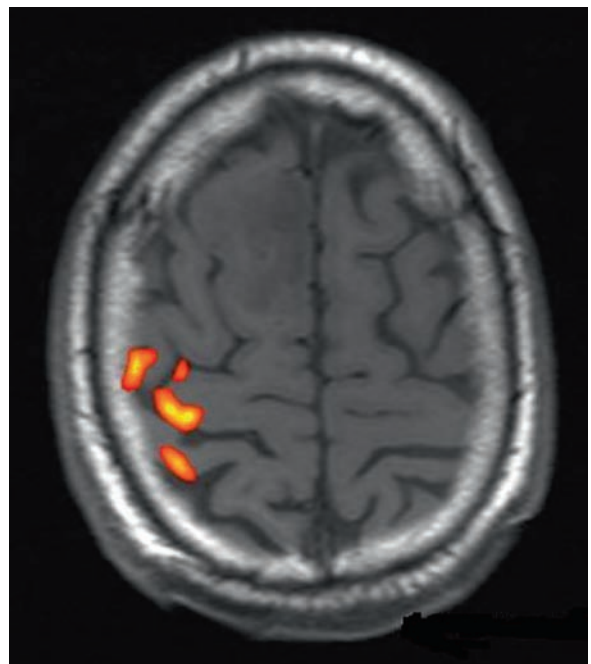


**Fig. 11.1** Axial T1-weighted brain activation study performed at 3 Tesla showing the area for finger tapping of the left hand. The tumor that is planned to be surgically resected is just anterior and medial to the cortical area of brain activation. The posterior aspect of the tumor is nicely delineated by a medial and lateral sulcus

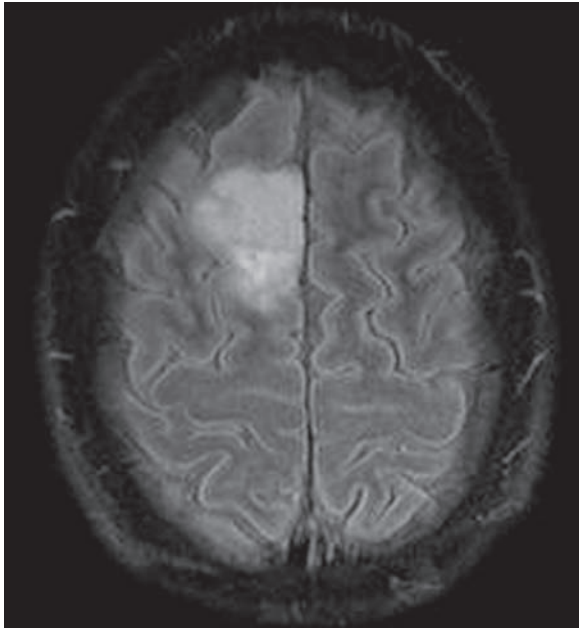


**Fig. 11.2** Three Tesla axial turbo FLAIR image demonstrating a right frontal area of increased signal that is consistent with a low grade glioma. This scan was obtained immediately prior to a brain activation study that was performed to identify the location of functional cortex in proximity to the presumed tumor

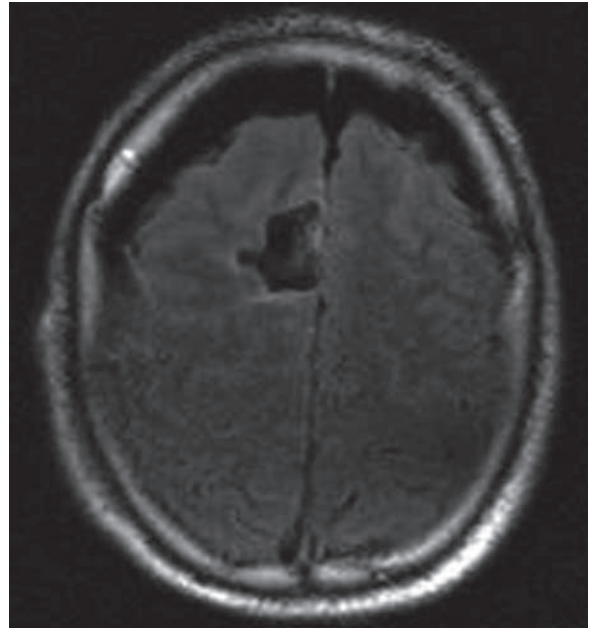


**Fig. 11.3** Intraoperative axial turbo FLAIR scan that was obtained at 1.5 Tesla showing a complete radiographic resection of the tumor footprint. The pathologic examination revealed an oligodendroglioma. The surgical resection cavity is filled with air and pneumocephalus is seen over both frontal lobes. Brain shift as a consequence of the egress of cerebrospinal fluid has occurred

did experience temporary neurologic worsening that included speech apraxia in two patients, motor apraxia in two patients and combined speech and motor apraxia in one patient. All patients experienced complete resolution of these deficits within 4 weeks of surgery. There were no safety issues that occurred in this series related to the inadvertent transport of ferromagnetic items too near to the magnet field.

## 11.9 Discussion

The use of ioMRI at various field strengths has been well described, and validated for safety and efficacy in achieving maximal tumor resection in adult and pediatric brain tumor surgery (Alexander et al. 1997; Berger et al. 1994; Bernays and Laws 1997; Bernstein et al. 2000; Black et al. 1999; Hall et al. 2003; Hall et al. 2005; Hall et al. 1998; Kremer et al. 2006; Lam et al. 2001; Martin et al. 1998; Nimsky et al. 2004; Schwartz et al. 1999; Trantakis et al. 2003). The addition of preoperative fMRI provides the neurosurgeon with a clear delineation of the areas of eloquent cortex that must be

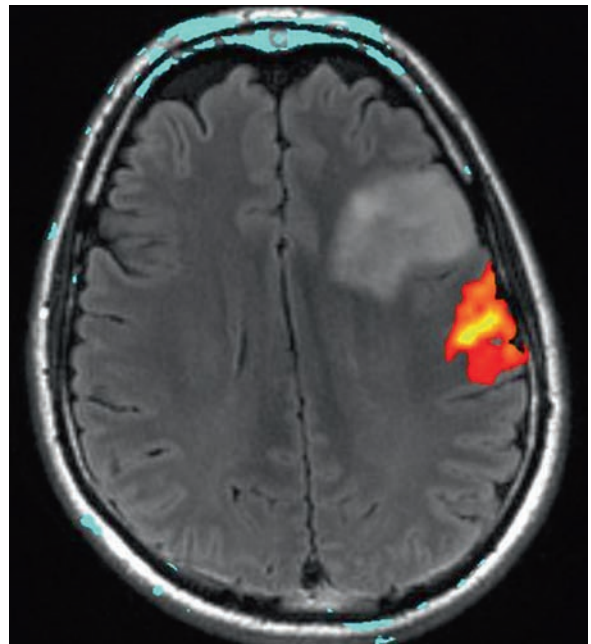


**Fig. 11.4** Axial turbo fluid-attenuated inversion recovery (FLAIR) magnetic resonance imaging scan demonstrating a left frontal low grade glioma that was found at surgery to be an oligodendroglioma. This brain activation study was performed at 3 Tesla and the task being performed was finger tapping of the right hand

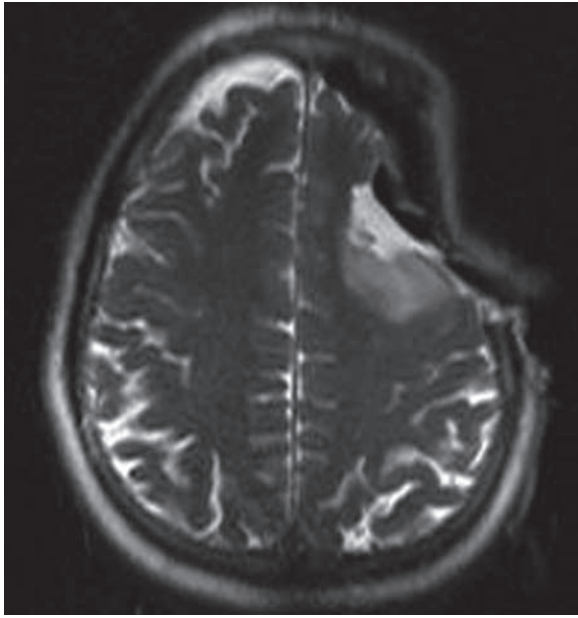


**Fig. 11.5** Intraoperative axial half-Fourier acquisition single-shot turbo spin echo (HASTE) magnetic resonance imaging scan demonstrating the presence of residual tumor just posterior to the surgical cavity that required additional resection before the completion of the procedure. The HASTE imaging technique is used for low grade gliomas because of its ability to clearly demonstrate residual disease and the rapid acquisition time that is possible during surgery. Note the presence of brain shift of the left frontal lobe

preserved during tumor resection; when combined with ioMRI, it has allowed for the safe resection of tumors near eloquent cortex that would otherwise have required awake craniotomy or intraoperative cortical stimulation, or that may even have been considered unresectable. A reasonable concern with fMRI is that it defines areas of functionality indirectly, most often due to oxygen consumption during the performance of a task. Differences between functional territories as defined by direct brain mapping and fMRI have been reported (Roux et al. 2003), supporting this concern. Moreover, our speech testing used the commonly accepted paradigm of silent speech to reduce artifact (Friedman et al. 1998; Hinke et al. 1993), although areas of brain activation are not identical to those where true speech is generated (Huang et al. 2002). Awake craniotomy does provide the most direct assessment of functionality of the brain tissue that is being resected; however, it requires stimulation to function or loss of function after resection to define eloquent areas. This may result in an irreversible neurological deficit.

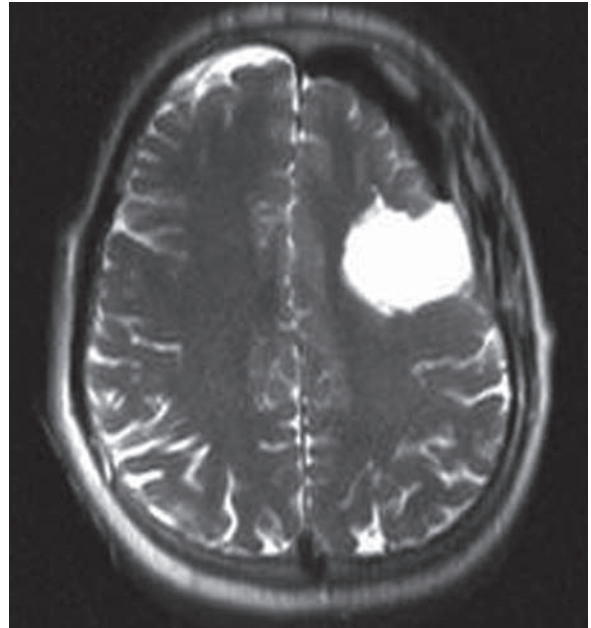


**Fig. 11.6** Intraoperative axial half-Fourier acquisition single-shot turbo spin echo (HASTE) magnetic resonance imaging scan demonstrating a complete radiographic resection of the left frontal oligodendroglioma footprint. The craniotomy has been closed completely at this point and there is a mixture of saline and cerebrospinal fluid seen filling the resection cavity

Most importantly, the lack of lasting postoperative deficits in the 29 patients in our combined series suggests that although indirect, fMRI does yield accurate information on the location of eloquent cortex and allows for the safe resection of tumors lying adjacent to that tissue. Regardless of the technique that is used for localizing tumors, those that infiltrate directly into functional cortex cannot be safely resected by the surgeon. Because of this limitation, there were patients who still underwent partial resection in both of our series despite the use of fMRI guidance and in other reported series (Nimsky et al. 2006a).

Increasing the field strength of the preoperative fMRI from 1.5 to 3 T improved the resolution of these images. Although the 1.5 T imaging allowed for safe aggressive resection of the lesions in the first series, the functional data was limited to one axial plane, whereas the 3 T data were visible on multiple slices, allowing for visualization of function in three dimensions. The success of increasing magnet strength intraoperatively raises the possibility of performing 3 T high field ioMRI to match preoperative functional imaging at 3 T, which obviously would add clarity to the intraoperative

imaging, affording a resolution equal to that of the preoperative functional images. Our experience in applying 3 T fMRI preoperative data intraoperatively to guide brain tumor resection at 1.5 T has been sufficient for most surgical decision making. However, intraoperative imaging at 3 T may clearly represent the next degree of sophistication for neurosurgeons working in this field.

In our series, intraoperative scans were obtained to demonstrate brain structure only; therefore, during surgery the neurosurgeon was required to extrapolate the preoperative fMRI data onto the newly acquired ioMRI structural scans. While intraoperative fMRI scans would obviate the need for preoperative acquisition, this would also add the time of multiple cycles of anesthesia reversal (for the performance of the intraoperative functional tasks) to the procedure. As with any imaging modality used during surgery, the data does not replace sound surgical judgment and familiarity with the neuroanatomy. Therefore, although our paradigm requires that the surgeon must mentally apply the preoperative fMRI data to newly acquired ioMRI images, this should not compromise the safety or efficacy of this technique.

Functional MRI data may also be coregistered with neuronavigation data as described above, although this has previously been reported to pose the risk of mislocalization (Roux et al. 2001) and still is subject to brain shift as with other frameless stereotactic techniques. Another way to compensate for brain shift that has been reported, involves the application of intraoperative high resolution 3D ultrasound data to registered MRI/fMRI data to allow for the correction of shift (Rasmussen et al. 2007). This is certainly an attractive option, although rigorous validation of computational algorithms is needed.

### 11.10 Low Grade Gliomas

Intraoperative MRI has been shown to help facilitate the resection of low grade gliomas (Martin et al. 1998); however, the lack of clearly defined borders in these infiltrating tumors does increase the risk of damage to adjacent neural structures during image-guided surgery. Because low grade glial tumors are often infiltrative and there exists controversy regarding the benefits of an aggressive resection of low grade gliomas; these tumors are often treated without surgery when they

occur in close proximity to eloquent cortex. The infiltrative nature of these lesions may obscure the border between tumor and functional cortex. We have reviewed our experience with resection of low grade gliomas using ioMRI-guidance combined with preoperative fMRI. Our method of combining preoperative fMRI acquired at 1.5 T with 1.5 T ioMRI-guided surgery, allowed for complete tumor resection in 10 (63%) patients without neurologic deficit at 1 month after surgery. Only one patient in this series received adjuvant radiation therapy and all patients enjoyed progression free survival at last follow up (median 25 months). The lack of recurrence or progression of disease is consistent with our belief that maximal resection is the optimal treatment for low grade gliomas. Furthermore, we interpret the fact that a significant number of the patients in this series exhibited transient postoperative neurologic deficits without permanent sequelae, as evidence that ioMRI allowed for the most aggressive resection possible by the neurosurgeon.

### 11.11 High Grade Gliomas

HGG represent the majority of primary intraparenchymal brain tumors in adults, and as mentioned previously, are treated by most neurosurgeons by surgical resection. Functional MRI neuronavigation as well as ioMRI combined with preoperative fMRI have been used in the treatment of HGG. Because these tumors usually enhance after contrast administration, a radiographic GTR can be defined as the removal of the enhancing mass on MRI. HGG are generally visible grossly, and the neurosurgeon is often able to determine when GTR has been achieved during surgery without imaging. Nonetheless, ioMRI is useful for judging the extent of the tumor resection and confirming whether additional tumor removal is warranted. In our practice, contrast is only given intraoperatively after the apparent removal of most of the grossly abnormal tissue to avoid the diffusion of contrast into the edematous brain around the resection cavity.

Although controversy continues as to whether gross total tumor resection extends survival in patients with HGG, the combination of fMRI and ioMRI provides increased protection of eloquent brain structures without the need for awake craniotomy and cortical

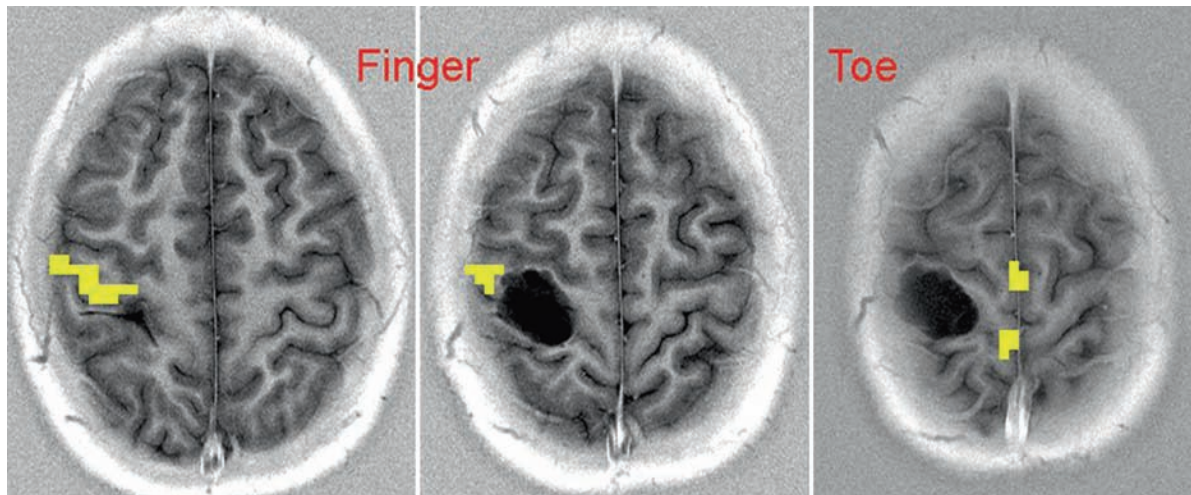


**Fig. 11.7** Brain activation study at 1.5 Tesla showing the location of finger and toe tapping of the left side of the body were present on three axial inversion recovery scans displayed on different slice images. The area of decreased signal represents a

brain metastasis from a sarcoma that originated in the thigh that is located in close proximity to eloquent motor function on this inversion recovery magnetic resonance imaging scans

stimulation. Class I data regarding the extent of surgical resection on prognosis is unlikely to be collected, given the improbability that patients will agree to be randomized into the deliberate subtotal resection group. However, we feel that the rationale for aggressive tumor removal as outlined in the introduction further justifies the use of iMRI as a tool to maximize tumor resections.

In a rare, prospective, randomized trial comparing neuronavigation with diffusion tensor imaging tractography compared to traditional structural neuronavigation for tumors near the pyramidal tract, subgroup analysis of 81 HGG revealed a significantly higher rate of GTR, with a corresponding statistically significant increase in median survival from 14.0 to 21.2 months (Wu et al. 2007). Although this approach represents a slightly different treatment modality, we believe that this is a demonstration of the advantage offered by surgical guidance with functional imaging.

## 11.12 Other Tumors

Although we have focused on gliomas, the strategies outlined in this chapter should be applicable to virtually any lesion near eloquent cortex. The role of aggressive surgical resection is less clear for metastatic brain tumors, and aggressive surgical resection for tumors

adjacent to eloquent cortex may be less appealing, especially given the excellent nonsurgical modalities presently available. Within the parameters of a rational approach to surgical resection, however, fMRI-guided neurosurgery likely has a role in a subset of patients with metastatic lesions (Figs 11.7 and 11.8). Certainly lesions located near eloquent structures will often be symptomatic, and the availability of fMRI-guided resection is likely to be useful in such situations.

Because meningiomas are extra-axial tumors, their surgical resection should pose a lower risk of postoperative neurologic injury. The benefit of radical resection in treatment of meningiomas is well documented (Simpson 1957). Neuronavigation is often used for planning the surgical resection of meningiomas and may be helpful in achieving complete resection (Keskil et al. 2006). We felt that iMRI with pre-operative functional imaging at 3 T was helpful in three meningiomas in our series that were located near eloquent cortex (Figs 11.9 and 11.10).

## 11.13 Conclusions

Functional MRI identifies those areas of cortex that are likely to result in neurologic compromise if resected by the neurosurgeon. Despite the fact that these data are indirectly measured, the use of fMRI has been

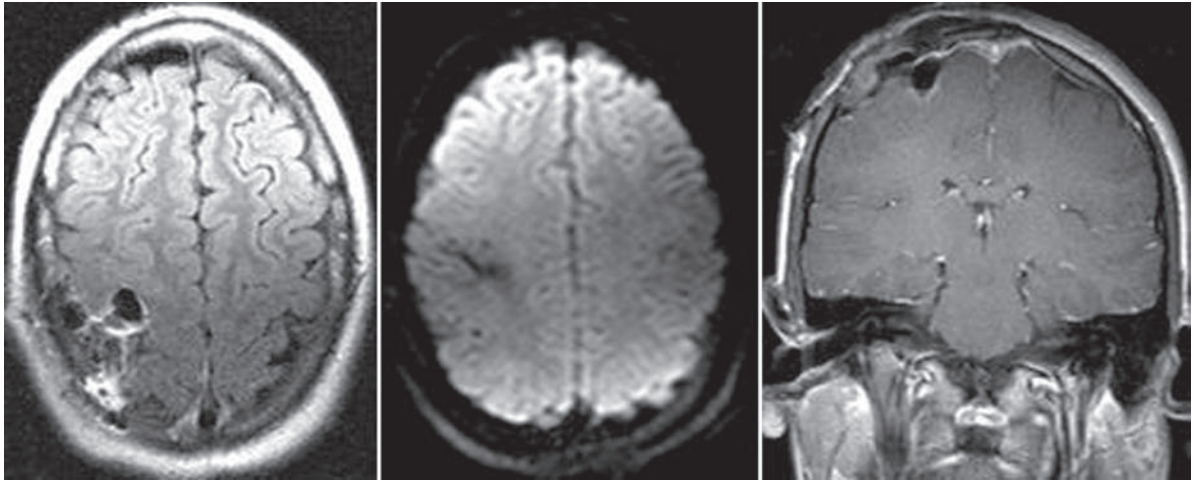


**Fig. 11.8** Intraoperative axial turbo FLAIR, axial gradient echo, and coronal T1-weighted contrast enhanced magnetic resonance imaging scans demonstrating the complete resection of the poste-

rior right frontal sarcoma brain metastasis. The patient sustained no postoperative transient or permanent neurologic injury and they were discharged from the hospital on the second postoperative day

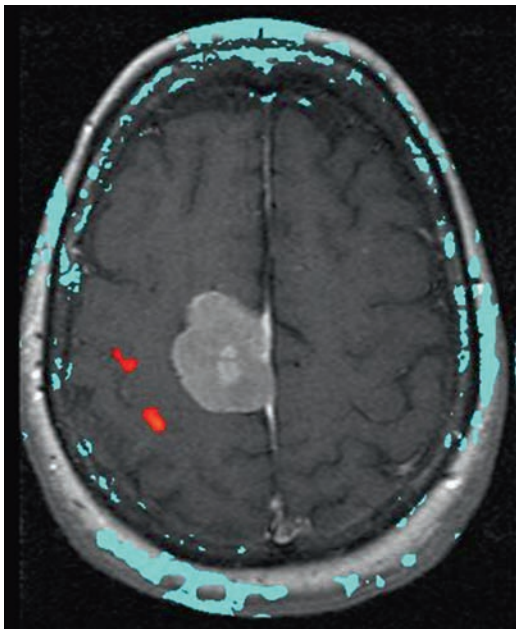


**Fig. 11.9** Axial brain activation study performed at 3 Tesla demonstrating the location of the functional area of the cortex for finger tapping of the left hand. The area of activation is just posterior and lateral to the contrast-enhancing tumor on this T1-weighted axial magnetic resonance imaging scan that was found to be a meningioma at surgery

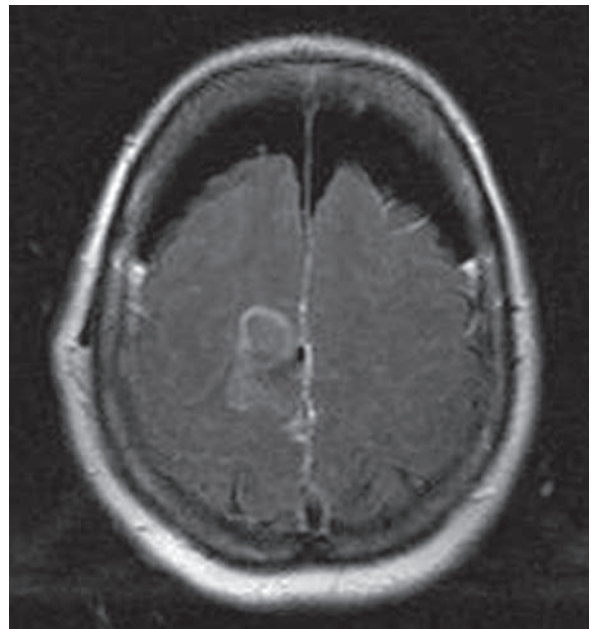


**Fig. 11.10** Intraoperative axial turbo FLAIR MRI scan that was obtained at 1.5 Tesla after the complete resection of the tumor. Of note is the pneumocephalus that is present over both frontal lobes and the degree of brain shift that has resulted from the loss of cerebrospinal fluid during surgery

validated as safe and effective for surgical guidance in the resection of tumors located near areas of functional cortex. We prefer a paradigm of preoperative high field fMRI combined with structural iMRI to guide the removal of tumors that we have described in this series. Others have found fMRI useful within the context of coregistered frameless neuronavigation and awake craniotomy.

## References

- Alexander E, Moriarty TM, Kikinis R, Black P, Jolesz FM (1997) The present and future role of intraoperative MRI in neurosurgical procedures. *Stereotact Funct Neurosurg* 68(1–4 Pt 1):10–17
- Amiez C, Kostopoulos P, Champod AS, Collins DL, Doyon J, Del Maestro R, Petrides M (2008) Preoperative functional magnetic resonance imaging assessment of higher-order cognitive function in patients undergoing surgery for brain tumors. *J Neurosurg* 108(2):258–268
- Archip N, Clatz O, Whalen S, Kacher D, Fedorov A, Kot A, Chrisochoides N, Jolesz F, Golby A, Black PM, Warfield SK (2007) Non-rigid alignment of pre-operative MRI, fMRI, and DT-MRI with intra-operative MRI for enhanced visualization and navigation in image-guided neurosurgery. *Neuroimage* 35(2):609–624
- Berger MS, Deliganis AV, Dobbins J, Keles GE (1994) The effect of extent of resection on recurrence in patients with low grade cerebral hemisphere gliomas. *Cancer* 74(6):1784–1789
- Bernays RL, Laws ER Jr (1997) Intraoperative diagnostic and interventional magnetic resonance imaging in neurosurgery. *Neurosurgery* 41(4):999
- Bernstein M, Al-Anazi AR, Kucharczyk W, Manninen P, Bronskill M, Henkelman M (2000) Brain tumor surgery with the Toronto open magnetic resonance imaging system: preliminary results for 36 patients and analysis of advantages, disadvantages, and future prospects. *Neurosurgery* 46(4):909–917
- Black PM, Alexander E III, Martin C, Moriarty T, Nabavi A, Wong TZ, Schwartz RB, Jolesz F (1999) Craniotomy for tumor treatment in an intraoperative magnetic resonance imaging unit. *Neurosurgery* 45(3):423–431
- Braun V, Dempf S, Tomczak R, Wunderlich A, Weller R, Richter HP (2000) Functional cranial neuronavigation. Direct integration of fMRI and PET data. *J Neuroradiol* 27(3):157–163
- Braun V, Dempf S, Tomczak R, Wunderlich A, Weller R, Richter HP (2001) Multimodal cranial neuronavigation: direct integration of functional magnetic resonance imaging and positron emission tomography data: technical note. *Neurosurgery* 48(5):1178
- Braun V, Albrecht A, Kretschmer T, Richter HP, Wunderlich A (2006) Brain tumour surgery in the vicinity of short-term memory representation – results of neuronavigation using fMRI images. *Acta Neurochir (Wien)* 148(7):733–9
- Buckner JC (2003) Factors influencing survival in high-grade gliomas. *Semin Oncol* 30(6 Suppl 19):10–14
- Chang EF, Potts MB, Keles GE, Lamborn KR, Chang SM, Barbaro NM, Berger MS (2008) Seizure characteristics and control following resection in 332 patients with low-grade gliomas. *J Neurosurg* 108(2):227–235
- Clatz O, Delingette H, Talos IF, Golby AJ, Kikinis R, Jolesz FA, Ayache N, Warfield SK (2005) Robust nonrigid registration to capture brain shift from intraoperative MRI. *IEEE Trans Med Imaging* 24(11):14171–27
- Claus EB, Horlacher A, Hsu L, Schwartz RB, Dello-Iacono D, Talos F, Jolesz FA, Black PM (2005) Survival rates in patients with low-grade glioma after intraoperative magnetic resonance image guidance. *Cancer* 103(6):1227–133
- Engle DJ, Lunsford LD (1987) Brain tumor resection guided by intraoperative computed tomography. *J Neurooncol* 4(4):361–370
- Fandino J, Kollias SS, Wieser HG, Valavanis A, Yonekawa Y (1999) Intraoperative validation of functional magnetic resonance imaging and cortical reorganization patterns in patients with brain tumors involving the primary motor cortex. *J Neurosurg* 91(2):238–250
- Feigl GC, Safavi-Abassi S, Garabaghi A, Gonzalez-Felipe V, El Shawarby A, Fruend HJ, Samii M (2008) Real time 3T fMRI data of brain tumour patients for intra-operative localization of primary motor areas. *Eur J Surg Oncol* 34(6):708–715
- Friedman L, Kenny JT, Wise AL, Wu D, Stuve TA, Miller DA, Jesberger JA, Lewin JS (1998) Brain activation during silent word generation evaluated with functional MRI. *Brain Lang* 64(2):231–256
- Gumprecht H, Ebel GK, Auer DP, Lumenta CB (2002) Neuronavigation and functional MRI for surgery in patients with lesion in eloquent brain areas. *Minim Invasive Neurosurg* 45(3):1511–1513
- Hall WA, Martin AJ, Liu H, Pozza CH, Casey SO, Michel E, Nussbaum ES, Maxwell RE, Truwit CL (1998) High-field strength interventional magnetic resonance imaging for pediatric neurosurgery. *Pediatr Neurosurg* 29(5):2532–2539
- Hall WA, Liu H, Maxwell RE, Truwit CL (2003) Influence of 1.5-Tesla intraoperative MR imaging on surgical decision making. *Acta Neurochir Suppl* 85:29–37
- Hall WA, Liu H, Truwit CL (2005) Functional magnetic resonance imaging-guided resection of low-grade gliomas. *Surg Neurol* 64(1):20–27
- Hinke RM, Hu X, Stillman AE, Kim SG, Merkle H, Salmi R, Ugurbil K (1993) Functional magnetic resonance imaging of Broca's area during internal speech. *Neuroreport* 4(6):6756–6758
- Huang J, Carr TH, Cao Y (2002) Comparing cortical activations for silent and overt speech using event-related fMRI. *Hum Brain Mapp* 15(1):39–53
- Jääskeläinen J, Randell T (2003) Awake craniotomy in glioma surgery. *Acta Neurochir Suppl* 88:31–35
- Jeremic B, Grujicic D, Antunovic V, Djuric L, Stojanovic M, Shibamoto Y (1994) Influence of extent of surgery and tumor location on treatment outcome of patients with glioblastoma multiforme treated with combined modality approach. *J Neurooncol* 21(2):177–185
- Joki T, Carroll R, Dunn IF, Zhang J, Abe T, Black PM (2001) Assessment of alterations in gene expression in recurrent malignant glioma after radiotherapy using complementary deoxyribonucleic acid microarrays. *Neurosurgery* 48(1):195–202

- Kamada K, Houkin K, Takeuchi F, Ishii N, Ikeda J, Sawamura Y, Kuriki S, Kawaguchi H, Iwasaki Y (2003) Visualization of the eloquent motor system by integration of MEG, functional, and anisotropic diffusion-weighted MRI in functional neuronavigation. *Surg Neurol* 59(5):352–361
- Kamada K, Todo T, Masutani Y, Aoki S, Ino K, Morita A, Saito N (2007) Visualization of the frontotemporal language fibers by tractography combined with functional magnetic resonance imaging and magnetoencephalography. *J Neurosurg* 106(1):90–98
- Keles GE, Lamborn KR, Berger MS (2001) Low-grade hemispheric gliomas in adults: a critical review of extent of resection as a factor influencing outcome. *J Neurosurg* 95(5):735–745
- Keskil S, Bademci G, Goksel M (2006) Tracing the dural tail with image-guided surgery. *Minim Invasive Neurosurg* 49(6):3573–3578
- Kober H, Nimsky C, Vieth J, Fahlbusch R, Ganslandt O (2002) Co-registration of function and anatomy in frameless stereotaxy by contour fitting. *Stereotact Funct Neurosurg* 79(3–4):272–283
- Kowalczyk A, Macdonald RL, Amidei C, Dohrmann G III, Erickson RK, Hekmatpanah J, Krauss S, Krishnasamy S, Masters G, Mullan SF, Mundt AJ, Sweeney P, Vokes EE, Weir BK, Wollman RL (1997) Quantitative imaging study of extent of surgical resection and prognosis of malignant astrocytomas. *Neurosurgery* 41(5):10281–10336
- Kremer P, Tronnier V, Steiner HH, Metzner R, Ebinger F, Rating D, Hartmann M, Seitz A, Unterberg A, Wirtz CR (2006) Intraoperative MRI for interventional neurosurgical procedures and tumor resection control in children. *Childs Nerv Syst* 22(7):6746–6748
- Krishnan R, Raabe A, Hattungen E, Szélenyi A, Yahya H, Hermann E, Zimmermann M, Seifert V (2004) Functional magnetic resonance imaging-integrated neuronavigation: correlation between lesion-to-motor cortex distance and outcome. *Neurosurgery* 55(4):904–914
- Kucharczyk J, Hall WA, Broaddus WC, Gillies GT, Truwit CL (2001) Cost-efficacy of MR-guided neurointerventions. *Neuroimaging Clin N Am* 11(4):767–772
- Lacroix M, Abi-Said D, Fournay DR, Gokaslan ZL, Shi W, DeMonte F, Lang FF, McCutcheon IE, Hassenbusch SJ, Holland E, Hess K, Michael C, Miller D, Sawaya R (2001) A multivariate analysis of 416 patients with glioblastoma multiforme: prognosis, extent of resection, and survival. *J Neurosurg* 95(2):1901–1908
- Lai DM, Lin SM, Tu YK, Kao MC, Hung CC (1993) Therapy for supratentorial malignant astrocytomas: survival and possible prognostic factors. *J Formos Med Assoc* 92(3):2202–2206
- Lam CH, Hall WA, Truwit CL, Liu H (2001) Intra-operative MRI-guided approaches to the pediatric posterior fossa tumors. *Pediatr Neurosurg* 34(6):295–300
- Laws ER Jr, Taylor WF, Clifton MB, Okazaki H (1984) Neurosurgical management of low-grade astrocytoma of the cerebral hemispheres. *J Neurosurg* 61(4):665–673
- Martin C, Alexander E III, Wong T, Schwartz R, Jolesz F, Black PM (1998) Surgical treatment of low-grade gliomas in the intraoperative magnetic resonance imager. *Neurosurg Focus* 4(4):e8
- Medbery CA III, Straus KL, Steinberg SM, Cotelingam JD, Fisher WS (1988) Low-grade astrocytomas: treatment results and prognostic variables. *Int J Radiat Oncol Biol Phys* 15(4):837–841
- Meyer FB, Bates LM, Goerss SJ, Friedman JA, Windschitl WL, Duffy JR, Perkins WJ, O'Neill BP (2001) Awake craniotomy for aggressive resection of primary gliomas located in eloquent brain. *Mayo Clin Proc* 76(7):677–687
- Nabavi A, Black PM, Gering DT, Westin CF, Mehta V, Pergolizzi RS Jr, Ferrant M, Warfield SK, Hata N, Schwartz RB, Wells WM III, Kikinis R, Jolesz FA (2001) Serial intraoperative magnetic resonance imaging of brain shift. *Neurosurgery* 48(4):787–797
- Nguyen LN, Maor MH, Oswald MJ (1998) Brain metastases as the only manifestation of an undetected primary tumor. *Cancer* 83(10):218121–218124
- Nicolato A, Gerosa MA, Fina P, Iuzzolino P, Giorgiutti F, Bricolo A (1995) Prognostic factors in low-grade supratentorial astrocytomas: a uni-multivariate statistical analysis in 76 surgically treated adult patients. *Surg Neurol* 44(3):208–221
- Nimsky C, Ganslandt O, Von Keller B, Romstöck J, Fahlbusch R (2004) Intraoperative high-field-strength MR imaging: implementation and experience in 200 patients. *Radiology* 233(1):67–78
- Nimsky C, Ganslandt O, Buchfelder M, Fahlbusch R (2006a) Intraoperative visualization for resection of gliomas: the role of functional neuronavigation and intraoperative 1.5 T MRI. *Neurol Res* 28(5):4824–4827
- Nimsky C, Ganslandt O, Keller BV, Fahlbusch R (2006b) Intraoperative high field MRI: anatomical and functional imaging. *Acta Neurochir Suppl* 98:87–95
- O'Shea JP, Whalen S, Branco DM, Petrovich NM, Knierim KE, Golby AJ (2006) Integrated image- and function-guided surgery in eloquent cortex: a technique report. *Int J Med Robot* 2(1):75–83
- Ogawa S, Lee TM, Kay AR, Tank DW (1990) Brain magnetic resonance imaging with contrast dependent on blood oxygenation. *Proc Natl Acad Sci U S A* 87(24):98689–72
- Patchell RA, Tibbs PA, Walsh JW, Dempsey RJ, Maruyama Y, Kryscio RJ, Markesbery WR, Macdonald JS, Young B (1990) A randomized trial of surgery in the treatment of single metastases to the brain. *N Engl J Med* 322(8):494–500
- Philippon JH, Clemenceau SH, Fauchon FH, Foncin JF (1993) Supratentorial low-grade astrocytomas in adults. *Neurosurgery* 32(4):5545–5549
- Picht T, Kombos T, Gramm HJ, Brock M, Suess O (2006) Multimodal protocol for awake craniotomy in language cortex tumour surgery. *Acta Neurochir (Wien)* 148(2):127–137
- Piepmeier J, Christopher S, Spencer D, Byrne T, Kim J, Knisel JP, Lacy J, Tsukerman L, Makuch R (1996) Variations in the natural history and survival of patients with supratentorial low-grade astrocytomas. *Neurosurgery* 38(5):8728
- Piepmeier JM (1987) Observations on the current treatment of low-grade astrocytic tumors of the cerebral hemispheres. *J Neurosurg* 67(2):177–181
- Preul C, Tittgemeyer M, Lindner D, Trantakis C, Meixensberger J (2004) Quantitative assessment of parenchymal and ventricular readjustment to intracranial pressure relief. *AJNR Am J Neuroradiol* 25(3):377–381
- Rasmussen IA Jr, Lindseth F, Rygh OM, Berntsen EM, Selbekk T, Xu J, Nagelhus Hernes TA, Harg E, Håberg A, Unsgaard G (2007) Functional neuronavigation combined with intra-operative 3D ultrasound: initial experiences during

- surgical resections close to eloquent brain areas and future directions in automatic brain shift compensation of preoperative data. *Acta Neurochir (Wien)* 149(4):365–378
- Reinertsen I, Lindseth F, Unsgaard G, Collins DL (2007) Clinical validation of vessel-based registration for correction of brain-shift. *Med Image Anal* 11(6):673–684
- Reinges MH, Nguyen HH, Krings T, Hütter BO, Rohde V, Gilsbach JM (2004) Course of brain shift during microsurgical resection of supratentorial cerebral lesions: limits of conventional neuro-navigation. *Acta Neurochir (Wien)* 146(4):369–377
- Roessler K, Donat M, Lanzenberger R, Novak K, Geissler A, Gartus A, Tahamtan AR, Milakara D, Czech T, Barth M, Knosp E, Beisteiner R (2005) Evaluation of preoperative high magnetic field motor functional MRI (3 Tesla) in glioma patients by navigated electrocortical stimulation and postoperative outcome. *J Neurol Neurosurg Psychiatry* 76(8):115211–115217
- Roux FE, Ibarrola D, Tremoulet M, Lazorthes Y, Henry P, Sol JC, Berry I (2001) Methodological and technical issues for integrating functional magnetic resonance imaging data in a neuronavigational system. *Neurosurgery* 49(5):11451–11456
- Roux FE, Boulanouar K, Lotterie JA, Mejdoubi M, LeSage JP, Berry I (2003) Language functional magnetic resonance imaging in preoperative assessment of language areas: correlation with direct cortical stimulation. *Neurosurgery* 52(6):13351–13445
- Schulder M, Maldjian JA, Liu WC, Mun IK, Carmel PW (1997) Functional MRI-guided surgery of intracranial tumors. *Stereotact Funct Neurosurg* 68(1–4 Pt 1):98–105
- Schulder M, Holodny A, Liu WC, Gray A, Lange G, Carmel PW (1999) Functional magnetic resonance image-guided surgery of tumors in or near the primary visual cortex. *Stereotact Funct Neurosurg* 73(1–4):31–36
- Schwartz RB, Hsu L, Wong TZ, Kacher DF, Zamani AA, Black PM, Alexander E III, Stieg PE, Moriarty TM, Martin CA, Kikinis R, Jolesz FA (1999) Intraoperative MR imaging guidance for intracranial neurosurgery: experience with the first 200 cases. *Radiology* 211(2):477–488
- Signorelli F, Guyotat J, Schneider F, Isnard J, Bret P (2003) Technical refinements for validating functional MRI-based neuronavigation data by electrical stimulation during cortical language mapping. *Minim Invasive Neurosurg* 46(5):2652–2658
- Simpson DJ (1957) The recurrence of intracranial meningiomas after surgical treatment. *J Neurol Neurosurg Psychiatry* 20(1):22–39
- Speigl-Kreinecker S, Pirker C, Marosi C, Buchroithner J, Pichler J, Silye R, Fischer J, Micksche M, Berger W (2002) Dynamics of chemosensitivity and chromosomal instability in recurrent glioblastoma. *Br J Cancer* 96:9609
- Stummer W, Reulen HJ, Meinel T, Pichlmeier U, Schumacher W, Tonn JC, Rohde V, Opperl F, Turowski B, Woiciechowsky C, Franz K, Pietsch T; ALA-Glioma Study Group (2008) Extent of resection and survival in glioblastoma multiforme: identification of and adjustment for bias. *Neurosurgery* 62(3):564–576
- Trantakis C, Tittgemeyer M, Schneider JP, Lindner D, Winkler D, Strauss G, Meixensberger J (2003) Investigation of time-dependency of intracranial brain shift and its relation to the extent of tumor removal using intra-operative MRI. *Neurol Res* 25(1):9–12
- Truwit CL, Hall WA (2006) Intraoperative magnetic resonance imaging-guided neurosurgery at 3-T. *Neurosurgery* 58(4 Suppl 2):ONS-338–345
- Ushio Y, Kochi M, Hamada J, Kai Y, Nakamura H (2005) Effect of surgical removal on survival and quality of life in patients with supratentorial glioblastoma. *Neurol Med Chir (Tokyo)*. 45(9):454–460
- Vecht CJ, Haaxma-Reiche H, Noordijk EM, Padberg GW, Voormolen JH, Hoekstra FH, Tans JT, Lambooij N, Metsaars JA, Wattendorff AR et al (1993) Treatment of single brain metastasis: radiotherapy alone or combined with neurosurgery? *Ann Neurol* 33(6):583–590
- Vidiri A, Carapella CM, Pace A, Mirri A, Fabis A, Carosi M, Giannarelli D, Pompili A, Jandolo B, Occhipinti E, Di Giovanni S, Crecco M (2006) Early post-operative MRI: correlation with progression-free survival and overall survival time in malignant gliomas. *J Exp Clin Cancer Res* 25(2):177–182
- Weber F, Riedel A, Köning W, Menzel J (1996) The role of adjuvant radiation and multiple resection within the surgical management of brain metastases. *Neurosurg Rev* 19(1):23–32
- Wilkinson ID, Romanowski CA, Jellinek DA, Morris J, Griffiths PD (2003) Motor functional MRI for pre-operative and intraoperative neurosurgical guidance. *Br J Radiol* 76(902):98–103
- Wu JS, Zhou LF, Tang WJ, Mao Y, Hu J, Song YY, Hong XN, Du GH (2007) Clinical evaluation and follow up outcome of diffusion tensor imaging-based functional neuronavigation: a prospective controlled study in patients with gliomas involving pyramidal tracts. *Neurosurgery* 61(5):935–948

## 12.1 Introduction

Intracranial space-occupying lesions, particularly glial tumors, may challenge the neurosurgeon who aims at preserving neuronal function as much as possible while removing as much of the lesion as possible. It has been repeatedly questioned whether radical resection of gliomas is the method of choice because of their invasive nature, but it has also been shown recently that patients can benefit from radical resection as much as possible both in primary (Stummer et al. 2006) and recurrent gliomas as well as in low-grade gliomas (Claus et al. 2006, Sanai et al. 2008). Radical resection of glial tumors, however, is hampered by the risk of damaging neuronal functions, particularly of speech and motor functions. Therefore, early on in the development of modern neurosurgery, brain tumor surgery under local anesthesia (LA) was suggested in order to reduce the risk of immediate severe and non-reversible postoperative neurological deficit (Berger et al. 1992; Black et al. 1987; Ojemann et al. 1989; Ojemann 1988). Most of the patients are initially frightened by the suggestion of undergoing brain tumor surgery under local anesthesia. However, they accept this method when the details are fully explained to them (Danks et al. 1998). Nevertheless, there are limitations, such as patients' inability to cooperate – in the case of very young and very old patients, or a tumor located and extending in

such a fashion that there is no good way to position the patient with sufficient comfort; patients with reduced cardio-pulmonary functions or seizures related to the tumor should be particularly well taken care of. Taking these precautions into account, it has been shown by many centers that it is possible to reduce the risk of a focal neurological deficit while increasing the chance to completely remove a tumor located in eloquent areas (Danks et al. 2000; Duffau 2005a, b; Duffau et al. 2003; Ebeling et al. 1995; Pinsker et al. 2007).

With the advent of Magnetic Resonance Imaging (MRI) and particularly functional MRI (fMRI), this technique is now widely accepted as being able to precisely localize brain functions (Brannen et al. 2001; Naidich et al. 2001), with a high degree of sophistication and reliability (with a 53% regional specificity (FitzGerald et al. 1997)): even different brain functions requiring complex interactions between various active brain areas. While the latter may be further explored in research projects, some indications for its use in a clinical setting have emerged over the recent years and led to its implementation into routine MRI scanner software. In routine clinical neurosurgical practice, these techniques mainly concern the definition of the dominant hemisphere, the various speech areas and motor cortex. Furthermore, relation between the most important areas can be demonstrated by fiber tracking, thus enabling the surgeon to prevent damage to the white matter tracts (Duffau 2005a, b, 2007; Nimsky et al. 2006a–c). However, there are certain limitations which may lead one to question the value of these fMRI results in relation to intraoperative application. This paper should elucidate some of the benefits and pitfalls of both techniques as experienced by the authors in a review of the literature.

---

M. H. Mehdorn (✉)

Department of Neurosurgery, University Hospital  
of Schleswig-Holstein (UKSH), Campus Kiel,  
Schittenhelmstrasse 10, 24105 Kiel, Germany  
e-mail: mehdorn@nch.uni-kiel

## 12.2 Indications for Direct Cortical Stimulation and/or Functional Magnetic Resonance Imaging (fMRI): Patient Selection

Two factors determine the indication for either direct cortical stimulation (DCS) during surgery under awake conditions or fMRI:

1. The clinical condition of the patient, particularly his presenting symptoms, and his neurological status.

If the patient's history and presenting symptoms, like temporary speech deficits or focal seizures, suggest a lesion affecting motor or speech areas, and the diagnosis of an intrinsic brain tumor in these areas is ascertained, the patient is considered for awake craniotomy using DCS. Special attention should be given to the patient's problems of understanding and his/her capability and willingness to cooperate with the surgeon and the OR team; these factors need to be analyzed preoperatively by the neurosurgical staff members and dedicated neuropsychologists.

These criteria obviously exclude the following patient groups from awake craniotomy: emergency tumor decompressions in comatose patients, small children and geriatric patients who would be unable to cooperate fully.

In all other patients with tumors in the above mentioned locations, the method of DCS was the method of choice, before fMRI was available in our institution as well as in others, to determine intraoperatively how much tumor could be removed safely without provoking too big a neurological deficit. In our experience as well in the experience of others, DCS has shown to improve surgical outcome when operating in functionally relevant areas, enhancing both the amount of tumor resection and the preserving function.

Now, since the advancement of MRI technology and introduction of fMRI in the armamentarium of preoperative evaluation this method needs to be taken into consideration and weighted against the DCS method.

2. Tumor localization and function of brain region

Following the first diagnostic imaging of the tumor which is made in order to grade it in a assumptive manner, its localization, as visualized by preoperative computed tomography (CT) scanning or more appropriately by MRI, is analyzed to determine whether functionally

relevant ("eloquent") brain structures incl. fiber tracts, are in vicinity to the tumor and could possibly be harmed during tumor removal. The initial grading should help to define the extent of surgical resection. While, resection of a WHO grade III or IV glioma should be attempted with the intent to completely preserve function at the preoperative level for the limited survival time, in grade I or II gliomas complete resection should be attempted in order to optimize survival times without adjunctive therapy. In these patients, particular workup is required in order to define the spatial relation between the tumor borders and the functionally relevant structures i.e., speech and motor cortical areas, optical regions and the fiber tracts, particularly the pyramidal tract and the bundles between the motor and sensory speech areas, and also the optical fiber tracts e.g., the Gratiolet tract.

While fMRI data acquisition can be applied to all patients who tolerate the narrow canal of MRI machines, and who understand the need to cooperate while performing the neuropsychological paradigms, the DWI measurements required for representation of fiber bundles demand that a patient lie for some additional time without moving his/her head until the data are acquired.

The fMRI data need to be processed and transferred to the neuronavigation consoles in order to be used for surgical planning.

On the basis of the above mentioned criteria the patient is advised to undergo surgery as awake craniotomy.

## 12.3 Methods

### 12.3.1 Surgery Under Local Anesthesia: Awake Craniotomy

Details of this technique have been described by our group (Pinsker et al. 2007) and others (Danks et al. 2000; Duffau 2005a, b; Duffau et al. 2003, 1999; Tonn 2007). We have implemented awake craniotomy since 1993 in our department in order to remove as much tumor as possible in or close to eloquent areas while preserving function. Prerequisite for this technique is, in our opinion, a good (neuro-) psychological preparation of the patient. The majority of our brain tumor patients undergo formal preoperative neuropsychological testing by our dedicated neuropsychologists who not only evaluate the aspects of the dominant hemisphere and, in a

very sophisticated manner, the neuropsychological deficits, but also talk to the patients concerning their individual fears related to the tumor and the upcoming surgery. In the initial phase, we also brought the patients into the operating room and positioned them onto the OR table to make them familiar with the setting; due to time restraints, this is no longer possible, but the patients are well familiarized with this particular type of surgery. Anesthesiologists also play a special role in this setting; they have to take care of the patient during surgery and are essential in keeping a balance between sedation of the patient during some parts of surgery e.g., craniotomy itself and having him/her awake for testing during tumor removal. Medications used in this regard are propofol and analgesics. Central lining is given to all our patients although this may not be the routine in other centers (Fig. 12.1).

LA is applied to the patient by the neurosurgeon using ropivacaine-HCl (Naropin®) 0.75% for the blocks around the 3-pin head-holder. Neuronavigation is used to define the optimal craniotomy site and delineation of the skin incision. Subsequently the line of the skin incision is anesthetized additionally; when a curved incision is required, particular care is paid to apply sufficient anesthesia to the underlying muscles, usually the temporal muscle. After careful aseptic preparation the surgical drapes are placed after having applied a semicircular or rectangular cage-like metal to hold the drapes with sufficient comfort for the patient to whom every single step of draping him/her is explained carefully (Fig. 12.2).



**Fig. 12.1** Brain Surgery in the awake patient. The patient is operated with standard microneurosurgical equipment while undergoing specific neurophysiologic and neuropsychological testing

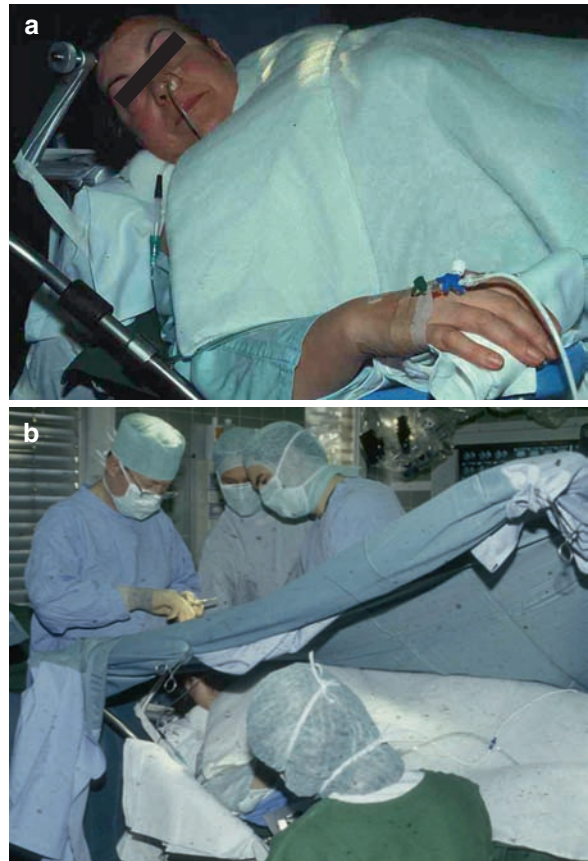


**Fig. 12.2** Positioning the awake patient in the 3-Pin Headholder using local anesthesia. (a) Close up view of the patient. (b) During surgery with the neuropsychologist calming and testing the patient

Then surgery is performed as usual, while always talking to the patient and explaining all the steps and adding LA as required; particular care is taken while the craniotomy is performed. Until this step and a little bit longer, the patient is also allowed to sleep under anesthesiological supervision and with the help of sedation and/or analgesic short lasting medication.

The dura is subsequently opened under the operating microscope and the brain inspected, and, again with the help of the neuronavigation, the brain tumor is localized.

### 12.3.2 Stimulation

Once the tumor has been outlined with inspection and neuronavigation, the functional mapping is required to define cortical brain areas which are functionally

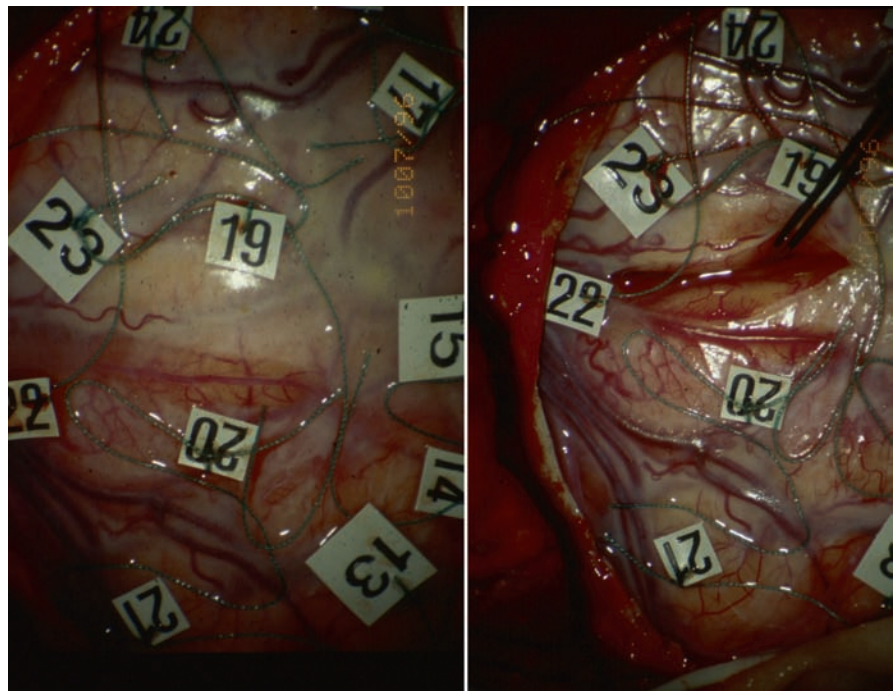
relevant. These areas can be outlined in the fashion as described by Ojemann (Ojemann et al. 1989; Ojemann 1988) and marked by cotton pledgets with numbers on it, or they can be virtually marked with neuronavigation. Results of preoperative fMRI studies defining functionally relevant areas, can be implemented during surgery, using particular computer programs, as provided commercially by BrainLAB and other companies, which help to blend them into a particular computer screen adjacent to a surgical microscope, or to implement them into light course of the microscope, thus overlaying them virtually onto the surgical field. Both methods are available, presenting the tumor either as outline onto the brain surface or the level of visual acuity or by defining the tumor as 3D volume (Fig. 12.3).

Stimulation itself is performed using the Ojemann stimulator with various settings and eliciting the patient's response to various levels of bipolar stimulation. The motor respective speech disturbances are carefully monitored by the neuropsychologist attending on the patient during the important phases of surgery, and this way, a mapping of cortical areas which are safe to remove and those whose removal may cause

neurological deficits, is ascertained. Particular attention needs to be paid to the vasculature of the cortical surface as it relates to the stimulated areas since one should always remind oneself that the cortical vessels, particularly the arteries, are nearly more important to be preserved than the cortical surface itself which they irrigate.

Once the area which can safely be removed has been defined, the interaction between the surgeon and the patient should not end. Care has to be taken depending on the correlation between the tumor borders and the white matter tracts e.g., the pyramidal tract (Nimsky et al. 2006a–c). Stimulation should therefore be continued, while the surgeon is entering the white matter, and combined with neuronavigation, in order to show the spatial correlation between these important structures (Bello et al. 2008; Duffau 2007; Duffau et al. 2002). In our experience, the voltage required to elicit some motor problems in the patient relates well with the distance to the pyramidal tract: the higher the voltage the longer the distance to the tract. This means that one has to monitor this distance continuously as the tracts may be displaced during surgical removal of the tumor, when compared to their preoperative position.

**Fig. 12.3** Cortical testing. The tumor encompasses the cortex, clearly visible by the discoloration in the *top* portion of the image. Direct cortical stimulation (DCS) results are registered using numbered cottonoids to map and documenting the elicited corresponding results. The identified safe access routes are taken for arachnoidal opening, corticotomy and resection of the tumor. The images show corresponding sites, left before, and right after arachnoid opening and during cortical testing of the sulcal cortical surface with the Ojemann bipolar probe



### 12.3.3 Intraoperative MRI

The implementation of a high-field MRI machine into a neurosurgical operating room (OR) has facilitated tumor removal further by allowing real-time imaging on a high level of imaging quality. This enables the surgeon to re-establish the true anatomical situation which changes permanently after opening of the dura due to CSF drainage, manipulation of the brain and during tumor removal (Nabavi et al. 2001; Nimsky et al. 2000). This phenomenon of brain-shift is also of high importance concerning the accuracy of fMRI data acquired preoperatively.

## 12.4 Practical Considerations

In order to optimize the situation for the patient, we have developed a protocol for patients with tumors in or near to eloquent brain areas. Formal neuropsychological testing as an initial step, as well as detailed neuro-imaging using MRI (T1 and T2, DWI and DTI and MPRage for 3D reconstruction and preparation for neuronavigation), fMRI data and DWI images are performed in order to determine the spatial relationship between tumor and functionally relevant structures, and then the situation is discussed with the patient to see whether awake craniotomy should be suggested. If the patient agrees, he undergoes surgery under LA as usual and under intraoperative high-field MRI control. This allows for re-registration of functionally relevant data and update into the neuronavigation (Nabavi et al. 2003; Nimsky et al. 2006a–c).

## 12.5 Results

In a previous paper (Pinsker et al. 2007), we have compared the results of surgery performed between 1998 and 2002 in 80 patients with gliomas located in eloquent areas, using awake craniotomy in 37 primary operations and 18 operations for recurrent gliomas, while using – on the patients’ request – general anesthesia in 27 patients. Comparing only patients with tumors located in the motor areas, patients operated

using awake craniotomy had a higher rate of complete resection as evaluated by MRI scans within the 48 h post surgery: 20 out of 26 (77%) as compared to 4 out of 12 (33%). Worsening of motor functions occurred and lasted more than 3 months in three patients (12%) following awake craniotomy, while it happened in four patients (33%) operated under general anesthesia.

Since the routine use of preoperative fMRI and fiber tracking and intraoperative high-field MRI, we have the “clinical feeling” that we may be less intense to persuade patients into awake craniotomy, but this feeling needs to be substantiated in a prospective fashion, and the results of this policy are presently evaluated with regard to long term outcome. Having the possibilities, however, to use elaborate neuropsychological evaluation, intraoperative monitoring, intraoperative MRI scanning and intraoperative application of local chemotherapy agents, the number of patients coming to us in a predetermined fashion has certainly risen, and such a study may be difficult to evaluate.

Intraoperative guidance by preoperatively acquired data with regard to position of eloquent areas may certainly be helpful (Nimsky et al. 2004; Pinsker et al. 2007), but still the surgeon has to be aware of intraoperative brain deformation, i.e., “Brain Shift”(Nabavi et al. 2001; Nimsky et al. 2000) and must therefore, still use his best surgical judgement while removing tumor tissue in or around eloquent areas. In this regard, intraoperative clinical control plays a substantial role in defining the extent of surgical resection around eloquent areas. A careful comparison of the location of eloquent areas as defined on fMRI studies and the intraoperative definition of these areas will be helpful in determining the clinical value of each of the methods described.

## 12.6 Perspectives

Further elaboration of preoperative evaluation of patients harboring those life-limiting tumors is warranted in order to further improve quality of life both during treatment and follow-up, while enhancing long-term survival. Initial surgery is essential to remove as much tumor as possible and thereby determine long-term results, while second or third surgery often must take compromises to preserve function.

## References

- Bello L, Gambini A, Castellano A, Carrabba G, Acerbi F, Fava E, Giussani C, Cadioli M, Blasi V, Casarotti A, Papagno C, Gupta AK, Gaini S, Scotti G, Falini A (2008) Motor and language DTI fiber tracking combined with intraoperative subcortical mapping for surgical removal of gliomas. *Neuroimage* 39(1):369–382
- Berger MS, Ojemann GA (1992) Intraoperative brain mapping techniques in neuro-oncology. *Stereotact Funct Neurosurg* 58(1–4):153–161
- Black PM, Ronner SF (1987) Cortical mapping for defining the limits of tumor resection. *Neurosurgery* 20(6):914–919
- Brannen JH, Badie B, Moritz CH, Quigley M, Meyerand ME, Houghton VM (2001) Reliability of functional MR imaging with word-generation tasks for mapping Broca's area. *AJNR Am J Neuroradiol* 22(9):1711–1718
- Claus EB, Black PM (2006) Survival rates and patterns of care for patients diagnosed with supratentorial low-grade gliomas: data from the SEER program, 1973–2001. *Cancer* 106(6): 1358–1363
- Danks RA, Aglio LS, Gugino LD, Black PM (2000) Craniotomy under local anesthesia and monitored conscious sedation for the resection of tumors involving eloquent cortex. *J Neurooncol* 49(2):131–139
- Danks RA, Rogers M, Aglio LS, Gugino LD, Black PM (1998) Patient tolerance of craniotomy performed with the patient under local anesthesia and monitored conscious sedation. *Neurosurgery* 42(1):28–34; discussion 34–26
- Duffau H (2005a) Intraoperative cortico-subcortical stimulations in surgery of low-grade gliomas. *Expert Rev Neurother* 5(4):473–485
- Duffau H (2005b) Lessons from brain mapping in surgery for low-grade glioma: insights into associations between tumour and brain plasticity. *Lancet Neurol* 4(8):476–486
- Duffau H (2007) Contribution of cortical and subcortical electrostimulation in brain glioma surgery: methodological and functional considerations. *Neurophysiol Clin* 37(6):373–382
- Duffau H, Capelle L, Denvil D, Sichez N, Gatignol P, Taillandier L, Lopes M, Mitchell MC, Roche S, Muller JC, Bitar A, Sichez JP, van Effenterre R (2003) Usefulness of intraoperative electrical subcortical mapping during surgery for low-grade gliomas located within eloquent brain regions: functional results in a consecutive series of 103 patients. *J Neurosurg* 98(4):764–778
- Duffau H, Capelle L, Sichez N, Denvil D, Lopes M, Sichez JP, Bitar A, Fohanno D (2002) Intraoperative mapping of the subcortical language pathways using direct stimulations. An anatomo-functional study. *Brain* 125(Pt 1):199–214
- Duffau H, Capelle L, Sichez J, Faillot T, Abdennour L, Law Koune JD, Dadoun S, Bitar A, Arthuis F, Van Effenterre R, Fohanno D (1999) Intra-operative direct electrical stimulations of the central nervous system: the Salpêtrière experience with 60 patients. *Acta Neurochir (Wien)* 141(11):1157–1167
- Ebeling U, Fischer M, Kothbauer K (1995) Surgery of astrocytomas in the motor and premotor cortex under local anesthesia: report of 11 cases. *Minim Invasive Neurosurg* 38(2):51–59
- FitzGerald DB, Cosgrove GR, Ronner S, Jiang H, Buchbinder BR, Belliveau JW, Rosen BR, Benson RR (1997) Location of language in the cortex: a comparison between functional MR imaging and electrocortical stimulation. *AJNR Am J Neuroradiol* 18(8):1529–1539
- Nabavi A, Black PM, Gering DT, Westin CF, Mehta V, Pergolizzi RS Jr, Ferrant M, Warfield SK, Hata N, Schwartz RB, Wells WM III, Kikinis R, Jolesz FA (2001) Serial intraoperative magnetic resonance imaging of brain shift. *Neurosurgery* 48(4):787–797; discussion 797–788
- Nabavi A, Gering DT, Kacher DF, Talos IF, Wells WM, Kikinis R, Black PM, Jolesz FA (2003) Surgical navigation in the open MRI. *Acta Neurochir Suppl* 85 121–125
- Naidich TP, Hof PR, Yousry TA, Yousry I (2001) The motor cortex: anatomic substrates of function. *Neuroimaging Clin N Am* 11(2):171–193, vii–viii
- Nimsky C, Ganslandt O, Buchfelder M, Fahlbusch R (2006a) Intraoperative visualization for resection of gliomas: the role of functional neuronavigation and intraoperative 1.5 T MRI. *Neurol Res* 28(5):482–487
- Nimsky C, Ganslandt O, Cerny S, Hastreiter P, Greiner G, Fahlbusch R (2000) Quantification of, visualization of, and compensation for brain shift using intraoperative magnetic resonance imaging. *Neurosurgery* 47(5):1070–1079; discussion 1079–1080
- Nimsky C, Ganslandt O, Fahlbusch R (2004) Functional neuro-navigation and intraoperative MRI. *Adv Tech Stand Neurosurg* 29 229–263
- Nimsky C, Ganslandt O, Fahlbusch R (2006b) Implementation of fiber tract navigation. *Neurosurgery* 58(4 Suppl 2):ONS-292–303; discussion ONS-303–294
- Nimsky C, Ganslandt O, Merhof D, Sorensen AG, Fahlbusch R (2006c) Intraoperative visualization of the pyramidal tract by diffusion-tensor-imaging-based fiber tracking. *Neuroimage* 30(4):1219–1229
- Ojemann GA (1988) Effect of cortical and subcortical stimulation on human language and verbal memory. *Res Publ Assoc Res Nerv Ment Dis* 66 101–115
- Ojemann G, Ojemann J, Lettich E, Berger M (1989) Cortical language localization in left, dominant hemisphere. An electrical stimulation mapping investigation in 117 patients. *J Neurosurg* 71(3):316–326
- Pinsker MO, Nabavi A, Mehdorn HM (2007) Neuronavigation and resection of lesions located in eloquent brain areas under local anesthesia and neuropsychological-neurophysiological monitoring. *Minim Invasive Neurosurg* 50(5):281–284
- Sanai N, Berger MS (2008) Glioma extent of resection and its impact on patient outcome. *Neurosurgery* 62(4):753–764; discussion 264–756
- Stummer W, Pichlmeier U, Meinel T, Wiestler OD, Zanella F, Reulen HJ (2006) Fluorescence-guided surgery with 5-aminolevulinic acid for resection of malignant glioma: a randomised controlled multicentre phase III trial. *Lancet Oncol* 7(5):392–401
- Tonn JC (2007) Awake craniotomy for monitoring of language function: benefits and limits. *Acta Neurochir (Wien)* 149(12):1197–1198

## 13.1 Introduction

Magnetic resonance imaging (MRI) has had an extraordinary impact on the diagnosis and management of epilepsy. Contemporary high-field strength MRI enables detailed in vivo imaging of lesions that underlie symptomatic epilepsies, for example, hippocampal sclerosis or malformations of cortical development. This routine use of high-field MRI in clinical epilepsy has also contributed to the increasing interest in the potential use of functional MRI (fMRI) to image the abnormal brain function that underlies epilepsy. Here, we give a brief overview of epilepsy, the current state of fMRI for the difficult problem of imaging epileptic seizures, and introduce the topic of neurovascular coupling in the epileptic brain and the constraints this imposes on fMRI interpretation.

## 13.2 Background

The term *epilepsy* derives from the Greek “to lay hold of” or “to be seized,” and is defined by the tendency to recurrent, spontaneous clinical seizures. Epileptic seizures vary in their forms, from seemingly minor seizures such as brief staring episodes, eye blinks, or myoclonic jerks, to generalized convulsions. All seizure types can be potentially debilitating regardless of their form, depending on the frequency of the events, and the age of onset, among other factors.

---

S. Glynn (✉)  
The Mahoney Institute of Neurological Sciences,  
University of Pennsylvania, 3 W Gates Building, 3400 Spruce  
Street, Philadelphia, PA 19104, USA  
e-mail: simongly@med.umich.edu

Epilepsy affects 50 million people worldwide and over 2.7 million people in the United States, more than multiple sclerosis, Parkinson’s disease, and motor neuron disease combined (Sander 2003; Hauser et al. 1990; Kurtzke 1982). Half of the persons with epilepsy are children, although recently there has been a sharp increase in epilepsy in persons over 65 years. In many people, particularly children, seizures will remit, but for the majority of persons epilepsy is a lifelong diagnosis (Hauser et al. 1991).

Importantly, the majority of persons with epilepsy have normal intellect. As a group, persons with epilepsy have impaired cognitive performance compared to age and education-matched normal controls. This cognitive impairment reflects (1) the etiology of their epilepsy, (2) the direct effects of the seizures, and (3) and the cognitive effects of the antiepileptic medicines used to control the seizures.

Only in a minority of newly diagnosed persons with epilepsy can a specific etiology be determined.

## 13.3 fMRI in Epilepsy

fMRI has the potential to contribute both to epilepsy research and clinical practice, although there is no currently approved or universally accepted clinical application for fMRI in epilepsy (Neuroimaging Subcommittee of the ILAE 2000). The best established use of fMRI in epilepsy practice is in the presurgical evaluation of patients being considered for temporal lobectomy. Temporal lobectomy is an effective therapy for medically refractory temporal lobe epilepsy (Wiebe et al. 2001), but can be complicated by cognitive deficits. In this application, fMRI is used

to lateralize language and, to a lesser extent, memory function (for reviews, see Swanson et al. 2007; Hwang et al. 2006, respectively) in an effort to predict postsurgical deficits following temporal lobectomy. It provides a safer and more repeatable alternative or complementary information compared to the more invasive intracarotid amobarbital test, which has been used for the same purpose for several decades. This application of fMRI is covered in a separate chapter in this volume by Binder (chapter 9).

A second application of fMRI in epilepsy, with both clinical and basic science implications, is its use for localizing seizure onset in the brain and for characterizing the physiology of seizures. This is an expanding area of investigation. A PUBMED query performed in 2008 using the terms (“fMRI” or “functional MRI”) and (“epilepsy” or “seizure”) returned nearly 500 articles, the first of these starting in 1994. Of these, nearly 100 papers were published last year. About 150 papers concern the technical development of concurrent electroencephalography (EEG) and fMRI, or the use of this concurrent EEG–fMRI technique to localize interictal (that is, recorded in the interval between seizures) epileptiform discharges. Briefly, simultaneous recordings of EEG during fMRI imaging enable experiments to be defined by the presence of an interictal epileptiform discharge on EEG. One can hypothesize that the cortical origin of these interictal discharges is concordant with changes in the BOLD signal modeled using these epileptiform discharges on EEG. In general, these studies have thus far failed to conclusively localize the cortical origin of interictal epileptiform discharges, but have demonstrated that these discharges are associated with remarkably extensive changes in distributed networks well beyond the presumed origin of the epileptic discharge. These papers have been the topic of several recent reviews (see, for example, Gotman 2008; or Laufs and Duncan 2007), and will not be reviewed in detail in this chapter. The other papers are on a variety of topics, including experimental design and analysis methods, and language or memory lateralization and dysfunction in patients with temporal lobe epilepsy.

In contrast, only very few papers have been published on the use of fMRI to image epileptic seizures. The obvious reason for this is that seizures are spontaneous, happening without warning (although there are important exceptions). For this reason, fMRI recordings of clinical seizures are either merely fortuitous; or are recorded in persons with very frequent seizures, or they

are seizures that may be deliberately induced in the subject (for example, hyperventilation-induced absence seizures).

For those fMRI recordings that *do* fortunately image a clinical seizure, there are several methodological issues that complicate the fMRI imaging. First, usually only one clinical seizure (on rare occasions, several) will be recorded, which in turn has implications for the modeling of the hemodynamic response. Second, imaging clinical seizures is complicated by uncontrolled movement. For obvious reasons of safety, convulsive seizures or seizures characterized by violent movements cannot be imaged in an MRI scanner without special accommodations. But even very small movements of the head seen in myoclonic jerks, absence seizures, or simple focal seizures may be problematic for the interpretation of voxel-based fMRI analyses, as this movement-related noise will be correlated to the experimental effect of interest (Lemieux et al. 2007). This is especially of concern in fMRI experiments to record seizures because acquisitions tend to be long, often as long as 2 h, and significant movement that complicates voxel-wise analysis is a virtual certainty over these intervals. For these reasons, technical advances in image registration, field-corrected image reconstruction, and techniques to detect activations that are robust to large-amplitude movements during scanning, are especially relevant to fMRI imaging in epileptic seizures (see, for example, Yeo et al. 2008).

In the following sections, we review the papers on fMRI imaging of epileptic seizures. We also describe briefly the different types of clinical epileptic phenomena and their suitability for fMRI imaging, as well as differences in models of neuronal physiology that inform the interpretation of these fMRI data.

### 13.4 Classification of Epileptic Seizures

Epileptic seizures are primarily divided into focal and generalized seizures. Focal seizures are seizures for which clinical features or EEG recordings demonstrate focal onset in one cerebral hemisphere. Conversely, generalized seizures are defined by the absence of clinical or EEG data that would indicate focal onset. Instead, generalized seizures appear clinically and on EEG to involve both cerebral hemispheres very early and rapidly at seizure onset.

### 13.5 Focal Epilepsies and the Concept of An “Epileptogenic Focus”

The concept of an “epileptogenic focus” is widely accepted in focal seizures, although recently a competing network or systems-oriented approach has been proposed (Spencer 2002). The details of exactly how this epileptogenic focus creates a seizure are complex and controversial (for reviews see McCormick et al. 2001; Avanzini 2003), but in outline form may be somewhat as follows: In normal brain, bursting pyramidal neurons in the neocortex and hippocampus form a recurrent excitatory network with nearby excitatory neurons; this network also activates GABAergic inhibitory interneurons, as well as other inhibitory mechanisms, that modulate this excitatory network.

In epileptic brain, failure of these inhibitory dynamics leads to increased excitability of these networks. As a consequence, spontaneously bursting pyramidal neurons in epileptic cortex may synchronously depolarize large populations of neurons. This phenomenon, termed the *paroxysmal depolarizing shift*, is seen on EEG as an epileptiform spike or sharp wave.

This abnormal network behavior is contained by GABAergic interneurons surrounding this spontaneously bursting focus (termed “surround inhibition”). Infrequently, this surround inhibition fails. Connected populations of excitatory neurons outside the epileptogenic focus that previously demonstrated normal firing patterns, then start phase locking to the epileptic bursting discharges seen on EEG. This, in turn, starts a cascade of neuronal and extracellular events, the result of which is a clinical seizure.

### 13.6 Neurovascular Coupling in Focal Epilepsy

Understanding this in outline is important, because this model has consequences for fMRI imaging of focal seizures. First, these neuronal dynamics, in contrast to cognitive experiments, probably result in a dramatic (or even supernormal) increase in the cerebral metabolic rate of oxygen (CMRO<sub>2</sub>) (Folbergrova et al. 1981). In response to this increased CMRO<sub>2</sub>, we would expect cerebral blood flow (CBF) and cerebral blood volume, capillary and venous blood oxygen, and BOLD contrast

to increase dramatically. Indeed, exactly these dynamics were directly observed and described by Penfield in induced epileptic seizures during epilepsy surgery in the 1930s: “... the cerebral arteries pulsate violently.... Their color becomes a bright red and arteries which were not seen to pulsate before the seizure may now begin to do so visibly. In fact this recovery may go so far that the veins themselves take on an arterial hue.” (Penfield 1933). Following this reasoning, one can hypothesize that imaging using these metabolic and hemodynamic signals may define the epileptogenic focus in these patients.

### 13.7 fMRI Imaging of Focal Seizures

These dynamics have been successfully imaged by several groups using BOLD fMRI in patients with frequent focal seizures. The inferences in these few papers are tentative, and probably incorrect in several respects. This is confounded by the fact that only a few experiments have used concurrent EEG–fMRI (Salek-Haddadi 2002; Kobayashi 2006; Di Bonaventura 2006); and fewer still have been performed in patients without lesions on anatomical MRI (Salek-Haddadi 2002). Nonetheless, these papers do describe several findings that are potentially very interesting:

First, the amplitude of the BOLD signal increase in focal seizures is large compared to cognitive experiments. In different papers, this varies from 2% for seizures without clinical accompaniment, to increases as large as 40% described in a patient with frequent focal motor seizures (Jackson et al. 1994), compared to the 0.5–1% increase in BOLD usually seen in cognitive fMRI experiments.

Second, this large increase in BOLD signal means that seizures may be identified even in the absence of a clinical or EEG correlate. This is demonstrated in several papers simply by visually inspecting the BOLD time series for stereotyped signal increases, without the use of spatial statistics or linear regression models (Jackson et al. 1994; Detre et al. 1995; Krings 2000). This, in turn, enables the mapping of the spatial and temporal sequence of a seizure that *precedes clinical onset*. This is important because clinical onset of a seizure may reflect propagation from the epileptogenic focus to other cortical areas. This is nicely demonstrated

in the paper by Krings et al. (2000) for a single seizure in a patient with a right central tumor and focal motor seizures of the left foot. Visual analysis of the BOLD time series demonstrated an increase in the BOLD signal 65 s preceding clinical onset in the epileptogenic focus adjacent to the tumor but distant from the somatotopic representation for the foot, then followed by a BOLD signal increase in the left foot area coincident with clinical seizure onset.

Third, EEG–fMRI enables fMRI imaging of seizures that do not have a clinical correlate (termed electrographic seizures). This technical advance is important because increases in the BOLD signal may reflect any number of physiological or technical influences, quite apart from seizure activity. Conversely, the interpretation of these BOLD signal increases is straightforward if the BOLD signal increases correspond in time and space to electrographic seizure discharges recorded on EEG. Reflecting this advance, the majority of recent papers in fMRI in epilepsy have concentrated on using EEG–fMRI to determine the BOLD signatures of various interictal epileptiform discharges on EEG. In contrast, only two papers, as yet, describe concurrent EEG–fMRI to image focal seizures.

The first of these papers by Salek-Haddadi et al. (2002) recorded continuous BOLD fMRI in a patient with frequent simple focal seizures of behavioral arrest only (this paper is also unique in describing the anatomical MRI as normal). Concurrent EEG recorded a left temporal electrographic seizure of 41 s duration; no clinical change was observed, and the patient did not report experiencing a seizure. This electrographic seizure was then modeled as a single neural event using a Fourier basis set to avoid assumptions about the shape of the HRF, and an F contrast was used to test for variance due to the effects of interest (the seizure). The time course for this cluster of time-locked variance on the F map was then extracted, and entered into a second model as a single covariate of interest. This demonstrated a BOLD signal increase of 2.5% over baseline at 6 s following EEG onset in the left anterior temporal lobe (maximum beta value, concordant with the EEG localization) and left inferior parietal cortex (statistical maximum).

A second paper by Kobayashi et al. (2006) used EEG–fMRI to record multiple electrographic seizures in a patient with right temporo-parietal gray matter nodular heterotopias and frequent clinical seizures consisting of a rising epigastric aura, followed by an out of

breath sensation and brief loss of awareness. Twenty-five brief focal electrographic seizures lasting 2–6 s were recorded; no clinical seizures were observed, and the patient did not report any seizures. Source modeling for these discharges estimated the maximum negativity in the inferior right temporal region. Maps of the t statistic were created using four different hemodynamic response functions (HRFs) with peaks at 3, 5, 7, and 9 s. These t-statistic maps demonstrated widespread and intense activation, including the abnormal right temporo-parietal cortex some distance from the inferior temporal localization on EEG. This was interpreted as indicating that the seizures started in the dysplastic cortex but did not generate a visible EEG change.

This last observation, that BOLD signal increases may also identify focal seizures *without EEG correlate*, also imposes a very strong constraint on the use of the EEG to model seizures. As an example of this from our laboratory, BOLD fMRI was successfully used in a patient with frequent focal motor seizures of his right face, but without EEG correlate. During the fMRI acquisition, no definite clinical seizures were recorded. Nonetheless, visual inspection of these BOLD signal changes demonstrated, clear, episodic BOLD signal increases of 3–4% in the posterior left frontal lobe that were consistent with the localization of focal seizures subsequently recorded on intracranial EEG (Detre et al. 1995). This is important because EEG is frequently normal in certain focal seizures, as well as in simple focal seizures arising from the medial, basal, or interhemispheric neocortex – that is, precisely in the seizure types amenable to fMRI imaging.

## 13.8 Benign Childhood Focal Epilepsies

Benign childhood focal epilepsies are of special interest in understanding focal seizures. These include the commonest epileptic seizures in children; interestingly, none of these syndromes occur in adults, probably due to age-related processes in the developing brain. Most children with these syndromes have only one or several seizures, and remission is expected in all children.

Reflecting this, no papers describe fMRI imaging of clinical seizures in children. These epilepsy syndromes are nonetheless well suited for EEG–fMRI experiments

due to the very high frequency of interictal discharges, and for this reason, several papers of interest are briefly reviewed here.

In the first of these, Archer et al. (2003a) performed spike-triggered EEG–fMRI in a child with benign epilepsy with centrotemporal spikes (BECTS; the most frequent of the benign childhood focal epilepsies). This demonstrated an increase in BOLD signal in sensorimotor cortex corresponding to the centrotemporal epileptiform discharges on EEG, and consistent with the prominent facial twitching and salivation described in these seizures. In this paper and in a separate paper, decreases as well as increases in BOLD signal were also described in the prefrontal cortex and in the anterior cingulate, interpreted as consistent with clinical observations of deficits in attention and concentration in these children (Archer et al. 2003a; Archer et al. 2003b; Lengler et al. 2007). In a separate paper, these observations were extended using EEG source modeling to distinguish focal abnormal BOLD signal in the face area in BECTS, from spatially more extensive propagated activity seen as BOLD activations (Boor et al. 2007).

In contrast to BECTS, other benign childhood focal epilepsies present with diverse clinical symptoms, despite a common EEG localization. In the childhood occipital epilepsies, for example, the EEG localizes the epileptic activity to the posterior head regions, but very often the abnormalities also involve the parietal and temporal areas. In several of these children, EEG/fMRI recordings have been helpful by demonstrating BOLD signal increases and, presumably, neuronal dysfunction in the posterior parietal lobes, distant from the occipital spike focus found using EEG source analysis and, importantly, more consistent with the clinical seizures in these children (Leal et al. 2006).

Finally, these papers raise important issues for modelling fMRI experiments of epilepsy in children. Specifically, Jacobs et al. (2008) analyzed 64 EEG–fMRI event types in 37 children from 3 months to 18-years. HRFs were calculated for each BOLD event type using a Fourier basis set. This demonstrated significantly longer peak times of the HRF in the youngest children (0–2 years), suggesting a different coupling between neuronal activity and metabolism or blood flow. Less easy to understand is the observation that even as the *t*-value increased with frequent spikes, the amplitude of the HRF decreased with increasing spike frequency. These observations would indicate that different HRF models may be required for fMRI in

children with high spiking rates, a quite common situation (Jacobs 2008).

### 13.9 Generalized Epilepsies

In contrast to focal seizures reviewed above, generalized seizures are defined by the absence of clinical or EEG data that would indicate focal onset. Instead, generalized seizures appear clinically and on EEG to involve both cerebral hemispheres very early and rapidly at seizure onset. Clinically, these are described as spells of impaired consciousness (“petit mal” or “absence”), myoclonic jerks, or tonic-clonic (convulsive) seizures.

Of these seizures, absence seizures are the prototype for generalized seizures. Absence seizures are brief spells of staring or unresponsiveness, as a rule less than 30 s in duration. Clinical seizures are frequent, usually (at least) every day, and are easily provoked by hyperventilation in nearly all untreated patients. On EEG, the essential feature is generalized 3–4 Hz spike-wave discharges, involving the entire brain.

### 13.10 The Concept of Hypersynchrony in Primary Generalized Seizures

The essential feature of generalized seizures is the sudden, spontaneous, and transient abnormal hypersynchronization of neuronal activity seen on EEG over both hemispheres. Two theoretical lines of reasoning have been proposed (for reviews see Meeren et al. 2005; Blumenfeld 2005). The first of these is the concept of a “centrencephalic” system located in the brain stem and diencephalon that imposes the 3–4 Hz spike-wave EEG pattern on the cortex via thalamo-cortical projections (Penfield 1954; Buzsaki 1991).

The second line of reasoning proposes that the 3–4 Hz spike-wave EEG pattern is a consequence of diffusely increased cortical excitability. According to this “cortico-reticular theory,” cortical neurons respond to normal thalamo-cortical input by generating spike-wave discharges via cortico-cortical excitation, in the context of impaired GABAergic inhibition (Gloor 1968). Intriguingly, two recent papers suggest – in an animal model of absence epilepsy – that this phenomenon may not require diffusely increased cortical excitability, but may be initiated by a cortical epileptogenic focus, that

then activates the thalamo-cortical network, amplifying and sustaining the discharge (Meeren et al. 2005; Polack et al. 2007).

### 13.11 Neurovascular Coupling in Generalized Seizures

What are the consequences of this concept of hypersynchrony for fMRI imaging of generalized seizures? First, the temporal resolution of fMRI (or any imaging that uses a hemodynamic signal) is limited by the delayed hemodynamic response to neural activity. This is important, as fMRI is unlikely to be helpful in imaging the fast cortico-cortical and cortico-thalamic dynamics described in these models.

Second, the hemodynamic changes described in focal seizures reflect increased neuronal activity. Conversely, in generalized seizures the characteristic feature – at least conceptually – is the transient, abnormal synchronization of neuronal activity, and not an increase (or decrease) in neuronal activity. For this reason, the expected hemodynamic changes in fMRI experiments of generalized seizures are less obvious than in focal seizures. Indeed, decreases as well as increases in BOLD signal, as well as no BOLD signal change, have all been described in fMRI experiments of generalized seizures, reflecting this different underlying physiology.

### 13.12 fMRI Imaging of Generalized Seizures

Spike-wave discharges modeled in EEG–fMRI experiments are often less than 3s, and usually do not have any obvious clinical correlate; although discharges as long as 30s are described (Moeller et al. 2008). These EEG–fMRI experiments describe a remarkably stereotyped fMRI correlate for generalized spike-wave discharges. This consists of a thalamic increase in the BOLD signal, as well as decreases in the frontal and parietal cortex, as well as posterior cingulate, that is apparently irrespective of the duration and morphology of the spike-wave discharge (Aghakhani et al. 2004; Gotman et al. 2005; Hamandi et al. 2006; Laufs et al. 2006; Moeller et al. 2008). For this reason, these data may be valid as well, for at least some types of clinical generalized seizures.

In contrast to focal seizures described earlier, increased BOLD signal is consistently seen only in the thalamus during generalized spike-wave discharges in humans (Moeller et al. 2008; Salek-Haddadi 2003; Laufs et al. 2006) and in animal models of absence seizures (Blumenfeld 2005; Tenney et al. 2004). These data would be consistent with the concept introduced above, that generalized spike-wave discharges activate a thalamo-cortical network. Conversely, no pages, to date, demonstrate a clear focal increase in cortical BOLD signal that is interpreted as an epileptogenic cortical focus triggering the spike-wave discharges – although group analyses may not be useful if this focus varies from individual to individual.

Instead, at the cortical level, the compelling finding has been a “negative BOLD response” or “deactivation” or decrease in the BOLD signal in the frontal, parietal, and posterior cingulate cortex (although these deactivations are variable and activations are also described). This negative BOLD signal closely matches the areas of cortex hypothesized to be involved in so-called “default mode” of brain activity (Greicius et al. 2003; Mazoyer et al. 2001; Raichle et al. 2001; Raichle 2003). If correct, then the “deactivation” or interruption of this network during generalized spike-and-wave may explain the symptom of absence as an interruption of an organized, baseline default mode of brain activity, and not the direct effect of the EEG discharge. This represents an important conceptual advance in our understanding of absence seizures.

A competing interpretation for these surprising widespread deactivations, is that the underlying physiology of neural activity and blood flow is not normal (that is, an increase in neural activity is not coupled to an increase in blood flow, hence the BOLD signal decreases). fMRI experiments to examine this question in selected regions of interest have, in fact, demonstrated normal coupling between CBF and BOLD responses, and CMRO<sub>2</sub> (Hoge et al. 1999; Stefanovic et al. 2005).

More recently, fMRI experiments have assessed this coupling between neural activity and blood flow over the entire brain using simultaneous BOLD and arterial spin labeling (ASL) perfusion contrast. Correlations were calculated for the BOLD and CBF signal in terms of percentage signal change on a voxel-by-voxel basis. This demonstrated that BOLD and CBF were positively correlated during normal EEG activity, and also during generalized spike-wave, although the value of this correlation varied over the brain, suggesting that

some areas may demonstrate a different hemodynamic response. These perfusion data would indicate that neurovascular coupling is intact, and that the negative BOLD signal is due to decreases in CBF. These perfusion data are in broad agreement with deactivations observed in normal subjects (Garraux et al. 2005).

Interestingly, widespread deactivations are also seen in focal seizures (as well as the expected BOLD increases). Currently, there is no agreed interpretation for these BOLD signal decreases. In the opposite hemisphere, or at a distance from the BOLD increase (Salek-Haddadi 2002; Federico et al. 2005; Krings 2000). Conceptually, deactivations in focal seizures may reflect GABAergic inhibition, but the relationship of the BOLD signal to inhibition is complex (Logothetis et al. 2001; Arthurs and Boniface 2002; Laurienti 2004). Nor do these deactivations in focal seizures appear to reflect deactivation of default-mode networks as proposed above for generalized seizures. (Kobayashi 2006).

### 13.13 Continuous Seizures

*Status epilepticus* refers to a “continuous seizure,” or recurrent seizures for more than 30 min – in contrast to the vast majority of epileptic seizures, that terminate spontaneously in several minutes. In these instances, recording the seizure, otherwise a serendipitous affair, becomes trivial. Imaging status epilepticus using fMRI is nonetheless at odds with the consensus that status epilepticus generally, and convulsive status epilepticus in particular, is a medical emergency. For this reason, control over clinical and electrographic seizures is a clinical imperative, and, with a few exceptions, precludes fMRI imaging. The two potential exceptions to this are (1) generalized absence status epilepticus, and (2) focal motor status epilepticus (termed *epilepsy partialis continua*).

#### 13.13.1 Absence Status Epilepticus

Absence status epilepticus is probably the commonest of all continuous seizures, and the most likely to be imaged using functional neuroimaging. Typical absence status presents as an impairment of consciousness that may last for hours, and occasionally for days before the

seizure is recognized, although most patients recognize what is happening. Once recognized, intravenous benzodiazepines usually stop absence status epilepticus abruptly. No papers to date describe the fMRI imaging of absence status epilepticus in humans. In a marmoset model of absence status, EEG–fMRI at 4.7 T of spike-wave discharges for more than 60-min duration, demonstrated BOLD increases in the thalamus and sensorimotor cortex (Tenney et al. 2004), resembling the fMRI correlates reviewed earlier for spike-wave discharges in humans. Interestingly, despite the higher field strength and robust clinical phenomena in this model, no significant negative BOLD changes were seen.

#### 13.13.2 Epilepsy *Partialis Continua*

Epilepsy *partialis continua* (EPC) is a focal, nonconvulsive form of status epilepticus, presenting as irregular myoclonic twitching or jerking of some muscle group, often involving the hand or face, for hours or days (and in some cases, even years). Implicit in this description is the observation that EPC is frequently resistant to antiepileptic medicines. Conversely, this presents unique opportunities to arrange for fMRI imaging. Lazeyras et al. (2000), for example, used multiple advanced MRI techniques including EEG–fMRI, in a patient with normal anatomical MR imaging and EPC. This demonstrated an area of increased BOLD signal that was concordant with a new hyperintensity in the occipital region on FLAIR imaging, and elevated lactate, decreased *N*-acetylaspartate (NAA), and elevated choline (Cho) on [(1)H] MR spectroscopy. This NAA level remained reduced even following seizure control, demonstrating irreversible focal neuronal injury from EPC despite the disappearance of the FLAIR signal abnormality.

Separately, two papers have used fMRI to study recurrent events previously diagnosed as movement disorders in two patients. In both instances, fMRI findings were interpreted as consistent with EPC. In the first of these, EEG–fMRI was performed in a patient with isolated hemifacial spasm. This demonstrated increased BOLD signal in the contralateral cortex responsible for facial movements, with widespread BOLD signal deactivations suggestive of epileptic network involvement and not facial nerve hyperexcitability (Espay et al. 2008).

In the second paper, [(18)F] fluorodeoxyglucose positron emission spectroscopy (FDG-PET) and fMRI were performed before and after benzodiazepine injection, in a patient with a right malformation of cortical development and unusual dystonic movements of his left hand (Zyss et al. 2007). Before benzodiazepine injection, no activation was seen on EEG–fMRI for the contrast of motor performance using the left (dystonic) hand vs. rest. Conversely, physiological activation was seen adjacent to the cortical malformation for this identical contrast after a benzodiazepine injection effectively diminished the abnormal movement, consistent with modulation of the baseline. Physiological activation of the left primary motor cortex was not influenced by the benzodiazepine injection. Finally, [18F] FDG-PET performed at rest demonstrated hypermetabolism located in the right paracentral area that was reduced after receiving benzodiazepine. These functional data were interpreted as favoring the diagnosis of EPC.

### 13.14 Reflex Seizures

In unusual cases of epilepsy, seizures may be provoked by recognizable stimuli. This may be a simple external stimulus such as flashing lights, startle, or touch; or a more elaborate stimulus, for example, reading, performing calculations, eating, or playing Rubik’s cube (an example of praxis-induced seizures; Senanayake 1987). These reflex seizures have the obvious advantage for fMRI that subclinical (seen on EEG only) or minor clinical events can be reproduced on demand during image acquisition. The several elegant fMRI experiments in persons with reflex epilepsies demonstrate that fMRI may be useful to localize epileptiform activity in these conditions, as well as advancing our understanding of the mechanisms of seizure onset. Several examples are reviewed here.

#### 13.14.1 Photosensitive Epilepsy

In this epilepsy syndrome, persons with generalized epilepsy demonstrate a paroxysmal response on EEG in response to flash stimulation. In the only fMRI

experiment to date to study this response, EEG–fMRI and [(1)H] MRS were performed in 16 persons with generalized epilepsy, including 9 persons with photosensitive epilepsy, and 12 normal subjects (Hill et al. 1999). Prominent visual cortex activation was seen in all normals and persons with epilepsy during flash stimulation. Photoparoxysmal spike-wave activity on EEG was evoked in only 3/9 epileptics; no BOLD correlate was seen for this photoparoxysmal response. Nonetheless, irrespective of the presence of a spike-wave response to the photic stimulation, photosensitive persons demonstrated a larger area of visual cortex activation with photic stimulation. Simultaneous with this activation, prominent BOLD signal attenuation was seen in the peri-rolandic cortex; as well as a marked, widespread undershoot in the BOLD signal following the end of photic stimulation. MRS performed without photic stimulation demonstrated a slight but significant increase in lactate levels in the visual cortex in photosensitive persons, compared to generalized epilepsy or controls. These intriguing findings would support the hypothesis of increased cortical hyperexcitability introduced earlier, at least for the subset of persons with generalized epilepsy and photosensitivity.

#### 13.14.2 Reading Epilepsy

Reading epilepsy is a reflex seizure disorder in which subjects complain of myoclonic movements of the mouth and throat when they read, especially aloud. Archer et al. (2003b) identified two individuals with reading epilepsy who agreed to EEG–fMRI imaging of their clinical seizures. The subjects were instructed to read silently for 30 s; this was then compared to visual fixation. In both subjects, reading recruited normal visual and language areas. In one subject, spike-related increases in the BOLD signal (17 spikes) were recorded in the left precentral gyrus, that overlapped with the activation pattern seen in reading.

Based on these data, the authors proposed that the mechanism for reading-induced seizures may start as a focal seizure in the left dorsolateral prefrontal cortex that is recruited in reading. Interestingly, reconstruction of the left central sulcal patterns in both subjects demonstrated an abnormal-appearing sulcus concordant with this BOLD signal.

### 13.14.3 Writing Epilepsy

Abreu et al. (2005) described this condition in a 33-year-old right-handed person in whom seizures started as dystonic posturing and then myoclonic jerks of the right hand one minute after starting to write, consistent with clinical localization of the seizure onset in the left hemisphere. Paradoxically, EEG during these seizures demonstrated generalized spike-wave discharges that were maximal over the right (not left) centro-parietal head regions. A SPECT injection performed during a seizure also was discordant, demonstrating increased cerebral perfusion over right fronto-parietal cortex.

In this patient, fMRI (performed without EEG) using a writing paradigm demonstrated extensive, intense, abnormal left frontal (supplementary motor area) activation induced by writing that then suddenly terminated with the onset of myoclonic jerking. These findings were interpreted as consistent with the clinical localization to the left hemisphere, as opposed to EEG and SPECT in this patient (Abreu 2005). More intriguingly, the spatial and temporal sequence of this BOLD signal preceding clinical onset of the seizure would be consistent with the hypothesis introduced earlier, that generalized discharges on EEG (as in this patient) may not require diffusely increased cortical excitability, but may alternatively be initiated by a cortical epileptogenic focus – in this instance, in the neuronal networks in the left frontal lobe that subserve writing.

### 13.14.4 Musicogenic Epilepsy

Musicogenic epilepsy is characterized by focal seizures precipitated by certain types of music, or sometimes music played by certain combinations of instruments. However, thinking about, remembering, or playing music may also precipitate a clinical seizure. The stimulus may also be exquisitely specific. Curiously, EEG recordings of seizures in musicogenic epilepsy has described seizure onset in either hemisphere, even though music function is considered to be lateralized to the right hemisphere (at least in non-musicians).

Morocz et al. (2003) performed fMRI (but not EEG) on one patient with musicogenic epilepsy triggered by the song “I Believe In You And Me,” by Whitney Houston. EEG recordings and ictal SPECT performed previously in this patient had localized seizure onset in

the left anterior temporal lobe. Music was played in a block-design, for 39 s per block, for 10 repetitions. A similar but different song, “Somebody Bigger Than You Or I,” from the same album was used as the control condition. Repeated exposure to the seizure-precipitating music resulted in two distinct patterns: The contrast of epileptic music to control music demonstrated BOLD increases in the frontal lobes and especially the right gyrus rectus; but no increased BOLD signal in the left temporal lobe. Conversely, for the contrast using only the five auras elicited by the music, BOLD increases were seen in the both the right gyrus rectus and left temporal lobe. As the left temporal lobe is not known to play any role in music, and was not activated by the epileptogenic music, the authors hypothesized that left temporal lobe onset on EEG and SPECT in this patient, could be secondary to the right gyrus rectus focus seen on BOLD, triggered perhaps by the emotional processing of music.

## 13.15 The Future

The advantages of fMRI to advance our understanding of epilepsy but also to identify the epileptic focus in persons with focal epilepsy compared to the surgical implantation of electrodes are so compelling it seems certain that the development of fMRI will continue. Several directions for future fMRI experiments in epilepsy seem especially interesting, in the context of the papers reviewed.

### 13.15.1 The Concept of a Preictal State

Perhaps the most surprising idea to emerge from the fMRI experiments reviewed here is the concept that changes in the BOLD signal may precede the clinical onset of a focal seizure. This observation underlines the concept of a “preictal state” in focal epilepsy advanced in several papers using linear (Litt et al. 2001) and nonlinear (Lehnertz et al. 1995; Elger and Lehnertz 1998) analysis of EEG time series that appear to demonstrate changes in the EEG, minutes to hours preceding clinical onset.

This idea that hemodynamic changes may define a preictal state has been investigated in experiments

using different modalities to measure CBF. Both increases (Adelson et al. 1999; Makiranta et al. 2005) and decreases (Hoshi et al. 1992) in tissue oxygenation have been found tens of seconds before seizure onset. Transcranial Doppler studies have been interpreted as demonstrating increases in lobar perfusion 20 min before focal as well as generalized spike-wave seizures (De Simone et al. 1998; Diehl 1998; Weinand et al. 1994). Indirect measurement of CBF in patients with TLE has demonstrated significant increases in CBF in the region of the seizure focus 10–12 min preceding onset on intracranial EEG (Weinand et al. 1997). Preictal hyperperfusion in the absence of clinical or EEG change has also been seen on SPECT scans fortuitously obtained minutes prior to seizure onset and during video-EEG monitoring (Baumgartner et al. 1998).

Two recent papers on fMRI experiments in epilepsy add to this idea that hemodynamic changes may define a preictal state. The first paper reviewed 143 concurrent EEG–fMRI studies of interictal epileptiform discharges performed at the Montreal Neurological Institute. Of these studies, BOLD changes in nearly half of the datasets preceded interictal epileptiform discharges on EEG used to model the BOLD signal, by several seconds (Hawco et al. 2007).

In the second paper, three persons with frequent frontal lobe seizures on falling asleep recorded their typical seizure in the fMRI scanner (Federico et al. 2005). BOLD changes over the entire brain were first analyzed using a t-contrast to compare a 1-min block immediately preceding seizure onset to a 1-min block beginning several minutes earlier. The time course was then extracted for the ROI defined by the maximal cluster on this t map, and for a mirror ROI in the contralateral hemisphere, and these time courses were compared. Each patient showed significant, focal BOLD signal changes (either increased or decreased) up to 20 min over the presumed seizure focus.

Obviously, the interpretation of the hemodynamic changes in these papers is complex. Nonetheless, the concept of a preictal state, if correct, would represent a tremendous advance in our understanding of how seizures happen. This, in turn, is potentially important clinically because, if a preictal state can be detected, then the use of various “closed loop” devices (for example, that give cortical stimulation) may be possible to prevent clinical seizures.

### 13.15.2 Low Frequency Noise in BOLD

Extending this idea, if we hypothesize that a preictal state exists for more than several minutes in epileptic networks preceding a clinical seizure, then we need to consider that detecting the BOLD signal correlate for this network activity will be complicated by the low frequency noise characteristics of BOLD time series. This noise refers to the fact that voxel intensities in BOLD fMRI data tend to demonstrate a slow variation over time, unrelated to the experimental design. This low frequency variability is typically removed by either high pass filtering, or by introducing terms into the linear model to model this low frequency drift. For this reason, BOLD contrast fMRI is not sensitive to detecting low frequency, or state-related changes that may be important in epilepsy.

Conceptually, the most direct approach to measuring these state-related changes, would be to directly measure, the changes in perfusion at different time points using bolus contrast agents, or noninvasive arterial spin-labeling (ASL; Detre et al. 1994). Perfusion-based methods such as ASL may be useful for these fMRI experiments, for several reasons. First, they do not rely on a comparison between an active and baseline condition. In our laboratory, for example, this has enabled ASL–fMRI imaging of focal hyperperfusion in EPC. Interictal hypoperfusion in temporal lobe epilepsy has also been demonstrated with both ASL (Wolf et al. 2001) and DSC methods (Wu et al. 1999). Because these techniques measure perfusion only, their interpretation is also considerably more straightforward compared to the multiple hemodynamic parameters encoded in BOLD (although these are dominated by changes in blood oxygenation). Because ASL methods do not rely on the detection of changes in local susceptibility as in BOLD contrast, they are particularly well suited to the detection of activation in regions of high static susceptibility, such as orbitofrontal cortex and the inferior temporal lobes.

### 13.15.3 Is Perfusion Matched to $CMRO_2$ ?

It follows from the papers reviewed that the BOLD signal increases during focal seizures, consistent with increases in blood flow and blood oxygenation (and

thus a decrease in deoxygenated hemoglobin). It nonetheless is not absolutely clear that this increase in blood flow is adequate to meet the increased  $CMRO_2$  in focal seizures. This uncertainty is motivated by recent studies using fast optical techniques in animal models and in humans to image these hemodynamic signals (for a superb review, see Schwartz 2007). Even in normal cognitive experiments, fast optical techniques demonstrate a rapid decrease in tissue oxygenation and an increase in deoxygenated hemoglobin that precedes the increase in blood flow, termed the “initial dip” of the BOLD response (Frostig et al. 1990).

Conversely, in epilepsy, fast optical measurements demonstrate that this increase in deoxygenated hemoglobin may persist, despite an increase in Suh et al. 2006a Suh et al. 2006b blood flow, during both interictal epileptiform discharges and epileptic seizures (Bahar et al. 2006; Shariff et al. 2006; Suh et al. 2006a, b). Similar data exists in earlier studies using implanted oxygen-sensitive electrodes in humans that recorded a decrease in tissue oxygenation preceding and during focal seizures (Dymond et al. 1976). These data, if correct, would indicate that CBF and blood oxygen, although increased during focal seizures, may be inadequate for the supernormal increase in  $CMRO_2$  seen in focal epilepsy.

This conjecture has implications for fMRI, as well. If the transient increase in deoxygenated hemoglobin is earlier and more focal than the subsequent increase, then imaging this transient hemodynamic change may be an excellent marker for the epileptic focus. For BOLD fMRI, this means future development of imaging techniques optimized to image this initial dip in hemoglobin oxygenation, as opposed to imaging increases in BOLD contrast, may be the smarter approach.

## References

- Abreu P, Ribeiro M, Forni A, Pires I, Sousa G (2005) Writing epilepsy: a neurophysiological, neuropsychological and neuroimaging study. *Epilepsy Behav* 6(3):463–466
- Adelson PD, Nemoto E, Scheuer M, Painter M, Morgan J, Yonas H (1999) Noninvasive continuous monitoring of cerebral oxygenation periictally using near infrared spectroscopy: a preliminary report. *Epilepsia* 40:1484–1489
- Aghakhani Y, Bagshaw AP, Bénar CG, Hawco C, Andermann F, Dubeau F, Gotman J (2004) fMRI activation during spike and wave discharges in idiopathic generalized epilepsy. *Brain* 127(Pt 5):1127–1144
- Archer JS, Briellman RS, Abbott DF, Syngieniotis A, Wellard RM, Jackson GD (2003a) Benign epilepsy with centro-temporal spikes: spike triggered fMRI shows somato-sensory cortex activity. *Epilepsia* 44(2):200–204
- Archer JS, Briellmann RS, Syngieniotis A, Abbott DF, Jackson GD (2003b) Spike-triggered fMRI in reading epilepsy: involvement of left frontal cortex working memory area. *Neurology* 60(3):415–421
- Arthurs OJ, Boniface S (2002) How well do we understand the neural origins of the fMRI BOLD signal? *Trends Neurosci* 25(1):27–31
- Avanzini G, Franceschetti S (2003) Cellular biology of epileptogenesis. *Lancet Neurol* 1(1):33–42
- Bahar S, Suh M, Zhao M, Schwartz TH (2006) Intrinsic optical signal imaging of neocortical seizures: the ‘epileptic dip’. *Neuroreport* 17(5):499–503
- Baumgartner C, Serles W, Leutmezer F, Patariaia E, Aull S, Czech T, Pietrzyk U, Relic A, Podreka I (1998) Preictal SPECT in temporal lobe epilepsy: regional cerebral blood flow is increased prior to electroencephalography-seizure onset. *J Nucl Med* 39(6):978–982
- Blumenfeld H (2005) Cellular and network mechanisms of spike-wave seizures. *Epilepsia* 46(Suppl 9):21–33
- Boor R, Jacobs J, Hinzmann A, Bauermann T, Scherg M, Boor S, Vucurevic G, Pfeleiderer C, Kutschke G, Stoeter P (2007) Combined spike-related functional MRI and multiple source analysis in the non-invasive spike localization of benign rolandic epilepsy. *Clin Neurophysiol* 118(4):901–909
- Buzsaki G (1991) The thalamic clock: emergent network properties. *Neuroscience* 41(2–3):351–364
- Carmichael DW, Hamandi K, Laufs H, Duncan JS, Thomas DL, Lemieux L (2008) An investigation of the relationship between BOLD and perfusion signal changes during epileptic generalised spike wave activity. *Magn Reson Imaging* 26(7):870–873
- De Simone R, Silvestrini M, Marciari MG, Curatolo P (1998) Changes in cerebral blood flow velocities during childhood absence seizures. *Pediatr Neurol* 18:132–135
- Detre JA, Zhang W, Roberts DA, Silva AC, Williams DS, Grandis DJ, Koretsky AP, Leigh JS (1994) Tissue specific perfusion imaging using arterial spin labeling. *NMR Biomed* 7(1–2):75–82
- Detre JA, Sirven JI, Alsop DC, O’Connor MJ, French JA (1995) Localization of subclinical ictal activity by functional magnetic resonance imaging: correlation with invasive monitoring. *Ann Neurol* 38(4):618–624
- Di Bonaventura C, Carnfi M, Vaudano AE, Pantano P, Garreffa G, Le Piane E, Maraviglia B, Bozzao L, Manfredi M, Prencipe M, Giallonardo AT (2006) Ictal hemodynamic changes in late-onset rasmussen encephalitis. *Ann Neurol* 59(2):432–433
- Diehl B, Knecht S, Deppe M, Young C, Stodieck SR (1998) Cerebral hemodynamic response to generalized spike-wave discharges. *Epilepsia* 39:1284–1289
- Dymond AM, Crandall PH (1976) Oxygen availability and blood flow in the temporal lobes during spontaneous epileptic seizures in man. *Brain Res* 102(1):191–196
- Elger CE, Lehnertz K (1998) Seizure prediction by non-linear time series analysis of brain electrical activity. *Eur J Neurosci* 10(2):786–789

- Espay AJ, Schmithorst VJ, Szaflarski JP (2008) Chronic isolated hemifacial spasm as a manifestation of epilepsy partialis continua. *Epilepsy Behav* 12(2):332–336
- Federico P, Abbott DF, Briellmann RS, Harvey AS, Jackson GD (2005) Functional MRI of the pre-ictal state. *Brain* 128(Pt 8):1811–1817
- Folbergrová J, Ingvar M, Siesjö BK (1981) Metabolic changes in cerebral cortex, hippocampus, and cerebellum during sustained bicuculline-induced seizures. *J Neurochem* 37(5):1228–1238
- Frostig RD, Lieke EE, Ts'o DY, Grinvald A (1990) Cortical functional architecture and local coupling between neuronal activity and the microcirculation revealed by in vivo high-resolution optical imaging of intrinsic signals. *Proc Natl Acad Sci U S A* 87(16):6082–6086
- Garraux G, Hallett M, Talagala SL (2005) CASL fMRI of subcortico-cortical perfusion changes during memory-guided finger sequences. *Neuroimage* 25(1):122–132
- Gloor P. (1968) Generalized cortico-reticular epilepsies. Some considerations on the pathophysiology of generalized bilaterally synchronous spike and wave discharge, *Epilepsia* 2 pp. 249–263
- Gotman J (2008) Epileptic networks studied with EEG-fMRI. *Epilepsia* 49(Suppl 3):42–51
- Gotman J, Grova C, Bagshaw A, Kobayashi E, Aghakhani Y, Dubeau F (2005) Generalized epileptic discharges show thalamocortical activation and suspension of the default state of the brain. *Proc Natl Acad Sci U S A* 102(42):15236–15240
- Greicius MD, Krasnow B, Reiss AL, Menon V (2003) Functional connectivity in the resting brain: a network analysis of the default mode hypothesis. *Proc Natl Acad Sci U S A* 100(1):253–258
- Hamandi K et al (2006) EEG-fMRI of idiopathic and secondarily generalized epilepsies. *Neuroimage* 31(4):1700–1710
- Hamandi K, Laufs H, Nöth U, Carmichael DW, Duncan JS, Lemieux L (2008) BOLD and perfusion changes during epileptic generalised spike wave activity. *Neuroimage* 39(2):608–618
- Hauser WA, Hesdorffer DC (1990) *Epilepsy: frequency, causes and consequences*. Demos Vermande, New York
- Hauser WA, Annegers JF, Kurland LT (1991) Prevalence of epilepsy in Rochester, Minnesota 1940–1980. *Epilepsia* 32:429–445
- Hawco CS, Bagshaw AP, Lu Y, Dubeau F, Gotman J (2007) BOLD changes occur prior to epileptic spikes seen on scalp EEG. *Neuroimage* 35(4):1450–1458
- Hill RA, Chiappa KH, Huang-Hellinger F, Jenkins BG (1999) Hemodynamic and metabolic aspects of photosensitive epilepsy revealed by functional magnetic resonance imaging and magnetic resonance spectroscopy. *Epilepsia* 40(7):912–920
- Hoge RD, Atkinson J, Gill B, Crelier GR, Marrett S, Pike GB (1999) Linear coupling between cerebral blood flow and oxygen consumption in activated human cortex. *Proc Natl Acad Sci U S A* 96(16):9403–9408
- Hoshi Y, Tamura M (1992) Cerebral oxygenation state in chemically induced seizures in the rat. A study by near infrared spectrophotometry. *Adv Exp Med Biol* 316:137–142
- Hwang DY, Golby AJ (2006) The brain basis for episodic memory: insights from functional MRI, intracranial EEG, and patients with epilepsy. *Epilepsy Behav* 8(1):115–126
- Jackson GD, Connelly A, Cross JH, Gordon I, Gadian DG (1994) Functional magnetic resonance imaging of focal seizures. *Neurology* 44(5):850–856
- Jacobs J, Hawco C, Kobayashi E, Boor R, LeVan P, Stephani U, Siniatchkin M, Gotman J (2008) Variability of the hemodynamic response as a function of age and frequency of epileptic discharge in children with epilepsy. *Neuroimage* 40(2):601–614
- Kobayashi E, Hawco CS, Grova C, Dubeau F, Gotman J (2006) Widespread and intense BOLD changes during brief focal electrographic seizures. *Neurology* 66(7):1049–1055
- Krings T, Töpper R, Reinges MH, Foltys H, Spetzger U, Chiappa KH, Gilsbach JM, Thron A (2000) Hemodynamic changes in simple partial epilepsy: a functional MRI study. *Neurology* 54(2):524–527
- Kurtzke JF (1982) The current neurologic burden of illness and injury in the United States. *Neurology* 32(11):1207–1214
- Laufs H, Duncan JS (2007) Electroencephalography/functional MRI in human epilepsy: what it currently can and cannot do. *Curr Opin Neurol* 20(4):417–423
- Laufs H, Lengler U, Hamandi K, Kleinschmidt A, Krakow K (2006) Linking generalized spike-and-wave discharges and resting state brain activity by using EEG/fMRI in a patient with absence seizures. *Epilepsia* 47(2):444–448
- Laurienti PJ (2004) Deactivations, global signal, and the default mode of brain function. *J Cogn Neurosci* 16(9):1481–1483. No abstract available
- Lazeyras F, Blanke O, Zimine I, Delavelle J, Perrig SH, Seeck M (2000) MRI, (1)H-MRS, and functional MRI during and after prolonged nonconvulsive seizure activity. *Neurology* 55(11):1677–1682
- Leal A, Dias A, Vieira JP, Secca M, Jordão C (2006) The BOLD effect of interictal spike activity in childhood occipital lobe epilepsy. *Epilepsia* 47(9):1536–1542
- Lehnertz K, Elger CE (1995) Spatio-temporal dynamics of the primary epileptogenic area in temporal lobe epilepsy characterized by neuronal complexity loss. *Electroencephalogr Clin Neurophysiol* 95(2):108–117
- Lemieux L, Salek-Haddadi A, Lund TE, Laufs H, Carmichael D (2007) Modelling large motion events in fMRI studies of patients with epilepsy. *Magn Reson Imaging* 25(6):894–901
- Lengler U, Kafadar I, Neubauer BA, Krakow K (2007) fMRI correlates of interictal epileptic activity in patients with idiopathic benign focal epilepsy of childhood. A simultaneous EEG-functional MRI study. *Epilepsy Res* 75(1):29–38
- Litt B, Esteller R, Echaz J, D'Alessandro M, Shor R, Henry T, Pennell P, Epstein C, Bakay R, Dichter M, Vachtsevanos G (2001) Epileptic seizures may begin hours in advance of clinical onset: a report of five patients. *Neuron* 30(1):51–64
- Logothetis NK, Pauls J, Augath M, Trinath T, Oeltermann A (2001) Neurophysiological investigation of the basis of the fMRI signal. *Nature* 412(6843):150–157
- Makiranta M, Ruohonen J, Suominen K, Niimäki J, Sonkajarvi E, Kiviniemi V, Seppänen T, Alahuhta S, Jantti V, Tervonen O (2005) BOLD signal increase precedes EEG spike activity, a dynamic penicillin induced focal epilepsy in deep anesthesia. *Neuroimage* 27:715–724
- Mazoyer B, Zago L, Mellet E, Bricogne S, Etard O, Houdé O, Crivello F, Joliot M, Petit L, Tzourio-Mazoyer N (2001)

- Cortical networks for working memory and executive functions sustain the conscious resting state in man. *Brain Res Bull* 54(3):287–298
- McCormick DA, Contreras D (2001) On the cellular and network bases of epileptic seizures. *Annu Rev Physiol* 63: 815–846
- Meeren H, van Luijckelaar G, Lopes da Silva F, Coenen A (2005) Evolving concepts on the pathophysiology of absence seizures: the cortical focus theory. *Arch Neurol* 62(3): 371–376
- Moeller F et al (2008) Changes in activity of striato-thalamo-cortical network precede generalized spike wave discharges. *Neuroimage* 39(4):839–1849
- Morocz IA, Karni A, Haut S, Lantos G, Liu G (2003) fMRI of triggerable auras in musicogenic epilepsy. *Neurology* 60(4): 705–709
- Neuroimaging Subcommittee of the ILAE (2000) Commission on Diagnostic Strategies recommendations for functional neuroimaging of persons with epilepsy. *Epilepsia* 41(10): 1350–1356
- Penfield W (1933) The evidence for a cerebral vascular mechanism in epilepsy. *Ann Internal Med* vol 7(3):303–310
- Penfield W and Jasper H. (1954) *Epilepsy and the functional anatomy of the human brain*. Boston: Little, Brown & Co., 896 pp
- Polack PO, Guillemain I, Hu E, Deransart C, Depaulis A, Charpier S (2007) Deep layer somatosensory cortical neurons initiate spike-and-wave discharges in a genetic model of absence seizures. *J Neurosci* 27(24):6590–6599
- Raichle ME (2003) Functional brain imaging and human brain function. *J Neurosci* 23(10):3959–3962
- Raichle ME, MacLeod AM, Snyder AZ, Powers WJ, Gusnard DA, Shulman GLA (2001) default mode of brain function. *Proc Natl Acad Sci U S A* 98(2):676–682
- Salek-Haddadi A, Merschhemke M, Lemieux L, Fish DR (2002) Simultaneous EEG-Correlated Ictal fMRI. *Neuroimage* 16(1):32–40
- Salek-Haddadi A, Lemieux L, Merschhemke M, Friston KJ, Duncan JS, Fish DR (2003). Functional magnetic resonance imaging of human absence seizures. *Ann Neurol*. 53(5):663–7
- Sander JW (2003) The epidemiology of epilepsy revisited. *Curr Opin Neurol* 16:165–170
- Schwartz TH (2007) Neurovascular coupling and epilepsy: hemodynamic markers for localizing and predicting seizure onset. *Epilepsy Curr* 7(4):91–94
- Senanayake N (1987). Epileptic seizures evoked by the Rubik's cube. *J Neurol Neurosurg Psychiatry*. 50(11):1553–4
- Shariff S, Suh M, Zhao M, Ma H, Schwartz TH (2006) Recent developments in oximetry and perfusion-based mapping techniques and their role in the surgical treatment of neocortical epilepsy. *Epilepsy Behav* 8(2):363–375
- Spencer SS (2002) Neural networks in human epilepsy: evidence of and implications for treatment. *Epilepsia* 43(3): 219–227
- Stefanovic B, Warnking JM, Kobayashi E, Bagshaw AP, Hawco C, Dubeau F, Gotman J, Pike GB (2005) Hemodynamic and metabolic responses to activation, deactivation and epileptic discharges. *Neuroimage* 28(1):205–215
- Suh M, Bahar S, Mehta AD, Schwartz TH (2006a) Blood volume and hemoglobin oxygenation response following electrical stimulation of human cortex. *Neuroimage* 31(1): 66–75
- Suh M, Ma H, Zhao M, Shariff S, Schwartz TH (2006b) Neurovascular coupling and oximetry during epileptic events. *Mol Neurobiol* 33(3):181–197
- Swanson SJ, Sabsevitz DS, Hammeke TA, Binder JR (2007) Functional magnetic resonance imaging of language in epilepsy. *Neuropsychol Rev* 17(4):491–504
- Tenney JR, Marshall PC, King JA, Ferris CF (2004) fMRI of generalized absence status epilepticus in conscious marmoset monkeys reveals corticothalamic activation. *Epilepsia* 45(10):1240–1247
- Weinand ME, Carter LP, Patton DD, Oommen KJ, Labiner DM, Talwar D (1994) Long-term surface cortical cerebral blood flow monitoring in temporal lobe epilepsy. *Neurosurgery* 35:657–664
- Weinand ME, Carter LP, el-Saadany WF, Sioutos PJ, Labiner DM, Oommen KJ (1997) Cerebral blood flow and temporal lobe epileptogenicity. *J Neurosurg* 86(2):226–232
- Wiebe S, Blume WT, Girvin JP et al (2001) A randomized, controlled trial of surgery for temporal-lobe epilepsy. *N Engl J Med* 345:311–318
- Wolf RL, Alsop DC, Levy-Reis I, Meyer PT, Maldjian JA, Gonzalez-Atavales J, French JA, Alavi A, Detre JA (2001) Detection of mesial temporal lobe hypoperfusion in patients with temporal lobe epilepsy by use of arterial spin labeled perfusion MR imaging. *AJNR Am J Neuroradiol* 22(7): 1334–1341
- Wu R, Bruening R, Noachtar S, et al (1999) MR measurement of regional relative cerebral blood volume in epilepsy. *J Magn Reson Imaging* 9:435–440
- Yeo DT, Fessler JA, Kim B (2008) Motion robust magnetic susceptibility and field inhomogeneity estimation using regularized image restoration techniques for fMRI. *Med Image Comput Assist Interv Int Conf Med Image Comput Comput Assist Interv* 11(Pt 1):991–998
- Zyzz J, Xie-Brustolin J, Ryvlin P, Peysson S, Beschet A, Sappey-Marinié D, Hermier M, Thobois S (2007) *Epilepsia partialis continua* with dystonic hand movement in a patient with a malformation of cortical development. *Mov Disord* 22(12): 1793–1796

Marko Wilke

## 14.1 Introduction

Several exciting neuroscientific questions can only be answered only when investigating the developing brain. However, children are not small adults, and imaging children therefore poses a number of special challenges on different levels. In this chapter, I will try to cover some specific aspects that may need to be considered when planning, conducting, or analyzing paediatric imaging studies.

When *planning* a neuroimaging study in children, special ethical issues arise, for example, subject consent. Subject recruitment is more difficult, and special emphasis must be placed on their exact characterization.

*Conducting* an fMRI study in children requires a special commitment in terms of time and personnel. Task design is another important issue, and additionally, technical adaptations may be necessary in order to achieve optimal results.

*Data analysis* poses a number of pitfalls, including spatial normalization and tissue segmentation. Finally, interpretation of results has to take into account known differences between the developing and the adult brain.

The developing brain has an enormous potential for learning (in the physiological setting; Elbert et al. 2001) and self-repair (when confronted with adverse events; Krägeloh-Mann 2004). These properties clearly

diminish with age; several exciting questions with wide-ranging implications can therefore be explored only when investigating children, as for example, neural reorganization following stroke. However, researchers must be aware of a number of issues that require special attention when investigating children using fMRI. This chapter aims at highlighting selected points that may require special consideration in this context.

## 14.2 Planning a Paediatric Neuroimaging Study

As children may be unable to fully understand the implications of participating in a research study, special regulations exist with regard to obtaining informed consent, which usually has to be signed by the legal guardian of the child. Most researchers will also obtain written assent from the child, which seems advisable, especially in older children or teenagers. The highest ethical standards must be met in order to justify the necessity of investigating children instead of adults (MRC 2008). In this context, it should also be noted that, for studies done in the US, there are now guidelines from the National Institutes of Health requiring researchers to establish a pathway to screen for and communicate incidental findings detected as part of a neuroimaging research study (NIH 2008), which is also a relevant issue in children (Kim et al. 2002).

When aiming at investigating normal children, it is imperative that all efforts be made to recruit a representative sample of subjects from the community. The much-used (but much less publicized) approach of scanning the children of co-workers and acquaintances

---

M. Wilke  
Department Paediatric Neurology and Developmental Medicine,  
University Children's Hospital, Hoppe-Seyler-Straße 3,  
72076 Tübingen, Germany  
e-mail: Marko.Wilke@med.uni-tuebingen.de

harbours the serious problem of studying a super-normal group which may not be representative of the population as a whole (Rivkin 2000). Substantial efforts may therefore be necessary to recruit truly normal children from different parts of the community and from different socio-economic and ethnic backgrounds (Evans et al. 2006). This is especially relevant when children are meant to serve as “normal controls” for a clinical population. For example, imaging data from subjects scanned for clinical reasons still show significant differences from truly healthy control subjects, even if the images were subsequently read as normal (Courchesne and Plante 1996). As also relevant in adults, the detection of previous conditions potentially interfering with normal brain development (significant head trauma, severe or long-standing illness or invasive therapies [e.g. chemotherapy], etc.) requires a thorough personal history to be taken. Moreover, shared pathology has been described in siblings of affected individuals with attention deficit disorder (Durstone et al. 2004) or schizophrenia (Falkai et al. 2007), underlining the necessity to screen for such disorders in first-degree relatives as part of the recruitment procedure. As to subject selection, it also seems important to remember that the age range of subjects should be as narrow as possible, in order to avoid the confounding effects of age. Conversely, if the effect of age is under study, the number of subjects must be sufficiently large in order to detect such effects and to account for the large variability in brain structure (Giedd et al. 1996; Wilke and Holland 2003). The age-dependent failure rate of children (Byars et al. 2002; see also next paragraph) must be taken into account when planning and budgeting for subject recruitment, in a way that children in the lower age brackets are overrepresented (allowing for a larger proportion of them to fail the scanning session).

Institutional review boards will impose special requirements for imaging studies in children which are especially relevant when imaging normal children. Incidental findings must be screened for. Researchers should aim at avoiding recruitment bias, and subject characterization should take into account the rapidly changing features of the developing brain.

Naturally, when investigating children for a clinical reason, many of the criteria mentioned above may not be relevant as the main indication and justification for MR-scanning is a clinical one. However, most, if not

all, of the following points may still need to be considered. For especially “difficult-to-scan” populations such as infants and toddlers, using imaging data obtained during a clinically-indicated scan under general anaesthesia may be the only option. In this context, it is important to remember the proven or suspected role sedative agents have on the hemodynamic response (Altman and Bernal 2001; Dueck et al. 2005) which may make data analysis using standard hemodynamic response functions difficult. As an alternative, studies have been done on babies and infants during natural sleep (Almli et al. 2007; Dehaene-Lambertz et al. 2002). With further efforts towards reducing scanner noise (de Zwart et al. 2002; Moelker and Pattynama 2003), such an approach may be easier in the future.

### 14.3 Conducting a Paediatric Neuroimaging Study

Children may be as willing but less able to comply with the high demands of participating in a neuroimaging study. In children taking part in such a study, there is a clear inverse correlation between age and failure rate (Byars et al. 2002). Interestingly, claustrophobia, rarely, is an issue in children (Eshed et al. 2007); instead, anxiety, insecurity and lack of understanding of the procedure are major concerns. The main lesson to be drawn from this is that adequate subject preparation is the key in achieving high success rates when scanning children. Several approaches have been suggested to achieve this, chief among them being the use of a mock scanner to desensitize children with regard to the intimidating scanner environment (Epstein et al. 2007). Our approach has been to reserve longer time slots (2h per subject) at the real scanner and to desensitize children by using life-sized dolls that are being scanned prior to the subject (see Fig. 14.1). Therefore, the child can actually see (and thus, more concretely understand) the procedure (Wilke and Holland 2008). Even with extensive preparation, a failure rate of about 50% in children at 5 years of age must be expected (Byars et al. 2002). The value of motivated, experienced personnel in this process of desensitization cannot be overestimated, as every preparation scheme may have to be individually adapted based on the child’s reaction.



**Fig. 14.1** Life-sized doll, to be scanned prior to the child as part of the desensitization procedure

Task design is an important point, and worth spending a lot of time on, before starting the study. A child's attention span is shorter, and its ability to lie still for an extended period of time is significantly reduced when compared to a motivated adult. It may also feel alone in the scanner, so addressing the child in an encouraging way between imaging series helps to keep it motivated. Age-appropriate stimulation material is important (see Fig. 14.2), and additionally, the level of difficulty needs to be adapted to the child's abilities (Thomas and Casey 2000; Wilke et al. 2003a). Failure to take these facts into account may result in a high likelihood to end up with a frustrated child in the scanner, which consequently will be unable to comply for the remainder of the session. The following points are therefore important to keep in mind:

- Short functional series (about 5 min/series), interlaced by talking to the child, improve the chances of acquiring usable data.

- Distraction in the form of a movie or music should be provided during non-fMRI parts of the exam (for example while acquiring the anatomical images).
- Easy-to-do, but not boring tasks that are matched to the child's abilities to solve them will keep the child motivated.
- Practice sessions before the scan where the child demonstrates that it can master the task are advisable.
- Objective documentation of task engagement should be incorporated so that continued task execution can be verified, ideally in real time.
- Task design should not be too technical; for example, using comics or cartoons to illustrate the task is advisable.
- Non-essential scanning parts should be kept as short as possible and should be strategically placed to ensure the successful processing of the whole dataset (many successfully completed tasks do not help if the anatomical dataset, which may be necessary for data processing, could not be acquired).

With regard to specific technical difficulties that are part of scanning children, these tend to increase as the age of the subject decreases. Factors such as coil loading or differing water content of the brain are not relevant when teenagers are under study. However, when imaging neonates, these factors are decisive with regard to the obtainable image quality (Erberich et al. 2003). MR-compatible incubators with matching RF-coils have been introduced that now allow for high-quality scanning of neonates in a protective environment (Blüml et al. 2004). In the first years of life, there are further issues with regard to sequence optimization as image contrast continues to change dramatically (Ball and Dunn 1997). Finally, fMRI in the first year needs to consider that the BOLD response in very young children is still changing (Marcar et al. 2004), which may also be an issue in older children (Schapiro et al. 2004).

Extensive, age-appropriate preparation is key when conducting imaging studies in children. A mock scanner or "child phantoms" are helpful for desensitization. Task design should always take into account the abilities of the subjects under study, and scanning time should be kept as short as possible. Especially when scanning very small children, technical adaptations (smaller coils, optimized sequences) may be necessary.

**Fig. 14.2** Illustration of child-friendly stimulation material as part of a language task, taken from a children's book (for details see Wilke et al. 2005). Images used with kind permission from Egmont Pestalozzi Verlag, Munich, Germany



#### 14.4 Analyzing a Paediatric Neuroimaging Study

Due to the vast amount of acquired data, analyses of functional MRI are now mainly done within specialized software suites like AFNI, BrainVoyager, FreeSurfer, FSL, or SPM. However, it is important to remember that, both to reduce the processing load and to increase the quality of the obtained results, many software solutions implicitly or explicitly make use of prior information in the form of reference data. Such reference data is routinely derived from a single (like the common space of Talairach and Tournoux 1988) or several healthy adults (like the now commonly-used MNI-Brain, Mazziotta et al. 1995). However, such adult spatial information may not be appropriate when processing paediatric brains, especially in crucial steps as spatial normalization or tissue segmentation (Wilke et al. 2002, 2003b). While it has been suggested that using a common stereotaxic space does not have a negative impact on the ensuing results

(Burgund et al. 2002), it seems clear, that, especially for processing brain imaging data from younger children, a significant impact of such procedures must be expected (Fig. 14.3). Similar to the increasing technical difficulties with the decrease in subject's age mentioned above, a number of issues, when processing neonatal or infant brain data, are still unexplored. Therefore, eliminating or at least exploring the extent of the impact of such reference data seems important.

With regard to interpreting results from brain imaging studies done in children, it seems important to remember that, again, the application of concepts derived from studying adult brains must be considered with caution. This is true for an anatomical delineation such as the Brodman label (Brodman 1909), the value of which is questionable due to the large interindividual variability even in adults where a combined approach has been advocated (Eickhoff et al. 2007). Moreover, functional differences also seem to be present: studies suggest that cortical specializations present in adults

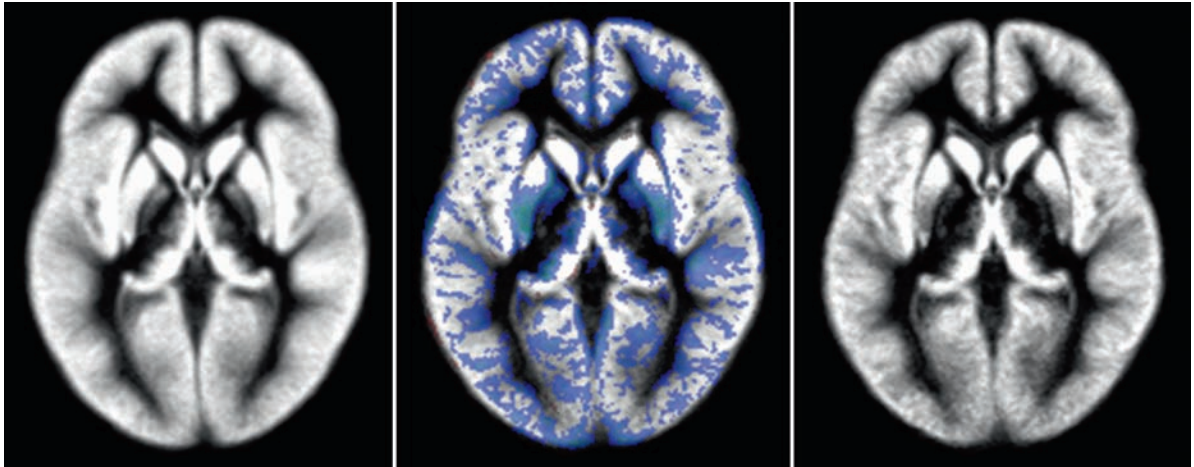


**Fig. 14.3** Illustration of age-related brain changes: gray matter template for 6 (*left*) and 17-year-old boys (*right*), and differences in gray matter concentration between them (*middle*, exceeding 10%; *blue* values indicate higher gray matter

concentration in younger children). Note substantial changes in the basal ganglia, but also throughout the whole cortical gray matter. Data generated with the TOM-toolbox (Wilke et al. 2008)



**Fig. 14.4** Reorganization of the language network in a 16-year-old boy following perinatal left-hemispheric stroke: note activation in typical anterior (*circle*) and posterior (*box*), but right-hemispheric brain regions while doing a language task. Data analyzed using SPM5,  $P \leq 0.05$ , FDR-corrected for multiple comparisons; note posterior co-activation due to visual processing (Wilke et al. 2005)

only evolve in normal children, likely paralleling the increase in functional specialization (Bitan et al. 2006; Brauer and Friederici 2007). Recently, the question of evolving networks of cortical processing as a function of normal development was hotly debated (Brown et al. 2006; Durston et al. 2006). In how far these functional differences are linked with structural maturation processes is currently unknown.

What is true for the healthy setting is even more relevant for the response to adverse events: the developing brain has distinct ways to compensate for early insults, both in the sensorimotor and the language domain (Carr et al. 1993, Staudt 2007; Staudt et al. 2002). Here, children have been shown to continue to use early patterns of motor organization or to reorganize the whole cortical language network to the opposite hemisphere (Fig. 14.4). Both patterns are specific to the developing brain. Taken together, these results suggest that caution must be used when interpreting paediatric imaging studies on the background of knowledge gained from adult studies.

Interpreting results from paediatric imaging studies requires an awareness of implicit or explicit influences from adult reference data on processing steps or analysis approaches. The developing brain shows distinct patterns of reorganization following external insults, so that especially in the pathological setting, applying information gained from studying adults may be inappropriate.

## 14.5 Conclusions

Much can be learned from studying the developing brain, and several questions will only be answered by understanding the processes underlying normal and abnormal brain development. When setting out to do imaging studies in children, it seems important to remember a number of specific points distinguishing paediatric from adult imaging studies, as laid out above. A multi-professional, collaborative effort involving researchers committed to working with children seems to be a prerequisite for successfully performing such studies.

## References

- Almli CR, Rivkin MJ, McKinstry RC; Brain Development Cooperative Group (2007) The NIH MRI study of normal brain development (objective-2): newborns, infants, toddlers, and preschoolers. *NeuroImage* 35:308–325
- Altman NR, Bernal B (2001) Brain activation in sedated children: auditory and visual functional MR imaging. *Radiology* 221:56–63
- Ball WS Jr, Dunn RS (1997) Computed tomography and magnetic resonance imaging. In Ball WS Jr (ed) *Pediatric neuroradiology*, 1st edn. Lippincott Raven, Philadelphia, PA, p 17
- Bitan T, Burman DD, Lu D et al (2006) Weaker top-down modulation from the left inferior frontal gyrus in children. *NeuroImage* 33:991–998
- Blüml S, Friedlich P, Erberich S et al (2004) MR imaging of newborns by using an MR-compatible incubator with integrated radiofrequency coils: initial experience. *Radiology* 231:594–601
- Brauer J, Friederici AD (2007) Functional neural networks of semantic and syntactic processes in the developing brain. *J Cogn Neurosci* 19:1609–1623
- Brodman K (1909) *Vergleichende Lokalisationslehre der Grosshirnrinde: in ihren Principien dargestellt auf Grund des Zellenbaues*. Johann Ambrosius Barth, Leipzig
- Brown TT, Petersen SE, Schlaggar BL (2006) Does human functional brain organization shift from diffuse to focal with development? *Dev Sci* 9:9–11
- Burgund ED, Kang HC, Kelly JE, Buckner RL et al (2002) The feasibility of a common stereotactic space for children and adults in fMRI studies of development. *NeuroImage* 17:184–200
- Byars AW, Holland SK, Strawsburg RH et al (2002) Practical aspects of conducting large-scale functional magnetic resonance imaging studies in children. *J Child Neurol* 7: 885–890
- Carr LJ, Harrison LM, Evans AL, Stephens JA (1993) Patterns of central motor reorganization in hemiplegic cerebral palsy. *Brain* 116:1223–1247
- Courchesne E, Plante E (1996) Measurement and analysis issues in neurodevelopmental magnetic resonance imaging. In Thatcher RW, Lyon GR, Rumsey J, Krasnegor N (eds) *Developmental neuroimaging: mapping the development of brain and behavior*, 1st edn. Academic, San Diego, CA, p 43
- Dehaene-Lambertz G, Dehaene S, Hertz-Pannier L (2002) Functional neuroimaging of speech perception in infants. *Science* 298:2013–2015
- de Zwart JA, van Gelderen P, Kellman P (2002) Reduction of gradient acoustic noise in MRI using SENSE-EPI. *NeuroImage* 16:1151–1155
- Dueck MH, Petzke F, Gerbershagen HJ et al (2005) Propofol attenuates responses of the auditory cortex to acoustic stimulation in a dose-dependent manner: a fMRI study. *Acta Anaesthesiol Scand* 49:784–791
- Durston S, Hulshoff Pol HE, Schnack HG et al (2004) Magnetic resonance imaging of boys with attention-deficit/hyperactivity disorder and their unaffected siblings. *J Am Acad Child Adolesc Psychiatry* 43:332–340
- Durston S, Davidson MC, Tottenham N et al (2006) A shift from diffuse to focal cortical activity with development. *Dev Sci* 9:1–8
- Eickhoff SB, Paus T, Caspers S et al (2007) Assignment of functional activations to probabilistic cytoarchitectonic areas revisited. *NeuroImage* 36:511–521
- Elbert T, Heim S, Rockstroh B (2001) Neural plasticity and development. In Nelson CA, Luciana M (eds) *Handbook of developmental cognitive neuroscience*. MIT, Cambridge, MA, p 193
- Epstein JN, Casey BJ, Tonev ST et al (2007) Assessment and prevention of head motion during imaging of patients with attention deficit hyperactivity disorder. *Psychiatry Res* 155: 75–82
- Erberich SG, Friedlich P, Seri I et al (2003) Functional MRI in neonates using neonatal head coil and MR compatible incubator. *NeuroImage* 20:683–692
- Eshed I, Althoff CE, Hamm B et al (2007) Claustrophobia and premature termination of magnetic resonance imaging examinations. *J Magn Reson Imaging* 26:401–404
- Evans AC; Brain Development Cooperative Group (2006) The NIH MRI study of normal brain development. *NeuroImage* 30:184–202
- Falkai P, Honer WG, Kasper T et al (2007) Disturbed frontal gyrification within families affected with schizophrenia. *J Psychiatr Res* 41:805–813
- Giedd JN, Snell JW, Lange N et al (1996) Quantitative magnetic resonance imaging of human brain development: ages 4–18. *Cereb Cortex* 6:551–560
- Kim BS, Illes J, Kaplan RT, Reiss A, Atlas SW (2002) Incidental findings on pediatric MR images of the brain. *AJNR Am J Neuroradiol* 23:1674–1677
- Krägeloh-Mann I (2004) Imaging of early brain injury and cortical plasticity. *Exp Neurol* 190:84–90
- Marcar VL, Strässle AE, Loenneker T et al (2004) The influence of cortical maturation on the BOLD response: an fMRI study of visual cortex in children. *Pediatr Res* 56:967–974
- Mazziotta JC, Toga AW, Evans A et al (1995) A probabilistic atlas of the human brain: theory and rationale for its development. *NeuroImage* 2:89–101
- Moelker A, Pattynama PM (2003) Acoustic noise concerns in functional magnetic resonance imaging. *Hum Brain Mapp* 20:123–141

- MRC (2008) MRC ethics guide: medical research involving children. [www.mrc.ac.uk](http://www.mrc.ac.uk)
- NIH (2008) Detection and disclosure of incidental findings in neuroimaging research. [www.ninds.nih.gov/news\\_and\\_events/proceedings/ifexecsummary.htm](http://www.ninds.nih.gov/news_and_events/proceedings/ifexecsummary.htm)
- Rivkin MJ (2000) Developmental neuroimaging of children using magnetic resonance techniques. *Ment Retard Dev Disabil Res Rev* 6:68–80
- Schapiro MB, Schmithorst VJ, Wilke M et al (2004) BOLD fMRI signal increases with age in selected brain regions in children. *Neuroreport* 15:2575–2578
- Staudt M (2007) (Re-)organization of the developing human brain following periventricular white matter lesions. *Neurosci Biobehav Rev* 31:1150–1156
- Staudt M, Lidzba K, Grodd W, Wildgruber D, Erb M, Krägeloh-Mann I (2002) Right-hemispheric organization of language following early left-sided brain lesions: functional MRI topography. *NeuroImage* 16:954–967
- Talairach J, Tournoux P (1988) Co-planar stereotaxic atlas of the human brain. Thieme Medical, Stuttgart
- Thomas KM, Casey BJ (2000) Functional MRI in pediatrics. In Moonen CTW, Bandettini PA (eds) *Functional MRI*. Springer, Berlin, pp 513–524
- Wilke M, Holland SK (2003) Variability of gray and white matter during normal development: a voxel-based MRI analysis. *Neuroreport* 14:1887–1890
- Wilke M, Holland SK (2008) Structural MR-imaging studies of the brain in children: issues and opportunities. *Neuroembryol Aging* 5:6–13
- Wilke M, Schmithorst VJ, Holland SK (2002) Assessment of spatial normalization of whole-brain magnetic resonance images in children. *Hum Brain Mapp* 17:48–60
- Wilke M, Holland SK, Myseros JS et al (2003a) Functional magnetic resonance imaging in pediatrics. *Neuropediatrics* 34:225–234
- Wilke M, Schmithorst VJ, Holland SK (2003b) Normative pediatric brain data for spatial normalization and segmentation differs from standard adult data. *Magn Reson Med* 50:749–757
- Wilke M, Holland SK, Altaye M et al (2008) Template-O-matic: a toolbox for creating customized pediatric templates. *NeuroImage* 14:903–913
- Wilke M, Lidzba K, Staudt M, Buchenau K et al (2005) Comprehensive language mapping in children, using functional magnetic resonance imaging: what's missing counts. *Neuroreport* 16:915–919

## 15.1 Introduction

The developing human brain possesses a superior potential of functional reorganization after lesions compared with the adult brain. Because of such reorganizational processes, children with early brain lesions often show abnormally located cortical representations of certain brain functions, e.g. of motor representations (Carr et al. 1993; Staudt et al. 2002a; 2004a) or of language functions (Rasmussen and Milner 1977; Staudt et al. 2002b). Nowadays, these abnormally located representations can be identified non-invasively using techniques such as functional MRI (fMRI), transcranial magnetic stimulation (TMS) or magnetoencephalography (MEG). Thus, these techniques can not only contribute to our general understanding of the processes involved in the reorganization of the developing human brain, but can also be used clinically in the pre-surgical evaluation of children who have to undergo brain surgery, e.g. for the relief of pharmaco-refractory epilepsies originating from their lesions (Hertz-Pannier et al. 2001; Staudt et al. 2001; 2004a, b; Liégeois et al. 2006).

The clinical application of these mapping techniques in this context is particularly challenging: first, most of these patients are children, often with various

degrees of cognitive impairments, so that their ability to comply with the experimental requirements is often reduced; second, the brain lesions often destroy or distort anatomical landmarks, which can normally be used for the identification of eloquent brain regions; and third, the cortical representations of brain functions may have shifted because of reorganizational processes following lesions acquired during ongoing brain development. This chapter gives typical examples of examinations of children, mostly in the pre-surgical evaluation before epilepsy surgery, highlighting a number of important aspects.

## 15.2 Example 1

A 3-year-old boy suffered from therapy-refractory focal seizures originating from a cortical dysplasia (yellow arrows in Fig. 15.1) in the central (Rolandic) region of the right hemisphere. On clinical examination, left hand function was normal. Prior to possible epilepsy surgery, fMRI during a simple active hand motor task (repetitive squeezing of a toy) was used to visualize the spatial relation between the dysplasia and the primary sensorimotor representation of the contralateral hand.

Based on these findings of fMRI activation in the immediate vicinity of the dysplasia, no total resection of the dysplasia was performed.

fMRI can be used even in pre-school children to localize the primary sensorimotor region (S1M1) in the vicinity of epileptogenic lesions.

---

M. Staudt  
Neuropediatric Clinic and Clinic for Neurorehabilitation/  
Epilepsy, Center for Children and Adolescents,  
Krankenhausstrasse 20, 83569 Vogtareuth, Germany  
e-mail: mstaudt@schoen-kliniken.de

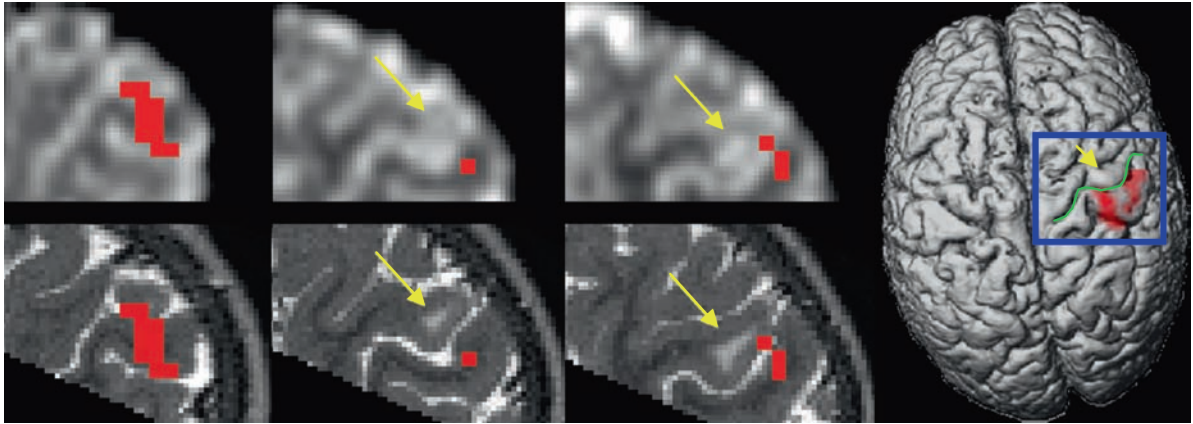


**Fig. 15.1** fMRI during active left hand movement in a 3-year-old boy with a focal cortical dysplasia (hyperintense on T2; *yellow arrows*) of the right central (Rolandic) region. The fMRI activation (in *red*) is superimposed directly on the (functional) EPI images (yielding the most reliable topographical localization, since no coregistration is involved; *upper row*), and,

after coregistration, to high-resolution structural T2-weighted images acquired in general anaesthesia during a separate session (*lower row*; courtesy of Prof. Winkler, Olgahospital Stuttgart) as well as onto a 3D surface reconstruction (*right*). *Green line* = central sulcus; *blue rectangle* = position of the enlarged details on the *left*

### 15.3 Example 2

A 16-year-old girl with congenital hemiparesis due to a pre- or perinatally acquired cortico-subcortical infarct

in the territory of the middle cerebral artery (MCA) showed a striking discrepancy between a large cystic lesion and relatively well-preserved sensorimotor functions (preserved grasp) of the contralateral (paretic)

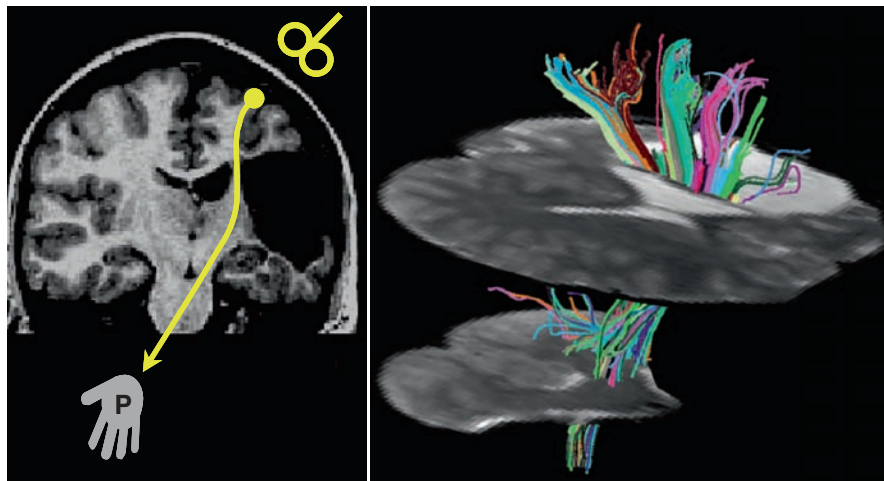


**Fig. 15.2** MRI and TMS findings of a 16-year-old girl with congenital hemiparesis due to a large cortico-subcortical infarct. *Left*: Coronal T1-weighted image depicting the cystic lesion. TMS (indicated by the *yellow figure-eight-coil symbol*) of the affected hemisphere elicited normal motor-evoked potentials in the paretic hand (P), confirming the presence of preserved crossed

cortico-spinal projections (*yellow arrow*). *Right*: MR diffusion tensor tractography (in random colours on unweighted diffusion images; tilted axial planes, anterior-lateral-superior view) visualized numerous fibre trajectories passing through the small bridge of preserved white matter between the cystic lesion and the lateral ventricle. Adapted from Staudt et al. 2006b, permission pending

hand (Staudt et al. 2006b). On neurophysiological examination, TMS revealed preserved crossed cortico-spinal projections from the affected hemisphere to the paretic hand, and MEG identified the first cortical response to repetitive tactile stimulation of the paretic thumb (N20m) in the affected hemisphere, indicating the presence of preserved crossed spino-thalamo-cortical somatosensory projections. Accordingly, diffusion tensor imaging (DTI) tractography with a seed region positioned in the small bridge of preserved white matter between the enlarged lateral ventricle and the cystic lesion visualized extensive connectivity provided by this area (Fig. 15.2).

### 15.4 Example 3

A 20-year-old young man with congenital right hemiparesis due to a large polymicrogyria in the left fronto-parietal region shows partially preserved sensorimotor functions (preserved individual finger movements) of the contralateral (paretic) right hand (Staudt et al. 2004b). On neurophysiological examination, TMS revealed preserved crossed cortico-spinal projections from the affected hemisphere to the paretic hand. Accordingly, fMRI during a simple active hand motor task (repetitive opening/closing of the paretic hand) revealed activation in the polymicrogyric cortex. Thus, both TMS and fMRI demonstrate that, in this patient, the polymicrogyric cortex harbours the primary motor representation of the paretic hand (Fig. 15.3).

Dysgenic cortex (here: polymicrogyria) can fulfil primary motor functions, with normal descending cortico-spinal motor projections. This can be confirmed by a combination of fMRI and TMS.

Small areas of preserved white matter can provide surprisingly extensive connectivity in patients with early brain lesions. Such projections can be visualized by DTI tractography.

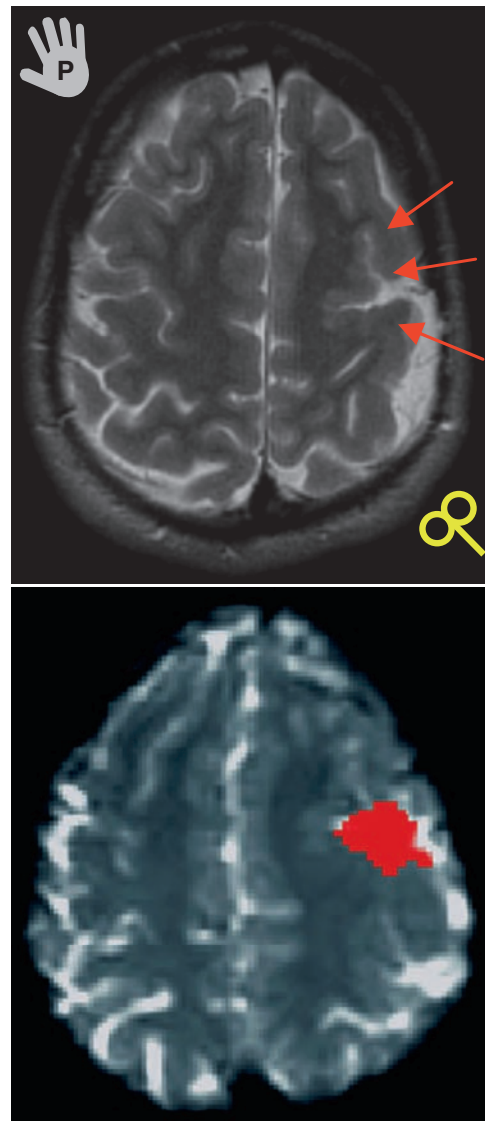


**Fig. 15.3** MRI and TMS findings of a 20-year-old man with congenital hemiparesis due to a large polymicrogyria. *Left:* Axial T2-weighted image depicting the polymicrogyria in the left fronto-parietal region (*red arrows*). TMS (indicated by the *yellow figure-eight-coil symbol*) of the affected hemisphere elicited normal motor-evoked potentials in the paretic hand (P), confirming the presence of preserved crossed cortico-spinal projections. *Right:* fMRI activation (in *red*; superimposed on the functional EPI) during active movement of the paretic hand revealed activation in the polymicrogyria, approximately opposing the Rolandic region in the contra-lesional hemisphere

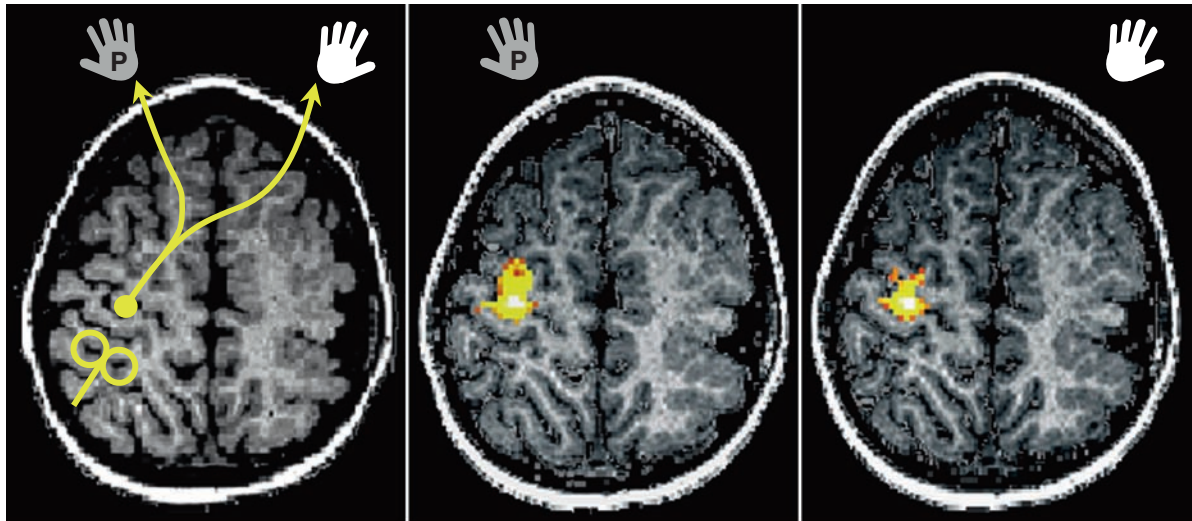


**Fig. 15.4** MRI and TMS findings of a 6-year-old boy with congenital hemiparesis due to a complex hemispheric malformation. *Left:* Axial T1-weighted image depicting the malformation of almost the entire hemisphere. TMS (indicated by the *yellow figure-eight-coil symbol*) of the contra-lesional hemisphere elicited not only the normal contralateral responses in the non-paretic

hand, but also ipsilateral motor-evoked potentials in the paretic hand (P), demonstrating the presence of ipsilateral cortico-spinal projections. fMRI during active movement of the paretic hand (*middle*) revealed activation in the hand knob area of the contra-lesional (ipsilateral) hemisphere, not different from the activation elicited by active movement of the non-paretic hand (*right*)

### 15.5 Example 4

A 6-year-old boy with congenital right hemiparesis due to a complex hemispheric malformation suffered from pharmaco-refractory seizures (Staudt et al. 2001). Clinical examination showed preserved individual finger movements in the paretic hand and massive mirror movements during voluntary movements of both the paretic and the non-paretic hand. Prior to epilepsy surgery, fMRI and TMS were performed to identify the primary motor representation of the paretic hand. TMS of the affected hemisphere did not elicit any response, whereas TMS of the contra-lesional hemisphere elicited bilateral responses with similar latencies. This indicated the presence of fast-conducting ipsilateral cortico-spinal projections, allowing the contra-lesional hemisphere to exert motor control over the paretic hand. Accordingly, fMRI during a simple active hand motor task (repetitive opening/closing of the paretic hand) revealed activation in the “hand knob” area of the contra-lesional hemisphere, not different from the fMRI activation elicited by movements of the non-paretic hand. Active grasping was still possible after functional hemispherectomy (Fig. 15.4).

Early brain lesions (malformations, but also defective lesions) can induce shifting of the primary motor

representation (M1) of the paretic hand to the contra-lesional hemisphere (with ipsilateral cortico-spinal tracts).

### 15.6 Example 5

A 19-year-old woman with congenital right hemiparesis due to a large unilateral periventricular brain lesion showed preserved individual finger movements in the paretic hand and massive mirror movements during voluntary movements of both the paretic and the non-paretic hand (Staudt et al. 2006a). As in the patient of example 4, TMS of the affected hemisphere did not elicit any response, but TMS of the contra-lesional hemisphere elicited bilateral responses with similar latencies. This indicated the presence of ipsilateral cortico-spinal projections, allowing the contra-lesional hemisphere to exert motor control over the paretic hand. Accordingly, fMRI during a simple active hand motor task (*active* opening/closing of the paretic hand) revealed activation in the “hand knob” area of the contra-lesional hemisphere, but also activation in the contralateral Rolandic region, an area from which no motor-evoked potentials could be elicited by TMS.



**Fig. 15.5** MRI, TMS, fMRI, MEG and DTI tractography findings of a 19-year-old female with congenital hemiparesis due to a unilateral periventricular brain lesion. *Left:* Coronal T1-weighted image depicting the periventricular lesion. TMS (indicated by the yellow figure-eight-coil symbol) of the contra-lesional hemisphere elicited not only the normal contralateral responses in the non-parietic hand, but also ipsilateral motor-evoked potentials in the paretic hand (P), demonstrating the presence of ipsilateral cortico-spinal projections. *Middle:* fMRI during active (*middle*

*left*) and passive (*middle right*) movement of the paretic hand. The blue circle indicates the position of the dipole reconstruction from MEG recording of the first cortical response to tactile stimulation of the paretic thumb. *Right:* Diffusion tensor imaging (DTI) tractography of ascending spino-thalamo-cortical projections, with seed regions in the dorsal brain stem (tegmentum pontis) and in the subcortical Rolandic white matter of both hemispheres (from Staudt et al. 2006a, permission pending)

fMRI during *passive* hand movement also elicited activation in the contralateral Rolandic region (i.e. of the affected hemisphere), suggesting preserved somatosensory functions in this region. And indeed, MEG recorded the first cortical response to repetitive tactile stimulation of the paretic thumb (N20m) in the contralateral Rolandic region, confirming this region to harbour the primary somatosensory representation (S1) of the paretic hand. Finally, DTI with a seed region in the dorsal brain stem (tegmentum pontis) visualized ascending spino-thalamo-cortical projections bypassing the lesion on their way to this preserved somatosensory representation of the paretic hand. This observation can be explained by the fact that developing thalamo-cortical somatosensory projections had not yet reached their cortical target areas by the time of the insult (the early third trimester of pregnancy; Kostovic and Judas 2002), so that these outgrowing fibres could find an alternative route in the preserved tissue, thus forming “axonal bypasses” around the defective areas (Staudt et al. 2006a).

This example and similar cases (Thickbroom et al. 2001; Staudt et al. 2006a) teach important lessons for the application of non-invasive imaging techniques in children with early brain lesions:

1. Different mechanisms are available for reorganization of primary motor and primary somatosensory representations (shifting to the contra-lesional hemi-

sphere for motor functions, forming axonal bypasses around a lesion for somatosensory functions).

2. This can lead to a “hemispheric dissociation” between the primary motor (M1) and the primary somatosensory (S1) representations of a paretic hand.
3. fMRI of passive hand movement alone is not suited to identify the “sensorimotor representation” of a paretic hand (see Fig. 15.5) – the reorganization of the primary motor representation in example 5 would have been missed with the “normal-looking” result for passive hand movement!

## 15.7 Conclusions

Non-invasive mapping techniques such as fMRI, TMS, MEG and DTI tractography are useful techniques in the pre-surgical diagnostic work-up of children with early brain lesions. These situations often require a combined use of complementary techniques.

The combination of fMRI (during active movements) and TMS is well suited to identify motor representations, with TMS being specific for areas from where cortico-spinal projections originate, and fMRI visualizing the entire sensorimotor network with a high spatial resolution in three dimensions (Thickbroom et al. 2001; Staudt et al. 2002a; 2004a, b). This is

important for the identification of (a) the spatial relation between M1 and an epileptogenic lesion (as in example 1), (b) of a preserved M1 in dysgenic cortex (as in example 3) and (c) of a reorganization of M1 into the contra-lesional hemisphere (as in examples 4 and 5). In this respect, patients with a “hemispheric dissociation” between M1 and S1 (Thickbroom et al. 2001; Staudt et al. 2006a) are particularly challenging, since here fMRI of active hand movements typically yields bilateral Rolandic activation.

The combination of fMRI (during passive movements) and MEG is well suited to identify somatosensory representations, with MEG (due to its high temporal resolution) being specific for primary somatosensory representations (e.g. the cortical projection areas of somatosensory fibres), and fMRI visualizing the somatosensory network with a high spatial resolution in three dimensions (Staudt et al. 2006a; Wilke et al. 2008). Similar to the motor system, this combination can identify (a) preserved somatosensory projections in preserved white-matter bridges (as in example 2), (b) a preserved S1 in Rolandic cortex overlying even large lesions (as in example 5) and (c) a preserved S1 in dysgenic cortex (no example included here, see Gerloff et al. 2006).

Finally, DTI tractography can visualize preserved projections in the vicinity of a lesion (as in example 2), or “axonal bypasses” around a lesion (as in example 5). Because of the uncertainties involved in this new technique, we still recommend to use such information only when additional evidence (e.g. neurophysiological evidence from TMS or MEG) for the existence of such projections is available.

## References

- Carr LJ, Harrison LM, Evans AL et al (1993) Patterns of central motor reorganization in hemiplegic cerebral palsy. *Brain* 116:1223–1247
- Gerloff C, Braun C, Staudt M et al (2006) Coherent corticomuscular oscillations originate from primary motor cortex: evidence from patients with early brain lesions. *Hum Brain Mapp* 27:789–798
- Hertz-Pannier L, Chiron C, Véra P et al (2001) Functional imaging in the work-up of childhood epilepsy. *Childs Nerv Syst* 17:223–228
- Kostovic I, Judas M (2002) Correlation between the sequential ingrowth of afferents and transient patterns of cortical lamination in preterm infants. *Anat Rec* 267:1–6
- Liégeois F, Cross JH, Gadian DG et al (2006) Role of fMRI in the decision-making process: epilepsy surgery for children. *J Magn Reson Imaging* 23:933–940
- Rasmussen T, Milner B (1977) The role of early left-brain injury in determining lateralization of cerebral speech functions. *Ann N Y Acad Sci* 30:355–369
- Staudt M, Braun C, Gerloff C et al (2006a) Developing somatosensory projections bypass periventricular brain lesions. *Neurology* 67:522–525
- Staudt M, Erb M, Braun C et al (2006b) Extensive peri-lesional connectivity in congenital hemiparesis. *Neurology* 66:771
- Staudt M, Gerloff C, Grodd W et al (2004a) Reorganization in congenital hemiparesis acquired at different gestational ages. *Ann Neurol* 56:854–863
- Staudt M, Grodd W, Gerloff C et al (2002a) Two types of ipsilateral reorganization in congenital hemiparesis: a TMS and fMRI study. *Brain* 125:2222–2237
- Staudt M, Krägeloh-Mann I, Holthausen H et al (2004b) Searching for motor functions in dysgenic cortex: a clinical TMS and fMRI study. *J Neurosurg* 101:69–77
- Staudt M, Lidzba K, Grodd W et al (2002b) Right-hemispheric organization of language following early left-sided brain lesions: functional MRI topography. *Neuroimage* 16:954–967
- Staudt M, Pieper T, Grodd W et al (2001) Functional MRI in a 6-year-old boy with unilateral cortical malformation: concordant representation of both hands in the unaffected hemisphere. *Neuropediatrics* 32:159–161
- Thickbroom GW, Byrnes ML, Archer SA et al (2001) Differences in sensory and motor cortical organization following brain injury early in life. *Ann Neurol* 49:320–327
- Wilke M, Staudt M, Juenger H et al (2008) Somatosensory system in two types of motor reorganization in congenital hemiparesis: topography & function. *Hum Brain Map* 30:776–788

## 16.1 Introduction

Transcranial magnetic stimulation (TMS) is a noninvasive and painless tool for the electrical stimulation of the human cortex (Barker et al. 1985). TMS depolarizes cortical neurons and can evoke measurable electrophysiological and behavioral effects. TMS is usually applied to one cortical area, but can also be given to two or more areas (i.e., multi-site TMS). Single or paired stimuli and short stimulus trains (i.e., high-frequency bursts) provide a means of transiently disrupting ongoing neuronal processing in the stimulated cortex. Repetitive TMS (rTMS) refers to the application of prolonged trains of stimuli, which are either given continuously as long trains at a constant rate (continuous rTMS), or intermittently as repetitive bursts (i.e., intermittent or burst-like rTMS). rTMS can modify the excitability of the cerebral cortex at the stimulated site and also at remote interconnected brain regions, beyond the time of stimulation. Its neuromodulatory effects make rTMS a valuable tool to study the functional plasticity of neuronal networks and may be used therapeutically in patients with neurological and psychiatric disorders.

### 16.1.1 How Does TMS Excite Cortical Neurons?

TMS causes inductive (electro-magneto-electric) stimulation of neuronal axons. A brief, high-current pulse

is produced in a stimulating coil. The time-varying electrical field produces a time-varying magnetic field with lines of flux oriented perpendicularly to the plane of the coil. The pulsed magnetic field is not attenuated by the skull and induces an electric field in the superficial brain tissue (i.e., cortex), which runs parallel to the plane of the coil but has a direction that is opposite to the electric field in the coil. Hence, the pulsed magnetic field is only used as a means to generate an electric field in the brain that is suprathreshold for exciting cortical axons.

How does the time-varying electrical field induced in the cortex excite neurons? The electrical field induced in the neuronal tissue drives transmembraneous ionic currents. The most relevant parameter is the rate of change of the electric field along the nerve. Depending on the gradient and the orientation of the electric field gradient relative to the course of the axon, the pulsed electrical field may generate an outward current and local depolarization at distinct sites of neuronal axons. If the outward current causes sufficient membrane depolarization, this will trigger an action potential. This action potential propagates along the axon and may cause a transsynaptic excitation of postsynaptic neurons. Crucial for an efficient depolarization of an axon is the spatial gradient of the induced electric field in relation to the orientation of the axon. At the cellular level, the events that lead to neuronal excitation are still poorly understood. For instance, the relevance of cellular and gyral shapes, the grey matter boundaries, the local variations in tissue conductivity, and the role of background neuronal activity for neuronal stimulation are largely unknown.

The majority of studies have investigated the physiological mechanisms of TMS in the human primary motor cortex (M1) because its effects can be quantified by recording the TMS evoked motor potential (MEP).

---

G. Hartwigsen (✉)

Department of Neurology, Neurocenter, University Hospital of Schleswig-Holstein, Schittenhelmstrasse 10, 24105 Kiel, Germany

e-mail: g.hartwigsen@neurologie.uni-kiel.de

For other brain regions, such direct quantification is difficult to obtain. Therefore, researchers have used neuroimaging techniques such as positron emission tomography (PET), electroencephalography (EEG), or functional magnetic resonance imaging (fMRI) to map TMS-evoked changes in regional neuronal activity throughout the brain (Bestmann et al. 2003b; Ilmoniemi et al. 1997; Lee et al. 2003; Massimini et al. 2005; Siebner et al. 2003). These studies have revealed that the TMS-induced changes in regional neuronal activity are not restricted to the stimulated cortex but give rise to functional changes in connected cortical areas, including subcortical brain regions (Bestmann et al. 2003b; Lee et al. 2003; Siebner et al. 2003).

Regarding fMRI, a critical question is whether the blood oxygen level dependent (BOLD) signal really captures the TMS induced changes in regional neuronal activity. Allen et al. (2007) combined optical imaging with electrophysiological recordings of neuronal activity in cat visual cortex to show that TMS-induced changes in neural activity are readily reflected by cerebral hemodynamics. Further, the quantitative coupling between TMS-evoked neural activity and cerebral hemodynamics was present over a range of stimulation parameters. These results demonstrate the usefulness of combined TMS–fMRI studies in humans showing that TMS-induced neural changes are “faithfully reflected in hemodynamic signals” (Allen et al. 2007).

### **16.1.2 Some Physical Aspects of Transcranial Magnetic Stimulation**

The induced magnetic and electric field decreases rapidly with increasing distance from the coil. The maximal depth of penetration depends on the shape and size of the coil, the employed stimulation intensity and the responsiveness of the targeted tissue. The decrease with distance is more rapid for small coils than for large ones. The coil should be placed tangentially on the skin to minimize the coil-cortex distance. Commercially used coils reach a penetration depth of approximately 2–6 cm. This implies that only cortical neuronal tissue is within the range of TMS while deep cerebral grey matter nuclei cannot be stimulated directly with TMS.

In general, TMS does not produce a focal stimulation of neuronal tissue at a small predictable site. The

geometry of the coil is an important factor in determining the magnitude and spatial extent of cortical stimulation. The two most commonly used coil shapes are circular (i.e., referred to as round coil) and figure-of-eight (referred to as figure-of-eight shaped coil or butterfly coil). The circular coil induces a concentric circular electric field. If the coil is placed with its entire surface tangentially to the skin, neuronal structures in the tissue underlying the circular coil will be activated. It should be noted that neuronal stimulation is minimal in the brain tissue underlying the center of the coil when the flat surface of the circular coil is placed on the scalp tangentially to the skin (Weyh and Siebner 2007). The other coil design has a figure-of-eight configuration. Figure-of-eight coils consist of two circular coils placed side by side and are wired such that the current from the stimulator passes in opposite directions in each. This produces a relatively clear defined maximum of the induced current where the two coils approach each other (i.e., in the geometrical center of the coil). With a spatial resolution of approximately 1–1.5 cm, the figure-of-eight coil is substantially more focal than the circular coil. This explains why the figure-of-eight coil is preferred to the round coil when TMS is used to map cortical functions (Walsh and Rushworth 1999). It needs to be borne in mind that commercially available stimulation devices may differ in terms of coil design. This may alter the characteristics of neuronal stimulation, including the heating properties during rTMS and the hardware design (Lang et al. 2006; Weyh et al. 2005).

### **16.1.3 Clinical and Neuroscientific Applications of TMS**

TMS can be used in several ways to study human brain function. Single-pulse or paired-pulse TMS can be applied to probe the excitability of intracortical inhibitory and facilitatory circuits in the motor and visual cortex. Since the action potentials induced by TMS spread along pre-existing axonal connections, TMS induced neuronal excitation is not limited to the stimulated cortex but leads to a transsynaptic spread of excitation to interconnected cortical areas. This renders TMS a very powerful means of studying functional and effective connectivity in the intact human brain (Kobayashi and Pascual-Leone 2003). For instance,

TMS has been extensively used to probe cortico–cortical and cortico–spinal connectivity in the motor system. In clinical neurology, TMS is commonly used as a routine evaluation of the excitability and conductivity of corticospinal pathways.

TMS can induce a transient dysfunction in the stimulated cortex (i.e., a “virtual lesion”). When being applied in its “virtual lesion” mode during an experimental task, TMS may produce measurable changes in task performance. These changes in behavior can be used to make inferences about the importance of the stimulated brain area for a specific cognitive, sensory or motor function (Walsh and Cowey 2000; Walsh and Rushworth 1999). Various rTMS protocols are being increasingly used by clinicians and neuroscientists to induce lasting changes in the status of the human brain (Siebner and Rothwell 2003). Conventional rTMS protocols consist of a continuous series of pulses with constant repetition rates. In the “continuous mode” of rTMS, stimulation rates of around 1 Hz are referred to as *low-frequency rTMS*, and stimulation rates between 5–50 Hz as *high-frequency rTMS*. Most studies regarding the motor cortex suggest inhibitory effects of low-frequency rTMS and facilitatory effects of high-frequency rTMS (Berardelli et al. 1998; Chen et al. 1997a; Pascual-Leone et al. 1998). Recent protocols use more complex temporal stimulation patterns such as double-pulse rTMS (Thickbroom et al. 2006), quadro-pulse rTMS (Hamada et al. 2007), or theta burst stimulation (TBS) which gives short, high-frequency *bursts* of pulses every 0.2 s (Huang et al. 2005). Ongoing research addresses the question whether the neuromodulatory effects of these rTMS protocols may have a therapeutic application in neurological and psychiatric disorders (Wassermann and Lisanby 2001).

TMS can be applied while subjects perform an experimental task (*online TMS*) or shortly before they perform the task (*offline TMS*). Offline TMS usually involves an rTMS protocol that induces a lasting alteration of cortical excitability, while online TMS may consist of single pulses or short high-frequency trains that are given at distinct time-points during task performance. Both approaches allow the testing of the functional relevance of the targeted brain area by measuring the acute (*online TMS*) or conditioning (*offline TMS*) effects of TMS on electrophysiological measures (e.g., the MEP amplitude), behavioral measures (e.g., response latencies or error rate) or more directly on regional brain activity using brain mapping techniques such as EEG, PET, or fMRI.

### 16.1.4 Adverse Effects and Safety Precautions

TMS has the capability of producing adverse effects, especially if rTMS is used. These side effects are extensively discussed in a recent review (Wassermann 2008). The most relevant adverse effect is the induction of epileptic seizures. Since rTMS induces stronger and more persistent effects on cortical excitability and function than single-pulse TMS, it bears a higher risk of provoking epileptic seizures even in healthy individuals. Therefore, safety guidelines were established which specify the maximal number of pulses per session, stimulus intensity and frequency that are considered to be safe in terms of seizure induction (Chen et al. 1997b; Wassermann 1998). Since the introduction of the safety guidelines, only a few cases of accidental seizures with TMS have been reported worldwide, and none of the individuals who had experienced rTMS-induced seizures has suffered lasting physical sequelae.

The rapid discharge through the coil produces a characteristic clicking sound in the frequency range of 2–7 kHz. The click is caused by mechanical deformation of the coil during the strong magnetic pulses. Peak sound pressure has been reported to be 120–130 dB at a distance of 10 cm from the coil (Starck et al. 1996). Sound levels will be higher when TMS is given inside the MRI bore because of the additional magnetic field generated by the MR scanner. Therefore, individuals who receive rTMS or are examined in the MR scanner should always wear ear plugs (cf. Sect. 16.3.2.1).

## 16.2 Placement of the Coil Over the Cortical Target Area

Accurate placement of the TMS coil over the cortex area that is to be stimulated with TMS is crucial. The motor response that is evoked by TMS can be used to localize the primary motor cortex. A similar approach can be chosen for TMS of the visual cortex by positioning the coil at the site where TMS most reliably elicits a phosphene. In both instances, TMS produces an overt response which can be used to functionally determine the appropriate site of stimulation. For most remaining cortical areas, no such responses can be elicited and other strategies have to be used to accurately place the coil over the cortical target.

Some researchers use the optimal site to stimulate the primary motor cortex as “anchor point” for the stimulation of pericentral cortical areas such as premotor or somatosensory areas (Gerschlagler et al. 2001; Koch et al. 2006; Lee and van Donkelaar 2006). However, this method is not sufficiently accurate for targeting more distant areas such as the dorsolateral prefrontal cortex (Bohning et al. 2003b).

The International 10–20 system for the placement of EEG electrodes (Jasper 1958) is often used for positioning of the TMS coil. The 10–20 system offers a grid of electrode sites located on the scalp that is derived from standard cranial landmarks, i.e., theinion, nasion, or preauricular points. This method assumes a consistent correlation between scalp locations and underlying brain structures across subjects. Greater accuracy can be obtained by acquiring structural MR images of the brain together with capsules containing a high-contrast marker attached to the head (Terao et al. 1998). The placement of the coil can then be referenced to the position of the marker.

Neuronavigated TMS guided by frameless stereotaxy represents the method of choice as it allows both, exact placement and monitoring of the coil throughout the TMS experiment (Denslow et al. 2005a; Herwig et al. 2003a; Neggens et al. 2004; Sack et al. 2006; Schonfeldt-Lecuona et al. 2005). Optical (infrared based) and acoustic (ultrasound based) devices are available for neuronavigation. These systems use passive (reflecting) or active (emitting) markers which are attached to the subject’s head and to the TMS coil (Ettinger et al. 1998). Sparing et al. (2008) compared different methods for the placement of the TMS coil over the primary motor cortex in terms of accuracy. The least accurate results were obtained when the 10–20 EEG system or function-guided procedures were used, although there was a great variation among different electrode positions as some can be located more reliably than others. In that study, fMRI guided neuronavigated stimulation yielded the highest spatial accuracy in the range of a few millimeters. Other studies have confirmed these results (Denslow et al. 2005a; Herwig et al. 2003b; Schonfeldt-Lecuona et al. 2005).

Neuronavigation requires a T1-weighted, high-resolution image of the subject’s brain. The anatomical images have to be transferred into three-dimensional space. Optionally, individual fMRI activation maps can be overlaid on the structural images. Predefined

anatomical landmarks are marked on the individual structural MRI with special neuronavigation software. Usually, the nasion, the nibs of the tragus of both ears, and the internal angle of the eyes are used. A headband is then strapped around the subject’s head. A tracker with at least three passive spheres or ultrasound reflecting transmitters is firmly attached to the headband, indicating the position of the subject’s head. Another tracker is fixed onto the TMS coil. These dynamic reference systems provide online information about the location of the head and the coil in space. A camera system detects the position of the dynamic reference systems and displays this information on a computer screen using navigation software for visual localization of the coil (see Fig. 16.1).

The subject’s head and the structural MR scans are coregistered by touching the predefined landmarks on the subject’s face using a pointer equipped with trackers. An accurate coregistration procedure is crucial to exact placement of the coil. The position of the coil is visualized in realtime on a computer screen relative to the individual three-dimensional anatomy of the brain. The exact position of the cortical target area can be defined either anatomically based on the gyral anatomy or functionally on the basis of activation maps that have been obtained with fMRI. In addition to the individual activation map, one can also use the stereotactic coordinates of a peak activation that has been identified in a group of subjects. In this instance, the coordinates from standardized space (MNI, Talairach) have to be transformed to the subject’s “native” space.

## 16.3 Combinations of fMRI with TMS

### 16.3.1 Why Combine TMS with fMRI?

fMRI provides a sensitive means of identifying brain regions where regional neuronal activity correlates with behavior. Due to its correlative nature, fMRI based activation maps cannot establish whether such activation makes a relevant contribution to the behavior. By temporarily disrupting ongoing neural activity, TMS permits to make causal inferences regarding the contribution of the stimulated cortex to a specific brain function. Since single-pulse TMS offers a high temporal resolution it can also be used to identify the period



**Fig. 16.1** Neuronavigated TMS guided by frameless stereotaxy. A tracker with three passive spheres is attached to the headband of the subject (a), to the TMS coil (b), and fixed on a pointer (c). These dynamic reference systems provide online information

about the location of the head and the coil in space. A camera system (d) detects the position of the dynamic reference systems and displays this information on a computer screen using navigation software for visual localization of the coil

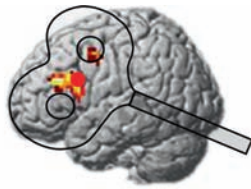
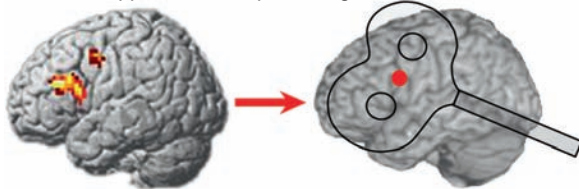
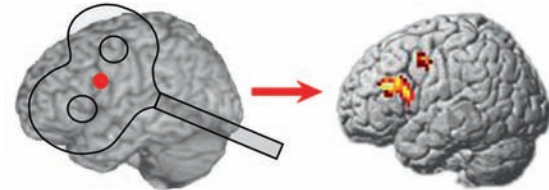
during which the stimulated area makes a critical contribution to the experimental task. Thus, combined TMS and fMRI gives access to noninvasive measuring of stimulation effects on the brain with a high spatial (fMRI: spatial resolution in the millimeter range) and temporal (single-pulse TMS: temporal resolution in the order of milliseconds) resolution.

The temporal relationship between TMS and fMRI defines which question can be addressed using a combined TMS–fMRI approach. TMS can be given in the MR scanner during fMRI data acquisition (online approach) to investigate the immediate effects of TMS on brain activity and behavior. Alternatively, TMS and

fMRI may be separated in space and time (offline approach). In this case, TMS is given outside the MRI suite before or after fMRI (see Fig. 16.2).

### 16.3.2 TMS in the MR Scanner During fMRI (Online TMS–fMRI Approach)

TMS during fMRI (interleaved TMS–fMRI) enables the researcher to probe the immediate impact of TMS on regional neuronal activity across the whole brain. By applying TMS during different functional states of

**a** “Online” approach: concurrent TMS & fMRI**b** “Offline” approach: fMRI preceding TMS**c** “Offline” approach: TMS preceding fMRI

**Fig. 16.2** Relative timing of TMS and fMRI determines the application of combined TMS–fMRI. TMS and fMRI can be performed interleaved, (i.e., “online” approach) to investigate immediate effects of TMS on brain functions (a). In the “offline” approach, fMRI precedes or follows TMS. fMRI preceding TMS is usually used to identify appropriate sites for focal TMS (b), while TMS preceding fMRI can be used to probe the lasting effects of TMS conditioning on brain functions (c)

the brain, the online TMS–fMRI approach can explore how the TMS influences on neuronal activity in the stimulated and distant areas vary with task demands.

### 16.3.2.1 Methodological Issues

Although the prerequisites to apply TMS during fMRI were already introduced by Bohning et al. (1997, 1998, 1999) approximately 10 years ago, interleaved TMS–fMRI failed to become a routine procedure yet. At present, most of the studies that used interleaved TMS–fMRI were carried out by three research groups in Charleston (North Carolina, USA), Göttingen (Germany), and London (UK) (for details, see Table 16.1). A simple implementation of TMS in the MRI environment is precluded by problems originating from the application of

magnetic pulses in the static magnetic field of the MR scanner and in the presence of magnetic field gradients required for image acquisition (Baudewig et al. 2001). Therefore, nonferromagnetic coils have to be used which are mechanically strengthened to prevent coils from breaking during fMRI. Subjects have to wear ear plugs and headphones because mechanical interactions between the TMS evoked local magnetic field and the static magnetic field of the MR scanner result in a louder click when the coil is discharged inside the scanner. The presence of the MR-compatible TMS coil may cause geometric image distortions (Baudewig et al. 2000; Bestmann et al. 2003a). These can be reduced by a shorter read-out time of echo-planar imaging (EPI) sequences, the use of stronger imaging gradients and parallel imaging.

The ferromagnetic stimulation device must be placed at sufficient distance from the magnetic field of the MR scanner, outside the scanner room or in a radiofrequency-shielded cabinet inside the scanner room. This requires a longer cable to connect the coil with the stimulator.

MR-compatible TMS coil holders help to ensure accurate placement of the coil inside the scanner. Yet spatial limitations imposed by the MR head coil may restrict the access to some cortical areas, especially in the basal, frontal and temporal lobe. TMS also evokes twitches of cranial muscles, somatosensory and auditory stimulation which may cause discomfort, movement artifacts and contribute to functional brain activation. Nonspecific auditory and somatosensory stimulation as well as the unpleasantness of TMS complicate the interpretation of TMS-induced brain activation by causing BOLD signal changes in subcortical and cortical areas involved in sensory or affective processing (Bestmann et al. 2005). It is therefore advisable to include a control condition which matches the auditory and somatosensory stimulation but does not cause transcranial cortical stimulation. Alternatively, the same TMS protocol might be applied to a control area in a separate fMRI session.

Dynamic artifacts pose a major problem to concurrent TMS during fMRI. Radiofrequency (RF) noise can markedly reduce the signal-to-noise ratio of MR images. TMS stimulators may themselves produce RF noise, and the antenna-like properties of the TMS coil cable can additionally guide RF noise into the scanner which can be reduced by customized RF filters. Leakage-currents that originate from the high-voltage capacitors of the TMS stimulator may induce additional image distortions and artifacts. Of note, these leakage-currents

**Table 16.1** Studies using interleaved TMS-fMRI in healthy volunteers

Target area	Task	TMS-fMRI protocol (frequency; %MT; total no. of pulses per train /session)	Reference
Left M1	Rest	0.83 Hz; 110; 20/session	Bohning et al. (1998)
Left M1	Rest	1 Hz; 80/110; 18/session	Bohning et al. (1999)
Left M1	Rest/finger movements	1 Hz; 110; 21/train	Bohning et al. (2000a)
Left M1	Rest	SP; 120; 15/session	Bohning et al. (2000b)
Left M1	Rest/finger movements	10 Hz; 110; 10/train	Baudewig et al. (2001)
Left PMd		10 Hz; 90/110; 10/train	
Left PFC	Rest	1 Hz; 80/100/120; 21/train	Nahas et al. (2001)
Left M1/S1	Rest	4 Hz; 90/110/110 AMT; 40/train	Bestmann et al. (2003b)
Left M1	Rest	1 Hz; 110; <i>not reported</i>	Bohning et al. (2003a)
Left M1	Rest	1 Hz; 120; 1,2,4,8,16,24/train	Bohning et al. (2003c)
Left M1	Rest	4 Hz; 150; 4/train	Kemna and Gembris 2003
Left M1	Rest	1 Hz; 110; 21/train	McConnell et al. (2003)
Left M1	Rest	3.1 Hz; 90/110 AMT; 30/session	Bestmann et al. (2004)
Left M1/S1	Rest/finger movements	1 Hz; 110; 21/train	Denslow et al. (2004)
Left PFC	Rest	1 Hz; 100; 21/session	Li et al. (2004a) <sup>a</sup>
Left M1	Rest	1 Hz; 110/120; <i>not reported</i>	Li et al. (2004b)
Left PFC			
Left PMd	Rest/finger movements	3 Hz; 90/110 AMT; <i>not reported</i>	Bestmann et al. (2005)
Left M1	Rest/finger movements	1 Hz; 110; 21/train	Denslow et al. (2005a)
Left M1	Rest	1 Hz; 110; 21/train	Denslow et al. (2005b)
Left M1	Rest	SP; ~90; 98/102; 110 SoM; 20; 40/session	Bestmann et al. (2006) <sup>b</sup>
Right FEF	Rest/visual judgement	9 Hz; 40/55/70/85 TOP; 10 Hz; 65 TOP; 5/train	Ruff et al. (2006)
Left PMd	Isometric left hand grips	11 Hz; 70/110; 5/train	Bestmann et al. (2007)
Left/right SPL	Visuospatial tasks	13.3 Hz; 100 TOP; 5/train	Sack et al. (2007)
Right IPS/FEF	Visual task (moving stimuli)	9 Hz; 40/55/70/85 TOP; 5/train	Ruff et al. (2008)

AMT active motor threshold; FEF frontal eye field; IPS intraparietal sulcus; M1 primary motor cortex; PFC prefrontal cortex; PMd dorsal premotor cortex; RMT resting motor threshold; SoM Sense of movement; SP single pulse; TOP total output

<sup>a</sup>Depressive patients

<sup>b</sup>Amputee patient

change with the intensity of TMS, and can give rise to intensity-dependent BOLD signal changes. Remote-controlled high-voltage relay-diode systems reduce leakage-currents flowing between the stimulator and the TMS coil and can thus be used to resolve this problem (Bestmann et al. 2007).

The strong magnetic pulses induced by TMS can severely distort MR images depending on TMS coil orientation, TMS pulse intensity, and MR magnetic field strength (Bestmann et al. 2003a; Shastri et al. 1999). Therefore, a direct interference between TMS pulse and EPI excitation pulses should be avoided, and images being perturbed by TMS pulses must be replaced (Bestmann et al. 2008). A feasible solution to this problem is to introduce a sufficiently long temporal gap between TMS pulses and subsequent MR image acquisition (for more technical details see Baudewig and Bestmann 2007; Bestmann et al. 2008).

### 16.3.2.2 Applications of Interleaved TMS-fMRI

Several researchers applied TMS over the motor cortex during rest and showed that TMS induced acute changes in BOLD signal in a dose-dependent fashion (Baudewig et al. 2001; Bestmann et al. 2003a, 2004; Bohning et al. 1998, 1999, 2000b). A single TMS pulse evoked regional increases in BOLD signal which were similar to those evoked by volitionally movements (Bohning et al. 2000b). Such BOLD signal increases were only observed at suprathreshold intensities which evoked a muscle twitch in the contralateral hand. Hence, it remains unclear whether the observed activation was directly induced by cortical stimulation or resulted from somatosensory feedback activation caused by the TMS-induced movement. However, Bestmann et al. (2005) applied short trains of 3 Hz rTMS over the left premotor cortex which produced an increase in BOLD

signal in the stimulated cortex and connected areas. Since the premotor TMS train did not produce overt muscle movements, it was concluded that these BOLD signal changes resulted from cortical stimulation rather than from somatosensory feedback activation.

Interleaved TMS–fMRI studies revealed that TMS can evoke changes in neural activity in connected cortical and subcortical areas (Baudewig et al. 2001; Bestmann et al. 2004, 2005; Bohning et al. 1998, 1999, 2000a; Ruff et al. 2008). These distant BOLD signal changes can occur even in the absence of consistent signal changes in the area that was directly targeted by TMS (Bestmann et al. 2004). This suggests that transsynaptic spread of excitation from the stimulated to connected brain areas makes a major contribution to neuronal stimulation that is induced by TMS in the human brain.

Interleaved TMS–fMRI opens up the possibility to examine how TMS interacts with intrinsic task-related activation and how these TMS-induced changes in task-related activity relate to changes in behavior. In a recent study, parietal rTMS was performed during fMRI to map TMS-induced changes in task-related brain activity that underly the TMS-induced impairment of visuospatial judgements (Ruff et al. 2008). Concurrent TMS–fMRI was employed, to investigate the influences of a short high-frequency rTMS train over the right frontal eye field (FEF) or intraparietal sulcus, on the BOLD response in occipital activity to visual stimulation. The authors showed that TMS induced changes in occipital activity critically depend on the actual state of the visual system at the time of TMS. Increased activity over visual area V5/MT+ was only found if moving stimuli were concurrently presented. Conversely, visual areas V1–V4 were specifically activated during the absence of input.

So far, very few interleaved TMS–fMRI studies have been carried out in patients. In a case study, Bestmann et al. (2006) investigated TMS induced activity changes in distinct cortical areas of an amputee. At an intermediate stimulus intensity, TMS over the motor hand representation contralateral to amputation, elicited a phantom sensation of a movement in half of the trials without producing overt activity in remaining muscles. The authors compared event-related BOLD signal changes in trials with versus without a phantom sensation of movement. Because the settings of TMS were identical, this comparison subtracted out any nonspecific TMS effects on regional neuronal activity. The sensation of a phantom movement was associated with increased activity in

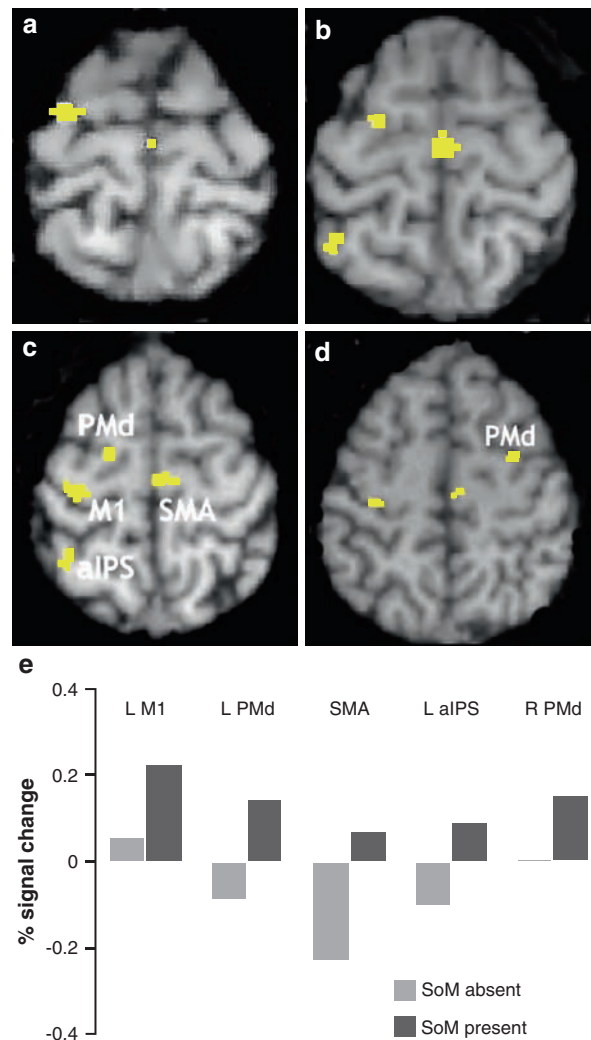


**Fig. 16.3** Activity changes for the comparison of trials with vs. without SoM reported, at intermediate TMS intensities (SPM(T) thresholded at  $T \geq 3$ ). When a conscious phantom SoM was perceived, activity increases were observed in several motor-related regions, including the left (stimulated) M1, left and right PMd, left anterior intraparietal sulcus (aIPS), and caudal SMA. Note that the intermediate stimulation intensities applied were held constant in this contrast, and were below threshold for evoking peripheral muscle responses. The results are displayed on the patient's anatomical T1-weighted MRI: (a) transverse section,  $z = 72$ ; (b)  $z = 67$ ; (c)  $z = 62$ ; (d)  $z = 57$ ; (e) fMRI percent signal change with respect to the session mean in peaks from these five motor-related regions (left M1, left and right PMd, SMA, left aIPS), for trials with or without evoked phantom SoM experienced. Reprinted from *Neuropsychologia*, 44 (14), Bestmann et al., Cortical correlates of TMS-induced phantom hand movements revealed with concurrent TMS–fMRI, pp. 2959–71, 2006, with permission from Elsevier

primary motor cortex, dorsal premotor cortex, anterior intraparietal sulcus, and caudal supplementary motor

area. Based on these results, it was argued that activity in these frontoparietal areas represents the neuronal correlate of the phantom sense of movement (see Fig. 16.3 for details). Concurrent TMS–fMRI may also be of value to study how “therapeutic” rTMS protocols acutely change neuronal activity in functional brain networks. For instance, fMRI has been used to probe the immediate effects of continuous 1 Hz TMS at 100% MT over the left dorsolateral prefrontal cortex in 14 patients with major depression (Li et al. 2004a).

### 16.3.3 Offline combination of TMS and fMRI

#### 16.3.3.1 TMS Following fMRI

There is consensus that fMRI can reliably identify brain regions in which increases in BOLD signal are correlated with the performance of an experimental task. Yet, the correlational nature of fMRI provides no information about the functional contribution of any activated brain region to the task. This question can be addressed using TMS. TMS can be applied over the area of interest to disrupt neuronal processing while participants perform the same experimental task. If the TMS-induced local perturbation affects task performance, this is taken as evidence that the stimulated cortical area is functionally relevant.

An elegant illustration of this approach was provided by Cohen and colleagues in a TMS study on blind subjects (Cohen et al. 1997). Previous neuroimaging studies had shown that Braille reading consistently activated visual cortical areas in blind subjects but not in those with sight. To investigate the significance of task-related activation in the occipital cortex, short trains of 10 Hz rTMS were given to several brain regions time-locked to Braille reading. Occipital rTMS induced errors and distorted the tactile perceptions of congenitally blind subjects, but had no effects on tactile performance in normal-sighted. This finding proved that the occipital visual cortex makes a relevant contribution to the processing of tactile input in blind subjects.

Functional MRI can be used to functionally localize the optimal site for TMS. In a study by Neggers and colleagues (2007), participants first performed a saccade task during fMRI. In each subject, the individual peak activation in the precentral sulcus was

identified and superimposed on the structural image of the subject’s brain. Then, frameless stereotaxy was used to place the coil over the fMRI defined FEF. This fMRI guided stereotactic approach is likely to be more precise than relying on structural anatomical landmarks because it takes into account the inter-individual variability of the functional representation of the FEF in the precentral cortex. An alternative strategy uses the results of a previous fMRI study that has used the same or a similar experimental task. The stereotactic coordinates of task-related peak activation in the area of interest define the site of stimulation. The individual site of stimulation is determined by using the inverse of the normalization transformation and transforming the coordinates from standard to “individual” space. Considering the high inter-individual variability of the therapeutic effects of rTMS in psychiatric and neurological disorders (e.g., Gross et al. 2007; Lefaucheur et al. 2007; Ridding and Rothwell 2007), the use of fMRI-guided TMS which takes into account the functional neuroanatomy of each individual may also increase the efficacy of rTMS as a therapeutic tool.

#### 16.3.3.2 fMRI Following TMS

Another way to combine rTMS and fMRI is to apply rTMS before fMRI. Here rTMS is used to induce an acute reorganization in the human brain (Siebner and Rothwell 2003). After rTMS, fMRI is performed to map the lasting functional impact of rTMS on task-related neuronal activity at a system level (O’Shea et al. 2007; Rounis et al. 2007). Performing fMRI after rTMS outside the scanner does not require specific methodological precautions because rTMS and fMRI are separated in space and time. This *condition-and-map approach* can be used to study the changeability of functional brain networks. Preferably, fMRI should start as quickly as possible after rTMS to capture the transient effects of rTMS (Baudewig and Bestmann 2007). The conditioning effects of rTMS on regional neuronal activity can be detected by comparing task-related activation before and after rTMS. It is important to control unspecific changes in task related activity that are simply due to the repetition of the experimental task in the MR scanner. This can be achieved by introducing a second session during which sham rTMS is given to the cortical target area. Sham rTMS should match real rTMS in terms of auditory and

**Table 16.2** Studies performing fMRI after a conditioning session of rTMS

Target area	Task during fMRI	TMS protocol (frequency; %RMT; total no. of pulses/session)	Reference
Left S1	Rest	5 Hz; 90; 2,500	Tegenthoff et al. (2005)
Left IFG	Semantic object classification	10 Hz; 110; 300	Wig et al. (2005)
Left S1	Tactile frequency discrimination	5 Hz; 90; 1,250	Pleger et al. (2006)
Right vs. Left DLPFC	Cued choice reaction	5 Hz; 90 AMT; 1,800	Rounis et al. (2006)
Left PFC	Face-name memory	5 Hz; 80; 500	Sole-Padullés et al. (2006) <sup>a</sup>
Right PFC	Tower of London	1 Hz; 110; 720 vs. 10 Hz; 100; 1,500	Fitzgerald et al. (2007) <sup>b</sup>
Left PMd, Left SM	Action selection	1 Hz; 90 AMT; 900	O'Shea et al. (2007)
Left DLPFC	Emotional stimuli	5 Hz; 120; 3,750	Cardoso et al. (2008) <sup>c</sup>
Right FEF	Saccade-fixation	30 Hz TBS; 80; 600	Hubl et al. (2008)
Contrales. M1	Hand grip movements	1 Hz; 100; 600	Nowak et al. (2008) <sup>d</sup>
Right M1	Sequential finger motor task, noxious tactile stimuli	10 Hz; 90; 1,000	Yoo et al. (2008)

AMT active motor threshold; DLPFC dorsolateral prefrontal cortex; FEF frontal eye field; IFG inferior frontal gyrus; M1 primary motor cortex; PFC prefrontal cortex; PMd dorsal premotor cortex; RMT resting motor threshold; S1 primary somatosensory cortex; SM sensorimotor cortex; TBS theta burst stimulation

<sup>a</sup>Elderly subjects with memory complaints

<sup>b</sup>Patients with treatment-resistant depression

<sup>c</sup>Depressive patients with Parkinson's disease

<sup>d</sup>Stroke patients

somatosensory stimulation but without inducing transcranial stimulation of the cortex. Alternatively, the same effective rTMS protocol might be applied to a second (control) area. A change in the pattern of activation after rTMS but not after control rTMS indicates a true reorganization in response to rTMS conditioning. The task specificity of functional reorganization can be shown by having participants perform a control task during the same fMRI session.

The condition-and-map approach has mostly been applied to study functional plasticity in healthy volunteers (see Table 16.2). For example, a recent study investigated the modulation and reorganization of networks associated with sensory perception and motor performance after subthreshold high-frequency (10 Hz, 90% resting motor threshold) rTMS of the right primary motor hand area (Yoo et al. 2008). Using a sham-controlled within-subject design, BOLD signal change during a sequential finger motor task and noxious tactile stimulation of the left hand were assessed before and after real and sham rTMS. Compared to sham rTMS, real rTMS led to increased activation in the motor network which was associated with enhanced motor performance. On the other hand, real rTMS caused deactivation in the sensory network which correlated with an increase in tactile sensory threshold. In another study, fMRI used in healthy right handers to

probe short-term reorganization in right PMd after 1 Hz rTMS induced a lasting disruption of neuronal processing in the dominant left PMd specialized for action selection (O'Shea et al. 2007). 1 Hz rTMS specifically increased activity in right PMd and connected medial premotor areas during action selection without affecting behavior. Based on additional experiments, it was claimed that, this increase in activity reflects compensatory short-term reorganization, that helps to preserve behavior after the "neuronal challenge" induced by rTMS.

To date patients have been rarely studied with the offline combination of rTMS and fMRI (Cardoso et al. 2008; Fitzgerald et al. 2007; Nowak et al. 2008). However, a large number of condition-and-map studies used offline rTMS followed by PET in patients with neurological and psychiatric disorders such as tinnitus (Richter et al. 2006; Smith et al. 2007), depression (Kuroda et al. 2006; Peschina et al. 2001; Speer et al. 2000), schizophrenia (Langguth et al. 2006), dystonia (Siebner et al. 2003) or Parkinson's disease (Strafella et al. 2005). These studies have shown that the condition-and-map approach is important to advance our understanding of the therapeutic effects of rTMS as well as the underlying pathological brain mechanisms and should encourage investigators to perform fMRI after rTMS in patients.

## 16.4 Conclusion

TMS can be used concurrently with fMRI (online approach), or it can be given before or after fMRI (offline approach). While online TMS during fMRI is technically demanding and requires specific safety precautions, the offline TMS before or after fMRI approach outside the MR scanner can be easily performed. The relative timing between TMS and fMRI defines the scientific and clinical questions that can be tackled with the combined TMS-fMRI approach. This approach provides unique opportunities to explore the dynamic aspects of functional neuronal networks in space and time, and how these functional interactions are affected by disease. It also bears great potential for studying the physiological impact of TMS on the human brain. This knowledge will be crucial to the increased efficacy of TMS as a therapeutic tool.

## References

- Allen EA, Pasley BN, Duong T et al (2007) Transcranial magnetic stimulation elicits coupled neural and hemodynamic consequences. *Science* 317:1918–1921
- Barker AT, Jalinous R, Freeston IL (1985) Non-invasive magnetic stimulation of human motor cortex. *Lancet* 1:1106–1107
- Baudewig J, Bestmann S (2007) Transkranielle Magnetstimulation und funktionelle Magnetresonanztomographie [Transcranial magnetic stimulation and functional magnetic resonance tomography]. In: Siebner HR, Ziemann U (eds) *Das TMS-Buch* [The TMS book]. Springer, Heidelberg
- Baudewig J, Paulus W, Frahm J (2000) Artifacts caused by transcranial magnetic stimulation coils and EEG electrodes in T(2)\*-weighted echo-planar imaging. *Magn Reson Imaging* 18:479–484
- Baudewig J, Siebner HR, Bestmann S et al (2001) Functional MRI of cortical activations induced by transcranial magnetic stimulation (TMS). *Neuroreport* 12:3543–3548
- Berardelli A, Inghilleri M, Rothwell JC et al (1998) Facilitation of muscle evoked responses after repetitive cortical stimulation in man. *Exp Brain Res* 122:79–84
- Bestmann J, Ruff CC, Diver J et al (2008) Concurrent TMS and functional magnetic resonance imaging: methods and current advances. In: Wassermann EM, Epstein CM, Ziemann U (eds) *The Oxford handbook of transcranial stimulation* Oxford University Press, New York
- Bestmann S, Baudewig J, Frahm J (2003a) On the synchronization of transcranial magnetic stimulation and functional echo-planar imaging. *J Magn Reson Imaging* 17:309–316
- Bestmann S, Baudewig J, Siebner HR et al (2003b) Subthreshold high-frequency TMS of human primary motor cortex modulates interconnected frontal motor areas as detected by interleaved fMRI-TMS. *Neuroimage* 20:1685–1696
- Bestmann S, Baudewig J, Siebner HR et al (2004) Functional MRI of the immediate impact of transcranial magnetic stimulation on cortical and subcortical motor circuits. *Eur J Neurosci* 19:1950–1962
- Bestmann S, Baudewig J, Siebner HR et al (2005) BOLD MRI responses to repetitive TMS over human dorsal premotor cortex. *Neuroimage* 28:22–29
- Bestmann S, Oliviero A, Voss M et al (2006) Cortical correlates of TMS-induced phantom hand movements revealed with concurrent TMS-fMRI. *Neuropsychologia* 44:2959–2971
- Bestmann S, Swayne O, Blankenburg F et al (2007) Dorsal premotor cortex exerts state-dependent causal influences on activity in contralateral primary motor and dorsal premotor cortex. *Cereb Cortex* 18(6):1281–1291
- Bohning DE, Pecheny AP, Epstein CM et al (1997) Mapping transcranial magnetic stimulation (TMS) fields in vivo with MRI. *Neuroreport* 8:2535–2538
- Bohning DE, Shastri A, Nahas Z et al (1998) Echoplanar BOLD fMRI of brain activation induced by concurrent transcranial magnetic stimulation. *Invest Radiol* 33:336–340
- Bohning DE, Shastri A, McConnell KA et al (1999) A combined TMS/fMRI study of intensity-dependent TMS over motor cortex. *Biol Psychiatry* 45:385–394
- Bohning DE, Shastri A, McGavin L et al (2000a) Motor cortex brain activity induced by 1-Hz transcranial magnetic stimulation is similar in location and level to that for volitional movement. *Invest Radiol* 35:676–683
- Bohning DE, Shastri A, Wassermann EM et al (2000b) BOLD-fMRI response to single-pulse transcranial magnetic stimulation (TMS). *J Magn Reson Imaging* 11:569–574
- Bohning DE, Denslow S, Bohning PA et al (2003a) Interleaving fMRI and rTMS. *Suppl Clin Neurophysiol* 56:42–54
- Bohning DE, Denslow S, Bohning PA et al (2003b) A TMS coil positioning/holding system for MR image-guided TMS interleaved with fMRI. *Clinical Neurophysiology* 114:2210–2219
- Bohning DE, Shastri A, Lomarev MP et al (2003c) BOLD-fMRI response vs. transcranial magnetic stimulation (TMS) pulse-train length: testing for linearity. *J Magn Reson Imaging* 17:279–290
- Cardoso EF, Fregni F, Martins Maia F et al (2008) rTMS treatment for depression in Parkinson's disease increases BOLD responses in the left prefrontal cortex. *Int J Neuropsychopharmacol* 11:173–183
- Chen R, Classen J, Gerloff C et al (1997a) Depression of motor cortex excitability by low-frequency transcranial magnetic stimulation. *Neurology* 48:1398–1403
- Chen R, Gerloff C, Classen J et al (1997b) Safety of different inter-train intervals for repetitive transcranial magnetic stimulation and recommendations for safe ranges of stimulation parameters. *Electroencephalogr Clin Neurophysiol* 105:415–421
- Cohen LG, Celnik P, Pascual-Leone A et al (1997) Functional relevance of cross-modal plasticity in blind humans. *Nature* 389:180–183
- Denslow S, Lomarev M, Bohning DE et al (2004) A high resolution assessment of the repeatability of relative location and intensity of transcranial magnetic stimulation-induced and volitionally induced blood oxygen level-dependent response in the motor cortex. *Cogn Behav Neurol* 17:163–173
- Denslow S, Bohning DE, Bohning PA et al (2005a) An increased precision comparison of TMS-induced motor cortex BOLD

- fMRI response for image-guided versus function-guided coil placement. *Cogn Behav Neurol* 18:119–126
- Denslow S, Lomarev M, George MS et al (2005b) Cortical and subcortical brain effects of transcranial magnetic stimulation (TMS)-induced movement: an interleaved TMS/functional magnetic resonance imaging study. *Biol Psychiatry* 57:752–760
- Ettlinger GJ, Leventon ME, Grimson WE et al (1998) Experimentation with a transcranial magnetic stimulation system for functional brain mapping. *Med Image Anal* 2:133–142
- Fitzgerald PB, Sriharan A, Daskalakis ZJ et al (2007) A functional magnetic resonance imaging study of the effects of low frequency right prefrontal transcranial magnetic stimulation in depression. *J Clin Psychopharmacol* 27:488–492
- Gerschlagner W, Siebner HR, Rothwell JC (2001) Decreased corticospinal excitability after subthreshold 1 Hz rTMS over lateral premotor cortex. *Neurology* 57:449–455
- Gross M, Nakamura L, Pascual-Leone A et al (2007) Has repetitive transcranial magnetic stimulation (rTMS) treatment for depression improved? A systematic review and meta-analysis comparing the recent vs. the earlier rTMS studies. *Acta Psychiatr Scand* 116:165–173
- Hamada M, Hanajima R, Terao Y et al (2007) Quadro-pulse stimulation is more effective than paired-pulse stimulation for plasticity induction of the human motor cortex. *Clin Neurophysiol* 118:2672–2682
- Herwig U, Abler B, Schonfeldt-Lecuona C et al (2003a) Verbal storage in a premotor-parietal network: evidence from fMRI-guided magnetic stimulation. *Neuroimage* 20:1032–1041
- Herwig U, Satrapi P, Schonfeldt-Lecuona C (2003b) Using the international 10–20 EEG system for positioning of transcranial magnetic stimulation. *Brain Topogr* 16:95–99
- Huang YZ, Edwards MJ, Rouinis E et al (2005) Theta burst stimulation of the human motor cortex. *Neuron* 45:201–206
- Hubl D, Nyffeler T, Wurtz P et al (2008) Time course of blood oxygenation level-dependent signal response after theta burst transcranial magnetic stimulation of the frontal eye field. *Neuroscience* 151:921–928
- Ilmoniemi RJ, Virtanen J, Ruohonen J et al (1997) Neuronal responses to magnetic stimulation reveal cortical reactivity and connectivity. *Neuroreport* 8:3537–3540
- Jasper HH (1958) The ten-twenty electrode system of the International Federation. *Electroencephalogr Clin Neurophysiol* 10:367–380
- Kemna LJ, Gembris D (2003) Repetitive transcranial magnetic stimulation induces different responses in different cortical areas: a functional magnetic resonance study in humans. *Neurosci Lett* 336:85–88
- Kobayashi M, Pascual-Leone A (2003) Transcranial magnetic stimulation in neurology. *Lancet Neurol* 2:145–156
- Koch G, Franca M, Albrecht UV et al (2006) Effects of paired pulse TMS of primary somatosensory cortex on perception of a peripheral electrical stimulus. *Exp Brain Res* 172:416–424
- Kuroda Y, Motohashi N, Ito H et al (2006) Effects of repetitive transcranial magnetic stimulation on [<sup>11</sup>C]raclopride binding and cognitive function in patients with depression. *J Affect Disord* 95:35–42
- Langguth B, Eichhammer P, Zowe M et al (2006) Neuronavigated transcranial magnetic stimulation and auditory hallucinations in a schizophrenic patient: monitoring of neurobiological effects. *Schizophr Res* 84:185–186
- Lang N, Harms J, Weyh T et al (2006) Stimulus intensity and coil characteristics influence the efficacy of rTMS to suppress cortical excitability. *Clin Neurophysiol* 117:2292–2301
- Lee JH, van Donkelaar P (2006) The human dorsal premotor cortex generates on-line error corrections during sensorimotor adaptation. *J Neurosci* 26:3330–3334
- Lee L, Siebner HR, Rowe JB et al (2003) Acute remapping within the motor system induced by low-frequency repetitive transcranial magnetic stimulation. *J Neurosci* 23:5308–5318
- Lefaucheur JP, Brugieres P, Menard-Lefaucheur I et al (2007) The value of navigation-guided rTMS for the treatment of depression: an illustrative case. *Neurophysiol Clin* 37:265–271
- Li X, Nahas Z, Kozel FA et al (2004a) Acute left prefrontal transcranial magnetic stimulation in depressed patients is associated with immediately increased activity in prefrontal cortical as well as subcortical regions. *Biol Psychiatry* 55:882–890
- Li X, Teneback CC, Nahas Z et al (2004b) Interleaved transcranial magnetic stimulation/functional MRI confirms that lamotrigine inhibits cortical excitability in healthy young men. *Neuropsychopharmacology* 29:1395–1407
- Massimini M, Ferrarelli F, Huber R et al (2005) Breakdown of cortical effective connectivity during sleep. *Science* 309:2228–2232
- McConnell KA, Bohning DE, Nahas Z et al (2003) BOLD fMRI response to direct stimulation (transcranial magnetic stimulation) of the motor cortex shows no decline with age. *J Neural Transm* 110:495–507
- Nahas Z, Lomarev M, Roberts DR et al (2001) Unilateral left prefrontal transcranial magnetic stimulation (TMS) produces intensity-dependent bilateral effects as measured by interleaved BOLD fMRI. *Biol Psychiatry* 50:712–720
- Neggess SF, Langerak TR, Schutter DJ et al (2004) A stereotactic method for image-guided transcranial magnetic stimulation validated with fMRI and motor-evoked potentials. *Neuroimage* 21:1805–1817
- Neggess SF, Huijbers W, Vrijlandt CM et al (2007) TMS pulses on the frontal eye fields break coupling between visuospatial attention and eye movements. *J Neurophysiol* 98:2765–2778
- Nowak DA, Grefkes C, Dafotakis M et al (2008) Effects of low-frequency repetitive transcranial magnetic stimulation of the contralesional primary motor cortex on movement kinematics and neural activity in subcortical stroke. *Arch Neurol* 65:741–747
- O'Shea J, Johansen-Berg H, Trief D et al (2007) Functionally specific reorganization in human premotor cortex. *Neuron* 54:479–490
- Pascual-Leone A, Tormos JM, Keenan J et al (1998) Study and modulation of human cortical excitability with transcranial magnetic stimulation. *J Clin Neurophysiol* 15:333–343
- Peschina W, Conca A, Konig P et al (2001) Low frequency rTMS as an add-on antidepressive strategy: heterogeneous impact on 99mTc-HMPAO and 18 F-FDG uptake as measured simultaneously with the double isotope SPECT technique. Pilot study. *Nucl Med Commun* 22:867–873
- Pleger B, Blankenburg F, Bestmann S et al (2006) Repetitive transcranial magnetic stimulation-induced changes in sensorimotor coupling parallel improvements of somatosensation in humans. *J Neurosci* 26:1945–1952
- Richter GT, Mennemeier M, Bartel T et al (2006) Repetitive transcranial magnetic stimulation for tinnitus: a case study. *Laryngoscope* 116:1867–1872

- Ridding MC, Rothwell JC (2007) Is there a future for therapeutic use of transcranial magnetic stimulation? *Nat Rev Neurosci* 8:559–567
- Rounis E, Stephan KE, Lee L et al (2006) Acute changes in frontoparietal activity after repetitive transcranial magnetic stimulation over the dorsolateral prefrontal cortex in a cued reaction time task. *J Neurosci* 26:9629–9638
- Rounis E, Yarrow K, Rothwell JC (2007) Effects of rTMS conditioning over the fronto-parietal network on motor versus visual attention. *J Cogn Neurosci* 19:513–524
- Ruff CC, Blankenburg F, Bjoertomt O et al (2006) Concurrent TMS-fMRI and psychophysics reveal frontal influences on human retinotopic visual cortex. *Curr Biol* 16:1479–1488
- Ruff CC, Bestmann S, Blankenburg F et al (2008) Distinct causal influences of parietal versus frontal areas on human visual cortex: evidence from concurrent TMS-fMRI. *Cereb Cortex* 18:817–827
- Sack AT, Kohler A, Linden DE et al (2006) The temporal characteristics of motion processing in hMT/V5+: combining fMRI and neuronavigated TMS. *Neuroimage* 29:1326–1335
- Sack AT, Kohler A, Bestmann S et al (2007) Imaging the brain activity changes underlying impaired visuospatial judgments: simultaneous FMRI, TMS, and behavioral studies. *Cereb Cortex* 17:2841–2852
- Schonfeldt-Lecuona C, Thielscher A, Freudenmann RW et al (2005) Accuracy of stereotaxic positioning of transcranial magnetic stimulation. *Brain Topogr* 17:253–259
- Shastri A, George MS, Bohning DE (1999) Performance of a system for interleaving transcranial magnetic stimulation with steady-state magnetic resonance imaging. *Electroencephalogr Clin Neurophysiol Suppl* 51:55–64
- Siebner HR, Rothwell J (2003) Transcranial magnetic stimulation: new insights into representational cortical plasticity. *Exp Brain Res* 148:1–16
- Siebner HR, Filipovic SR, Rowe JB et al (2003) Patients with focal arm dystonia have increased sensitivity to slow-frequency repetitive TMS of the dorsal premotor cortex. *Brain* 126:2710–2725
- Smith JA, Mennemeier M, Bartel T et al (2007) Repetitive transcranial magnetic stimulation for tinnitus: a pilot study. *Laryngoscope* 117:529–534
- Sole-Padullés C, Bartres-Faz D, Junque C et al (2006) Repetitive transcranial magnetic stimulation effects on brain function and cognition among elders with memory dysfunction. A randomized sham-controlled study. *Cereb Cortex* 16:1487–1493
- Sparing R, Buelte D, Meister IG et al (2008) Transcranial magnetic stimulation and the challenge of coil placement: a comparison of conventional and stereotaxic neuronavigational strategies. *Hum Brain Mapp* 29:82–96
- Speer AM, Kimbrell TA, Wassermann EM et al (2000) Opposite effects of high and low frequency rTMS on regional brain activity in depressed patients. *Biol Psychiatry* 48:1133–1141
- Starck J, Rimpilainen I, Pyykko I et al (1996) The noise level in magnetic stimulation. *Scand Audiol* 25:223–226
- Strafella AP, Ko JH, Grant J et al (2005) Corticostriatal functional interactions in Parkinson's disease: a rTMS/[11C]raclopride PET study. *Eur J Neurosci* 22:2946–2952
- Tegenthoff M, Ragert P, Pleger B et al (2005) Improvement of tactile discrimination performance and enlargement of cortical somatosensory maps after 5 Hz rTMS. *PLoS Biol* 3:e362
- Terao Y, Ugawa Y, Sakai K et al (1998) Localizing the site of magnetic brain stimulation by functional MRI. *Exp Brain Res* 121:145–152
- Thickbroom GW, Byrnes ML, Edwards DJ et al (2006) Repetitive paired-pulse TMS at I-wave periodicity markedly increases corticospinal excitability: a new technique for modulating synaptic plasticity. *Clin Neurophysiol* 117:61–66
- Walsh V, Cowey A (2000) Transcranial magnetic stimulation and cognitive neuroscience. *Nat Rev Neurosci* 1:73–79
- Walsh V, Rushworth M (1999) A primer of magnetic stimulation as a tool for neuropsychology. *Neuropsychologia* 37:125–135
- Wassermann EM (1998) Risk and safety of repetitive transcranial magnetic stimulation: report and suggested guidelines from the International Workshop on the Safety of Repetitive Transcranial Magnetic Stimulation, 5–7 June, 1996. *Electroencephalogr Clin Neurophysiol* 108:1–16
- Wassermann EM (2008) The motor-evoked potential in health and disease. In: Wassermann EM, Epstein CM, Ziemann U (eds) *The Oxford handbook of transcranial stimulation*. Oxford University Press, New York
- Wassermann EM, Lisanby SH (2001) Therapeutic application of repetitive transcranial magnetic stimulation: a review. *Clin Neurophysiol* 112:1367–1377
- Weyh T, Siebner HR (2007) Hirnstimulation - Technische Grundlagen [Stimulation of the brain - technical basics]. In: Siebner HR, Ziemann U (eds) *Das TMS-Buch [The TMS book]*. Springer, Heidelberg
- Weyh T, Wendicke K, Mentschel C et al (2005) Marked differences in the thermal characteristics of figure-of-eight shaped coils used for repetitive transcranial magnetic stimulation. *Clin Neurophysiol* 116:1477–1486
- Wig GS, Grafton ST, Demos KE et al (2005) Reductions in neural activity underlie behavioral components of repetition priming. *Nat Neurosci* 8:1228–1233
- Yoo WK, You SH, Ko MH et al (2008) High frequency rTMS modulation of the sensorimotor networks: behavioral changes and fMRI correlates. *Neuroimage* 39:1886–1895

Steven M. Stufflebeam

## 17.1 Introduction

Over the past two decades, numerous studies have demonstrated that functional magnetic resonance imaging (fMRI) conveniently maps brain activity, both at rest and during a task. The spatial resolution of fMRI in clinical scanners can exceed 1 mm in plane resolution. The temporal resolution, however, is limited to around 1 s or perhaps a few hundred milliseconds depending on the technique and the paradigm used. Today, in the clinical and research setting, MEG often supplements the spatial information from fMRI with high temporal information.

For purposes of identifying eloquent cortex, typically evoked activity from somatosensory, motor, auditory, visual, and language stimulation is recorded with MEG. During an MEG examination, the weak magnetic fields generated by neuronal currents in the brain are recorded. By measuring the magnetic field at several sites over the head, the most probable brain sources are estimated. The technique is best suited for measuring the activity in the fissural cortex of the cerebral hemispheres. Such areas are generally positioned so that they are difficult to measure even with invasive intracranial recordings. Thus, MEG detects brain activity that would be difficult to measure even in an operating room environment (Hämäläinen and Hari 2002).

This chapter reviews the history of clinical MEG, introduces basic concepts about biophysics and analysis

unique to MEG and electroencephalography (EEG), and compares and contrasts its clinical use with fMRI.

## 17.2 Clinical MEG Instrumentation

In 1968, David Cohen recorded the first magnetoencephalogram using a room-temperature copper coil as a detector, at the university of Illinois (Cohen 1968). After moving to the Massachusetts Institute of Technology, he built a more elaborate shielded room. At about the same time, James Zimmerman and colleagues developed the superconducting quantum interference device (SQUID), which uses the Josephson junction to measure tiny magnetic fields. It requires cooling to liquid helium temperatures, and has a sensitivity that is several hundreds times that of a copper coil. Zimmerman brought this detector to Cohen's room, and this combination of shielding and detector allowed the first clear measurements of the body's magnetic fields. After they had measured the heart, Cohen recorded the first MEG measured with a SQUID (Cohen 1972). The initial measurements of magnetic brain activity were done by physicists who used a single magnetometer.

Most MEG devices now have hundreds of channels that can provide whole-head coverage. This makes it possible to map activity throughout the cerebral cortex, or beyond, and is critical for detecting propagating or widespread epileptic activity. Because of interference from extraneous magnetic fields, all MEG measurements must be performed in a magnetically shielded room, which typically consists of two layers of aluminum and multiple layers of ferromagnetic shielding.

---

S. M. Stufflebeam  
Harvard Medical School/Massachusetts Institute of Technology,  
Athinoula A. Martinos Center for Biomedical Imaging,  
Massachusetts General Hospital, 149 Thirteenth Street - 2301,  
Charlestown, MA 02129  
e-mail: sms@nmr.mgh.harvard.edu

## 17.3 Magnetoencephalography and Electroencephalography Basic Biophysics

MEG and EEG both measure electric currents in the brain. There are critical differences between MEG and EEG that make them complementary. Importantly, MEG preferentially detects activity in superficial, non-radial areas of cortex, i.e., the fissural cortex of the cerebral hemispheres. This is particularly advantageous if the area of activity is in the walls of the sulci, such as in the somatosensory or the auditory areas.

Much of the neural activity measured by MEG is related to postsynaptic activity in the pyramidal cells of the cerebral cortex. It measures the neural activity directly, as contrasted with BOLD fMRI, which measures neural activity indirectly via the hemodynamic response. MEG localizes neural activity more accurately than EEG because magnetic fields are less perturbed than electrical potentials by overlying brain structures: scalp, skull, cerebrospinal fluid, meninges, and vascular structures. Recently, the advancements in the statistical combination of structural MRI, fMRI, and MEG have taken a great stride forward by yielding the maximum benefit from each technique into a single image (Dale and Halgren 2001; Dale et al. 2000).

The calculation of the magnetic field is more straightforward than that of the electric field because of the symmetries and conductivity distribution of the human head. As the EEG electrodes are in direct contact with the head, they measure the extracellular volume currents. All currents, both intracellular and extracellular, generate magnetic fields, but, because of the near spherical shape of the head, one can calculate the resultant magnetic fields due to primary currents without taking into account the conductivity layers of the head.

### 17.4 Analysis of MEG

In order to intelligently interpret the results of a clinical MEG measurement, the data is examined in both the sensor space and in the brain (source space). The basic measurement with MEG is magnetic field strength as a function of time. In order to improve the signal-to-noise ratio of measured signals, it is often necessary to average several (typically around 100

trials) responses from an identical stimulus. This tends to average the extraneous activity to around zero in the evoked response, thus effectively improving the overall signal-to-noise ratio.

#### 17.4.1 Source Modeling

Source modeling is necessary to determine the neural origin of the measured magnetic fields. The mathematical approach to this problem is known as the inverse problem. Generally, the inverse solution is nonunique and ill-posed. If proper assumptions are made, however, the solution becomes solvable.

##### 17.4.1.1 Equivalent Current Dipole

In order to make the inverse solution tractable, one can approximate that the activity from primary sensory or motor cortex originates as a single equivalent current dipole (ECD). This is physiologically plausible, given that a limited patch of cortex is synchronously activated and that the sensors are at least a few centimeters from the source. The ECD provides spatial information, magnitude (current dipole moment), and direction. It is typically computed using a standard iterative least-square algorithm (Marquardt 1963), which can also provide a measure of dipole parameter confidence, as well as the best-fitting parameters such as goodness of fit (GOF) measure (Hämäläinen et al. 1993).

Thus, by assuming a single source, the inverse problem has a unique solution. This works particularly well for primary sensory areas, focal epilepsies, and for higher cognitive areas that have a focal source. Further advances in the ECD approach, for both EEG and MEG, has made it possible to find multiple ECDs with a multidipole approach, such as that developed by Hari and colleagues for somatosensory activation (Hari et al. 1993). One approach to investigate temporal changes in different areas of the brain is known as the time-varying dipole model. In this model, a series of dipoles are modeled such that the locations are fixed, but allowing the amplitudes to vary over time. This ECD approach works quite well for sequentially or simultaneously activated cortical sources, although the fine spatial details are lost due to the fact that the measurements are obtained at least 3 cm from the sources (Hämäläinen et al. 1993).

### 17.4.1.2 Distributed Solutions

If a large area of cortex is activated, the single ECD solution may be misleading. In practice, this may be suspected when a dipole localizes too deep to be physiologically plausible, i.e., in the deep white matter. In such cases, distributed solutions such as the minimum norm estimate (MNE) or the minimum current solution (MCE) maybe more accurate. Although numerous other inverse solutions exist (Mosher et al. 1999; Mosher and Leahy 1998), this review concentrates on MNE and MCE.

#### Minimum Norm Estimate (MNE)

Originally pioneered by Hämäläinen (Hämäläinen and Ilmoniemi 1984), and recently improved by Dale and colleagues (Dale and Halgren 2001; Dale et al. 2000), MNE is now available in commercial software packages. The basis of the MNE is that a leadfield describes the contribution to the surface magnetic field from a series of dipoles in the brain. Although computationally expensive, the leadfield can be expressed as a matrix computed from a realistic head model from a head MRI.

The MNE does have some important limitations that must be kept in mind especially when they are used clinically: a depth bias, and the difficulty in determining the extent of activation. In its most elementary expression, the source variance is assumed to be equal throughout the volume, and the MNE solution is biased towards the most superficial currents. One approach to lessen this effect is to use a cortical constraint obtained from the anatomic MRIs (Dale and Sereno 1993). In addition to a depth bias, determining the extent of the sources is also problematic. Simulations (Dale and Sereno 1993) show that the point-spread function of estimates is a function of location. Further, the spread depends on the assumed source variance.

In order to further compensate for the superficial bias of current estimates, and also give a more accurate estimation of the extent of activation, Dale has suggested producing a statistical parametric map (SPM) by normalizing the estimate MNE by source noise (Dale et al. 2000). Simulations have determined that the point-spread function is then a much lesser function of location (Liu et al. 2002). Additionally, the SPM can be used for hypothesis testing of the spatial

extent of estimated activity in individuals across stimulus conditions, or between groups of subjects.

### 17.4.2 Combination with Other Imaging Technologies

In order to improve the spatial localization capabilities of MEG, the inverse solution can be combined with the spatial information provided from other sources, such as fMRI, positron emission tomography (PET), or optical imaging. As noted above, the spatial information from anatomic MRI can be used to restrict the solution to the cortical surface. For example, Dale and Halgren (2001) report the ability to create spatiotemporal “movies” of the processing of the brain during reading, by statistically combining the information from fMRI and MEG done with identical stimulus conditions, performed on different sessions (See Fig 17.1 for example). It might thus be possible to use such a technique to locate and quantify complex language and cognitive tasks presurgically.

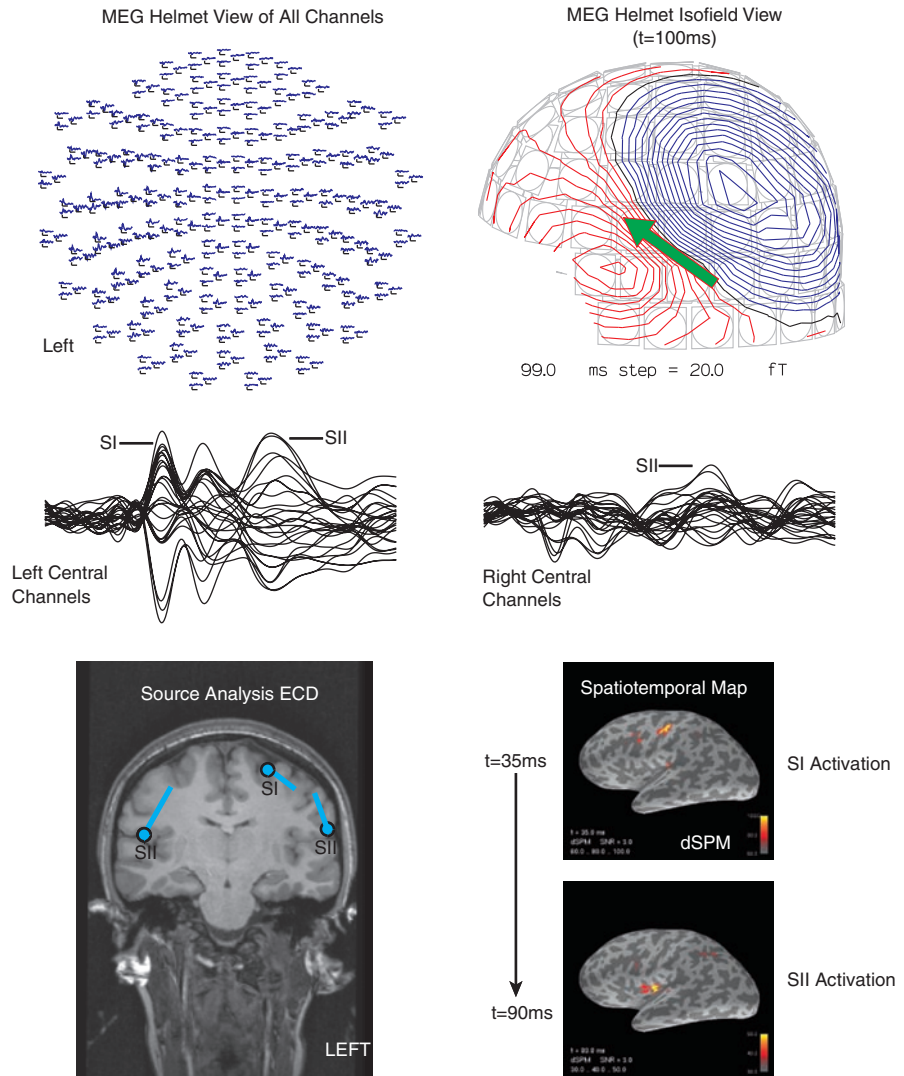
## 17.5 Presurgical Mapping

### 17.5.1 Somatosensory Mapping

Using a tactile stimulator, the somatosensory cortex homunculus can be easily mapped by successively stimulating finger digits, foot digits, and lip using MEG. Alternatively, an electrical nerve stimulator can be used to map the median, tibial nerve, and lip representative areas. If an electrical nerve stimulator is used, the electrodes are placed, and the intensity set, such that thumb twitching or toe twitching is elicited. Typically, 100 repeated stimuli are required to obtain adequate signal-to-noise ratio. Both the primary (SI) and secondary (SII) somatosensory cortices are detectable with MEG (see Fig. 17.2).

After recording the evoked magnetic fields, the primary somatosensory cortex is typically localized with an ECD (Hari 1991, 1990; Hari and Forss 1999). If the median nerve electrical stimulation technique is used, the N20m – the first “fast” component of the evoked magnetic field – is easily obtained in nearly all patients, including ones under deep anesthesia or in a coma

**Fig. 17.1** Somatosensory evoked field using MEG in an epilepsy patient. Upper left shows all 306 channels in a helmet view during electrical stimulation of the right median nerve. Upper right shows the isofield map of the current dipole (green arrow) over the SII area of the somatosensory cortex. Middle panels show enlargement of the channels over the somatosensory cortex of the right and left sides. Lower left shows the equivalent current dipole (ECD) of the contralateral SI and bilateral SII estimates superimposed on a T1-weighted MRI. Lower right shows two time frames (35msec & 90msec post-stimulation of the right median nerve) demonstrating the activity location and magnitude (F-statistic) of SI (upper) and SII (lower). This activity can be converted to a millisecond resolution ‘movie’ of the cortical current activity after a stimulus

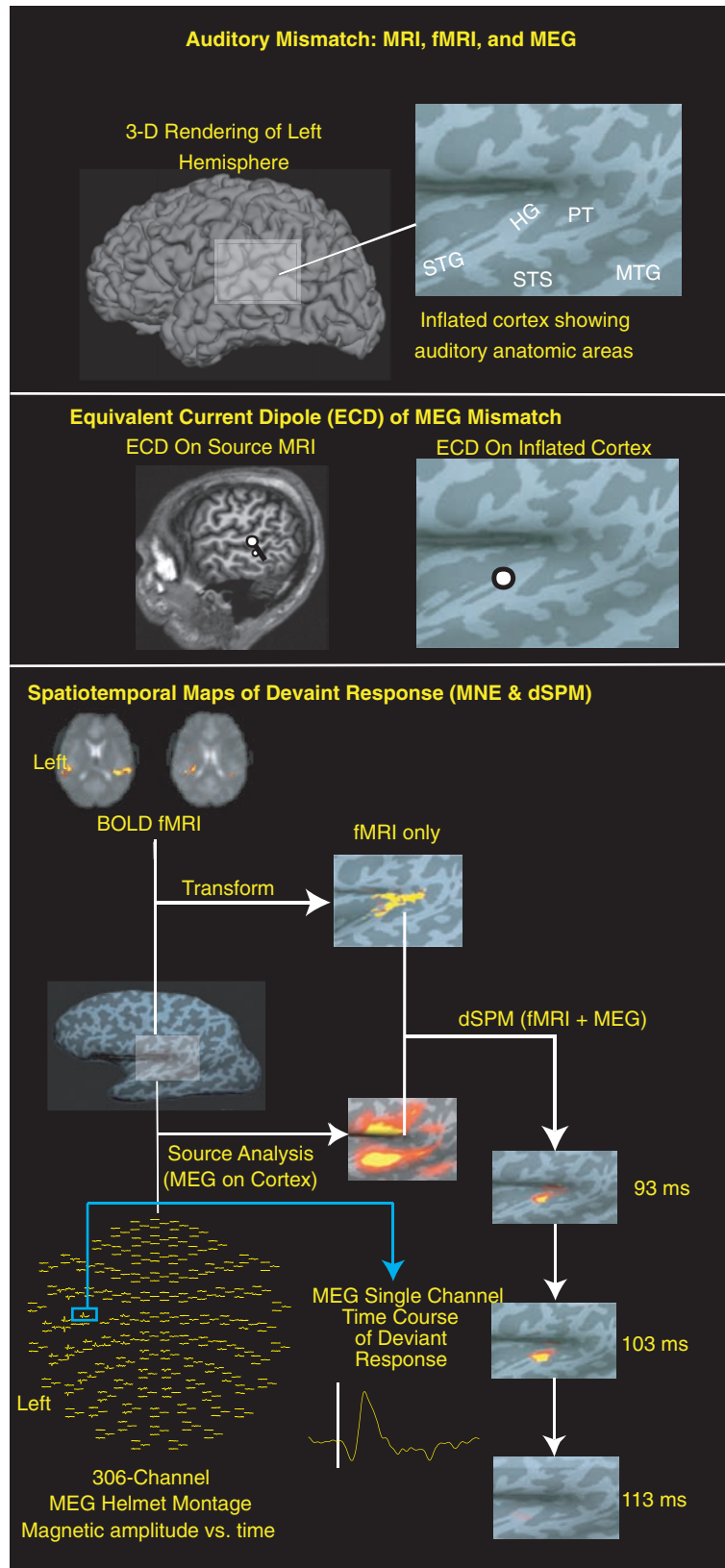


(Hoshiyama et al. 1996; Kakigi 1994). The N20 m generator is located in the anterior wall of the somatosensory gyrus (area 3b), with a nonradial orientation, which is ideal for detection with MEG (Hari 1990, 1991, 1993; Hari and Forss 1999; Hoshiyama et al. 1996). It is a preconscious field that bypasses the thalamus and, due to a high signal-to-noise ratio, has a very repeatable localization, usually within a few millimeters of the hand area of the somatosensory cortex.

MEG identification of the central sulcus, has been validated by several groups using intraoperative measurements (Beisteiner et al. 1995; Inoue et al. 1999; Kober et al. 2001a; Schiffbauer et al. 2001). Firsching

et al. (1992, 2002), recently reported that in 30 patients, ECD localization of the tactile neuromagnetic response localized in the somatosensory cortex, and was in agreement with phase reversal measurements at the time of surgery, without exception. Recent reports of noninvasive multimodal technologies – MEG, fMRI, and others, – have noted that when combined, they enhance the reliability of identification of the central sulcus. Some have suggested using a functional risk profile (FRP), based on MEG findings to improve surgical decision-making (Hund et al. 1997). It should be kept in mind that brain tumor patients with known sensory or motor deficits often have diminished evoked fields (Hund et al. 1997).

**Fig. 17.2** Auditory mismatch response preliminary data using multiple imaging technologies in a control subject. Stimuli were narrow band standard tones (220Hz center, 1/8 octave widths) and deviants (3 Octaves above standard, with 1/8 octave width) presented rarely (5%). Labeled areas are Heschl's gyrus (HG), planum temporale (PT), superior temporal gyrus (STG), superior temporal sulcus (STS), and middle temporal gyrus (MTG). The next panel shows a focal source analysis technique, the equivalent current dipole (ECD) method, which is traditionally used for MEG source estimation. On the left is a sagittal MRI with the ECD source estimate location with the black bar indicating the dipole direction. On the right, the dipole representing the peak in the magnetic mismatch response (MMNm) is registered onto the inflated cortex. Notice that in this case the dipole is near the anterior portion of Heschl's gyrus. The 3rd panel illustrates how the actual pilot data from fMRI, MEG data, and the inflated cortex data are combined to create a 'movie' or spatiotemporal map. The fMRI data superimposed on source EPI BOLD MRI images, which is then transformed onto the inflated cortex. The lower panel illustrates how the activity from the 306 channels of MEG data are transformed using the minimum norm estimate (MNE), a distributed source estimate method, onto the inflated cortical source. Note that only the auditory areas in the rectangular region over the STG are shown for the fMRI, MNE, and dSPM panels. Next, the fMRI data and the MNE results are combined into a spatiotemporal movie, or dSPM. With this pilot data from a normal control, some activity of the mismatch response is seen at 93ms, which peaks at approximately 103ms, and is diminished by 113ms



### 17.5.2 Motor Mapping

As noted above, many functional imaging techniques, such as fMRI and PET, can accurately identify the central sulcus (Bittar et al. 1999). However, isolating pure motor activity with fMRI is difficult due to inevitable activation of the adjacent somatosensory cortex or other components of the motor system. MEG, however, can be used to isolate pure motor activity. In practice, it requires precise timing of the onset of motor movement in order to produce an averaged evoked field. This can be achieved by a self-paced button press, or by the use of a trigger, a photo-optic switch. Activity that peaks between 20 and 50 ms before the onset of movement reflects activity in the primary motor cortex (Lewine and Orrison 1995).

Alternatively, the motor cortex can be mapped by performing a coherence analysis of the activity over the motor cortex with the electromyogram (EMG) waveform, as suggested by Makela et al (Makela et al. 2001). By placing bipolar electrodes over the first interosseous muscle, and instructing the patient to press the thumb against the index finger, the coherence of the MEG–EMG yields a spectrum with a peak near 20 Hz, most concentrated in the MEG sensors over the motor cortex. This coherence calculation isolates the primary motor cortex response from the rest of the motor system (Makela et al. 2001). MEG can be combined with neuronavigational systems in the neurosurgical suite to guide neurosurgeons of motor cortex (Ganslandt et al. 1999; Rezai et al. 1996, 1997). More recently, MEG has been reported to be useful in identifying the entire neural network, activated during the planning and the act of motor movement, including supplementary cortex (Erdler et al. 2000, 2001) and premotor cortex (Gross et al. 2000, 2001).

### 17.5.3 Auditory Cortex

It is possible to localize the middle (50–200 ms) and late components (>400 ms) of the auditory response with MEG. Localization of the primary auditory cortex can be used as surgical reference, especially when using a neuronavigational system (Jannin et al. 2000, 2002). More importantly, the later components of the auditory evoked response can be used to map higher level functioning such as language processing. The

N1 m peak is the largest and most robust, displaying a strong dipolar response, which localizes to the posterior superior temporal gyrus in or near the primary auditory cortex (See Fig 17.1). The auditory cortex has multiple tonotopic maps, and some report the ability to use the neuromagnetic response from a series of tone pips at various frequencies (i.e., 100 Hz, 200 Hz, 500 Hz, 1 kHz, 5 kHz) to define a dominant tonotopic organization (Pantev et al. 1995).

### 17.5.4 Visual Cortex

In patients with tumors lying near visual eloquent areas, mapping of the visual cortex is possible. The primary visual cortex can be mapped by a simple ECD of the first visual evoked peak from a strong visual stimulus, such as a checkerboard flash. Mapping of the visual areas is theoretically difficult with ECD mapping due to synchronously active sources. In practice, however, it does yield valid results (Hatanaka et al. 1997; Nakasato et al. 1996; Nakasato and Yoshimoto 2000). Mapping of the magnetic equivalent of visual evoked potentials N75, P100, and N145 components is robust with large visual stimuli with phase reversal techniques, and can be performed to detect visual field deficits (Hatanaka et al. 1997; Nakasato et al. 1996; Nakasato and Yoshimoto 2000). During a visual language task, it is often possible to fit ECDs to dipole locations, so that it does not necessarily have to be a separate stimulation which can save time during the MEG measurement.

### 17.5.5 Language Mapping

In patients with brain tumors in the perisylvian region, as well as in patients with epilepsy, lateralization, and localization of language processing are critical. Although fMRI has become standard at some institutions, the intracarotid injection of amobarbital, known as the Wada test, is still considered the gold standard for a presurgical determination of hemispheric dominance. Still, the Wada test has been criticized because of potential cross-flow to the contra-lateral hemisphere, and the lack of testing of territory supplied by the posterior circulation. There are several reports of MEG being used in determining both hemispheric dominance

for language, as well as regional language mapping of individual language areas (Breier et al. 1999a, b; Castillo et al. 2001; Floel 2001; Simos et al. 1999a, b, 2001; Szymanski et al. 1999, 2001). MEG of language areas holds the promise of providing a noninvasive method of mapping language areas, with the goal of prolonging survival and making possible more extensive resections of brain tumors, yet preserving language function, in order to increase the survival. Such a test could reduce the need for invasive Wada tests and stimulation-based intraoperative mapping techniques.

### 17.5.5.1 Functional Language Paradigms

Determining hemispheric dominance or regional language processing in a brain tumor patient requires choosing the task that best activates the desired stream of language processing. Specific language processes include phonological, lexical, and syntactic processing. In addition, memory storage and retrieval occurs concurrently. Supporting processes include attention, motor planning (speech), and basic visual or auditory processing. Semantic decision tasks are probably the most popular as they require a response from the patient, such as a forced binary decision, allowing one to monitor the quality of the patient's responses. Otherwise, covert responses are desirable, as overt (spoken) responses can lead to unacceptable motion artifacts. Still, some passive sensory paradigms requiring no patient response have been reported in the literature, to be successful (see below).

### 17.5.5.2 Hemispheric Dominance for Language

Determination of the language dominant hemisphere is critical in the presurgical work-up of tumors near language processing areas. There are several reports of using MEG to determine hemispheric dominance of language. The most commonly reported methods fall into two broad categories: (1) Sequential equivalent current dipole mapping and (2) Distributed solutions.

Wada and Rasmussen determined that over 93% of patients are left language dominant, and that over 96% of right-handed patients are so, as well, although more recent studies indicate that many patients have more bilateral representation of language than the original studies (Beisteiner et al. 1995). In left-handed patients,

only about 70% demonstrate left hemispheric dominance for language, with about 15% of patients demonstrating bilateral language lateralization.

Recently, sequential dipole fitting has been proposed to determine language dominance. First proposed by Papanicolaou (Papanicolaou et al. 1999), statistical criteria based on the ECD are used for filtering a sequential equivalent current dipole fit. The stimuli may consist of auditory and/or visual words. The results concur with Wada test results (Breier et al. 1999a) and electrical stimulation mapping (Panagiotis 1999). Szymanski et al. (Szymanski et al. 2001) reported using simple phonetic stimuli, such as the vowel sounds /a/ and /u/, for determining the language hemispheric dominance by summing the number of selective dipoles in the late auditory magnetic field on each hemisphere, and calculating a lateralization index. Multiple groups report a strong correlation with both intraoperative mapping techniques and the results of the Wada test (Simos et al. 1999a; Szymanski et al. 2001).

It also been reported that MEG finds the posterior language areas, in and around Wernicke's area, and is less sensitive for the anterior frontal areas, in and around Broca's area. Kober et al. (2001b) propose using a spatial filter, continuous localization by spatial filtering (CLSF), to determine language hemispheric dominance which can image simultaneously active sources. CLSF requires parcellating the brain into approximately 6,000 "voxels" and calculating the current produced in each "voxel."

### 17.5.5.3 Spatiotemporal Regional Language Mapping

MEG can localize, with a high temporal resolution, both receptive (auditory and visual) and productive brain areas, either alone or in combination with fMRI. There are number studies of the language system activation under a variety of passive and task-activated language paradigms, usually done for the purposes of understanding how the brain processes language. This has led to a revolution in mapping brain function and understanding how the brain processes information. However, the practical needs for the presurgical workup of brain tumor patients and the needs of basic neuroscience are fundamentally different in several respects. First, the neurosurgical application requires precise localization in the individual patient, while the neuroscientist can average

the response over several subjects in order to increase the signal-to-noise ratio of small activations. Second, the neurosurgeon usually requires mapping the *essential language areas*, not just the participating areas. Essential language areas are those that, when removed, result in a language deficit. *Participating* areas are activated during language paradigms, but do not result in a postoperative language deficit after resection, either because there are areas of redundant processing, or because other areas learn to take over the same function. Currently, there is no way to distinguish essential areas from participating areas with noninvasive imaging, and this is a major goal of clinical functional imaging. Combining the fMRI, DTI tractography, and MEG source analysis can be used to guide neurosurgery (See Figure 2).

By simply applying a source localization procedure, the same techniques described for determining hemispheric dominance can be used for regional language mapping. The mapping of ECDs of the late auditory evoked fields can be used for both posterior temporal and frontal operculum mapping (Papanicolaou et al. 1999; Breier et al. 2001). Temporal maps of activation have similar profiles as determined by invasive electrocorticography (ECoG). The latency of Wernicke's area is typically between 210 and 420ms, and Broca's area between 400–1,100ms, depending on the individual subject and the particular language paradigm. Generally, the peak activation of Wernicke's area precedes Broca's area, although occasionally, other temporal profiles have been reported (Kober et al. 2001b).

## 17.6 Spontaneous Activity: Epileptic Spike Localization

Localization of seizure activity can be performed both within the context of a low-grade brain tumor or as part of the workup of surgical epilepsy. Although interictal activity is most easily captured with MEG, ictal activity is also being detected and localized with whole head MEG systems – particularly if the instrument is located in a hospital where antiepileptic medicines can be tapered and stopped. The most effective workup of epilepsy with MEG is with a whole-head system and is usually performed with simultaneously recorded EEG. A standard EEG electrode array, which has no magnetic material, is convenient and provides a way of producing a standard EEG classification of ictal or interictal

activity. Higher density caps are also available if EEG source localization is contemplated.

## 17.7 MEG and fMRI: What's the difference?

The precise relationship between the evoked neuro-magnetic response and the BOLD signal are complex, and incompletely understood. One might, for example, assume that increased signal in MEG or EEG would be positively correlated with an increase in fMRI BOLD, but this is not always the case. This phenomenon is partly due to the fact that electromagnetic response is a weighted sum of the postsynaptic potentials in the brain occurring on a millisecond scale, and the BOLD signal is a hemodynamic response resulting from a convolution over several seconds of the temporal mean of cortical activity. fMRI appears to be related to changes in the neural firing rate, which also decreases with increased inhibition.

fMRI easily and conveniently detects multiple areas activated during a particular sensory or motor task. For example, during motor activation, the supplementary and premotor areas are activated in addition to the primary motor cortex. MEG also detects premotor activity but the detected signal from the supplementary motor is weaker. Therefore, fMRI can image activity in some regions that are problematic with MEG. MEG can, however, detect the activity exclusively from the primary motor cortex with the use of EMG–MEG coherence, as described above. BOLD activity is not subject to spatial cancellation effects as surface MEG and EEG are (Ahlfors and Simpson 2004). Another advantage of fMRI over MEG is that it does not require increasingly sophisticated models to solve the inverse problem (Hämäläinen and Hari 2002).

A disadvantage of fMRI is that, especially at lower field strengths (3.0 T and below), significant activity detection is due to large draining veins, which can be at some distance from the cortical sites, leading to confusion in the localization of central sulcus (Ugurbil et al. 2003). MEG is useful in cases of a compromise to the hemodynamic compensatory mechanisms, such as arteriovenous malformations and, importantly, tumors (Roberts et al. 2000). This is especially true if the functional cortex is located within the radiologically defined extent of the tumor, such as those of a

slow-growing, low-grade nature. This has been emphasized in a study by Inoue et al. (1999) who found two examples where the tumor and edema mass effect led to the disruption of normal hemodynamic response that caused an incorrect localization. Holodny et al. (1999, 2000) found decreased BOLD activation of the motor and somatosensory cortices adjacent to brain tumors, despite normal neurological function. Thus, abnormal vascular supply may decrease the hemodynamic response measured by fMRI. MEG, on the other hand, is a direct measure of neural activity and is immune to the constraints imposed by the vascular system (Roberts et al. 2000).

## 17.8 Conclusion

MEG/EEG and fMRI have excellent temporal and spatial resolution. Clinically, they can be used together to accurately map eloquent cortex and epileptic cortex in both healthy and diseased populations.

## References

- Ahlfors SP, Simpson GV (2004) Geometrical interpretation of fmri-guided MEG/EEG inverse estimates. *Neuroimage* 22(1):323–332
- Beisteiner R et al (1995) Comparing localization of conventional functional magnetic resonance imaging and magnetoencephalography. *Eur J Neurosci* 7(5):1121–1124
- Bittar RG et al (1999) Presurgical motor and somatosensory cortex mapping with functional magnetic resonance imaging and positron emission tomography. *J Neurosurg* 91(6):915–921
- Breier JI et al (1999a) Lateralization of cerebral activation in auditory verbal and non-verbal memory tasks using magnetoencephalography. *Brain Topogr* 12(2):89–97
- Breier JI et al (1999b) Language dominance determined by magnetic source imaging: a comparison with the Wada procedure. *Neurology* 53(5):938–945
- Breier JI et al (2001) Language dominance in children as determined by magnetic source imaging and the intracarotid amobarbital procedure: a comparison. *J Child Neurol* 16(2): 124–130
- Castillo EM et al (2001) Mapping of expressive language cortex using magnetic source imaging. *Neurocase* 7(5):419–422
- Cohen D (1968) Magnetic field measurements of human alpha rhythm. *Science* 161:784–786
- Cohen D (1972) Magnetoencephalography: detection of the brain's electrical activity with a superconducting magnetometer. *Science* 175(22):664–666
- Dale AM, Halgren E (2001) Spatiotemporal mapping of brain activity by integration of multiple imaging modalities. *Curr Opin Neurobiol* 11(2):202–208
- Dale AM, Sereno MI (1993) Improved localization of cortical activity by combining EEG and MEG with MRI cortical surface reconstruction: a linear approach. *J Cogn Neurosci* 5(2): 162–176
- Dale AM et al (2000) Dynamic statistical parametric mapping: combining fMRI and MEG for high-resolution imaging of cortical activity. *Neuron* 26:55–67
- Erdler M et al (2000) Supplementary motor area activation preceding voluntary movement is detectable with a whole-scalp magnetoencephalography system. *Neuroimage* 11(6 Pt 1): 697–707
- Erdler M et al (2001) Dissociation of supplementary motor area and primary motor cortex in human subjects when comparing index and little finger movements with functional magnetic resonance imaging. *Neurosci Lett* 313(1–2):5–8
- Firsching R et al (1992) Lesions of the sensorimotor region: somatosensory evoked potentials and ultrasound guided surgery. *Acta Neurochir (Wien)* 118(3–4):87–90
- Firsching R et al (2002) Practicability of magnetoencephalography-guided neuronavigation. *Neurosurg Rev* 25(1–2):73–78
- Floel A et al (2001) Language and spatial attention can lateralize to the same hemisphere in healthy humans. *Neurology* 57(6):1018–1024
- Ganslandt O et al (1999) Functional neuronavigation with magnetoencephalography: outcome in 50 patients with lesions around the motor cortex. *J Neurosurg* 91(1):73–79
- Gross J et al (2000) Cortico-muscular synchronization during isometric muscle contraction in humans as revealed by magnetoencephalography. *J Physiol* 527(Pt 3):623–631
- Gross J et al (2001) Dynamic imaging of coherent sources: studying neural interactions in the human brain. *Proc Natl Acad Sci U S A* 98(2):694–699
- Hämäläinen M, Hari R (2002) Magnetoencephalography. In: Toga AW, Mazziotta JC (eds) *Brain mapping: the methods*. Academic, Amsterdam, p. xvii, 877
- Hämäläinen M et al (1993) Magnetoencephalography – theory, instrumentation, and application to noninvasive studies of the working human brain. *Rev Mod Phys* 65: 413–497
- Hämäläinen MS, Ilmoniemi RJ (1984) Interpreting measured magnetic fields of the brain: estimates of current distributions. Vol. Report TKK-F-A559, Helsinki University of Technology, Helsinki, Finland
- Hari R (1990) Magnetic evoked fields of the human brain: basic principles and applications. *Electroencephalogr Clin Neurophysiol Suppl* 41:3–12
- Hari R (1991) On brain's magnetic responses to sensory stimuli. *J Clin Neurophysiol* 8(2):157–169
- Hari R et al (1990) Separate finger representations at the human second somatosensory cortex. *Neuroscience* 37(1): 245–249
- Hari R et al (1993) Functional organization of the human first and second somatosensory cortices: a neuromagnetic study. *Eur J Neurosci* 5(6):724–734
- Hari R, Forss N (1999) Magnetoencephalography in the study of human somatosensory cortical processing. *Philos Trans R Soc Lond B Biol Sci* 354(1387):1145–1154
- Hatanaka K et al (1997) Striate cortical generators of the N75, P100 and N145 components localized by pattern reversal

- visual evoked magnetic fields. *Tohoku J Exp Med* 182(1): 9–14
- Holodny AI et al (1999) Correlation between the degree of contrast enhancement and the volume of peritumoral edema in meningiomas and malignant gliomas. *Neuroradiology* 41(11):820–825
- Holodny AI et al (2000) The effect of brain tumors on BOLD functional MR imaging activation in the adjacent motor cortex: implications for image-guided neurosurgery. *AJNR Am J Neuroradiol* 21(8):1415–1422
- Hoshiyama M et al (1996) Somatosensory evoked magnetic fields following stimulation of the lip in humans. *Electroencephalogr Clin Neurophysiol* 100(2):96–104
- Hund M et al (1997) Magnetoencephalographic mapping: basic of a new functional risk profile in the selection of patients with cortical brain lesions. *Neurosurgery* 40(5):936–942; discussion 942–943
- Inoue T et al (1999) Accuracy and limitation of functional magnetic resonance imaging for identification of the central sulcus: comparison with magnetoencephalography in patients with brain tumors. *Neuroimage* 10(6):738–748
- Jannin P et al (2000) A data fusion environment for multimodal and multi-informational neuronavigation. *Comput Aided Surg* 5(1):1–10
- Jannin P et al (2002) Integration of sulcal and functional information for multimodal neuronavigation. *J Neurosurg* 96(4): 713–723
- Kakigi R (1994) Somatosensory evoked magnetic fields following median nerve stimulation. *Neurosci Res* 20(2):165–174
- Kober H et al (2001a) Correlation of sensorimotor activation with functional magnetic resonance imaging and magnetoencephalography in presurgical functional imaging: a spatial analysis. *Neuroimage* 14(5):1214–1228
- Kober H et al (2001b) New approach to localize speech relevant brain areas and hemispheric dominance using spatially filtered magnetoencephalography. *Hum Brain Mapp* 14(4): 236–250
- Lewine JD, Orrison WW Jr (1995) Magnetic source imaging: basic principles and applications in neuroradiology. *Acad Radiol* 2(5):436–440
- Liu AK, Dale AM, Belliveau JW (2002) Monte Carlo simulation studies of EEG and MEG localization accuracy. *Hum Brain Mapp* 16(1):47–62
- Makela JP et al (2001) Three-dimensional integration of brain anatomy and function to facilitate intraoperative navigation around the sensorimotor strip. *Hum Brain Mapp* 12(3):180–192
- Marquardt DW (1963) An algorithm for least-squares estimation of nonlinear parameters SIAM. *J Appl Math* 11(2): 431–441
- Mosher JC, Leahy RM (1998) Recursive MUSIC: a framework for EEG and MEG source localization. *IEEE Trans Biomed Eng* 45(11):1342–1354
- Mosher JC, Leahy RM, Lewis PS (1999) EEG and MEG: forward solutions for inverse methods. *IEEE Trans Biomed Eng* 46(3):245–259
- Nakasato N, Yoshimoto T (2000) Somatosensory, auditory, and visual evoked magnetic fields in patients with brain diseases. *J Clin Neurophysiol* 17(2):201–211
- Nakasato N et al (1996) Clinical application of visual evoked fields using an MRI-linked whole head MEG system. *Front Med Biol Eng* 7(4):275–283
- Panagiotis B (1999) Grand mal seizures with liver toxicity in a case of clozapine treatment. *J Neuropsychiatry Clin Neurosci* 11(1):117–118
- Pantev C et al (1995) Specific tonotopic organizations of different areas of the human auditory cortex revealed by simultaneous magnetic and electric recordings. *Electroencephalogr Clin Neurophysiol* 94:26–40
- Papanicolaou AC et al (1999) Magnetoencephalographic mapping of the language-specific cortex. *J Neurosurg* 90(1): 85–93
- Rezai AR et al (1996) The interactive use of magnetoencephalography in stereotactic image-guided neurosurgery. *Neurosurgery* 39(1):92–102
- Rezai AR et al (1997) Integration of functional brain mapping in image-guided neurosurgery. *Acta Neurochir Suppl* 68: 85–89
- Roberts TP et al (2000) Latency of the auditory evoked neuro-magnetic field components: stimulus dependence and insights toward perception. *J Clin Neurophysiol* 17(2):114–129
- Roberts TP et al (2000) Presurgical mapping with magnetic source imaging: comparisons with intraoperative findings. *Brain Tumor Pathol* 17(2):57–64
- Schiffbauer H et al (2001) Functional activity within brain tumors: a magnetic source imaging study. *Neurosurgery* 49(6):1313–1320; discussion 1320–1321
- Simos PG et al (1999a) Atypical temporal lobe language representation: MEG and intraoperative stimulation mapping correlation. *Neuroreport* 10(1):139–142
- Simos PG et al (1999b) Localization of language-specific cortex by using magnetic source imaging and electrical stimulation mapping. *J Neurosurg* 91(5):787–796
- Simos PG et al (2001) Mapping of receptive language cortex in bilingual volunteers by using magnetic source imaging. *J Neurosurg* 95(1):76–81
- Szymanski MD, Rowley HA, Roberts TP (1999) A hemispherically asymmetrical MEG response to vowels. *Neuroreport* 10(12):2481–2486
- Szymanski MD et al (2001) Magnetic source imaging of late evoked field responses to vowels: toward an assessment of hemispheric dominance for language. *J Neurosurg* 94(3): 445–453
- Ugurbil K, Toth L, Kim DS (2003) How accurate is magnetic resonance imaging of brain function? *Trends Neurosci* 26(2):108–114

# Index

## A

- Action potential, 155, 156
- Activation
  - functional magnetic resonance imaging (fMRI) studies, 101
  - by language, 96–99
  - positron emission tomography (PET) studies, 99
- Angular gyrus, 9, 12
- Anterior commissure, 8
- Aphasia, 72
  - after stroke, 96, 101
  - effect of repetitive transcranial magnetic stimulation (rTMS), 101, 102, 104
  - effects of piracetam, 101
  - metabolic disturbance *vs.* recovery, 98–101
  - metabolic disturbance *vs.* severity, 98
  - over-activation, 101, 104
  - treatment effects, 100–101
- Arterial spin labeling (ASL)
  - use in imaging seizures, 136–137
- Awake craniotomy, 122

## B

- Block design, 43, 55, 56
- Blood oxygen level dependent (BOLD), 54, 65, 156,
  - 160–164, 174, 175
  - extravascular contribution, 17, 18
  - intravascular contribution, 17
  - low frequency noise in, 136–137
  - spatial resolution, 16–18
  - spin-echo technique, 18
- Bracket-sign, 5, 8
- Brain activation, 108, 111–114, 116, 117
- Brain neoplasms, *see* Brain tumor
- Brain shift, 55, 65, 125
- Brain tumor, 103, 107–118

## C

- Calcarine sulcus, 12
- Callosal sulcus, 8
- Capillary bed, 65
- Caudate nucleus, 7
- Central sulcus (CS), 5, 7, 56, 62
- Cerebral blood flow (CBF), 19, 20
- Cerebrospinal fluid (CSF), 17, 18
- Children

- imaging studies in, 142, 143
- Cingulate gyrus, 8
- Cingulate sulcus, 5, 8
- Clastrum, 7, 10, 11
- Coactivation, 63
- Cognitive, 73
- Condition-and-map approach, 163, 164
- Congenital hemiparesis, 150–153
- Connectivity, 156, 157
- Consensus, 64
- Control, 57
- Coregistration, 150–153
- Corpus callosum, 8
- Cortical dysplasia, 149
- Cortical mapping, 124
- Cortico-spinal, 151–153
- Cuneus, 8
- Current procedural terminology (CPT)-code, 55
- Cycle, 58, 59

## D

- Dephasing, 35, 37
- Development, 149
- Diffusion tensor imaging (DTI), 51, 64
- Direct cortical stimulation (DCS), 121–125
- Duration, 58

## E

- Echo planar imaging (EPI), 36–38, 40, 160, 161
- EEG–fMRI, 128
  - in focal seizures, 130
  - in generalized seizures, 132
- Electrocorticography (ECoG), 64
- Electrophysiology, 31
- Energy demands of nervous tissue, 95
- Epilepsy, 51, 127. *See also* Seizures
  - benign childhood focal, 130–131
  - focal, 129
  - generalized, 131
  - musicogenic, 135
  - photosensitive, 134
  - reading, 135
  - reflex, 134
  - writing, 135
- Epilepsy, 174

- Epilepsy surgery, 149, 152  
 Epileptic seizure, 157  
 Equivalent current dipole, 170  
 Error, 64, 65  
 Extreme capsula, 10, 11
- F**  
 False negative, 44  
 False positive, 44  
 Feasibility, 53  
 Field potentials, 24–27, 30, 31  
 Fingers, 57, 62  
 Flow-sensitive alternating inversion recovery (FAIR), 19, 20  
 fMRI data analyses, 43  
 Frameless stereotaxy, 158, 159, 163  
 Frontal operculum, 7–12  
 Functional diagnosis, 64  
 Functional magnetic resonance imaging (fMRI), 69, 73, 77–88, 108–116, 118
- G**  
 General linear model (GLM), 44  
 Glioma, 121, 122  
 Globus pallidum, 7, 10, 11  
 Guidelines, 64
- H**  
 Hahn-spin-echo sequence, 37  
 Hand knob, 51, 56, 59, 152, 153  
 Head motion, 45, 47, 48  
 Hemispherectomy, 152  
 Hemispheric dissociation, 153, 154  
 Hemodynamic response function (HRF), 45  
 Heschl's gyrus, 11, 12  
 Heschl's sulcus, 11, 12  
 Homunculus, 59  
 Hook, 8
- I**  
 Inaccuracies, 65  
 Inferior frontal gyrus, 7  
 Inhibition  
   collateral, 96, 101, 103  
   transcallosal, 96, 99, 101, 103  
 Insula, 9, 10, 12  
 Interleaved TMS–fMRI, 159–162  
 Internal capsule, 7  
 Intracortical stimulation (ICS), 53  
 Intraoperative MRI, 125  
 Ipsilateral, 62, 63
- L**  
 Landmarks, 51, 59, 64  
 Language, 69, 70, 73  
   functional network, 96, 98–104  
   lateralization, 77–88  
   mapping, 173, 174  
 Lateral ventricles, 7, 8  
 Layers, 16, 18  
 Lentiform nucleus, 7, 10, 11
- Limitations, 64–65  
 Lips, 62  
 Local anesthesia  
   in brain tumour surgery, 121–125
- M**  
 Magnetic resonance imaging (MRI), 108, 113, 114, 116, 117  
 Magnetoencephalography (MEG), 149, 151, 153, 169–175  
 Malformation, 152  
 Medial frontal gyrus, 7  
 Mirror movements, 152  
 Morbidity, 64  
 Mortality, 64  
 Motion artifact, 57  
 Motion correction, 44, 46, 55  
 Motor, 43, 149, 151–154  
 Motor hand area, 51, 56, 59, 63, 64  
 Motor hand knob, 7  
 Motor (evoked) potential (MEP), 155, 157  
 Motor threshold, 161, 164  
 Motor tract, 122
- N**  
 Neovascularization, 65  
 Neuronal activity, 23, 24, 27–29  
 Neuronavigation, 45, 51, 65, 122  
 Neuroplasticity, 52  
 Neuro-vascular coupling, 31  
 Non-rigid normalization (realignment), 44
- O**  
 Operating microscope, 123  
 Optic radiation, 7
- P**  
 Pain, 51  
 Paracentral lobule (pars marginalis), 5, 8  
 Paradigm, 56–59  
 Parallel imaging, 37, 38, 40  
 Paresis, 54, 55, 57, 58, 62–64  
 Parieto-occipital sulcus, 8  
 Pars opercularis, 8, 10  
 Pars orbitalis, 8, 10  
 Pars triangularis, 8, 10  
 Patient safety, 64  
 Perfusion, 19–20  
   and CMRO<sub>2</sub> in seizures, 137  
 Periventricular, 152, 153  
 Planum temporale, 11, 12  
 Polymicrogyria, 151  
 Postcentral gyrus (postCG), 5, 7, 8, 12, 56, 62  
 Posterior commissure, 8  
 Precentral gyrus (preCG), 5, 7, 8, 11, 56, 62  
 Precentral hook, 51  
 Precentral sulcus, 62  
 Precuneus, 5, 8  
 Press button, 43–48  
 Primary motor, 56

Primary motor cortex, 155, 157, 158,  
161, 162, 164  
Putamen, 7, 10, 11

## R

Real-time fMRI, 55  
Recommendations, 64  
Recovery, 95–104  
    in brain tumors, 92, 99, 100  
    in hierarchical organization, 103–104  
Referencing, 65  
Region of interest (ROI), 44  
Reorganization, 52, 149, 153, 154, 163, 164  
Resection border, 54, 56  
Rest, 57, 59  
Rim, 47  
Risk, 64

## S

S1, 59  
S2, 59  
Scanning time, 55, 59  
Secondary motor, 57  
Seizures, 127. *See also* Epilepsy  
    absence status epilepticus, 133  
    epilepsy partialis continua  
    (EPC), 133–134  
    focal, 129  
    generalized, 131  
    neuronal hypersynchrony, 131–132  
    neurovascular coupling, 132  
    preictal state, 136  
    status epilepticus, 133  
Sensorimotor processing, 38  
Sensory-motor integration, 72–73  
Shim, 36, 37  
Signal intensity changes, 44–46, 48  
Signal time curves, 65  
Signal-to-noise ratio (SNR), 35–37, 39, 40  
Software, 43  
Somatosensory, 151, 154  
Somatotopy, 55, 56  
Speech, 43  
Speech perception, 70  
Speech production, 69–74

Spiking activity, 24, 25, 27, 30, 31  
Splenum, 7  
Status epilepticus. *See* Seizures  
Steal phenomenon, 54  
Stimulation, 57, 59  
Subcortical structures, 40  
Sulcus intermedius of Beck, 11  
Superior frontal gyrus (SFG), 5, 7, 8  
Supplementary motor area (SMA), 8, 54  
Supramarginal gyrus, 9, 12  
Sylvian fissure, 5, 7–12

## T

Temporal lobectomy, 81  
Thalamo-cortical, 153  
Thalamus, 7  
Threshold, 45  
Toes, 57, 62  
Tongue, 57  
Training, 55  
Transcranial magnetic stimulation (TMS),  
    96, 101–102, 149–153, 155–165  
    offline, 157, 160  
    online, 157–160, 165  
    sham, 163, 164  
Transmit and receive coils (t/r), 37, 38, 40  
Tumor, 51

## U

Ultra-high field, 35, 38–40  
User-friendliness, 45

## V

Vein, 65  
Venography, 16, 18  
Ventricle III, 7  
Verb generation task, 40, 41  
Vessel  
    functional response, 16  
    structure, 15, 16, 18  
Vessels, 36  
Virtual lesion, 157  
Visual stimuli, 38